

Contrail mitigation through flight planning

MSc Thesis Report

K.P.A.M. Barten

September 2017

Faculty of
Aerospace Engineering



Contrail mitigation through flight planning

by

K.P.A.M. Barten

to obtain the degree of **Master of Science**
at the **Delft University of Technology**

to be defend publicly on **September 29th, 2017**

Supervisors: Dr.ir. S. Hartjes
 Dr.ir. H.G. Visser



Faculty of Aerospace Engineering
Delft University of Technology

PREFACE

This document contains the results of my Master Thesis project. Its completion ends my time as a student at Delft University of Technology, where I have been able to challenge myself and develop my future more than anticipated. The flame of Prometheus as logo for this institution could not be more accurate in my opinion.

As a strong believer in the power of collaboration I cannot refrain from thanking the coaches that helped me along the way. I would like to thank my daily supervisor Sander Hartjes for his enthusiasm and guidance. My thanks also goes out to Dries Visser for his support and feedback as second supervisor. And finally, I could list family and friends that have helped shape me personally, emotionally and professionally, but I am confident they already know how much they mean(t) to me. You allow me to become a better version of myself. I find it fitting to end with the first and one the most important equations I was taught. Verantwoordelijkheid krijgen = verantwoordelijkheid nemen. I think this thesis serves as proof of its value.

Amsterdam, September 14, 2017

EXECUTIVE SUMMARY

This thesis explores the fuel and time cost associated with mitigating condensation trails of commercial aviation through flight planning. These white lines that can often be seen trailing high altitude jet aircraft add to anthropogenic global warming. Mitigating contrails should therefore help reduce climate change. Research has shown that reduction of a majority share of contrails is possible at very low fuel and time cost. Contrail reduction of over 50% is possible at the expense of at most a few percent additional fuel and very low additional flight time in free flight. Many models however are based on assumptions that do not hold in commercial operations. In order to further bridge the gap between these studies and commercial operations, flight planning is introduced as potential solution. This thesis investigates to what extent the results in literature hold when flight planning is used as a mitigation tool.

A model was developed that simulates a set of flights from Europe to North-America. First, an optimal ground track is found which complies with existing route structures. Second, a velocity-altitude profile is obtained from simulation of the flight along the ground track. To emulate ATC requirements flights are only allowed at certain flight levels and use step climbs between them. Mitigation of contrails is achieved in three ways. 1) Inclusion of contrail cost in the edge cost along the ground network is used to achieve lateral mitigating action. 2) Step climbs and descents along the flight profile allow for mitigation by altitude adjustment. 3) Combining both lateral and altitude changes provides a hybrid mitigation strategy.

Through ground track alterations nearly half of all contrails can be mitigated against 2-3% additional fuel and flight time. Mitigation by altitude profile alterations shows a different image for fuel optimal flights compared to time optimal. For fuel optimal flights there is a trend of increasing fuel consumption up to 0.1% with decreasing contrail distance, albeit very case dependent. For time optimal flights the case is reversed. Due to operational constraints any profile alteration leads to a lower cruise velocity which comes with increases in flight time and reduced fuel consumption. Over 80% of contrails can be mitigated while reducing fuel approximately 1.2% and increasing flight time by 0.4-0.8%. For hybrid mitigation results are also very case dependent. What is clear is that at least 50% of contrails can be mitigated at less than 2% additional fuel which exceeds ground track selection only strategy (i.e. hybrid outperforms a single dimension strategy). The results have confirmed the hypothesis that large shares of contrails can be mitigated against a few percent additional fuel consumption and flight time. Compared to literature the mitigation potential shows similar results. Compared to Hendriks [1] the results show more additional fuel for ground track selection strategy and less for profile alterations. In order to minimize the environmental impact of contrails, future research should further investigate the incorporation of contrail mitigation in commercial flight planning tools.

TABLE OF CONTENTS

Preface	I
Executive Summary	II
1 Introduction	1
2 Condensation Trails	3
2.1 Formation	3
2.2 Persistence	6
2.3 Modelling effort	8
2.4 Observation and validation studies	10
3 Environmental Impact	12
3.1 Anthropogenic climate change	12
3.2 Contrails and global warming	15
3.3 Contrail environmental impact studies	16
3.4 Metrics of climate impact	18
4 Flight Planning	21
4.1 Modelling flight planning	21
4.2 Current tools	22
5 Model Development	25
5.1 Approach	25
5.2 Equations of motion	26
5.3 Initial flight plan and simulation	27
5.3.1 Ground track determination	28
5.3.2 Optimal altitude and velocity profile	34
5.3.3 4D trajectory simulation	38
5.4 Incorporation of atmospheric data	40
5.5 Contrail prediction model	44
5.6 Ground track contrail optimization	45
5.7 Profile contrail optimization	46

6 Model Verification	51
6.1 Aircraft performance	51
6.1.1 Operational envelope	51
6.1.2 Aircraft drag and engine model	51
6.1.3 Step climb and steady horizontal flight	53
6.2 Simulation and integration	55
6.2.1 Optimal cruise condition generation	55
6.2.2 Cruise conditions grid	56
6.2.3 Climb phase interpolation	57
6.3 Contrail prediction model	58
6.4 Optimization method	61
6.4.1 Ground track selection	61
6.4.2 Profile optimization	62
7 Scenarios	65
8 Results	66
8.1 Baseline flight plan	66
8.1.1 Baseline flight plan in ISA to Washington D.C.	66
8.1.2 Baseline flight plan in NWP without wind	69
8.1.3 Baseline flight plan in NWP with wind	70
8.1.4 Baseline flight plans to Winnipeg and Vancouver	72
8.2 Ground track selection	72
8.2.1 Fuel optimal flights	72
8.2.2 Time optimal flights	73
8.3 Altitude profile optimization	74
8.4 Hybrid contrail mitigation	76
8.5 Sensitivity of contrail mitigation	79
8.5.1 Ground track selection sensitivity	79
8.5.2 Altitude profile optimization sensitivity	79
8.5.3 Hybrid contrail mitigation sensitivity	81
8.6 Alternative scenarios and constraints	82
8.6.1 Fixed North Atlantic Tracks	82
8.6.2 500 ft step climb	84
8.6.3 Other aircraft types	84
8.6.4 Eastbound flights	86
9 Discussion	88
10 Conclusion	91
References	94
Nomenclature	101
List of Abbreviations	104
List of Figures	106
List of Tables	109

TABLE OF CONTENTS

Appendix A	Numeric results - Baseline	110
Appendix B	Numeric results - Ground track	111
Appendix C	Numeric results - Altitude profile	121
Appendix D	Numeric results - Hybrid mitigation	139

CHAPTER 1

INTRODUCTION

Commercial aviation has enabled travel of people and goods at speeds and cost that changed the world. As the industry has grown, more and more large jet aircraft take to the sky, consuming fuel and releasing exhaust gasses along their trajectory. These exhaust gasses contain mainly carbon dioxide (CO_2), water vapour (H_2O) and some other oxides. Even though the exhaust gasses are mostly invisible, they are often seen as white lines behind jet aircraft. In some cases these lines even stay visible for hours after they form and many may be seen simultaneously across a clear sky. Condensation trails, or contrails for short, is what the white lines behind jet aircraft are called. They form when hot and humid air from the engines mixes with cold air and water vapour condenses to form plumes in the wake of these aircraft.

Experts have shown that global warming is a real and significant problem. As aviation is a large and increasing contributor to anthropogenic climate change the impact of jet aircraft on the climate has become a subject of research. Much of it focuses on carbon dioxide emissions which have been proven to add to the greenhouse effect. Reduction policies have been put in place and there is a societal awareness that its emission should be avoided as much as possible to combat global warming. What is much less well known is the contribution of contrails to global warming. As they form and persist, contrails change the local energy balance of the atmosphere, leading to a nett warming effect. Therefore, just like for carbon dioxide, reducing contrails where possible should help reduce anthropogenic global warming.

One could argue that the founding fathers of contrail research were Schmidt [2] and Appleman [3]. Modern day consensus on the required conditions for contrail formation is based on their work, along with a 1996 review of their work by Schumann [4]. These conditions are referred to as the Schmidt-Appleman criterion. Contrail formation is dominated by the local properties during isobaric mixing of the exhaust of jet aircraft and surrounding air. If saturation with respect to liquid water occurs contrails will form. Their persistence depends on whether final conditions are sufficiently saturated with respect to ice. If so, the young contrails will persist until conditions no longer satisfy this criterion. The long term environmental impact of contrails is relatively unknown compared to other direct emissions of aircraft. Nonetheless, research has shown strategies with great contrail mitigation potential at relatively small fuel and/or time cost. 50% or more of potential contrails can be mitigated through a few percent additional fuel and/or time cost in free flight [1, 5, 6, 7, 8, 9]. Various methods for contrail modelling have been explored. An example of successful microphysical modelling of individual contrails and their development is the Contrail Cirrus Prediction (CoCiP) model [10]. Other models take another approach and use straight forward application of the criteria for forma-

1. Introduction

tion and persistence (binary; yes or no) along with validated assumptions to make predictions in various scenarios [1] or use probability and statistics [11] or regression analysis [12]. For contrail mitigation to be effective in a realistic setting there are some rules and regulations the proposed flight should abide. Before a flight can take off a flight plan needs to be submitted and approved. Many airlines make use of flight planning tools (often software) that plan flights (semi)automatically and generate the corresponding flight plan, taking into account ATC, airport, airspace and other operational constraints and preferences.

Previous work by Hendriks developed a tool for mitigating total contrail time of a single flight through four dimensional trajectory optimization [1]. His and most other contrail mitigation studies have however remained rather separated from real life operations. Their conclusions rely heavily on specific conditions and ignore practical constraints. Examples include the assumption of free four dimensional path control and ignoring winds. Current research lacks the ability to translate conclusions of carefully crafted models to practical situations. Therefore, as flight planning is widely used to plan flights and optimize them, it is a promising solution to practical application of mitigation strategies. As such, this thesis aims to take a step towards assessing and mitigating the environmental cost of contrails caused by aviation by evaluating the fuel and time cost of contrail mitigation through flight planning.

Research question: What fuel and time cost is associated with mitigating the environmental impact of contrails through flight planning for flights between Europe and North America?

Research objective: To assess the fuel and time cost associated with mitigating the environmental impact of contrails caused by flights in the selected domain by developing a realistic flight planning tool that includes a measure of the contrails generated and using it to optimize a set of characteristic flights

The method used to investigate this contrail mitigation potential in a realistic flight planning context consists of a number of steps. Each flight is first assigned a minimum cost ground track, which is generated from a network of airways and corresponding edge costs. A flight is then simulated following optimal cruise conditions along this ground track. Contrail regions are identified along the way and are mitigated by horizontal (ground track), vertical (altitude profile) or hybrid flight path alterations. Subsequently their impact on fuel consumption and flight time for the selected scenarios is examined.

This report is structured as follows. Chapters 2 to 4 start by introducing some relevant literature and common practices concerning condensation trails, their environmental impact and flight planning. The theory that is covered in these is subsequently applied in creating a trajectory simulation and contrail mitigation model. Chapter 5 describes this model including ground track, profile and integrated trajectory generation, contrail prediction and contrail mitigation elements. Chapter 6 covers some aspects of the model in more detail and describes the verification and validation that is performed. The different scenarios that are evaluated are introduced in Chapter 7 after which their results are shown in Chapter 8. This includes baseline, ground track selection, altitude profile mitigation and hybrid results as well as a sensitivity analysis for them. Lastly, Chapters 9 and 10 cover the conclusion, discussion and recommendations regarding the results.

CHAPTER 2

CONDENSATION TRAILS

This chapter describes relevant theory concerning condensation trails, their formation, persistence as well as relevant modelling, observation and validation efforts in literature.

Condensation trails or contrails for short are the white stripes that can often be seen trailing high altitude aircraft. These are a common phenomenon in commercial aviation and can be seen to either dissipate quickly or stay for extended periods of time depending on circumstances. Similarly to breath in cold air, relatively hot and humid exhaust gasses are ejected in the wake of the aircraft at which point the water vapor in the air condenses and freezes to form a contrail. Section 2.1 describes the Schmidt-Appleman condition on which formation of contrails depends. Section 2.2 continues by covering the conditions under which they persist after formation. Section 2.3 covers some contrail modelling efforts in literature and their conclusions after which Section 2.4 briefly describes the results of observational studies and validation of previous contrail models.

2.1 Formation

Contrails have been studied ever since aircraft started reaching altitudes that are required for contrail formation in the midlatitudes around 1914-1919 [13]. The first article on contrails was published in 1919 by Ettenreich [14] who reported "the condensation of a cumulus stripe from the exhaust gases of an aircraft". Following this article, early research in contrail physics and modelling can be found in meteorological and climatological science. One could argue that Schmidt [2] and Appleman [3] are among the most influential authors and founders of modern contrail research. In 1996 Schumann [4] redefined their combined work into modern version of the well known Schmidt-Appleman criterion, which is important in contrail research since it can predict if contrails form under specified conditions or not.

In 1941 Schmidt [2] presented his research into the physics of contrail formation. In his work he investigated isobaric mixing between two air masses with varying enthalpy and water content. He showed that the critical conditions for contrail formation are dependent on ambient pressure, humidity and exhaust temperature and water content. Following Schmidt's work, in 1953 Appleman [3] published an article in which he introduced the same concept as Schmidt previously did and constructed curves that are used to determine the critical temperature for formation of a visible contrail in a given ambient pressure and humidity and the amount of air in the exhaust stream.

2. Condensation Trails

After the works of Schmidt [2] and Appleman [3] a review article was written in 1996 by Ulrich Schumann. This article on the conditions for contrail formation re-examined previous work and proposed the modern version of the Schmidt-Appleman criterion we work with today [4]. In his research Schumann included the effects of converting combustion heat into kinetic energy of flows in the wake area. Inclusion of this effect lead to higher critical temperatures and therefore less stringent conditions in which the criterion predicts contrails to form compared to previous work.

When looking at contrail formation one of the key concepts is that of saturated vapour pressure. Saturated vapour pressure is the thermodynamic equilibrium pressure of a vapour that is in contact with its solid or liquid form. This is the pressure at which there is a perfect equilibrium between the amount of molecules evaporating from the surface into a gaseous state as there are molecules returning to the condensed phase. When ambient pressure is greater than vapour pressure, more molecules will condense than evaporate and when ambient pressure is lower than vapour pressure, nett evaporation will occur. Since contrails are formed by condensation of water vapour, the conditions under which these phase shifts occur can be used to predict them. As can be seen in Figure 2.1 a curve can be constructed for liquid water and ice particles suspended in the atmosphere that relates the saturated vapour pressure to ambient temperature. Given these lines one can conclude that if local pressure is below the water saturation pressure, liquid water will evaporate and if it is above the water saturation pressure, the air has become saturated and vapour may condense back to solid or liquid.

When exhaust gasses exit the engine they are relatively hot. When plotting the exhaust conditions in Figure 2.1, due to the scale the location of this point cannot be seen; however one can image this point exists and is located above and to the right of the frame. From these exhaust conditions a line can be plotted that shows the mixing with ambient conditions. Mixing implies a decrease in temperature and saturated vapour pressure and thus a line going down and to the left is expected. Schumann shows that this line of mixing of exhaust and ambient gasses follows a gradient G [4]. The mixing line is plotted and can be seen in Figure 2.1. Gradient parameter G is a function of a range of inputs as seen in Equation (2.1) which are further elaborated on.

As mentioned, conditions above the saturated vapour pressure line will cause condensation. Given that using specific exhaust and ambient conditions a mixing line can be constructed, also a critical mixing line can be constructed that just touches the saturated vapour pressure line at a single point. This line can be seen in Figure 2.1. The critical mixing line provides the critical conditions for contrail formation. Any lower temperature will cause contrails to form as the mixing line crosses the vapour pressure line which implies mixing conditions in which condensation occurs. Any higher temperature and mixing conditions will keep contrails from forming. The critical temperature can be approximated graphically as Appleman did in 1953 [3] or determined through numerical methods that were later developed [15].

Given the mixing lines and vapour saturation pressure lines there are some specific points in Figure 2.1 that are relevant in Schumann's contrail formation theory [4]. The most straight forward location is T_{amb} at the end of the actual mixing line. At that temperature the exhaust has mixed completely. This temperature is used as one of the key values to determine whether or not the Schmidt-Appleman criterion is fulfilled. What can also be seen is the critical temperature T_c , which is the location where the critical mixing line and the vapour saturation

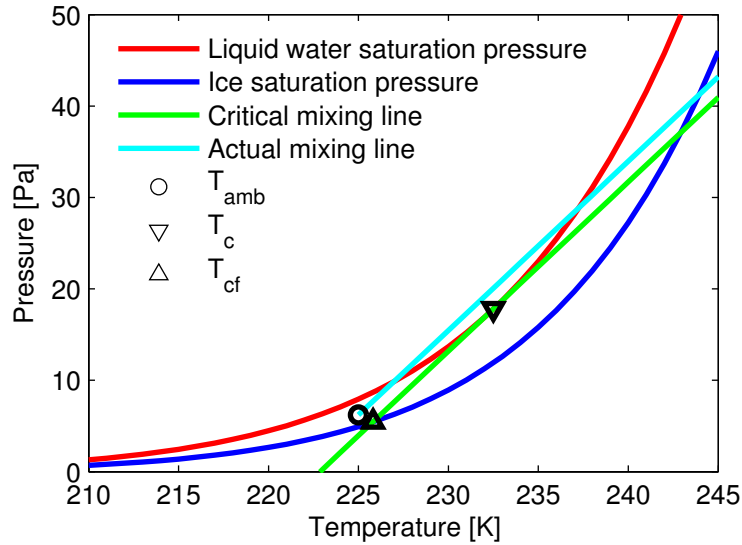


Figure 2.1: Contrail formation conditions

pressure line meet (where the red and green lines touch). Lastly, one can see the intersection of the critical mixing line and the ice saturation pressure which is referred to as T_{cf} . The temperature at this point represents the critical temperature point for contrail formation and is located on the critical mixing line.

When considering the slope of the ideal mixing line (which is equal to G) one can determine a set of input variables. Gradient parameter G is a function of specific heat capacity c_p ($Jkg^{-1}K^{-1}$), total pressure p (Nm^{-2}), ratio of molar masses of water and air ε , emission index of water vapour EI_{H_2O} ($kg kg^{-1}$), propulsive efficiency η and specific combustion heat Q ($MJ kg^{-1}$) [4]. Dimensional analysis proves that the unit of G is $N m^{-1} K^{-1}$ which matches expectations from the fact that the line is plotted in a pressure-temperature plot. From Equation (2.1) it is clear that G is dependent on atmospheric conditions, engine and combustion parameters and the type of aircraft propelled. Typical values for these are as follows. c_p is in the order of $1.00 \cdot 10^3 J kg^{-1} K^{-1}$ [4]. Total pressure at a cruise altitude of $10 km$ is approximately $260 hPa$ as dictated by the International Standard Atmosphere (ISA) [16]. Furthermore the molar masses of water is $18.02 gr mol^{-1}$ [17] and that of dry air is $28.97 gr mol^{-1}$ [18]. This combination gives a molar mass ratio of $\varepsilon = 18.02/28.97 = 0.622$. The emission index of water vapour expresses the mass of the emitted water vapour in the combustion process in relation to the mass of fuel consumed, which for kerosene is approximately $1.25 kg kg^{-1}$ [19]. As the propulsive efficiency of aircraft keeps improving, when Schumann wrote his paper he used an efficiency of $\eta = 0.308$ [4] however modern airliners are more efficient which implies a higher value for G . Lastly the specific combustion heat of the most commonly used jet fuels Jet A and Jet A-1 are 43.02 and $43.15 MJ kg^{-1}$ respectively [20].

$$G = \frac{c_p \cdot p}{\varepsilon} \cdot \frac{EI_{H_2O}}{(1 - \eta) \cdot Q} \quad (2.1)$$

The critical temperature T_c is determined from the observation that the critical mixing line is tangent to the saturated vapour pressure line. Tangency of these lines implies the slope G is equal to the derivative of the saturated vapour pressure line with respect to temperature. This

2. Condensation Trails

condition can be seen in equation form in Equation (2.2).

$$G = \frac{dp_{sat}(T)}{dT} \quad (2.2)$$

In Schumann's research on the Schmidt-Appleman criterion he took the condition as can be seen in Equation (2.2) and determined the critical temperature numerically through Newton iteration [4]. In his paper he describes that as a first guess one could use the relation as shown in Equation (2.3). For T_c he used units of $^{\circ}C$ and G in units of $N m^{-1} K^{-1}$.

$$T_c = -46.46 + 9.43 \cdot \ln(G - 0.053) + 0.720 \cdot [\ln(G - 0.053)]^2 \quad (2.3)$$

It is relevant to know the value of T_c is because it represents the critical temperature for contrail formation at a relative humidity of 100%. In order to take a final step towards developing a generalized critical contrail formation temperature as indicated by T_{cf} a final relation is required. Schumann used the relation as showed in Equation (2.4) to determine exactly this temperature. It is a function of the critical temperature T_c , the vapour saturation pressures (expressed by e_L) of critical temperature and to-be-determined contrail formation temperature and the relative humidity U . Since the Schmidt-Appleman criterion simply compares ambient temperature T_{amb} and critical contrail formation temperature T_{cf} it can be expressed in equation form as can be seen in Equation (2.5).

$$T_{cf} = \frac{T_c - [e_L(T_c) - U e_L(T_{cf})]}{G} \quad (2.4)$$

$$T_{amb} \leq T_{cf} \quad (2.5)$$

From the input as previously mentioned, along with the ISA temperature model, Schumann investigated the likelihood of contrails occurring at various altitudes [4]. He concluded that in kerosene jet aircraft at the time, contrails may form typically above $8.4 km$ and below $14 km$ altitude. This can also be seen in Figure 6.8. If hydrogen fuels are used instead of kerosene contrails may form above $6.3 km$ up to $19.5 km$ altitude. Their exhaust is of course pure water vapour which could (partially) explain the difference.

2.2 Persistence

In Section 2.1 a description of contrail formation is given. However as can be seen in many cases these contrails may initially form but disappear again in a matter of minutes. This shows the relevance of not only knowing when they form but also when contrails persist and become the long white lines in the sky. In this section the theory behind contrail persistence is expanded on.

Fundamentally, the question whether contrails persist depends on whether the condensed particles in a young contrail (albeit in solid or liquid form) are likely to evaporate or not. Of course this depends on similar atmospheric properties to those that were used to determine when contrails form, namely saturated vapour pressure and temperature.

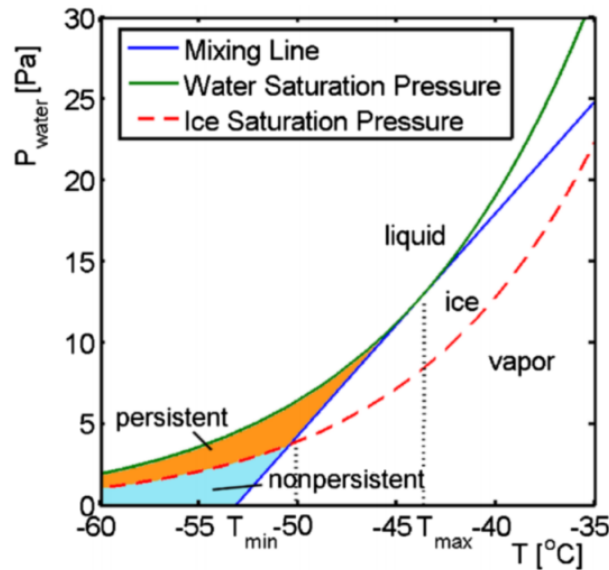


Figure 2.2: Persistence of contrails [21]

The relative humidity of the environment is critical in contrail persistence. As mentioned, distinction should be made to the relative humidity with respect to liquid water or ice. Just like there are two distinct saturated vapour pressure curves for liquid water and ice, also the relative humidity can be defined for both. It was shown that relative humidity with respect to ice is the value that determines whether contrails persist or not [22, 15, 23]. For contrail persistence, a distinction can be made between two states of saturation with respect to ice of the atmosphere. As one would expect the air can have a saturation level of 0 to 100% and will therefore hold all the vapour and typically not show condensation. We call this a state of subsaturation. Here, jet exhaust may cause humidity increases and temperature changes which may cause contrails to form, however as the wake mixes the ice crystals will sublime rather quickly [24, 25] and the contrail will vanish. The second state of saturation the atmosphere can take is that of supersaturation. In this case the air has a relative humidity of more than 100%. If ambient air is sufficiently supersaturated with respect to ice, contrails will persist [22, 24, 25].

An example from Schrader [15] as seen in Figure 2.3 helps illustrate exactly the conditions in the temperature-pressure plot that cause contrails to persist or evaporate after formation. The example shows an illustration of the aircraft and contrail with a set of points indicated. Underneath the aircraft and contrails the pressure-temperature graph is shown with the mixing line and corresponding points. One should note the following. The region above the saturated vapour pressure line for liquid water corresponds to conditions in which condensation will occur. As explained in Section 2.1 contrails will form in this part of the graph. In both cases the contrail only forms when the water saturation line is crossed because at this moment condensation is first initiated. After this point two things can happen. If the ambient air is not sufficiently saturated with respect to ice, the contrail particles sublime in the mixing process and the contrail vanishes. This can be seen in case of the non-persistent example between points three and four. If the air however is sufficiently saturated with respect to ice the contrail remains as can be seen from the conditions in point three in the persistent contrail example.

As is shown, contrails form if liquid saturation is reached and they persist as long as the air

2. Condensation Trails

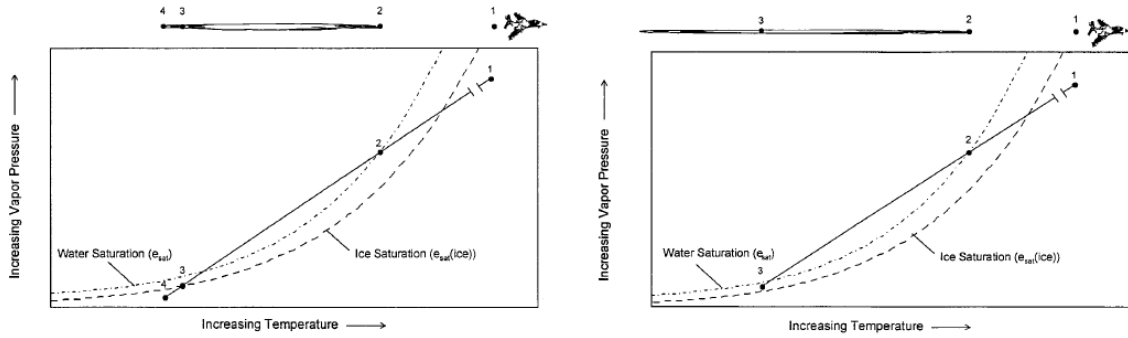


Figure 2.3: Illustration of contrail persistence by Schrader [15]

remains sufficiently saturated with respect to ice [24]. Sonntag showed that the saturated vapour pressure lines with respect to water and ice can be approximated as can be seen in Equation (2.6) and Equation (2.7) [26]. Especially the ice saturation pressure line is very accurate as shown by Murphy and Koop [27].

$$p_{liquid}^{sat}(T) = 100 \cdot e^{-6096.9385/T + 16.635794 - 0.02711193 \cdot T + 1.673952 \cdot 10^{-5} \cdot T^2 + 2.433502 \cdot \ln(T)} \quad (2.6)$$

$$p_{ice}^{sat}(T) = 100 \cdot e^{-6024.5282/T + 24.7219 + 0.010613868 \cdot T - 1.3198825 \cdot 10^{-5} \cdot T^2 - 0.49382577 \cdot \ln(T)} \quad (2.7)$$

In humidity measurements there are three basic metrics. These include absolute humidity which expresses the water vapour content of air in $gr\ m^{-2}$ and relative humidity, which gives the ratio of the current absolute humidity to the maximum humidity for that temperature in percentage (%). Finally there is specific humidity which is the ratio of the water vapour mass related to the entire air mass, expressed in $kg\ kg^{-1}$. As mentioned, contrail persistence requires sufficient saturation with respect to ice. In order to calculate this relative humidity one needs to be aware of the relationship between relative humidity and saturated vapour pressure. It has been shown that the saturated vapour pressure lines give the vapour pressure p in $N\ m^{-2}$ as a function of ambient temperature T_{amb} in $^{\circ}K$. Since the relative humidity is simply the ratio of the partial pressure of water vapour over the equilibrium vapour pressure (the saturated vapour pressure) one can use the known saturation pressure over water and ice to convert between RH_w and RH_i . The relation can be seen in Equations (2.8) and (2.9). It should be noted that RH_w refers to the relative humidity with respect to liquid water and RH_i is the relative humidity with respect to ice.

$$RH_w = 100 \cdot \frac{p_{vapour}^{partial}}{p_{liquid}^{sat}} \quad (2.8)$$

$$RH_i = 100 \cdot \frac{p_{vapour}^{partial}}{p_{ice}^{sat}} = RH_w \cdot \frac{p_{liquid}^{sat}}{p_{ice}^{sat}} \quad (2.9)$$

2.3 Modelling effort

In Section 2.1 the Schmidt-Appleman criterion has been introduced and in Section 2.2 contrail persistence has been elaborated on. Most contrail prediction and mitigation studies have relied

heavily on this theory and as such have been fundamentally similar. However, as shown in this section different models make use of different assumptions and put emphasis on different aspects of the theory or even take a different approach entirely by for example embracing probability and regression techniques to build models. This section gives an overview of different contrail prediction models that were developed.

One of the most sophisticated models that was developed is the Contrail Cirrus Prediction (Co-CiP). This model was developed by Schumann at Deutschen Zentrums für Luft- und Raumfahrt (DLR) [10]. Since the author is one of the leading authors on the subject this model makes extensive use of the theory that he developed over time. As expected the Schmidt-Appleman criterion is used to determine whether or not contrails form. It should be noted that due to the spatial nature of supersaturated regions the critical relative humidity with respect to ice was relaxed slightly. Because they are often shallow and narrow the discrete humidity field may not accurately describe it. In this model the critical humidity with respect to ice was chosen to be 80% in the mid-troposphere, 100% in the stratosphere and follows a smooth transition with pressure altitude between these two values in the upper 20% of the troposphere.

In 2016 a review article was written by Paoli which aimed to review the main physical processes and simulation efforts in contrail research [28]. The article defines four distinct phases namely, the jet, vortex, vortex dissipation, and diffusion phases as described by Gerz [29]. Each of these are governed by processes that are elaborated on extensively in the paper.

Rather than developing a model for contrail formation, development and other properties such as optical depth, some authors choose to use a different approach. Mannstein for example uses the frequency of an aircraft flying through an Ice Super Saturated Region (ISSR) as a proxy for the quantity of contrails that a particular strategy causes [5]. In his research he shows that the frequency of flying through these regions is decreased if the aircraft changes altitude when an ISSR is encountered regardless of the direction (upwards or downwards). A general altitude change regardless of atmospheric conditions will not lead to sufficient reduction in contrails. Moreover, a small increase in altitude will likely increase the probability of flying through contrail prone areas. If the change is directed towards the closest non-ISSR region some of the desired mitigation can be attained. In this case, an altitude change of 1000 *ft* is enough to reduce the frequency of flying through contrail prone regions by 50%.

There are researchers that believe the Schmidt-Appleman criterion has drawbacks due to its heavy dependence on accurate input data and try to overcome that through the creation of logistical models. Duda reports that logistic regression techniques can be used if the phenomenon of interest is a dichotomous (yes/no) variable, which is arguably true for prediction of contrails [12]. In his paper he tests 21 atmospheric parameters as predictors and includes random errors to test their effect. It was shown that the model correctly predicts the outcome approximately 85% of the time when large errors are introduced. The paper shows that logistical models could be valuable in contrail prediction. Especially when input data will be more accurate the models can be better calibrated which improves the quality of their output. Additional research is required to include regional and seasonal effects.

Just like Duda, Travis took a step back from contrail physics and used statistics to create an empirically based model for contrail prediction [11]. As input data he made use of 99 obser-

2. Condensation Trails

variations of which 33 with contrails, 33 with a clear sky and no contrails and 33 with a cloudy sky and no contrails. He initially used the average temperature of the 300–100-mb level and the column-integrated water vapor in the 700–100-mb layer as primary independent variables on contrail persistence. In the model he also tested for nonlinear dependencies by including the squares of temperature and water vapour and interaction between them by including the multiplication of temperature and humidity and the square of the interaction value. Three of these were concluded to be statistically significant which are the water vapour, water vapour temperature interaction and water vapor–temperature interaction squared. Finally the authors test the model they have created and its potential use in climate research. In the paper, usage of the model is suggested for micro-physical studies on contrails but these studies have yet to be carried out.

As contrails can often be clearly seen from the ground, this is also true for the trails of military jet aircraft. Given that the military invests significant resources in technologies like stealth to keep their aircraft from being detected, contrails are an obvious liability in their operations. Therefore also military research laboratories have developed contrail prediction models. In 1992, Bjornson wrote a paper on the improvement of the models that were at that point used due to an unacceptable probability of false outcomes [30]. By improving the input data for the model that was based on the Schmidt-Appleman criterion he could obtain a better fit for the contrail formation curves as a function of temperature, altitude and vertical motion. The previous model used the curves as developed by Appleman in 1953 [3] and by reconsidering the curves of governing relations, the accuracy of the model was improved. It was however concluded that not the atmospheric condition curves but inclusion of engine fuel-to-air ratio into the curves had the greatest improvement on the model and was consequently adopted. In 2001, in another piece of military contrail research Jackson describes how up to that point the Air Force Weather Agency had relatively poor contrail forecasts due to the accuracy of atmospheric measurements and numerical prediction of humidity and temperatures [31]. The newly developed statistical regression contrail prediction model was compared to a model based on the Schrader algorithm which represented the currently used model closely. It produced in 85% of cases a correct prediction whereas the original model only did in 58% of cases. It is clear that the military has developed contrail prediction models and will keep developing them. Although the Schmidt-Appleman criterion is a powerful tool in predicting contrails, the accuracy of input data should be considered carefully.

2.4 Observation and validation studies

It is one thing to develop advanced models to predict phenomena, but their validation is critical if they are to deliver any reliable results. It was also emphasised by Travis that one cannot underestimate the value of empirical studies [11] and going out collecting measurements and testing contrail models in real life. In this section an overview is given of selected validation and observation studies.

There have been studies that aim to quantify contrail coverage globally and regionally. Studies show estimates for global contrail coverage of 0.084% [32], 0.07% [33], 0.06% [34] and 0.05% [35]. Sausen determined that in the period 1983-1993 global contrail coverage was 0.09% [36]. It was also shown that there were significant seasonal patterns on a regional scale. In the

mid-latitudes winter showed more contrail coverage compared to summer. As might be expected, the pattern of air routes can be seen in geographical distribution of contrail coverage. As shown by Mannstein the daytime contrail coverage of Central Europe was $0.50\% \pm 0.25$ with regional maxima of 1.2% [37]. This was confirmed by Pultau who also reports a value of 0.5% with maxima during spring and winter [38]. Contrail coverage over the continental US is determined at 1.44% [36] to 1.7% [39]. Mannstein reports that South-East Asia has a coverage of approximately 0.13% with low values in the south and higher in the north [39]. Mannstein and Schumann continued to show that air traffic increases contrail coverage of the sky over Central Europe with an additional 3% [40]. Stubenrauch confirms this trend of increasing contrail cover due to increasing air traffic density [41]. It was shown that contrail coverage increases 0.20% – 0.25% per decade over Europe and 0.08% – 0.24% over the North Atlantic flight corridor. A 1999 study by Gierens predicts global contrail coverage to increase with a factor of three by 2050 [42]. This is mainly attributed to the assumed increase in propulsive efficiency as well as air traffic density worldwide. Contrail coverage during the day is reported to be two [43] to three [37] times that during the night. In summary, despite variations in methods and results of previous research it is safe to assume that global contrail coverage around the turn of the century was in the order of 0.05% – 0.1% and is increasing. Local peaks occur in high traffic density regions.

As shown in Sections 2.1 and 2.2 contrails only form under specific atmospheric conditions. Given that only a fraction of the atmosphere complies to these conditions, one could define a maximum potential contrail coverage fraction. This represents the fraction of the sky that could be covered by persistent contrails if an aircraft were to fly through it. Noppel calculated a value of $11.8 - 14.5\%$ globally and in the range of 17% for regions with high air traffic density in the northern hemisphere [44]. Sausen determined global potential contrail coverage to be approximately 16% [36]. Stubenrauch estimated the potential contrail coverage in areas of high air traffic density to be in the order of 5% – 10% [41]. Williams showed that seasonal changes have a significant effect on potential contrail coverage over much of Europe [45]. In summer the coverage is close to 5% in high traffic density areas while in winter local values of 25% are not uncommon. This shows the impact of choices with respect to input data. Daily and seasonal changes or weighting methods must be kept in mind in new contrail research.

CHAPTER 3

ENVIRONMENTAL IMPACT

Chapter 2 explains contrail physics and modelling efforts. In the context of this thesis however it is also important to know why they should be mitigated. This chapter goes into detail regarding the impact that aviation exhaust has on the global climate and how contrails contribute to it. Some relevant studies are introduced including previous contrail mitigation studies. Finally, a closer look is taken at various metrics of climate impact.

3.1 Anthropogenic climate change

One of the most cited pieces of work on the role of aviation in global climate change is a report by the Intergovernmental Panel on Climate Change (IPCC) from 1999 [46]. This report along with its follow up [47] and numerous other works explain why and how much burden aviation puts on the environment. There is general consensus on the way that aviation impacts the environment, as listed below [48]. Section 3.1 aims to provide an overview with the ways in which aviation contributes to climate change, as well as explaining some opportunities for the industry to limit their growing contribution.

- CO₂ results in a warming effect
- NO_x results in a warming effect
- Emissions of soot particles result in a warming effect
- Emissions of sulphate particles result in a cooling effect
- Persistent linear contrails result in both warming and cooling (nett result is warming)
- Contrail-cirrus clouds result in both warming and cooling (nett result is warming)

It was shown that international aviation contributes to 2.5-3% of anthropogenic CO₂ emissions [49]. As can be seen from Figure 3.1 aircraft emissions add in many ways to climate change. The different types of direct emissions correspond to the list by Lee [48] that was shown. Each of the components contribute in their own way to climate change. Apart from sulphate particles, the other direct emissions all cause a nett warming effect. It should be noted that some lead to both positive and negative effects. An example is the increased albedo effect by widespread clouds which cause cooling during the day and warming during the night. However, when both effects are taken into account and added, the nett effect is warming [48]. What is also clear from Figure 3.1 is that there is a difference between complete combustion products and the actual combustion products. Expulsion of carbon monoxide, hydrocarbons, soot and nitrous oxides are the result of incomplete combustion which add to the warming effects with respect to the ideal case. It can be seen that one-to-one relations are difficult to establish

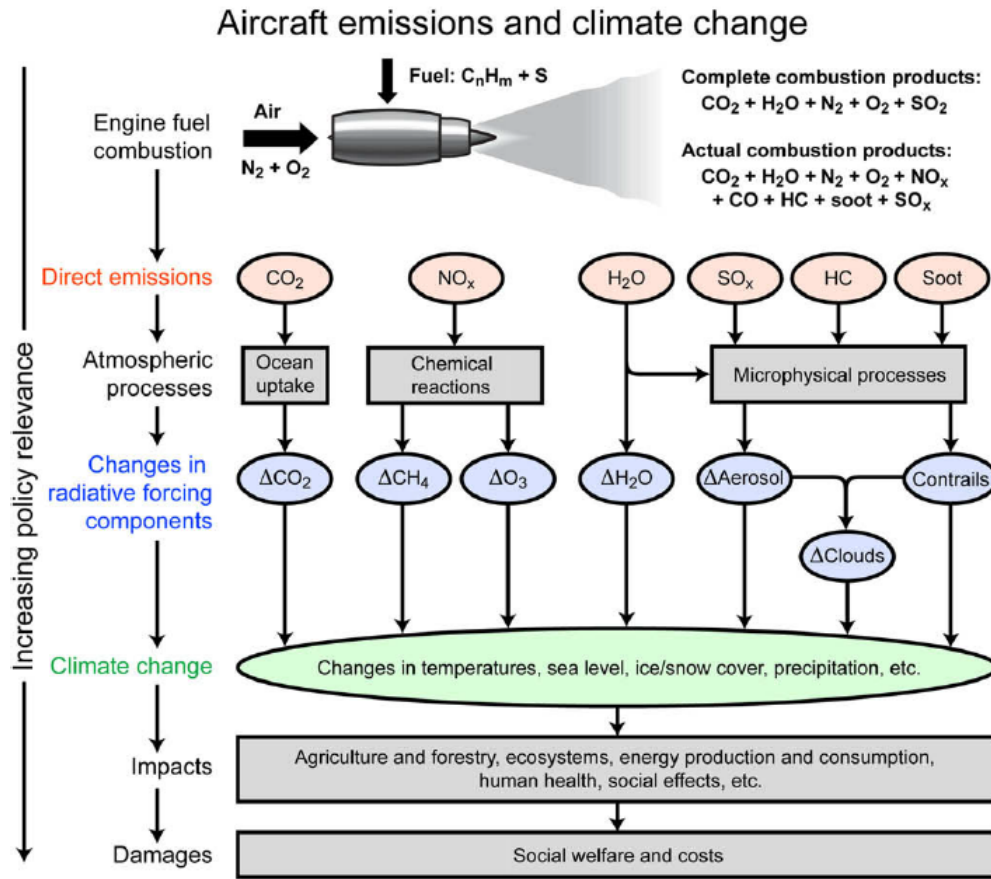


Figure 3.1: Overview of aviation emissions and their impact on climate change and damages [50]

between direct emissions and climate change. Atmospheric processes, chemical reactions and microphysical processes need to be considered before an estimate of the change in radiative forcing can be made. Translation to climate change and even potential impacts and damages are not straight forward. This makes it difficult to quantify the "cost" of direct emissions, however some efforts have been made to create a common measure for climate impact. Section 3.4 covers these in more detail.

Given that aircraft have been around for little over 100 years, their impact on the environment has only been significant during the past decades. What is clear however from Figure 3.2 is that the industry is growing very fast. Since the 1970s the number of passengers transported worldwide has increased a factor ten and the total freight moved by aircraft shows a similar growth. This is paired by an increase in fuel consumption and emissions albeit less than the growth in pax due to increased efficiency. The 2016 annual review by IATA mentions that the the industry is trying to decouple the the growth in traffic from the increase in emissions. In order to do so it has committed to three targets. The first is a nett annual improvement of 1.5% in fuel efficiency until 2020. From 2020 onwards any new growth needs to be carbon neutral and finally, by 2050 the nett emissions need to be half of what they were in 2005 [51]. It seems evident that given that an average airliner has a lifespan in the order of 30 years [52] (dependent on many factors), innovations in new aircraft alone cannot is not sufficient to meet these goals.

Environmental impact mitigation measures can be occur in three categories. First, they can be

3. Environmental Impact

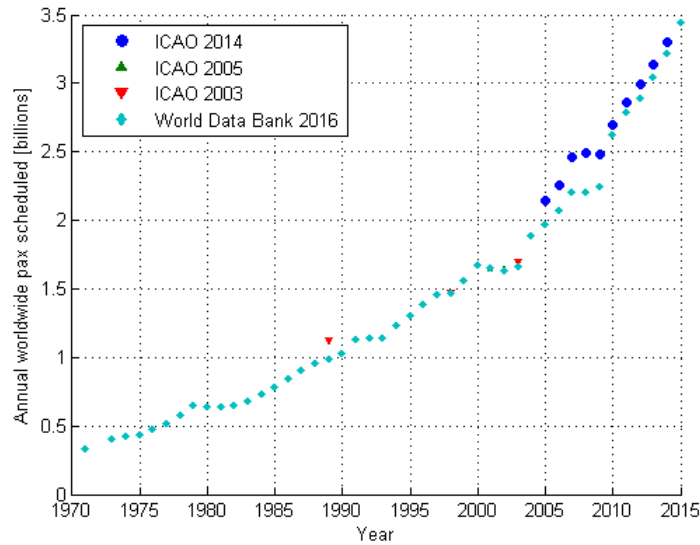


Figure 3.2: Worldwide annual number of scheduled pax [53, 54, 55, 56]

forced by a regulatory body such as a (local) government or organization that has the power to push certain rules, policies or measures. Abiding these is obviously not done on a voluntary basis. The second category consists of economic measures. Examples are taxes, subsidies and other measures that give a financial incentive to act in a way that reduces climate impact. There are already many states that put heavy taxes on fuel, ticket prices and subsidies on other technologies. Also conditional tax exemptions based on KPI's or even fines are applied to incentivize airlines financially. The final category contains voluntary measures. These include the participation to environmental research or voluntary agreement to meet certain targets. Of course implementation and enforcement of these can vary widely.

One of the ways of enforcing measures that improve the environmental impact of aviation is by standards, policies and principles by International Civil Aviation Organization (ICAO). It has rules covering aircraft emissions, fuel taxation and even charging principles that are relevant in an environmental context [46]. Many of these rules are overseen by Committee on Aviation Environmental Protection (CAEP) which examines them and researches what can be changed to improve from a technical, economic and environmental point of view [46]. In addition to that, improvements in engine and Communication, Navigation and Surveillance (CNS) technology enables airlines to become more (fuel) efficient with obvious environmental benefits. This effect is enhanced by globalization and opening up of markets in an already very competitive sector. Of course mitigation starts with knowing who emits how much. A major point of discussion in aircraft related emissions is how to allocate emissions between parties. The international character and large number of parties involved makes it difficult to allocate emissions to specific states, firms or individuals.

The Kyoto Protocol sets targets for states to meet by certain periods. If it does not meet these targets, the the United Nations (UN) can sanction the state in various ways. As of 2012 the European Union has included emissions of aviation in their so-called Emissions Trading System (ETS) [57]. This system works by allowing participants to buy and sell the rights to emit greenhouse gasses like carbon dioxide [58]. They are given a certain amount of expulsion

rights for a certain period. If at any point emissions rights are left unused they can be sold to others that do not meet their target. By introducing a clear financial incentive the European Union aims to accelerate the reduction of emissions of anthropogenic greenhouse gases. It was shown that for low (5 euro per ton CO₂) to moderate (20 euro per ton CO₂) carbon emission prices, the macroeconomic impact of including aviation in this system is negligible [59]. The high price scenario (40 euro per ton CO₂) predicts additional 0.2% growth by 2020. When looking at the actual trading price it can be seen that even the moderate scenario overestimates the price by a factor two. The actual price has not been over 10 euro per ton CO₂ since the beginning of 2012 and is currently around 5, which corresponds to the low scenario. In terms of carbon dioxide, emissions reduction for the low price scenario were found to be in the range of 0.3-0.5%, whereas the medium price lead to 4.0-6.3% reduction and the high price even 7.0-11.0% [59]. Low cost and regional airlines are predicted to be impacted more significantly than network carriers due to the difference in their business model, however given their above average margins they should remain profitable [49].

3.2 Contrails and global warming

This section provides insight into how exactly contrails contribute to climate change. Clouds, contrails as well as airborne water droplets in general contribute both in a positive and negative way to global warming. This has to do with the fact that during the day the surface of the earth is warmed by the sun. Because of this heat, the earth also radiates energy out to space which in turn causes it to cool. During the day more energy is absorbed than emitted and the reverse is true at night. Clouds and contrails change these ratios by reflecting part of the solar energy back during the day through the albedo effect. During the night they also reflect part of the radiative energy from the surface and keep it from advancing into space. If the two effects are integrated over time the warming effect has the upper hand [33, 60]. It was shown that, even though the effect was initially overestimated, contrails have the largest effect in terms of radiative forcing of all aviation related components [61].

Of course the reflective properties of very thin contrails are different from thicker ones. The contribution of a certain gas to the energy budget of the earth is usually compared through radiative forcing. Positive radiative forcing leads to warming and negative radiative forcing causes cooling and is usually expressed in watts per square meter ($\frac{W}{m^2}$). Research shows that there are a number of factors that affect the influence contrails have on the earth's energy budget. According to Meerkotter, the radiative forcing of contrails is mainly determined by product of the coverage area of the contrail and the optical depth [62]. Optical depths of 0.2 to 0.7 are commonly used for contrails, however models are rather sensitive to this parameter. Frömring showed that a detection threshold of 0.05 instead of 0.02 in the model yields a 146% increase of global mean contrail radiative forcing [63]. Of course it is difficult to estimate the mean optical depth as it varies through the cross section of the contrail and evolves over time as it dissipates or spreads. Probabilistic approaches including Gaussian distributions are often used to achieve a mean depth that models can work with. In addition to the size and optical depth, also the local radiative properties are important to consider. As one can imagine the time of day, surrounding natural clouds and location on the globe all influence the properties and quantity of energy that passes through the contrails. Espinoza published a review paper concerning parametrization of radiative properties of cloud layers [64]. Parametrizations have also been developed by Schumann [10].

3. Environmental Impact

Estimates for radiative forcing by contrails span a wide range. According to Minnis the global mean for line shaped contrails is 0.02 W/m^2 in 1992 and 0.1 W/m^2 in 2050 [60]. Minnis finds a global mean of $0.006\text{--}0.025 \text{ W/m}^2$ [65]. When looking at the spectrum of radiation it can be seen that contrails have negative forcing for shortwave radiation but larger positive forcing for long waves [62]. The IPCC reported in 1999 that the mean radiative forcing by aviation emissions is approximately 0.05 W/m^2 in 1992 [46], however the 2005 update on this reduces the effects of contrails and brings the new total to 0.048 W/m^2 for 2000 [47]. Lee shows a global mean forcing of $0.023\text{--}0.087 \text{ W/m}^2$ in 2005 [50]. It should be noted that these estimates do not include aviation induced cirrus clouds, but only contrails. According to Burkhardt this contrail induced cloudiness is the single largest contributor to aviation related radiative forcing. Taking into account natural cloud feedback he estimates radiative forcing by global contrail induced cloudiness to be 0.031 W/m^2 [66]. Marquart estimates an increase in global mean radiative forcing due to contrails increasing from approximately 0.01 W/m^2 in 2015 to 0.015 in 2050 [34]. Meerkötter shows that radiative forcing increases with optical depth and area of coverage [62]. Instead of computing a global mean he determines the radiative forcing for an area covered by contrails to be in the range of $10\text{--}30 \text{ W/m}^2$ using an optical depth of $0.2\text{--}0.7$. Using a global contrail coverage of 0.1% this gives a global mean of $0.01\text{--}0.03 \text{ W/m}^2$ which is comparable to previous estimates. According to Stuber, the majority of forcing comes from night and winter flights. Night flights which represent 25% of traffic contribute to $60\text{--}80\%$ of radiative forcing and the 22% of flights that fly during winter contribute to half of the forcing [67].

3.3 Contrail environmental impact studies

Previous contrail mitigation studies have investigated a number of strategies. They need to be effective in preventing climate change as much as possible as well as abiding safety, feasibility and cost constraints [50]. Overall it is clear that technology or different fuel (additives) are not a feasible mitigation option. Operational avoidance is seen as the best option in reducing contrail climate effects [50]. This section gives a quick overview on the strategies that were investigated and their main conclusions.

A review on contrail avoidance strategies was published in 2008 [61]. As described in Chapter 2 the conditions under which contrails form are dependent on the thermodynamics and atmospheric conditions during mixing of exhaust gasses. Gierens concludes that technical measures are only feasible if they can either decrease the water vapor emission index (EI_{H_2O}), decrease the overall propulsive efficiency (η) or increase the specific combustion heat of the fuel (Q) [61]. One way of changing these values is by changing the fuel that is used. According to the IPCC only liquid hydrogen and methane as possible alternative to kerosene, however they would both lead to more contrails rather than less given their EI_{H_2O} and Q values. Another strategy could be to add certain chemicals to the fuel to suppress contrail formation. An example would be an additive that coats the exhaust particles in a hydrophobic coating which counteracts condensation nuclei. Gierens showed that fuel additives are not a viable option for contrail mitigation due to their relatively small influence on the Schmidt-Appleman criterion [68]. They could however contribute to reducing the optical depth to some extent. A major contributor to the inability of technology to help mitigate contrails is the ever increasing propulsive efficiency of jet aircraft [21]. Overall, future engine technology is likely to only increase contrails.

Generally, operational strategies seem to give much more promising results than the previously mentioned ones. Since contrails require relatively cold and humid air (like often seen in ISSRs) aircraft can prevent contrails from forming by simply avoiding air that has these properties. Implementation of such avoidance strategies depends heavily on the shape and locations of ISSRs, which are reported as flat and widespread [69, 5], similar to the shape of a pancake. The thickness is typically around 200-500 meters [69]. Over 80% of ISSRs have a thickness less than 1500 meters and about 30% are less than 100 meters thick [70]. The horizontal size is more difficult to measure, however by measuring the length of the path of flights that traverse these areas an estimate can be made. Gierens shows that the average path is 150-250 kilometers in length [71] indicating that the horizontal dimension is much larger than the vertical one. Other research generally confirms this.

Given the shape and size of areas that are prone to contrails it should come as no surprise that changing altitude is an often proposed strategy. This comes in three basic variations, namely global altitude restrictions, local and temporal altitude restrictions and changes to the altitude of individual flights [21]. In the first category Fichter showed an almost linear relation between lowering cruise altitude and contrail reduction [35]. Contrails were found to decrease by 1% with every 133ft (40m) altitude reduction until 6000 ft (1830m) with a reduction of 45%. A 2000ft (610 m) rise was found to increase contrails by 6%. Williams investigated a monthly revision of the maximum flight level above Central Europe. The study suggests an increase of 4% fuel consumption as a consequence and increased air traffic controller workload [45]. Flight times were not significantly impacted in most cases. Williams shows that an overall cruise altitude decrease over the US and North-Atlantic would likely not counteract the corresponding increased CO₂ emissions [72]. Mannstein shows that it is more effective to change altitude once an ISSR is encountered compared to general altitude changes [5]. As can be seen in Figure 3.3 the probability of creating contrails could potentially be decreased by over 80% using less than 2000ft (610m) altitude changes if there is information on the ISSR geometry available and over 50% in case there is none. Soler confirms the effectiveness of altitude changes by showing increased fuel consumption in the order of 3% when taking into account contrail cost compared to purely operational cost optimization [6]. Flights between 12 city pairs in the United States were found to be able to reduce the time they fly through contrail prone regions by 70% at the expense of 2% additional fuel burn [7]. Klima shows that at the expense of -10 to 5 % of operating cost approximately 45-75% of contrails could be mitigated [8]. In case of a custom reroute that minimizes fuel 55-85% of contrails could be mitigated at the expense of 0.5-1.0% increased flight time and 2.5-3.5% increased fuel burn. Campbell shows a contrail decrease of 50% at 1.48% additional fuel burn and 100% at 6.19% increased fuel consumption [9]. Hendriks shows that 90% of contrails can be mitigated at less than 1.5% increased fuel consumption [1].

What remains however is a practical strategy that airlines can implement. Flight planning and operational constraints are hardly ever considered. Even though studies show great potential they are based on specific situations and often impractical assumptions, not even to mention operational considerations (e.g. neglecting Air Traffic Control or airspace structure). Actual flight planning algorithms in combination with an altitude change strategy for contrail mitigation are the missing link to estimating practical implications.

3. Environmental Impact

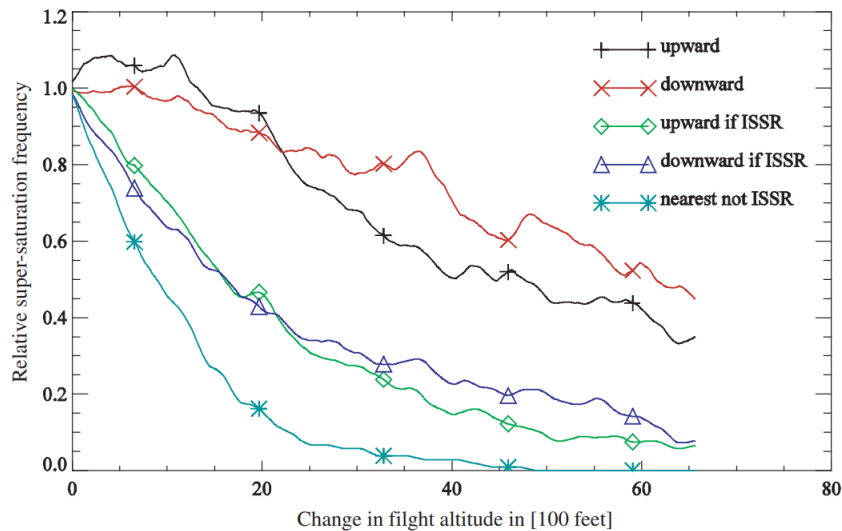


Figure 3.3: Probability of flying in ISSR after various altitude change policies [5]

3.4 Metrics of climate impact

This section covers various metrics that can be used to estimate and draw conclusions on climate impact. There are many ways of looking at a complex system like the Earth's atmosphere and even more ways of trying to quantify the impact of contrails and other aviation related phenomena. One could simply consider the physical metrics that can be evaluated by measuring (e.g. CO₂ released) or use more elaborate physical model based metrics. Moreover, metrics that assess softer criteria such as economic impact and thus more difficult to objectively quantify are also proposed. As there is something to say for all methods, picking a metric is often a matter of choice. The overview given here should make the choice easier and more informed by making the reader aware of some of the strengths and weaknesses of these metrics. This chapter will cover both methods that can be used in a flight planning algorithm as well as metrics that might be difficult to use in practice but have an interesting angle on evaluation of human induced climate change. It should be noted that there are also metrics that are not described here for practical reasons. The metrics that are however discussed in Section 3.4 are listed below [50, 73].

- Radiative forcing
- CO₂ equivalent
- Global Warming Potential (GWP)
- Global Temperature (Change) Potential (GTP)
- Mean Global Temperature Potential (MGTP)
- Global Damage Potential (GDP)
- Monetary cost
- Welfare

Radiative forcing is the measure used by the IPCC [46] and many others [50]. As mentioned it measures a gas' ability to influence the energy balance of the atmosphere. In other words, it determines how much energy from the sun is absorbed and how much is radiated out from the earth to space. It is arguable the most direct way of comparing the effect of different emissions

on the climate. It is clear that for aviation this metric is desirable as emissions are in gaseous form and through radiative forcing can be compared with relative ease. For other applications however (e.g. deforestation) it is much more difficult to use. Radiative forcing does not include thermal inertia of the system.

CO₂ equivalent is another way to create a common measure of emission. When looking at Figure 3.1 it can be seen that in this case direct emissions and radiative forcing components are translated to one of the primary direct emissions. Given the focus on this gas in global warming discussions to many it "feels" like an appropriate metric. It should be noted that there are some difficulties translating between quantities as with most metrics. By choosing a metric that requires both the relation between CO₂ and climate impact and the subject it is compared to with respect to climate change, one essentially introduces a double potential error. Based on the current or historic price for CO₂ emissions as listed for the Emissions Trading System the quantity of gas can be transformed to a monetary value. The cost of emissions in monetary units are also a possible metric. It should be noted that a transformation from CO₂ equivalent is only one of many ways. The cost as given in the ETS is supposed to represent a measure of societal cost, however the question remains whether this is actually the case. Price have ranged from 1 euro per ton CO₂ in March 2007 to almost 30 in July 2008 and are currently around 5.

Global Warming Potential (GWP) was adapted from the IPCC's second assessment by the Kyoto Protocol as a way of comparing the climate effect of different gasses [74]. The formal definition is that GWP is the cumulative of the radiative forcing between the moment of evaluation and a chosen time horizon caused by the emission of a unit of gas now, compared to that of a reference gas [75]. The Kyoto Protocol typically used CO₂ as a reference gas. The key element here is the time horizon. Typically 100 years is used however other horizons have been used as well (e.g. 20, 200 or 500 years) with sometimes considerably different implications for policy makers. It should be noted that compared to GTP and MGTP, Global Warming Potential uses radiative forcing as a proxy, whereas the others use temperature change which is much more difficult to predict [73].

Global Temperature (Change) Potential (GTP) was proposed as an alternative to GWP because the latter does not reflect the effect of emissions on global temperature nor does it relate to damages caused by them [76]. When looking at Figure 3.1 the relevance of impact increases as one moves down from direct emissions to damages. Therefore there was a desire for a metric that was more "relevant". This however also implies an increase in the required model complexity and dependency on assumptions. GTP exists in two forms, namely as the temperature change due to a pulse emission of gas and as a measure of the effect of a sustained emission [76]. The distinction is often indicated using a subscript (GTP_p and GTP_s). Instead of focusing on the cause of global warming it looks at the effect; temperature increases [50]. It does so by estimating the influence of emissions by combining the change in radiative forcing (ΔRF), the heat capacity of the system (C) and a climate sensitivity parameter (λ) on the mean surface temperature (ΔT). The formal solution of the GTP can be seen in Equation (3.1) [76]. Just like GWP it requires a predefined time horizon over which emissions are evaluated.

$$\Delta T(t) = \frac{1}{C} \int_0^t \Delta RF(t') \exp\left(\frac{t' - t}{\lambda C}\right) dt' \quad (3.1)$$

3. Environmental Impact

Mean Global Temperature Potential (MGTP) was introduced by Gillett as an alternative to GWP and GTP [77]. In essence it is simply the time integrated version of the GTP. The main advantage is that MGTP changes much less strongly for different time horizons. This of course makes it easier to compare different horizons. It was shown that the ratio of MGTP between CH₄ or N₂O to CO₂ over 100 years is very similar to the ratio of the temperature responses [77]. Compared to GTP which puts relatively strong emphasis on initial emissions, MGTP divides weighting of impact much smoother [73]. This implies that the latter puts less emphasis on relatively temporary phenomena such as contrails and more on long term effects like increased CO₂ levels.

Global Damage Potential (GDP), also referred to as Economic Damage Index (EDI) is a socio-economic metric [78]. This means that rather than looking at climate change at a physics level it goes all the way to the bottom level of Figure 3.1 and aims to quantify the social and economic damage caused by emissions. In essence it is the sum of discounted future economic damages. It is clear that the relation between these damages and the emission of a unit of greenhouse gasses is difficult to establish. This means that compared to the previous metrics, it shows a high level of uncertainty and dependency on assumptions. Therefore and due to the fact that the previously mentioned metrics are much more widely used it seems unlikely that GDP is a suitable metric for trajectory optimization algorithms that include contrail mitigation objectives.

The final two metrics that are discussed are monetary cost and welfare. As one can imagine these are difficult to quantify and therefore not likely to be used in trajectory optimization. Even though the translation of CO₂ equivalents through the ETS seems inviting, prices are not stable enough for long term predictions. If an accurate model was available it would be more desirable to be able to express the impact of emissions in terms of financial cost or welfare. These metrics are the most relevant and may even create an increased sense of urgency but the reality of their widespread use seems far away.

CHAPTER 4

FLIGHT PLANNING

Chapter 4 aims to describe the practical side of implementing trajectory optimization methods in a real life scenario. Airlines make use of flight planning to do so. Section 4.1 introduces some key concepts and rules and regulations as well as describing the process of planning a flight. Section 4.2 gives an overview of key players in the business of flight planning.

4.1 Modelling flight planning

Flying a commercial aircraft is not like driving a car. The pilot does not have full autonomy in deciding when and how to fly, nor does he decide how much fuel is necessary to get to the destination. Instead, a flight plan has to be submitted before each flight, specifying details about it like aircraft type, the estimated weight and time at a set of waypoints from departure to arrival, potential alternative landing sites etc. This document needs to be approved by the aviation authorities before departure. For the US this is the FAA. For flights into, around or out of Europe the flight plan needs to be submitted to Eurocontrol.

There are a number of parties involved with the flight planning process and subsequent flight execution. The most relevant parties that bear responsibilities and that have influence on key flight parameters are the following:

- Airlines - Plan flights, submit flight plan and subsequently execute flights. Generate optimal path based on fuel and time (and environmental) cost while respecting practical constraints as much as possible
- Airports - Facilitate ground support and CNS equipment including ILS and lighting systems. Need to approve take-off and landing rights of in- and outbound flights
- Air traffic control - Control air traffic in a specific three dimensional area. Ensures separation and efficient movement of aircraft under their responsibility. May refuse or delay flights or alter path in case of overloading
- Aviation authorities - Are the regulator of the aviation industry. Set and maintain standards, rules and regulations and enforce them to guarantee mainly safety as well as fairness, security and environmental improvement. Need to approve flight plan before execution

Flights follow a certain procedure from takeoff to landing. The most basic phases of any commercial flight is takeoff - climb - cruise - descent - touch down. The typical flight phases as

4. Flight Planning

described by Belobaba [79] can be seen in Figure 4.1. It should be noted that most research in contrail avoidance is concerned with situations similar to the cruise phase (high speed, horizontal, high altitude flight). For flight planning it is important to know exactly how the three dimensional routes that commercial aircraft fly are generated. Some airports only have a single runway, however others may have multiple. Amsterdam Airport Schiphol for example has six runways whose use is dependent on various conditions. As a consequence during flight planning it may not be certain what runway flights will use. After takeoff, flights will have to follow a departure procedure named Standard Instrument Departure (SID). The SID is a standard route that describes the aircraft path from the end of the runway to a waypoint from which it can continue the intended path, usually via an airway. Waypoints are three dimensional locations that are historically based on the location of a navigational aid such as a VOR or NDB. Waypoints are often used as the intersections between highways in the sky. They connect airways through which aircraft find their way from one airfield to another. From the moment the aircraft exits the SID the route is defined from waypoint to waypoint. These are predefined and are indicated using a 5 letter code. In case there is no airway connecting them it is possible to fly directly between them using the indication DCT in the flight plan. Otherwise the airway name would be used. In case no suitable waypoint is available it is also possible to manually pick a location and include it in the flight plan by using its latitude and longitude (e.g. 51N2959 003E3715 which is in Middelburg, Netherlands). In any case, the location of each waypoint is included in the flight plan. An example route from Schiphol to Gatwick could be routed as such: EHAM→EH195→GORLO→RATLO→DET10→EGKK. This includes both airways and non-airway (DCT) connections. Figure 4.3 shows an example airway structure above Brazil. The ground track is created from a combination of airways and waypoints as can be seen in this figure. At each waypoint the estimated distance, time and fuel consumption is given along with their cumulative values (or remaining in case of fuel). When the aircraft is getting relatively close to the arrival airport it will follow another predefined path from the final waypoint to touchdown called Standard Terminal Arrival Route (STAR). An example completed flight plan is shown in Figure 4.2.

The flight planning software uses a set of inputs to generate a path that is both feasible and optimal with respect to fuel and time cost. It does so by generating a route that minimizes direct variable operating cost including fuel cost, navigation charges, variable crew cost, variable maintenance costs, airport charges and delay costs [80]. A feasible path determined by the available waypoints and airways between them and SID and STAR of origin and destination airport. Using aircraft performance parameters, air traffic control requirements and other operational and practical constraints the flight plan is generated and submitted. After approval the pilot uses it to execute the flight.

4.2 Current tools

Given the legal requirement of filing a flight plan and the potential benefits of optimizing routes, airlines make extensive use of flight planning software. This is either developed internally or by specialized firms who provide the software or service. Due to the investment involved with developing such software, not much information is available about the internally developed packages. It is however clear that airlines have a choice between a set of externally developed packages if they are willing to pay for it. Provided in Table 4.1 is a list of systems that larger airlines use [83].

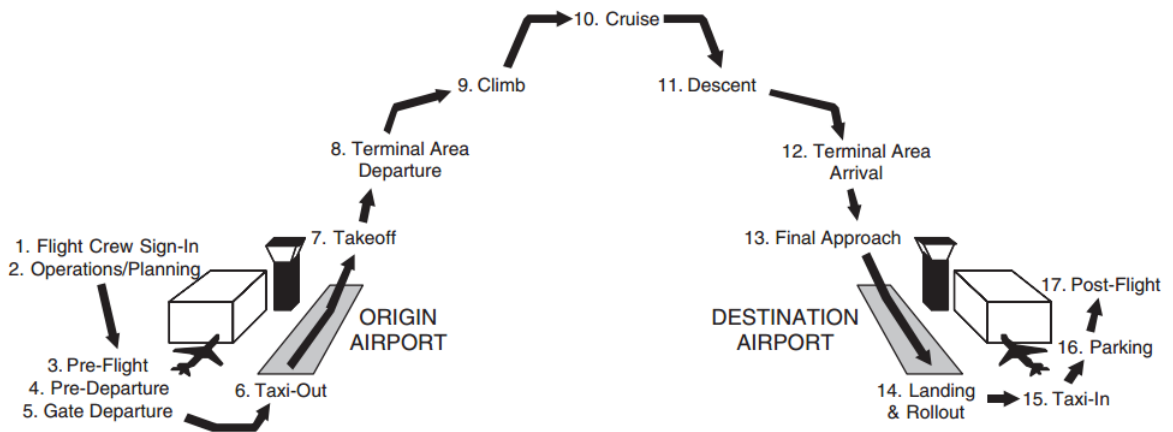


Figure 4.1: Typical flight phases [79]

Department of Transportation Federal Aviation Administration		International Flight Plan	
1 MESSAGE: <<= FF ->> 2. ADDRESS(S): EHAZQZX EBURZQZX EDDYZQZX LFFZQZX LFRZQZX LFBZQZX LECMZQZX LPFCZQX			
3. FLIGHT TIME: 190836 4. ORIGINATOR: EHAMZPX			
SPECIFIC IDENTIFICATION OF ADDRESSEE(S) AND/OR ORIGINATOR			
1 MESSAGE: <<= FPL 2. NUMBER: 1 3. DEPARTURE AERODROME: EHAM 4. CRUISING SPEED: 0830 5. LEVEL: F290 6. AIRCRAFT IDENTIFICATION: ACFA02 7. TYPE OF AIRCRAFT: EA30 8. WAKE TURBULENCE CAT: H 9. FLIGHT RULES: I 10. EQUIPMENT: SC 11. DEPARTURE TIME: 0940 12. ROUTE: LEK 2B LEK UA6 XMM/MO78F330 UA6 PON URION CHW UA5 NTS DCT 4611N00412W DCT STG UA5 FTM FATIMIA			
13. DESTINATION AERODROME: LPPT 14. TOTAL SET: 0230 15. ALTN AERODROME: LPRR 16. 2ND ALTN AERODROME:			
17. OTHER INFORMATION: REG/FBVG SEL/EJFL EET/LPFC0158			
SUPPLEMENTARY INFORMATION (NOT TO BE TRANSMITTED IN FPL MESSAGES)			
18. ENDURANCE: E/0345 19. PERSONS ON BOARD: P/300 20. SURVIVAL EQUIPMENT: POLAR [X], DESERT [X], MARITIME [M], JUNGLE [X] 21. DINGHIES: D/11 22. CAPACITY: 330 23. COVER: C 24. COLOUR: YELLOW 25. AIRCRAFT COLOUR AND MARKINGS: A/WHITE 26. REMARKS: X/ 27. PILOT-IN-COMMAND: C/DENKE		28. EMERGENCY RADIO: R/U, V, E 29. LIGHT: J/L, F, X 30. FLOURE: X, X	
FILED BY: AIR CHARTER INT.		ACCEPTED BY: ADDITIONAL INFORMATION:	

Figure 4.2: Example flight plan [81]

4. Flight Planning

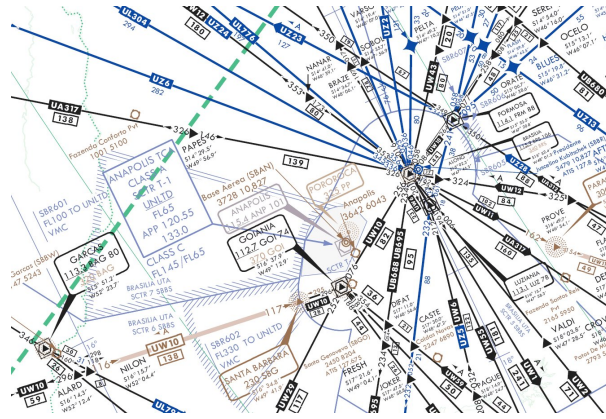


Figure 4.3: Example airway structure above Brazil [82]

Table 4.1: Overview of selected flight planning software

Name	Company	Client airlines
AirCentre FLight Plan Manager	Sabre Airline Solutions	18+
AIRCOM FLightPlanner	SITAONAIR	2+
AirPlan4	AirData	4+
CTO Flight Planning	Skyplan	n.a.
FLightkeys 5D	Flightkeys	n.a.
Jeppesen Dispatch Control	Jeppesen	n.a.
JetPlanner	Jeppesen	4+
Lido/Flight 4D	Lufthansa Systems	120+
N-Flight Planning	NAVBLUE	10+
NOTAM filtering (YOUNOTAM)	ACFTPERFO	n.a.
PPS - Preflight Planning System	Air Support	8+
Smart NOTAM MANAGER	Smart4Aviation	n.a.
SOAP Development	Jeppesen	n.a.
WSI Fusion	WSI Corporation	n.a.

As can be seen in Table 4.1 one of the most widely used tools for flight planning is Lido/Flight 4D, currently in use by over 120 airlines worldwide including KLM, Air France, China Southern, Emirates, Norwegian Air Shuttle and Wizz Air [83]. It was developed by Lufthansa Systems GmbH and supports the dispatch process of the airline using it. It does so by taking into account air traffic, air spaces, weather and aircraft performance parameters and generates an optimized flight route for each individual flight. It provides dispatchers with options for minimizing fuel, flight time or (operating) cost of the flight. Unfortunately not much information is publicly available about the methods and data Lido/Flight 4D uses. Just like other flight planning tools it uses public data like the Aeronautical Information Publication (AIP) and Route Availability Document (RAD) as well as information concerning SIDs and STARs. For aircraft performance it could use BADA data which is often used for this purpose, although this cannot be confirmed from public data. Further investigation is required for scientific tools in contrail mitigation studies to accurately emulate commercial tools.

CHAPTER 5

MODEL DEVELOPMENT

The flight plan as generated and simulated in this thesis consists of a set of scripts. The various functions and sequence are explained in this chapter. Together these form a model which is verified as presented in Chapter 6. Scenarios that are evaluated are presented in Chapter 7. Results obtained from these various simulations are elaborated on in Chapter 8.

The model can be divided into several subjects that each need to be solved for a flight plan to emerge. Given the complexity of the problem and dependency of current ideal state on many previous and future parameters there is a need for simplification. Section 5.1 describes the general approach through which the flight plan and simulation is achieved. The equations of motion used herein are introduced in Section 5.2. The decision has been made to initially separate the flight plan in 1) a ground track which finds a sequence of navigational aids that dictate the path of the aircraft over the surface and 2) a flight profile that describes the velocity and altitude of the aircraft at a given mass along the ground track. These are described in Section 5.3 and used to form an integrated 4-D flight plan. It should be noted that the first two stages generate what is the input for the ideal flight path, however actual simulation of the entire flight does not occur until integration takes place. Of course the flight plan would not be useful in a realistic scenario if it relied on a standard atmosphere rather than actual realistic atmospheric data. Section 5.4 elaborates on the incorporation of numerical weather predictions in the model. Given that the objective of this thesis is to determine the potential of contrail mitigation in a flight planning setting there is an obvious need to assess whether contrails occur under given conditions. Section 5.5 describes the contrail prediction module in more detail. Finally, contrail mitigation in both ground track and velocity-altitude profile is achieved by identifying contrails along the track and avoiding areas where they form. Mitigation processes for these are presented in Sections 5.6 and 5.7.

In summary, the subjects that make up the contrail mitigating flight planning model are discussed in this chapter. It starts with the approach and equations of motion after which each sub-process is elaborated on. Atmospheric data, contrail prediction and mitigation action are finally described.

5.1 Approach

As mentioned, due to the complexity of modelling high fidelity aircraft trajectories and dependencies on previous and future states some simplification is required. This is done by first generating a ground track, after which simulation of a flight along pre-processed optimal cruise

5. Model Development

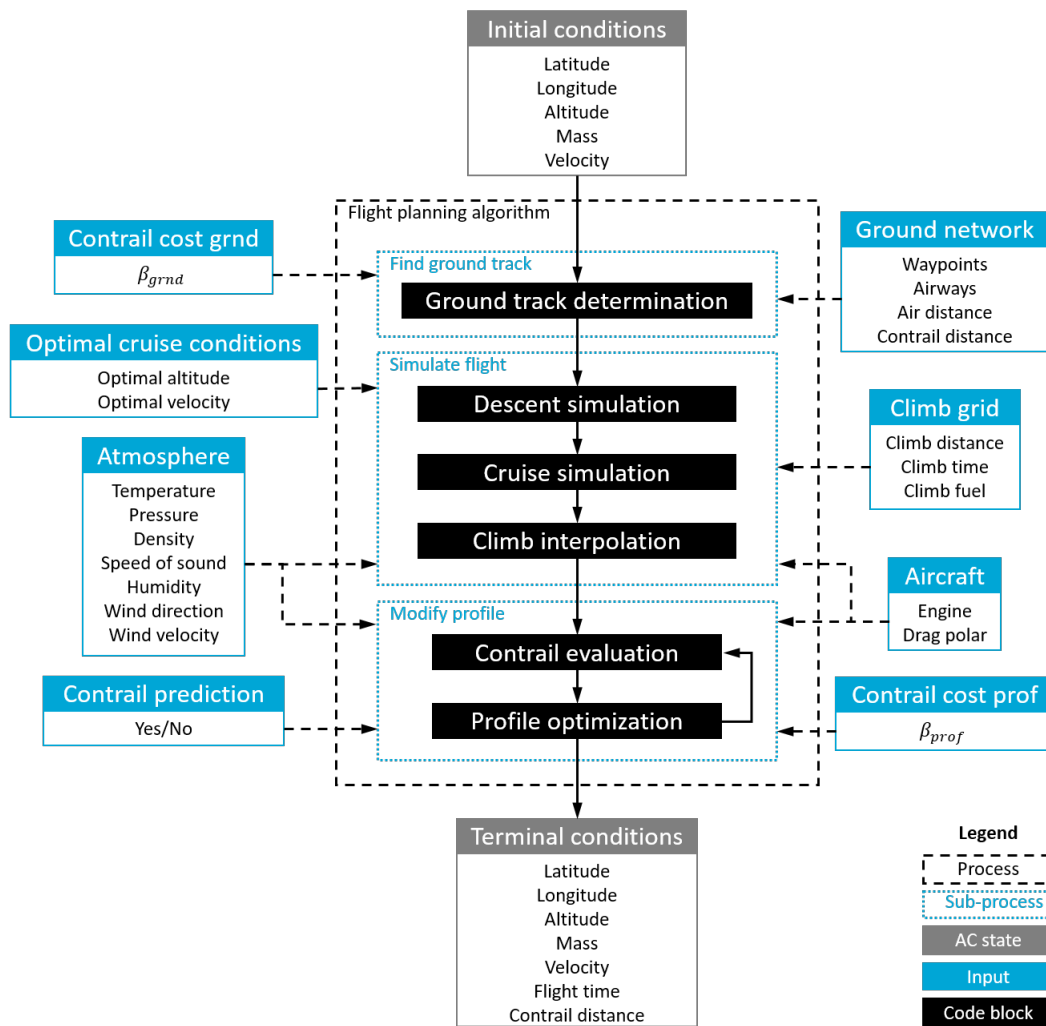


Figure 5.1: Schematic representation of flight planning algorithm

altitude and velocity yields the final trajectory. The flight is simulated backwards due to the fact that the landing weight is known whereas the take-off weight depends on how much fuel is required for a certain flight. Mitigating contrails along the way is possible at two moments in the planning algorithm. The first is during determination of the ground track. By including the contrail distance along each edge a ground track can be found to go around contrail areas. The second moment is after simulation of the non-mitigated flight by modifying the altitude profile for regions where contrails will form. A schematic overview of the flight planning algorithm can be found in Figure 5.1. Here, all elements including input, initial state, final state and sequence of the processes that the algorithm goes through can be found. Sections 5.3 to 5.7 describe the component parts of the process in more detail.

5.2 Equations of motion

To model the aircraft behaviour a two dimensional point mass model was used. The point mass model that was selected is fairly customary in aircraft performance modelling. Also, because control and stability issues are outside the scope of this thesis and the computational effort they require, higher dimensional models are disregarded. Moreover, the aircraft spends very little time banking compared to the time it spends with its wings level. The bank angle is

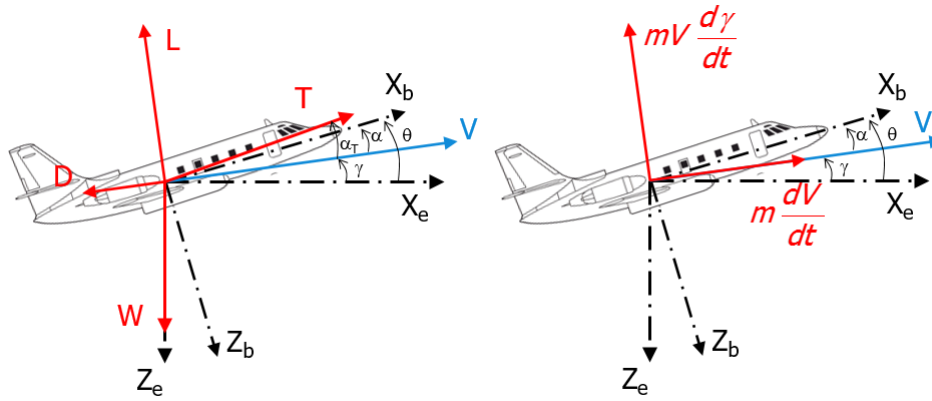


Figure 5.2: Free body diagram of forces acting on point mass and resulting acceleration

therefore disregarded in the point mass model which effectively changes it from three dimensional to two dimensional. A free body diagram of the forces acting on the point mass can be found in Figure 5.2.

The free body diagram in Figure 5.2 shows the forces acting on the point mass model and resulting acceleration. From this, the equations of motion can be derived as shown in Equations (5.1) to (5.4).

$$\dot{x} = V \cdot \cos\gamma \quad (5.1)$$

$$\dot{h} = -V \cdot \sin\gamma; \quad (5.2)$$

$$\dot{V} = \frac{T - D}{m} + g \cdot \sin\gamma \quad (5.3)$$

$$\dot{\gamma} = \frac{-L}{mV} + \frac{g \cdot \cos\gamma}{V} \quad (5.4)$$

The previous equations of motion are used to simulate the flight in climb, cruise and descent phase. However, due to ATC restrictions commercial jet aircraft are not allowed to follow a continuous climb profile during cruise. Instead, a combination of horizontal cruise and step climbs are used to approximate the optimal altitude profile as closely as possible. As a consequence of this the cruise phase simulation can be simplified even further. Due to the steady horizontal flight conditions that nearly the entire flight consists of, in this phase the flight path angle (γ) is assumed to be 0. This implies that the total lift is equal to the weight of the aircraft and the thrust is equal to the drag. As described in Section 5.3.2 the required thrust during the steps is adjusted to achieve a target climb rate.

5.3 Initial flight plan and simulation

As mentioned in Section 5.1 and shown in Figure 5.1 the sequence that the flight planning algorithm follows is first generating a ground track and subsequently simulating a flight along a pre-processed optimal altitude and velocity profile. This section describes how both ground track and optimal conditions profile are generated as well as briefly describing the aerodynamic and engine model.

5. Model Development

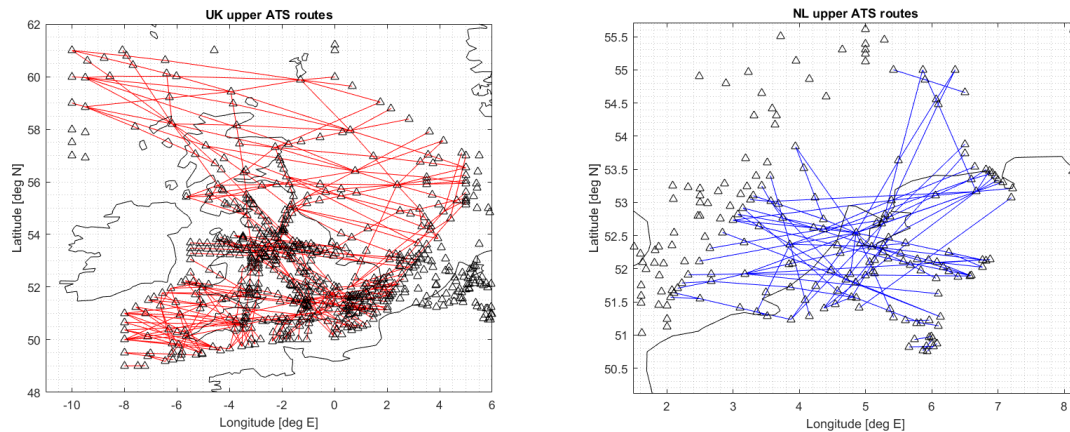


Figure 5.3: Upper ATS routes above the UK and Netherlands

5.3.1 Ground track determination

One of the factors that differentiates this thesis with respect to previous work is the degree of realism involved in creating the flight plan. Abiding existing airspace structure where possible in that respect adds greatly to the realism of the output. Given that this research focuses on transatlantic flight between the Netherlands and the US and Canada, there are some obvious regions such as in European airspace and above the North-East US where commercial air traffic is bound to a set of airways between navigational aids and fixes. Some areas however are less restrictive in horizontal and vertical navigation and allow airlines and flight crew to select their flight path more freely.

Traffic in European airspace is assisted and/or monitored by a regional Air Navigation Service Provider (ANSP) at lower altitudes or by Eurocontrol at higher altitude. In the Netherlands this is Luchtverkeersleiding Nederland (LVNL) and in the UK this is the Civil Aviation Authority (CAA). Each of these ANSPs provides a set of documents that describe relevant requirements, procedures and other information that pilots need to be aware of when flying in their airspace. Both make an Aeronautical Information Publication (AIP) publicly available in which airways that commercial airliners similar to those used in this thesis use, are described. More specifically, for cruise conditions it is assumed that aircraft above European airspace abide airways known as "Upper ATS routes". These routes are described in detail in both AIPs under section *ENR 3.2 UPPER ATS ROUTES*. Figure 5.3 shows the airways considered on the European side of the Atlantic Ocean.

Flights in airspace belonging to the US are monitored by the Federal Aviation Administration (FAA). Just like the European ANSPs it also provides an AIP. Figure 5.4 shows the airways considered in US airspace.

Flights that cross the Atlantic Ocean from Europe to the US and vice versa encounter long periods of time in which Communication, Navigation and Surveillance (CNS) is more difficult due to the distance from land based communication stations and nav aids. This increased uncertainty in both the own position and that of other nearby aircraft gave, in combination with the desire to keep airborne aircraft at a safe distance from each other, rise to the North At-

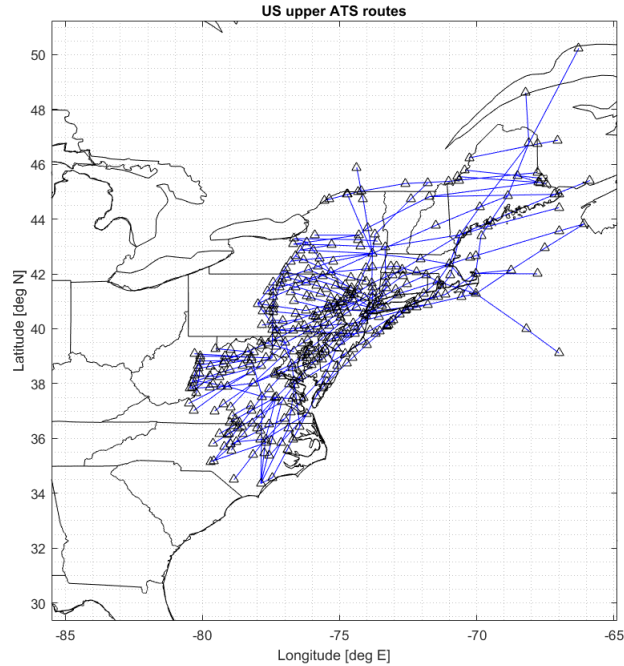


Figure 5.4: Upper ATS routes above North-Eastern United States

lantic Organized Track System (NAT-OTS). This system is aimed to ensure separation along the Atlantic crossing without the need for additional equipment. It does so by setting a number of ground tracks that define the track along which flights are allowed to cross the Atlantic Ocean. Approximately five to eight separate tracks are published daily for both eastbound and westbound traffic. These publications also state which flight levels are permitted on each track. Finally, a velocity constraint in combination with sufficient temporal separation between flights that enter the same track ensures separation. It is important to note that with every advancement in CNS technology these tracks become less necessary and therefore over-constraining of flights. Some claim that current technology no longer requires the NAT-OTS for adequate separation. It is therefore expected that in the near future, this system will become obsolete and free flight (to a certain extent) is allowed across the Atlantic Ocean.

As mentioned, the NATs are published daily by Shanwick Center (EGGX) and Gander Center (CZQX). These messages are formatted in such a way that flight crew and their equipment can easily read and use them. A database was composed containing all NATs dating January 27th, 2016 to January 27th, 2017. From this database, either a single track can be selected as input for the flight plan or the complete set of fixes used on any NAT in this period is used as a basis for transatlantic (semi-) free flight. These fixes create a grid between which virtual airways are defined. Since the majority of the fixes are arranged on north-south lines, it is assumed that westbound flights have a heading between 180 and 360 degrees (positive westward component at all times) and similarly for eastbound traffic. The resulting network gives enough freedom to ensure that every realistic option is possible while highly unrealistic scenarios, such as flying directly over a fix without it being part of the track, are avoided. As a rule, segments that respect the NAT perimeter, stay within a reasonable margin of the nominal flight direction and do not skip obvious fixes along the way are considered feasible.

5. Model Development

For many westbound NATs the ground track is followed by so called North American Route (NAR)s. These routes are an extension from the final fix of the NAT towards the North-American continental route system. Often a few NARs are listed as options which can be selected depending on ATC and airline preference. Descriptions of the NARs are provided by the FAA and processed. The database that was composed for the previously mentioned NATs is supplemented with the NAR routes and waypoints and similarly converted to a network of nodes and airways between them.

The NAT-OTS is only used in case flights cross the North Atlantic Ocean and through this leave the proximity of adequate ground based CNS equipment. Some transatlantic destinations that take a route closer to the North Pole therefore do not use the NATs. It should at this point be noted that although Canada does provide air navigation services including guidance and distribution of required publications, airways are much more sparsely located and flights are allowed much more freedom in their trajectory. In addition to that, Canada's ANSP (NAV CANADA) is a privately run corporation that does not provide public access to their publications but instead requires the purchase of these documents. To allow for the simulation of such flights, including to additional destinations halfway across the US-Canadian border (Winnipeg) and on the west coast (Vancouver) a set of fixes needs to be added. Careful consideration was taken of the route commercial air traffic uses to get from European origins to destinations in the Vancouver/Seattle area and vice versa. While applying a large margin of error around this area, a grid was created that allows the simulation of flights to Winnipeg and Vancouver. The grid was constructed by inserting virtual fixes on latitude-longitude intersections such as the 70°N and 40°W intersection. The grid expansion stretches from just north of the UK to Vancouver at 123°W and as high as 80°N . This allows the freedom that is required to explore potential contrail mitigation strategies, yet keeps computation time within practical limits. In the east-west direction NAT fixes are generally separated by 5° . This separation is also used for the additional fixed to the north of the NAT system and in Canadian airspace. In the north-south direction the resolution is much higher at 0.5° in the center of NAT regions and 1° closer to the north and south boundaries. The resolution of 1° was adopted for the additional fixes as well. By creating this additional grid on latitude-longitude intersections north of the NAT area and across Canadian airspace the missing AIP for these regions is replaced. Given the mentioned properties of the airspace it occupies and trajectories of commercial flights through it, it can be assumed that the grid provides sufficient flexibility and coverage to realistically model trajectories in this region. In short, Canada does not provide public maps so a grid was created to substitute it.

From the previous paragraphs it is clear that a network of airways is constructed that spans Western Europe and the North-Eastern US as well as across the North-Atlantic and Canada. What remains is to add the connecting edges between US and European airways and the grid created between them that spans the Atlantic Ocean. Similarly to the creation of the North Atlantic grid, as a rule of thumb segments that respect the area perimeter, stay within a reasonable margin of the nominal flight direction and do not skip obvious fixes along the way are considered feasible and added to the network. Figure 5.5 shows the final combined network topology.

As explained, a network of nodes and edges was constructed through which a ground track is found. This ground track is the basis over which an altitude and velocity profile is laid out

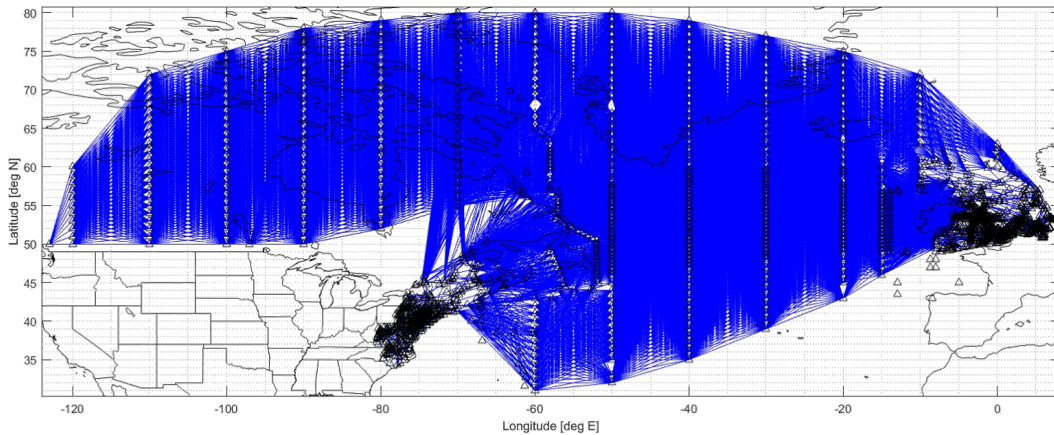


Figure 5.5: Complete Europe to United States network topology used for simulation

form a 4D trajectory. Before going into more detail how the edges in the network are weighed, it is important to note a few core properties that help determine which algorithms could be used to find the ground track. First, these edges are non-uniform. In a square grid where only up, down, left and right connections are allowed, each one has the same length. Given the topology of the airways and fixes, in combination with wind and other condition dependent variables this is not the case here. Second, assuming the aircraft never encounters wind speeds higher than its own airspeed, there are no negative edge weights. Based on this, it can also be concluded that there are no negative loops in the network. Third, the network has both bi- and unidirectional edges as some airways allow traffic in both directions and others do not. Given this network topology, cycles are possible though as mentioned they are never negative. Listed is a set of path finding algorithms. It should be noted that this is not an exhaustive list of every known path finding algorithm, but rather a shortlist of potential solution strategies to the problem to be solved.

- Dijkstra
- A*, fringe search, IDA*
- B*
- Bellman-Ford
- Floyd–Warshall
- Johnson’s
- Breadth-first search
- Depth-first search

One of the most well known algorithms is Dijkstra’s. It was conceived by Edsger W. Dijkstra in 1956 and has since been used on an enormous range of path finding problems. It has been further developed for specialized cases, some of which variants have been given separate names such as A*. In general, Dijkstra’s algorithm is one of the most reliable solution algorithms for arbitrary directed graphs with unbounded non-negative weights. This reliability and extensive documentation and validation in literature makes it a attractive option. Even though faster algorithms may exist, greedy, depth-first and other strongly steering strategies may fail to examine parts of the solution space, which decreases their reliability. After testing the input network using Dijkstra’s algorithm, it is obvious that time constraints for the 2D network is

5. Model Development

not an issue. Solutions spanning from the Netherlands to Vancouver take in the order of 0.05 to 0.1 second to generate. Application in the setting of this thesis does not require faster algorithms. Therefore its reliability and extensive validation in literature is the leading reason for selecting Dijkstra's algorithm for finding the optimal ground track.

Dijkstra's algorithm works by keeping track of a number of lists and sequentially checking nodes and distance to their connecting nodes. There is a "current" node, list of visited nodes and list of unexplored nodes. Each node has an initial distance of infinity from the origin. The initial "current" node is the origin node with obvious distance of zero to the destination. At each iteration, each node connected to the "current" node is checked. If the sum of the distance from the "current" node and edge weight is smaller than the listed distance of that node, it is replaced. Otherwise the smaller distance is kept. The "current" node is then added to the list of visited nodes and the unexplored node with the smallest distance is set as the new "current". Once the destination node is the "current" node the algorithm can be stopped. This procedure can also be listed as a set of steps as often seen in elaborations of how algorithms work.

1. Assign distance of infinity to each node except 0 for starting node
2. Set current node to starting node. Create list of unexplored nodes containing all other nodes.
3. For the current node, consider each neighboring node and calculate its distance from summing the edge cost and distance of current node. If this distance is smaller than the distance the node already has assigned, replace it. Otherwise keep the original distance.
4. After considering each neighbor, add current node to visited list. From the list of unexplored nodes, select the one with the lowest distance and set it as new current node.
5. If the current node is the destination node or if the lowest distance in the the unexplored list is infinite the algorithm is stopped.

In order for the Dijkstra algorithm to find an optimal path that corresponds to the real life scenario, it needs an adequate network topology as input as well as the cost incurred on each edge. In many types of problems the ground distance is a great way to find an optimal path. When the distance along each segment is used as edge cost in the ground track network, the solution of the Dijkstra algorithm closely resembles a great circle arc between origin and destination. This path is literally the shortest path one could take in terms of meters traveled over ground. Unfortunately, just like a boat sailing across moving water, the optimal path of an aircraft is not given by the shortest ground distance. Instead, the ideal path of an aircraft can be defined as the path along which the minimal distance is flown through air. In other words, instead of flying the shortest path over ground against the wind or in stagnant areas, one tries to take advantage of wind that takes the aircraft towards its destination, even if it incurs additional distance traveled over ground. This balance can be found by changing the edge cost from ground distance to air distance.

The air distance on an edge is obtained by dividing it into smaller segments and applying the wind triangle method on each interval. Since the optimal airspeed V_{air} is given, along with the desired ground path angle α , the wind direction β and speed V_{wind} the cosine rule as shown in Figure 5.6 and Equation (5.5) can be used to obtain the resulting velocity over ground V_{ground} when flying from location A to B through a uniform wind field. B* indicates the location the

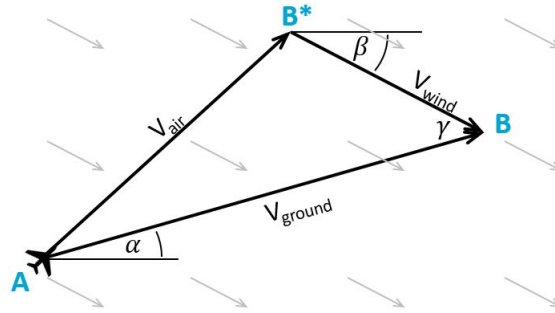


Figure 5.6: Wind triangle method

aircraft would fly to in case there was no wind. Due to the drifting effect in the wind though, it ends up at location B as desired. Division of the ground distance of the segment by the aircraft ground speed V_{ground} gives the time required to travel from A to B. During this period however, the aircraft travels a distance from A to B* through the air. Air distance on segment A to B is therefore given by the previously determined time it takes the aircraft to travel between those locations, multiplied by the aircraft's velocity with respect to air V_{air} during that time. Summing the air distances of all segments along an edge gives the total air distance between two connected nodes. Note that this distance is dependent on the direction of flight. Traffic that flies with the wind encounters less air distance compared to traffic that flies against it which implies that in a bi-directional connection between two nodes, two different edge costs are used.

$$V_{air}^2 = V_{ground}^2 + V_{wind}^2 - 2 \cdot V_{ground} \cdot V_{wind} \cdot \cos(\gamma) \quad (5.5)$$

Of course the previous assumes knowledge of the local atmospheric conditions and the optimal airspeed. When applying the International Standard Atmosphere there is no wind component, leading to air distances that are equal to the ground distance on that segment. Real life scenarios however do not feature a stagnant atmosphere. As is clear from Section 5.4 the atmosphere is a very dynamic system that can be described using a large set of parameters. Wind velocity and direction is not only dependent on latitude and longitude, but also on altitude and moment in time. As explained in Section 5.4 the temporal element is covered by the assumption of a single time step along which the simulation takes place. The optimal (pressure) altitude and airspeed of an aircraft however is dependent on atmospheric conditions and the aircraft mass. Section 5.3.2 goes into more detail as to how the optimal altitude and velocity are determined. Since they are a function of the aircraft mass and the mass is dependent on the to-be-determined trajectory an assumption has to be made.

Based on ISA an optimal profile is generated that relates an input aircraft mass and cost index to an optimal airspeed and altitude as can be found in Figure 5.9. Furthermore, verified data and range modelling shows the expected fuel consumption in realistic operations between each origin and destination airport. By using a linear extrapolation of this expected fuel required on a trip with respect to the ground distance to a node, an estimate of the aircraft mass at each node is obtained. From this mass along with an input cost index, the optimal velocity and altitude can be obtained from the ISA-based profile. Both mass and corresponding flight level estimates for a flight from the Netherlands to Washington D.C. (KIAD) can be seen in Figure 5.7. Note that some waypoints are not connected and therefore given a default weight

5. Model Development

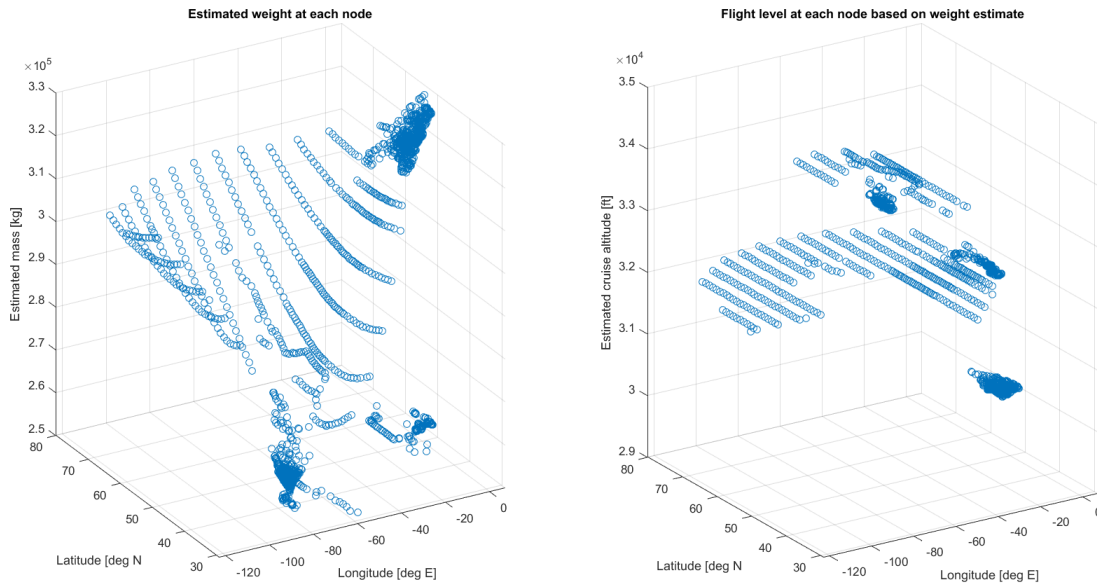


Figure 5.7: Mass and cruise altitude estimates for NL to Washington D.C. (KIAD) flight

equal to the landing weight. Since these are not connected to the rest of the grid, they are by definition never part of a track and can be disregarded. Simulation of various flights shows that the linear interpolation of mass along the track is in fact very reasonable as can be seen from Figure 8.4.

The final result of the ground track generation function on a track from the Netherlands to Washington D.C. can be seen in Figure 5.8. It shows the result of applying the Dijkstra algorithm to the edges weighted with in one case the ground distance and in another with the air distance. The first closely resembles a great circle arc as expected, while the second takes a more northern route to take advantage of wind direction and speed along the way. In this case the atmospheric conditions on February 12th 2014 were used to calculate the edges. It should be noted that the air distance is calculated using the estimate of cruise conditions that varies along the flight, whereas the wind arrows in the figure are of a single altitude only (250hPa) and merely provide the input to develop an intuitive understanding of the algorithm.

5.3.2 Optimal altitude and velocity profile

After generation of the ground track, the flight plan simulation is completed by following an optimum velocity and altitude profile. This profile is generated from local atmospheric conditions and the aircraft state. In short, local steady flight is simulated using models of the aircraft drag polar and engine characteristics. The subsequent cost of fuel and time on an interval is evaluated and by finding the minimum of the combined cost an optimum velocity and altitude is obtained. Section 5.3.2 describes the method and assumptions made to find the optimal cruise conditions

The altitude and velocity profile is generated using two steps. First, a solution is generated which respects the flight envelope. After this, a constraint is put on the altitude of the optimal solution. Intervals of 2000 ft are used to emulate level flight imposed by ATC restrictions.

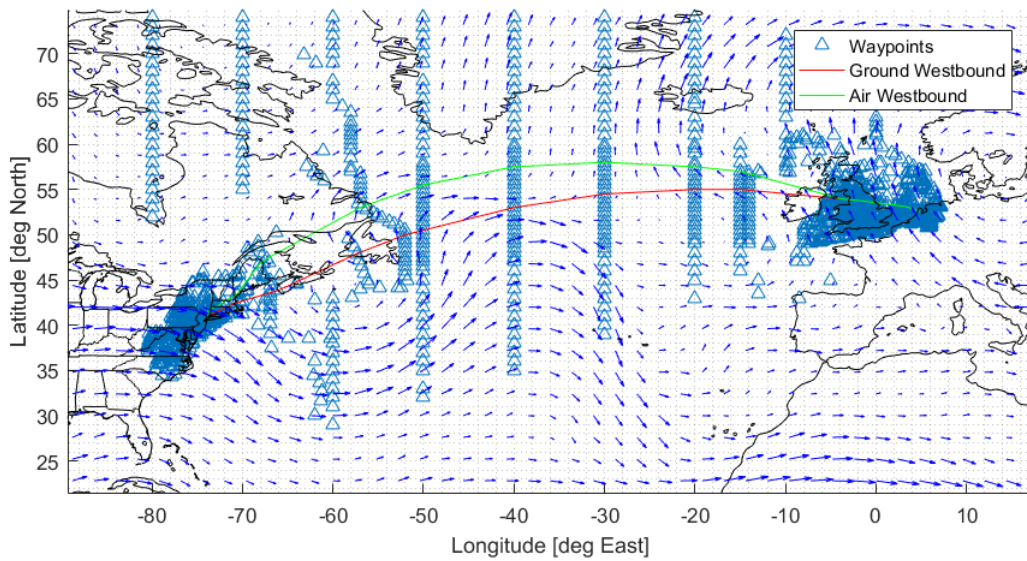


Figure 5.8: Ground track from NL to Washington D.C. (KIAD) in wind field at 250 hPa

Similar to this altitude restriction also a constant velocity on each flight level is required to accurately simulate ATC restrictions. The last step does just this by selecting the lowest velocity on each flight level and setting every solution associated with this altitude to this minimum velocity. An overview of the final profile is shown in Figure 5.9.

Profiles are generated by finding the optimal altitude and velocity for the aircraft to fly at given mass and cost index in steady horizontal cruise. Optimal is defined as the condition at which a cost function is minimized, keeping in mind a set of constraints. For the optimization routine, a built-in function is used. It minimizes an input objective function, while respecting linear and nonlinear constraints. The objective function to be minimized collects the unit cost along a kilometer of steady horizontal flight and a nonlinear constraint function is used to constrain the solution to a feasible region. To find the optimal cruise conditions both velocity V and altitude h are simultaneously optimized from initial point $V = 250$ and $h = 30000$. The solution is determined using a Sequential Quadratic Programming (SQP) algorithm with stopping criterion on the objective function and solution being 10^{-15} . Justification for these can be found in Section 6.2. The time required for each evaluation is approximately 0.5 seconds. Since the profile is constructed from linear interpolation along 50 points from minimum weight (m_{land}) to maximum weight (MTOW), the generation of a full profile takes in the order of 25-30 seconds.

Conventional flight computers use different values to weigh the cost of fuel and time. These variances are caused by the use of different units in Boeing aircraft compared to Airbus, as well as difference in individual airline strategies. To avoid picking one over another the cost was kept to a unit cost for both (1 monetary unit/minute and 1 monetary unit/kg). In all cases, a cost index of zero implies the most fuel efficient option and a large cost index a less fuel efficient though faster flight. From the input, local drag, thrust and fuel flow are determined for steady horizontal flight. Over a fixed distance (1 km), the time cost is determined by Equation (5.6) and fuel cost by Equation (5.7). The total cost is subsequently calculated by weighing the cost of time with the cost index as shown in Equation (5.8).

5. Model Development

$$Timecost = \frac{C_{time}}{60} \cdot \frac{ds}{V} \quad (5.6)$$

$$Fuelcost = C_{fuel} \cdot fuelflow \cdot \frac{ds}{V} \quad (5.7)$$

$$Totalcost = fuelcost + costindex \cdot timecost \quad (5.8)$$

In case the optimizer did not take various practical constraints into account, the output would be useless in a realistic flight planning scenario. Therefore a flight envelope constraint is taken into account. It restricts the solution space by setting three boundaries. Firstly, it restricts the velocity to a maximum. It does so by taking the maximum allowed Calibrated Airspeed (CAS) and Mach number and determining which results in a lower local True Airspeed (TAS). The most restrictive of the two is kept as maximum allowed velocity. Secondly, in a similar way to the maximum velocity, the minimum calibrated airspeed is converted and set as a boundary. Lastly, an operational service ceiling is defined by setting a minimum rate of climb that the aircraft should be able to attain of 500 ft/min. This climb rate requires a certain amount of energy to be converted to potential energy. The power required to attain this rate is assumed to be converted from surplus thrust. The equations used to construct this operational service ceiling can be found in Equations (5.9) to (5.11).

$$dE = m \cdot g \cdot climbrate \cdot dt \quad (5.9)$$

$$dThrust = \frac{dE}{V} \quad (5.10)$$

$$Thrust_{req} = D + dThrust \quad (5.11)$$

As mentioned, the unbound profile gives the optimal altitude and velocity for a range of aircraft weights. This profile however does not meet an important requirement for realism. Aircraft are bound to specific flight levels and as a consequence are not allowed to follow the continuous profile as generated. In order to obtain a profile that does meet the requirement of sticking to flight levels a second iteration is required. This takes the optimum input and determines the optimal velocity along both the flight level above and below the optimal solution with increments of 2000 ft. For example, if the optimal altitude is 31000 ft, the optimal velocity at 32000 ft (FL320) and 30000 ft (FL300) are found. The solution with the lowest cost associated with it is selected as the flight level bound optimal solution.

The final step in completing the optimal profile is the following. Reasoning similarly to the flight level constraint, ATC also requires aircraft to keep their velocity predictable. In practice this often means having a constant velocity between two step climbs. However, when introducing flight level constraints the solutions shows a larger change in velocity. Since variations in altitude are heavily restricted the velocity is optimized instead. This produces in some cases a pattern in the velocity plot that resembles a saw tooth between the location of two climbs. A more extensive elaboration on this can be found in Section 6.2.1. The solution to this is very simple. Because the highest velocity is not always attainable due to thrust constraints, the lowest velocity on a flight level is set for all segments associated with that altitude in order to guarantee feasibility of the simulation. It should be noted that velocity in this case refers to the mach number. The final profile with all three stages of its development is shown in Figure 5.9.

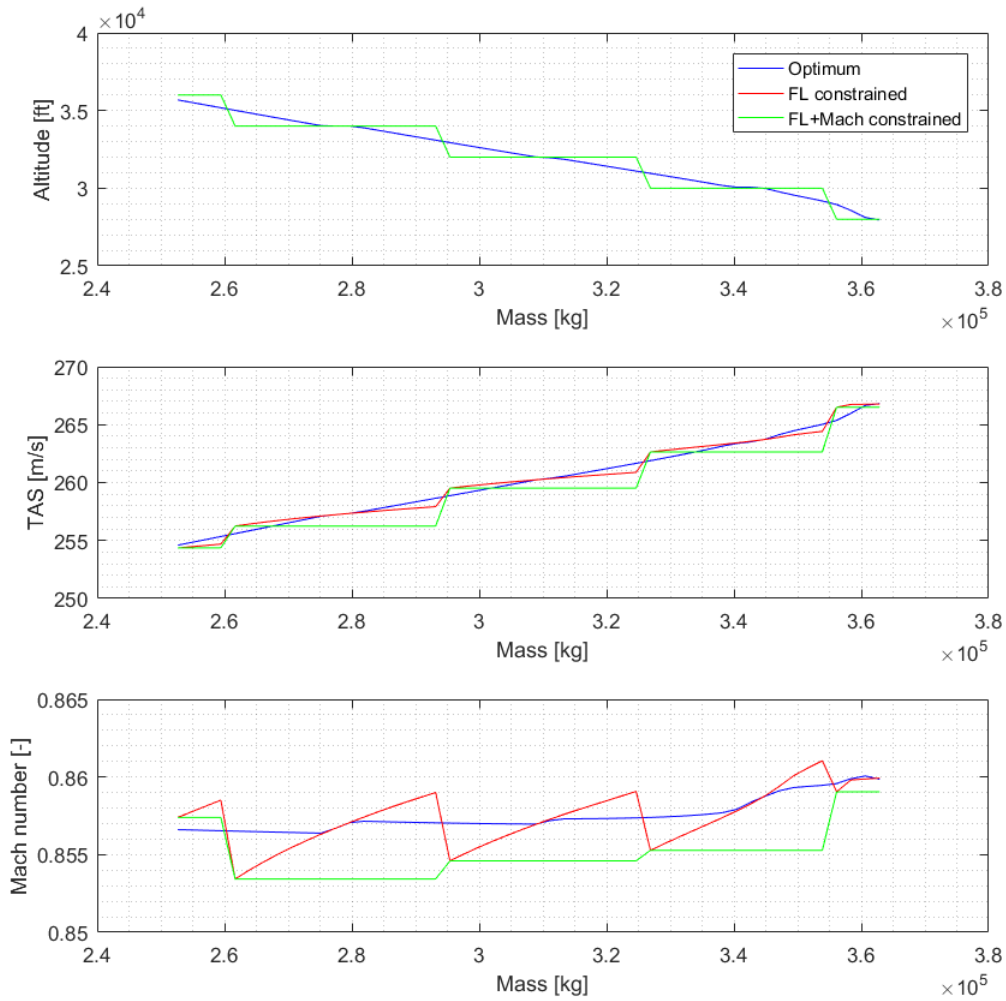


Figure 5.9: Altitude profile of unbound optimum, flight level constrained and flight level + Mach number constrained at $CI = 0$

The method of generating the altitude and velocity profile is elaborated. However, without accurate input from the underlying aerodynamic and engine model this has no value. That is why the following goes into more detail regarding the models used to approximate the aerodynamic drag and engine thrust and fuel flow in a given condition.

The aerodynamics are modelled by taking the mass, velocity and position of the aircraft and determining the aerodynamic drag associated with steady horizontal flight under these conditions. In case the latitude and longitude are not given, ISA is used to determine local atmospheric conditions. Otherwise local atmospheric properties from the NWP data are used. From the assumption of steady horizontal flight, the lift coefficient is determined as shown in Equation (5.12). An aerodynamic model is used to obtain the drag coefficient from an input lift coefficient and Mach number. From a grid of nodes, linear interpolation is used to obtain values for the complete domain. Figure 5.10 shows an overview of the domain and corresponding drag coefficients. Section 6.1.2 goes into more detail on this model. The drag is calculated as can be seen in Equation (5.13).

5. Model Development

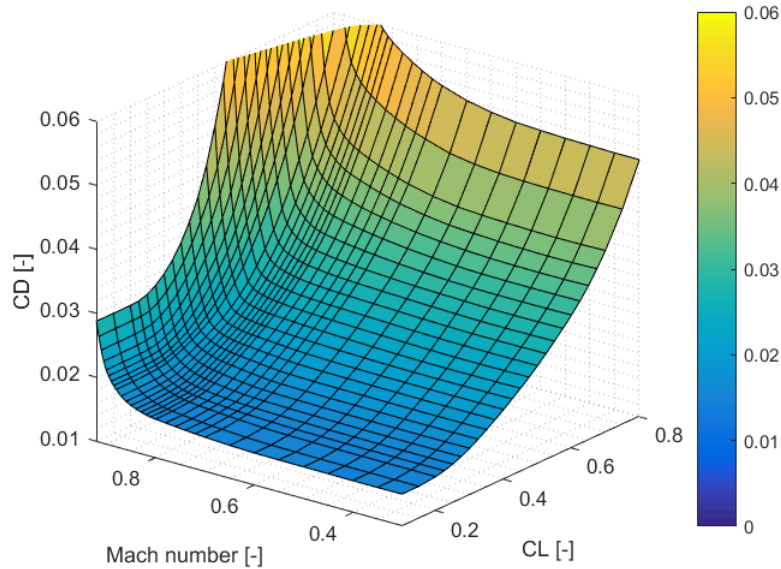


Figure 5.10: Drag polar used to model aerodynamic behaviour

$$C_L = \frac{L}{\frac{1}{2}\rho V^2 S} = \frac{m \cdot g}{\frac{1}{2}\rho V^2 S} \quad (5.12)$$

$$D = \frac{1}{2}\rho V^2 \cdot S \cdot C_D \quad (5.13)$$

The engine model used to simulate the thrust and fuel flow in any given conditions exist in two forms. One uses the throttle setting from 0 to 100% to calculate the thrust and fuel flow. The other one uses a desired thrust to determine the corresponding throttle setting and fuel flow. Linear interpolation between the maximum and minimum thrust gives the throttle setting and vice versa. Both minimum thrust, maximum thrust and fuel flow are obtained from linear interpolation of data from a performance database. Given that the database covers all regions that can be expected in an operational context, extrapolation of any kind is not considered. The maximum thrust in Newton and fuel flow in kg/s is shown in Figure 5.11.

5.3.3 4D trajectory simulation

Sections 5.3.1 and 5.3.2 cover the generation of the ground track and ideal altitude and velocity to keep while flying this track. The two do need to be integrated for a full 4D flight plan to emerge. This integration is attained by simulating a flight that follows the track and profile, with additional climb and descent stages and step climbs incorporated. By doing so, a final flight plan is created which both follows a trajectory close to, or optimal and is operationally feasible.

The amount of fuel an aircraft takes on board before departure is heavily dependent on the flight which is to be performed. Since a heavier aircraft requires more lift to stay airborne, it generates more drag, which in turn requires more thrust and thus a higher fuel consumption. Too keep the fuel consumption to a minimum it is therefore necessary to keep the aircraft as

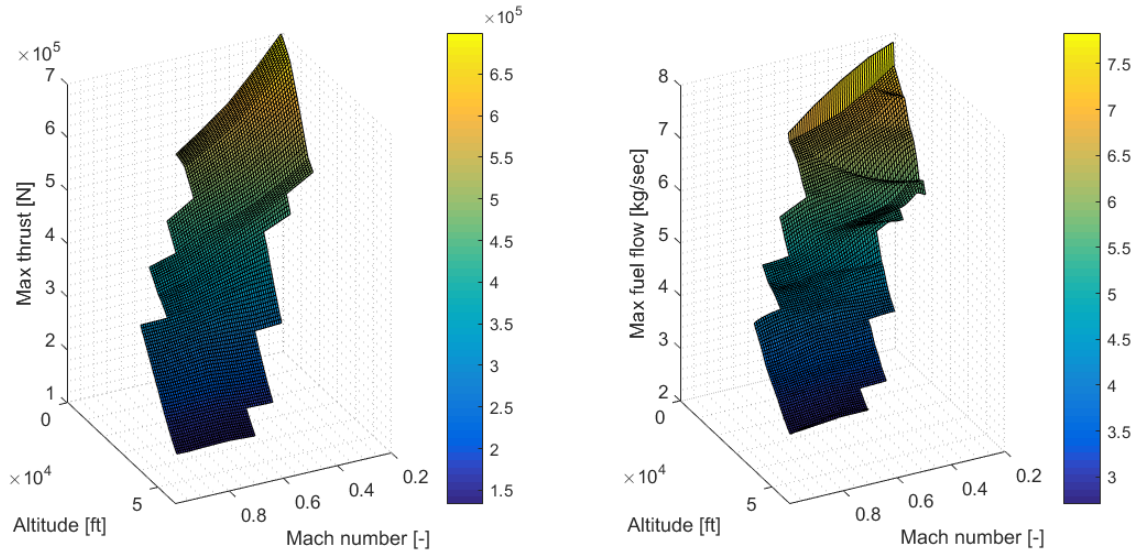


Figure 5.11: Max thrust in Newton and fuel flow in kg/s used to model engine characteristics

light as possible. One of the easiest ways to do this is by taking on as little fuel as possible (or allowed) to complete the journey. In practice this implies that the landing weight of an aircraft is known, since it has only a minimum amount of fuel left. Take-off weight however is not as predicable. For simulation purposes this has a major implication, namely, the flight is simulated backwards. Rather than forward integration in which fuel is subtracted from the take-off weight and one ends with the landing weight, the opposite is done. Backwards simulation means that the algorithm starts at a known end state. In this case at 15000 ft above the end node, at a fixed CAS. Backwards integration along the descent phase gives the state of the aircraft at the top of descent, at which point the cruise phase simulation is started. Using steady horizontal cruise segments and step climbs the cruise phase is simulated up to the top of climb, at which point the climb is evaluated and eventually the aircraft ends at 15000 ft above the starting node, at a fixed CAS.

The descent phase is initiated right above the end node at 15000 ft. The aircraft is assumed to have a throttle setting of 0% during the entire phase and maintain a velocity that corresponds to a schedule. By using throttle and velocity as a control, the glide path can be calculated and the descent trajectory simulated. The point mass model used for the calculations can be seen in Figure 5.2. The calculations corresponding to this figure, which form the backbone of the descent simulation are found in Equations (5.1) to (5.4) [84].

As mentioned, the cruise phase is simulated using two different modes. Either the aircraft flies at the flight level it is supposed to according to the optimal profile, or it requires a step climb to get there. In case the first is true, the input state is considered and the drag and corresponding thrust and fuel flow are calculated for steady horizontal flight. From backwards integration over the cruise phase and using a sufficiently small segment length, the total flight is simulated. It is important to note that the optimal conditions change not only with aircraft weight but also with latitude and longitude. In order to accurately follow the optimal conditions throughout the NWP based atmosphere a three dimensional grid (latitude, longitude and mass) was created from which these conditions can be retrieved. Section 6.2.2 goes into more detail about this grid. It should be mentioned that the 0.5 second evaluation time forces

5. Model Development

a trade-off between the grid resolution and computation time.

The second mode in simulation of the cruise phase is the step climb. If the aircraft is at a different altitude compared to the optimal conditions, this one is used rather than steady horizontal cruise. A target climb or descent rate of 500 ft/min is considered and converted into a thrust difference using the assumption that all potential energy is obtained from surplus thrust. Just like for the operational ceiling constraint, Equations (5.9) to (5.11) show the equations used to do so. In order to increase the accuracy of the fuel flow estimate, the fuel flow is evaluated at 60 intervals during each step and compounded. The fuel flow on this segment is evaluated and a new latitude, longitude, altitude and aircraft mass determined. By adding fuel flows over all segments the total fuel required for the step is found.

During simulation of the cruise phase, the aircraft gets heavier and closer to the origin of the flight. This creates an interesting situation. The climb phase of the aircraft is simulated in exactly the same way as the descent phase, except instead of 0% thrust, 100% is used. In order to end up exactly at 15000 ft above the origin node using backwards integration, the exact location of the top of climb needs to be known. Of course this is dependent on the altitude at which cruise is started, the velocity and most of all, the mass of the aircraft at the start of the climb. To solve this problem caused by backwards integration, the climb is simulated many times and the results stored to create a large matrix from which an accurate estimate of the starting position (top of climb), time and fuel required to execute this phase. Section 6.2.3 goes into more detail regarding creation of the climb matrix.

5.4 Incorporation of atmospheric data

The atmospheric model in which the simulation and optimization algorithms are conducted exist in two forms. Either the International Standard Atmosphere (ISA) is used or data is retrieved from a Numeric Weather Prediction (NWP) data set. The properties that are retrieved are the following.

- Pressure p in N/m^2
- Temperature T in K
- Air density ρ in kg/m^3
- Speed of sound a in m/s
- Relative pressure $\delta = \frac{p}{p_0}$ with no unit

The International Standard Atmosphere (ISA) is a standard for modelling atmospheric conditions. It defines the pressure, temperature and density across a wide range of altitudes in the earth's atmosphere. For accurate and reliable evaluation instead of using a data table, the underlying equations are used. Equations (5.14) to (5.18) show them written out completely [16]. These are valid in the troposphere and tropopause. This altitude range from 0 to 20km is more than enough in the context of commercial jet aircraft trajectory simulation. Figure 5.14 shows the development of the output values as the input altitude changes. It should be noted that $T_0 = 288.15$ K, $T_{11km} = 216.65$ K, $p_0 = 101325$ Pa, $p_{11km} = 22632$ Pa, $R = 287.15$ J/kg/K and $\gamma = 1.4$.

$$T = \begin{cases} T_0 - 6.5 \cdot 10^{-3} \cdot h & \text{if } h \leq 11km \\ T_{11km} & \text{otherwise} \end{cases} \quad (5.14)$$

$$p = \begin{cases} p_0 \cdot \left(1 - 6.5 \cdot 10^{-3} \cdot \frac{h}{T_0}\right)^{5.2561} & \text{if } h \leq 11km \\ p_{11km} \cdot e^{-\frac{g}{R \cdot T_{11km}} \cdot (h - h_{11km})} & \text{otherwise} \end{cases} \quad (5.15)$$

$$\rho = \frac{p}{R \cdot T} \quad (5.16)$$

$$a = \sqrt{\gamma \cdot R \cdot T} \quad (5.17)$$

$$\delta = \frac{p}{p_0} \quad (5.18)$$

Given the scope of this thesis, incorporation of realistic atmospheric data is essential. Therefore instead of relying purely on the ISA model, a data source is required from which to retrieve local atmospheric properties. Fortunately there are a number of sources available. Selection criteria for the data are the following.

- Spatial coverage (latitude, longitude and altitude)
- Spatial resolution (latitude, longitude and altitude)
- Data type available
- Data accuracy and reliability
- Temporal coverage
- Availability
- Required processing

As one can imagine, key requirements are for the data to cover the entire space along which the flight is simulated. This implies coverage of the longitudes 10°E to 125°W and latitudes 25°N to 85°N as well as an altitude range between 15000 and 45000 ft. Since commercial jet aircraft use pressure altitude to indicate their altitude during the majority of operations the latter can be translated to a pressure range between 571.81 and 147.47 hPa. These are hard requirements which rules out many options that only cover specific areas (e.g. only above US or European airspace).

Another key requirement is for the data to supply the information required for both simulation of the flight and evaluation of contrail formation and persistence. As a minimum, both temperature and humidity need to be part of the data pack. Moreover, this data needs to be both accurate and reliable for the conclusions from the thesis to hold. Accuracy in this context refers to the precision of the data that is supplied. If temperature is provided in steps of 10 °K, this is obviously not accurate enough for simulation. Reliability refers to the magnitude of errors induced by measurements and modelling of atmospheric data. These should also be kept to a minimum.

Besides the hard requirements there are also a number of softer conditions that are taken into account in data source selection. A denser atmospheric data grid yields more accurate simulation. Therefore, in addition to sufficient spatial coverage, a high resolution is desirable given the dependence of the trajectory on atmospheric conditions. Having a set of days/times to choose from when performing the simulation also helps enforce the validity of results by reducing the dependency on a single moments' evaluation. Inclusion of wind data would also

5. Model Development

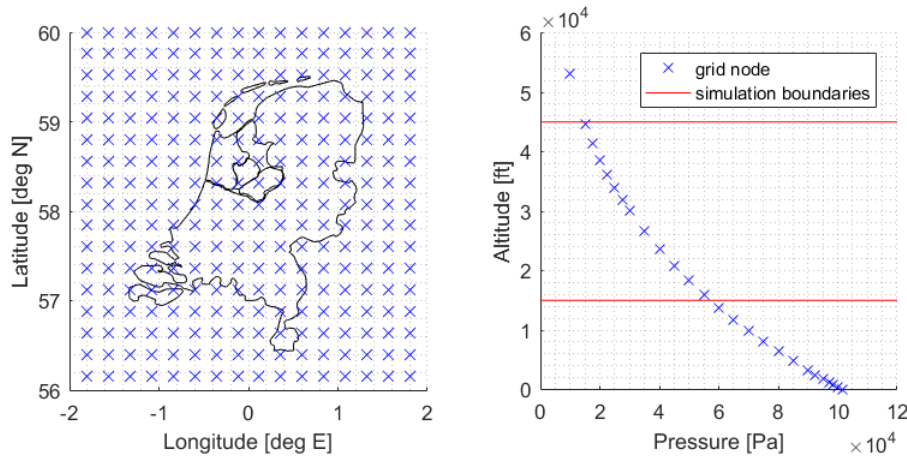


Figure 5.12: Horizontal (left) and vertical (right) resolution of Canadian GDPS NWP data

add greatly to the level of realism that this thesis pursues.

Based on the criteria presented in this section there is a source of publicly available data which very suited as input. The department of "Environment and natural resources" of the Government of Canada provides Numeric Weather Prediction data from their Global Deterministic Forecast System (GDPS) [85]. This data covers numerical predictions of the global atmosphere in a grid format sized 1500 by 751 nodes as can be seen in Figure 5.12. This grid of $.24 \times .24$ degrees corresponds to about 25 km resolution. On this rectangular grid the third dimensional component is added by data covering 28 isobaric levels. On the range of 15000 to 45000 ft this gives around a dozen distinct levels between which interpolation can be used to approximate conditions. A visualization of the spatial resolution can be seen in Figure 5.12. Among others the NWP data provides temperature, humidity, geopotential altitude associated with pressure levels and wind direction and velocity. The accuracy of the temperature data can be seen in Figure 5.13. It shows the deterioration of the RMSE as the model forecasts further into the future. In this thesis, only the 0-hour prediction is used for simulation. In other words, only the input data with corresponding highest possible accuracy is used for input, namely less than 1.5% error for temperature which is considered acceptable. This also implies the simulation is conducted using the atmospheric conditions of a single moment. The benefit of incorporation of potential atmospheric changes during an 8-12 hour transatlantic flight is easily offset by the huge increase in complexity and computational burden that is associated with including temporal variation of atmospheric data. It was therefore decided to only use the 0-hour prediction.

Based on the GDPS NWP data provided by the Government of Canada, an atmospheric model is built. The data only provides information on specific nodes. For simulation however, also an estimate of the atmospheric conditions between nodes is necessary which requires an interpolation method. The atmospheric model is create using a built-in function. This offers four kinds of interpolation for multidimensional uniformly spaced data, namely: nearest, linear, cubic and spline. In order to avoid a discontinuous function value, the first option is ignored. Due to the non-uniform vertical separation of data the cubic option is also not a feasible solution. Lastly, in order to avoid unwanted oscillatory behaviour and local extremes the spline option is disregarded. This leaves the very predictable and reliable option of linear interpolation. Figure 5.14 shows output data for three sets of NWP data (12 Feb 2014, 14 Feb 2017 and 11 May 2017) as well as the ISA output. Since the NWP data uses pressure as a proxy for

5.4. Incorporation of atmospheric data

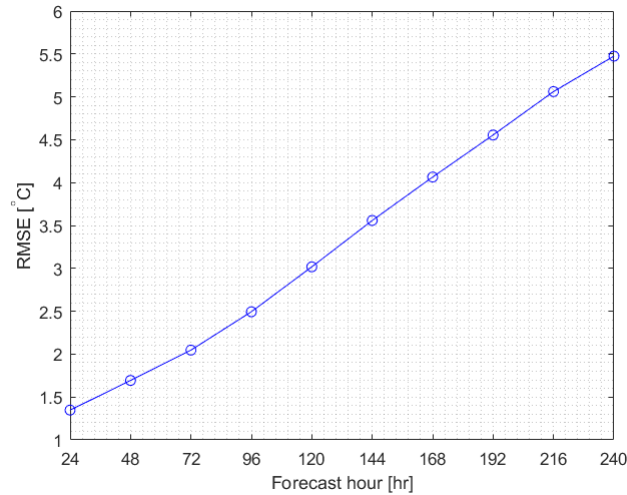


Figure 5.13: Canada GDPS NWP accuracy development with respect to prediction horizon [85]

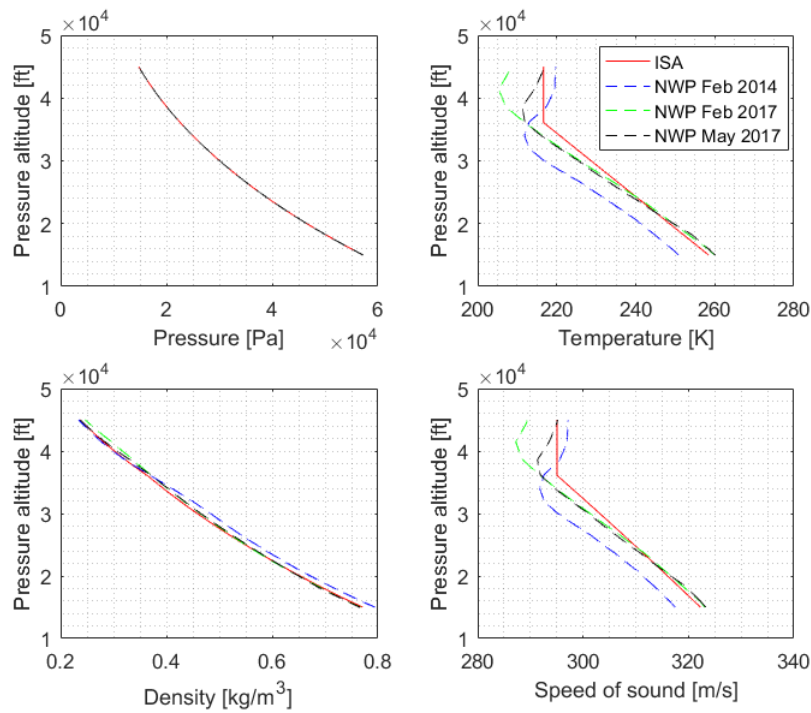


Figure 5.14: Comparison of ISA and 2014 and 2017 Canada GDPS NWP data at Spijkerboor fix

altitude, the pressure graphs overlap completely. Temperature varies quite a bit as expected but still follows the trend. Density shows very little deviation. Since speed of sound is directly proportional to temperature, it shows identical relative variation.

It should be noted that there are three NWP data sets. The first is identical to the one use by Hendriks [1], which covers February 12th, 2014. This is not a coincidence because this thesis follows directly from his work. In order to improve the validity of results however, additional input was retrieved. The second and third set cover 14 February 2017 and 11 May 2017. These are arbitrary dates which happen to be when this research was conducted. The GDPS unfortunately does not provide historic data which makes it impossible to retrieve data

5. Model Development

from any other day than the current one. Moreover, due to the size of data required and computational effort involved in processing it into the profile grid described in Section 5.3.2 it was decided that these three sets suffice.

5.5 Contrail prediction model

The contrail prediction model hinges on two separate binary outcomes. It first determines whether contrails form or not under input conditions and then determines whether a formed condensation trail would persist. Only when both are true are conditions determined to produce environmentally harmful condensation trails. The formation and persistence criteria are elaborated on in more detail in Sections 2.1 and 2.2. Their translation towards code that accurately predicts them is explained here. The contrail prediction module uses the local temperature, pressure and specific humidity from the atmospheric model as input. While converting these to a contrail prediction, a number of equations is used. The expressions for water vapour pressure are shown in Equations (5.19) and (5.20) [26]. One of the first operations is to convert the specific humidity to relative humidity with respect to water using these and Equation (5.21) [1]. It is important to note that the constants used in the entire contrail module are the following: $T_0 = 273.15$ K, $c_p = 1 \cdot 10^3$ J/kg/K, $EI_{H_2O} = 1.25$, $\varepsilon = 0.6220$, $Q = 43 \cdot 10^6$ J/kg and $\eta = 0.35$.

$$p_{liq} = 100 \cdot e^{\frac{-6096.9385}{T} + 16.635794 - 0.02711193 \cdot T + 1.673952 \cdot 10^{-5} \cdot T^2 + 2.433502 \cdot \log(T)} \quad (5.19)$$

$$p_{ice} = 100 \cdot e^{\frac{-6024.5282}{T} + 24.7219 + 0.010613868 \cdot T - 1.3198825 \cdot 10^{-5} \cdot T^2 - 0.49382577 \cdot \log(T)} \quad (5.20)$$

$$RH_w = \frac{SH \cdot p}{(\varepsilon + SH(1 - \varepsilon)) \cdot p_{liq}} \quad (5.21)$$

The first step in predicting contrail formation is calculating the ratio G , describing the change in water vapour pressure and temperature during mixing. Equation (5.22) shows the expression for it. At this point an initial estimate is made for T_{LM} as shown in Equation (5.23) [4] and finally calculated using Newton iteration as described by Schumann in 1996 [4]. This iteration works on the principle that a root of a function can be approximated using the first derivative of this function. A generalized formulation would be $x_{n+1} = x_n - \frac{f(x_n)}{f'(x_n)}$. In this case, the function that is approximated is the difference between the angle of the saturation vapour pressure line (p_{liq}) and G . In short, $f = p_{liq} - G$. Expressions for first and second derivatives of Equation (5.19) are determined. Subsequently iterating Equation (5.24) until a sufficiently small tolerance is obtained yields the final T_{LM} . Since this is a rather quick process the tolerance on the temperature increment is set to 10^{-3} which is sufficiently small to ensure the final value for T_{LM} is accurate.

$$G = \frac{EI \cdot c_p \cdot p}{\varepsilon \cdot Q \cdot (1 - \eta)} \quad (5.22)$$

$$T_{LM} = T_0 - 46.46 + 9.43 \cdot \log(G - 0.053) + 0.720 \cdot \log(G - 0.053)^2 \quad (5.23)$$

$$T_{LM_1} = T_{LM_0} - \frac{\dot{p}_{liq}(T_{LM_0}) - G}{\ddot{p}_{liq}(T_{LM_0})} \quad (5.24)$$

After calculation of T_{LM} the critical temperature for contrail formation is determined. There are three different cases defined for this, some of which require less computations. In case the relative humidity is either practically 0 or 1, the critical temperature follows directly from Equation (5.25). This relation and the method for determining the critical temperature T_{LC} is also described by Schumann [4].

$$T_{LC} = \begin{cases} T_{LM} - \frac{p_{liq}(T_{LM})}{G} & \text{if } RH_w = 0 \\ T_{LM} & \text{if } RH_w = 1 \end{cases} \quad (5.25)$$

If however the humidity is not close to 0 or 1, a Taylor series expansion around T_{LM} is required. The equations used to obtain T_{LC} in this case can be found in Equation (5.26) [4]. Contrail formation is now a simple comparison between the ambient temperature and now determined critical formation temperature. In case the ambient temperature is equal to or lower than critical, contrails are expected to form. In other cases, regardless of persistence, they do not form so do not add to radiative forcing.

$$T_{LC} = T_{LM} + A - (A^2 + 2B)^{\frac{1}{2}} \quad (5.26)$$

where $A = \frac{(1-RH_w) \cdot G}{RH_w^2 \cdot p''_{liq}(T_{LM})}$ and $B = \frac{(1-RH_w) \cdot p_{liq}(T_{LM})}{RH_w^2 \cdot p''_{liq}(T_{LM})}$

Determination of contrail persistence is much more straight forward compared to formation. Equation (5.27) shows the relation between relative humidity with respect to liquid water (RH_w) and ice (RH_i). Since the relative humidity with respect to water and the saturation vapour pressure over liquid water ($p_{sat_{liq}}$) are known, the partial vapour pressure ($p_{partial}$) can be calculated. This value can subsequently be used to determine the relative humidity with respect to ice. The reason for calculating RH_i is because contrail persistence is directly related to it. Formally for persistence it needs to be 100% or higher. Due to local variations in atmospheric conditions and a relatively large grid size compared to the scale at which contrail dynamics occur a lower boundary of 80% was used, just like Schumann and Hendriks did previously [1, 4, 86].

$$\left. \begin{aligned} RH_w &= \frac{p_{partial}}{p_{sat_{liq}}} \\ RH_i &= \frac{p_{partial}}{p_{sat_{ice}}} \end{aligned} \right\} RH_i = RH_w \cdot \frac{p_{sat_{liq}}}{p_{sat_{ice}}} \quad (5.27)$$

Using this theory and the NWP data described in Section 5.4 a prediction can be made where contrails form and persist. Figure 5.15 shows an overview of regions in the simulation domain where contrails will both form and persist. The figure depicts the situation at a realistic altitude of 250 hPa or approximately 34000 ft on the February 12, 2014. Persistent contrail regions are shown in yellow in contrast to where either they don't form, persist or both. These areas are colored blue.

5.6 Ground track contrail optimization

As can be found in Chapter 8 the mitigation of contrails is achieved using two separate strategies and finally a hybrid of the two. These follow a similar division to flight track simulation which first generates the ground track and subsequently a velocity-altitude profile over it. In short, contrails are avoided using either horizontal track alteration or changes to the profile, or a combination of the two. Section 5.6 describes the approach for mitigation by ground track alteration.

The target of this thesis is to explore feasibility of contrail mitigation in a more operationally realistic setting compared to previous research. One of the key insights in this context is a sensitivity of the contrail avoidance parameters β_{grnd} on contrail distance, fuel and time. It is therefore desirable to create a ground track mitigation algorithm which uses β_{grnd} as a weighting

5. Model Development

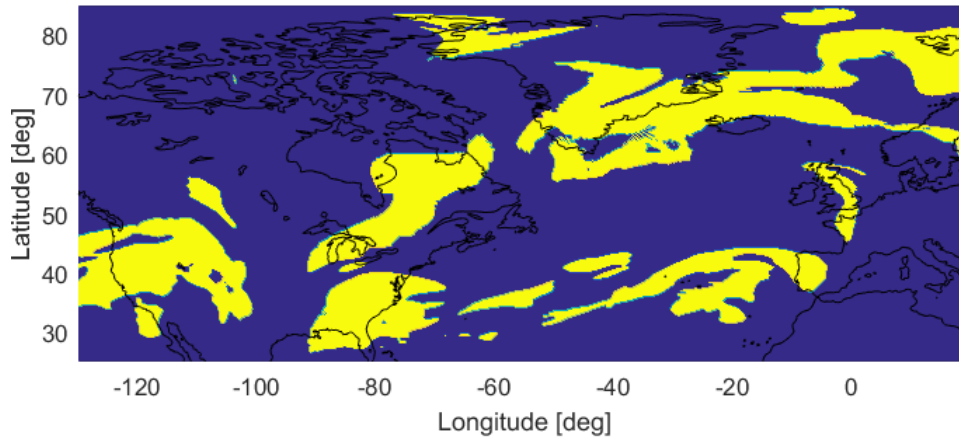


Figure 5.15: Persistent contrail formation regions (yellow) at 250hPa (34000ft)

factor for the contrail cost, relative to other factors to obtain the edge cost. Fortunately the solution to this is both obvious and relatively easy to implement. Equation (5.28) describes the edge cost between each node.

$$cost = s_{air} + \beta_{grnd} \cdot s_{contrail} \quad (5.28)$$

As described in Section 5.3.1 an estimation of aircraft mass is used to determine the corresponding cruise altitude and velocity at each node. These estimated cruise conditions can in turn be used to predict whether the aircraft will encounter atmospheric conditions that lead to persistent contrail formation. Each edge that is part of the network therefore not only obtains a cost in the form of air distance, but an additional second cost in the form of contrail distance penalty. The edge is divided into segments on which flight conditions are predicted and corresponding atmospheric conditions evaluated. The length of segments that generate persistent contrails are summed to obtain the total potential contrail distance along the edge. Just like in the non-mitigated case, the Dijkstra algorithm is used to find a ground track. However, instead of air distance as edge cost the cost as defined by Equation (5.28) is used. The resulting tracks can be seen in Figure 5.16.

5.7 Profile contrail optimization

Contrails are avoided using either horizontal track alteration or changes to the profile, or a combination of the two. The previous section describes the first approach for mitigation by ground track alteration. This section goes into detail regarding the model used for profile modification in order to mitigate contrails.

Similarly to the ground track optimization, it is desirable to have an input parameter β_{prof} which determines the extent to which contrails are avoided in the profile mitigation function. It is the contrail penalty parameter that enables a sensitivity analysis which provides critical insight in the effectiveness of contrail mitigation using profile alteration.

The global atmosphere is a very complex system. Regions in which contrails form are therefore very diverse in shape, size and location. Depending on the situation either an altitude increase,

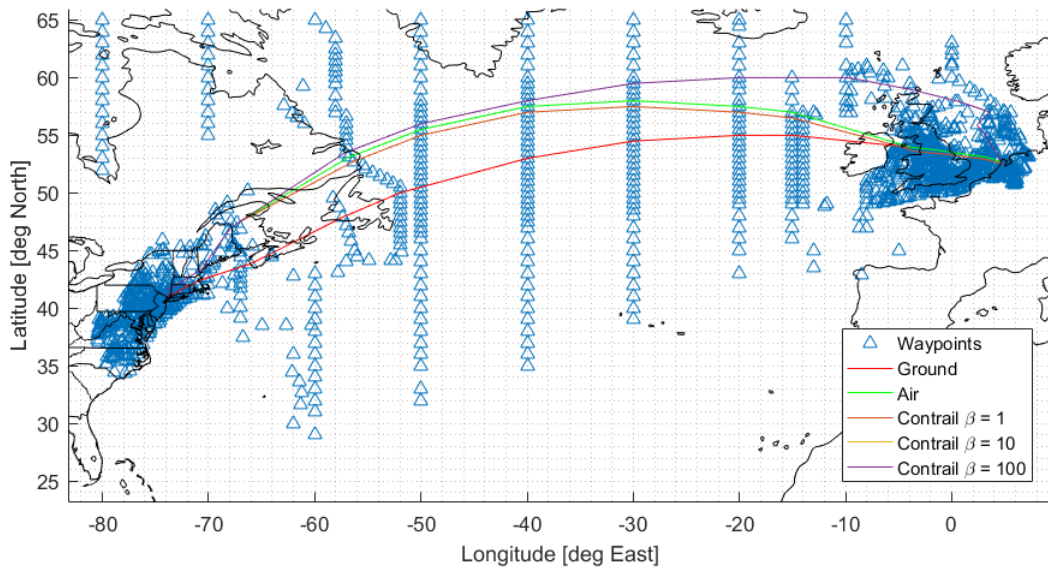


Figure 5.16: Ground track alterations NL to Washington DC (KIAD) at given values of β_{ground}

decrease or combination of the two is required for contrail avoidance. This makes even a general form of solution very difficult to predict beforehand. Moreover, a strong likelihood of encountering local minima yields many conventional gradient-based optimization routines ineffective. The complex problem with many local optima is in this case best solved by (meta)heuristic methods. These methods are used in limited computation capacity and work by sampling a set of solutions when the entire solution space is too large to be completely explored. From this category a specific method is selected. The profile optimization is conducted using a differential evolution algorithm. Apart from the fact that this is one of only a few options where both in-depth knowledge and the code is readily available within the TU Delft ATO department, it is very well suited for the problem at hand. It deals well with non-smooth nature of contrail occurrence and complex atmospheric conditions as well as having the ability to use parallel optimization and most importantly, it can avoid local optima.

Genetic algorithms emulate the process of natural selection to come up with a solution with the best performance according to the objective function. Similar to real life evolution, a set of potential solutions is generated and their fitness is evaluated using the objective function after which a new set of potential solutions is generated. Each iteration is referred to as one generation. Genetic algorithms use a set of operators to search for the optimal solution, those being crossover and mutation [87]. Using a crossover function, pairs of "parent" solutions are selected to produce a "child" solution. The properties of the child solution are created from its parents and may include a random mutation. The stochastic mutations insure that the genetic algorithm can avoid local minima/maxima. As solutions are produced generation after generation the goal is to have them converge towards a global optimum. The mutation probability may decrease over time to achieve this convergence. It should be noted that after each fitness evaluation, the candidates are selected and mutated with a certain probability p_s, p_m after which a selection criterion (e.g. tournament selection) is used to eliminate weak candidates [88]. Since genetic algorithms do not use gradient information in their search, they can be effectively applied to non-differentiable functions [89].

5. Model Development

Differential evolution is a method for approximating global optima when the objective function is non-differentiable, non-continuous or otherwise difficult to solve analytically [90]. It was shown that it generally outperforms evolutionary algorithms and particle swarm optimization methods with the exception of noisy functions [88]. It works, just like other evolutionary algorithms, by initially generating a population of candidate solutions and in an iterative process evaluating their performance and subsequently generating a set of new candidates by selecting, recombining and mutating. It is similar to an evolutionary algorithm except for the way in which it generates new potential solutions and due to its use of a "greedy" selection scheme [88]. Each new candidate is generated by the weighted difference of the parent solutions. The new candidate replaces them if it is fitter than its parent, otherwise the parents solutions are kept [88]. The method should adhere to a set of requirements. These are that they should find the true global minimum, they should converge fast and they should be easy to use by requiring a minimum of input parameters [91]. The algorithm that was used is a customized version of an adaptive elitist differential evolution algorithm [92].

In order to implement the differential evolution in a contrail mitigation context the scope of the algorithm needs to be defined from which an objective function, decision variables and constraints are obtained. Due to the complexity of the atmosphere and available computing resources individual contrail region optimization was selected. In practice this means that on a profile, the moment right before the aircraft flies into and right after it flies out of a contrail region are determined. On this section of flight, differential evolution is used to generate a profile that better suits the objective compared to the original profile. This profile is constructed using four decision moments (s_n) and decisions to be taken (f_n). Both the values of the entry location (s_1) and exit location (s_4) are fixed. Between these, two arbitrary locations are defined (s_2 and s_3). At locations 1, 2 and 3 a decision is made to either stay level, climb 2000 feet or descend 2000 feet. At location 4, the profile is forced to return to the original profile as can be seen in Equation (5.30). Note that the deviation to the original profile is the sum of the decisions taken at decision points that have been crossed at that particular distance. The logical consequence of the situation as described is that five variables determine the shape of the profile. s_1 and s_4 are fixed and f_4 is a function of f_1 to f_3 . The population in the differential evolution algorithm has the format $[s_2 \ s_3 \ f_1 \ f_2 \ f_3]$ where

$$s_1 \leq s_{2,3} \leq s_4 \quad \text{and} \quad f_{1,2,3} = \begin{cases} +2000 \\ 0 \\ -2000 \end{cases} \quad (5.29)$$

$$f_4 = - \sum_{i=1}^3 f_i \quad (5.30)$$

Figure 5.17 shows a depiction of two hypothetical situations in which a contrail region is encountered. As mentioned, there are four decision moments on which one of the three decisions with regard to altitude can be made. On the left $f = [+2000 \ 0 \ 0 \ -2000]$ and on the right $f = [+2000 \ -2000 \ -2000 \ +2000]$. As is clear from the right situation, because the decisions are made with respect to the original profile, steps in the original profile remain part of the solution unless they are counteracted explicitly by a decision variable. Between s_2 and s_3 the location and magnitude of the original step remains intact, though altitude can change depending on potential altitude changes at s_1 and s_2 .

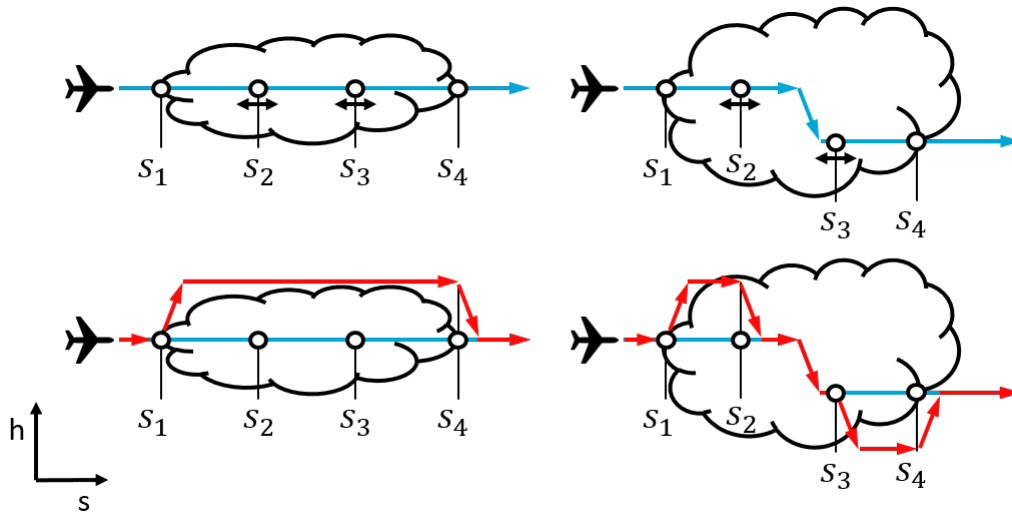


Figure 5.17: Hypothetical situations (blue) with potential profile alterations (red)

Given the goal of generating a contrail sensitivity plot, both contrail cost and time and fuel cost need to be reflected in the objective. This can be seen in Equation (5.31). In essence, the objective function script which evaluated by the differential evolution code generates an alternative profile in accordance with the decisions as defined by the decision variables. Along this trajectory the contrail distance is evaluated and potential envelope violations checked. The final state is compared to the original and changes in mass and time determined. The objective is to minimize the total change in fuel, time and total contrail distance generated along the profile. In case the operational envelope constraint is violated, the objective is automatically set to infinite.

$$\min : J = dm + dt + \beta_{prof} \cdot s_{contrail} \quad (5.31)$$

As mentioned, the differential evolution algorithm is capable of finding global optima when local ones also exist. This however should not be confused with finding a global optimum profile for the entire flight. The way the algorithm is set-up merely optimizes over a single contrail region. A non-contrail mitigating cruise phase is added from the final state of the mitigation profile. After this, the next contrail area is identified and contrails mitigated using the differential evolution method. In short there are three steps in generating the total profile mitigated trajectory, excluding step 0 which is to generate an overall non-mitigated flight profile. This sequence ensures the compounding effect of potential extra fuel and/or time of the mitigation profile on the part of the flight before it. For example, additional fuel in one stage of the flight leads to a higher weight prior to consuming it, which leads to higher fuel consumption and therefore even higher take-off weight. Merely adding the local differences across each contrail region therefore does not suffice. This process is shown in Figure 5.18 and steps listed below.

1. Identify locations of entry into and exit from contrail region
2. Mitigate contrails over contrail region using differential evolution
3. Generate non-mitigated trajectory along ground track starting from mitigated profile

It is important to note that the profile optimization routine only considers the cruise part of the flight. The number of decision variables is kept small on purpose since this directly reduces

5. Model Development

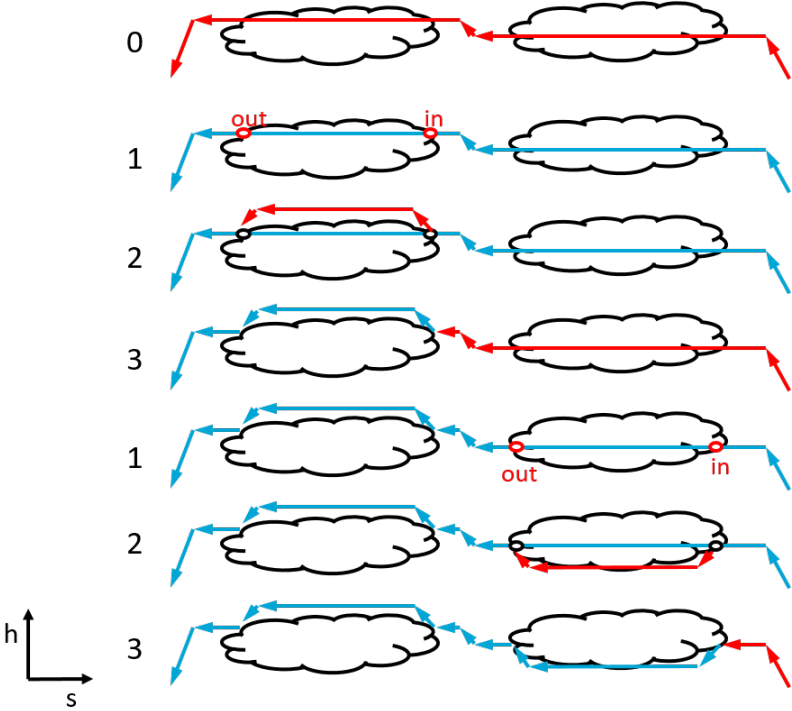


Figure 5.18: Mitigation profile generation on flight passing through two contrail regions

the computation time needed for reliable results. This does however restrict the variation in potential solutions. Given these discrete choices (+2000, 0 -2000 ft) and their frequency (4 times per contrail region) the profile mitigation algorithm is not suited to deal with the climb and descend phases of the simulation.

CHAPTER 6

MODEL VERIFICATION

Chapter 5 introduces the model used for simulation and explains how it works. This chapter builds on that by going into more detail regarding the simulation model and assumptions that are made during simulation, thereby verifying that it meets requirements and checking its output against other sources. First the aircraft performance is checked after which some simulation properties and assumptions are evaluated. After this the contrail prediction module is looked at more closely and finally some optimization parameters are verified.

6.1 Aircraft performance

For an accurate flight plan to be created, the underlying aircraft performance needs to resemble real operational conditions as close as possible. The models used for this thesis differ slightly from the ones used by Hendriks [1], which is one of the main reasons they are analyzed in more detail.

6.1.1 Operational envelope

Figure 6.1 shows the operational envelope that the aircraft is bound to by CAS and Mach number constraints. It also shows the simulation data for non-mitigated flights to each destination in the May 2017 NWP. The color shows the relative total cost associated with 1km of steady horizontal flight at the given conditions. Red corresponds to relatively high cost, whereas blue represents condition of lower unit cost. The total cost is of course the sum of fuel and time cost which is equal to the fuel cost in A and the time cost in B. Please note that the situation changes as the aircraft weight changes. As can be seen the velocity constraints are respected and an operational ceiling is obtained from the requirement of being able to keep a certain climb rate. It can also be seen that the simulation data starts and ends at the scheduled velocity at 15.000 feet. As expected the majority of the flight is spent in the dark blue region of the plot which corresponds to the lowest cost (optimal fuel or time) conditions. This confirms that the simulation works as it should and gives confidence in the results.

6.1.2 Aircraft drag and engine model

Figure 6.2 shows the difference in drag coefficient which results from the aerodynamic model used by Hendriks [1] and the one used in this work. It is clear that their results remain within 10% of each other across practically the whole domain. Near the edges at very high speed (Mach 0.9) or low lift coefficient (0.1) they do deviate more. It should be noted that fuel optimal flights remain mostly within conditions at which the two models do not differ more

6. Model Verification

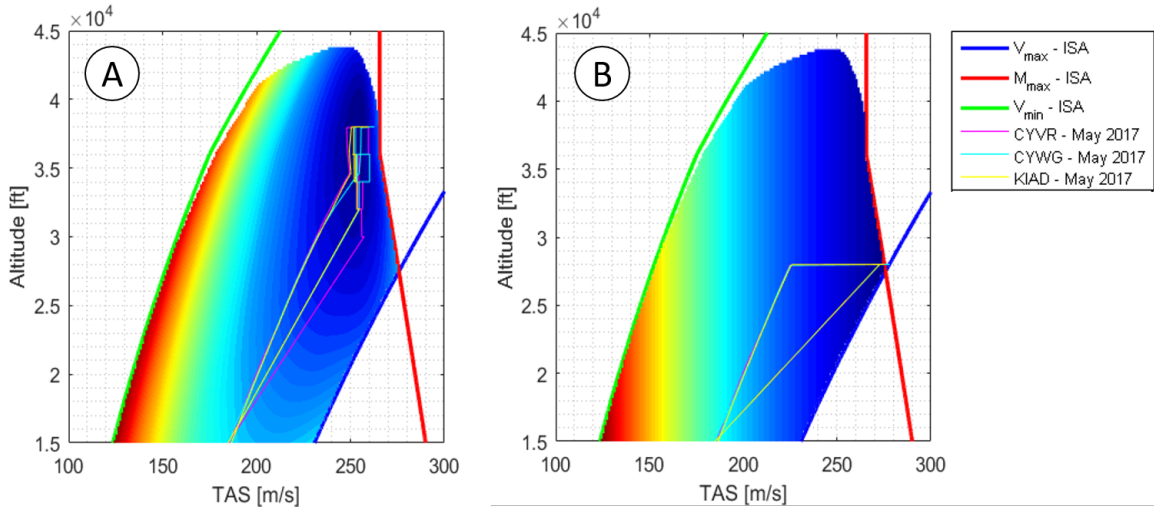


Figure 6.1: Steady horizontal flight unit cost at m_{land} in ISA with CAS and Mach constraints and fuel optimal (A) and time optimal (B) cases in May 2017 NWP

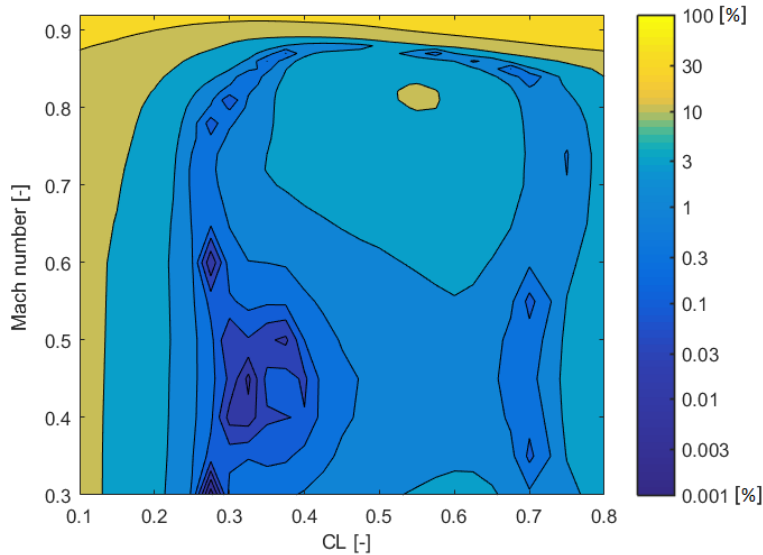


Figure 6.2: Absolute percentage difference between drag coefficient (C_D) in this thesis and the one used by Hendriks [1]

than a few percent. High lift coefficients and low velocities do not lead to large differences between them. It seems that between Mach 0.4 and 0.6 and between C_L 0.25 and 0.4 the two match very closely.

As for interpolation there are a number of options available. For gridded data like that of the aerodynamic drag this can be nearest, linear, cubic or spline. If the input data is scattered as is the case for the engine model linear, nearest or natural interpolation can be used. To avoid discontinuous second order derivatives which are often used in gradient based optimization algorithms, linear interpolation is avoided. After testing various options it was decided that spline interpolation was best suited for the aerodynamic drag data and nearest neighbor was best suited for the engine model. Extrapolation is disabled for both.

Figure 6.3 shows on the left (A) the difference in maximum thrust and on the right (B) the

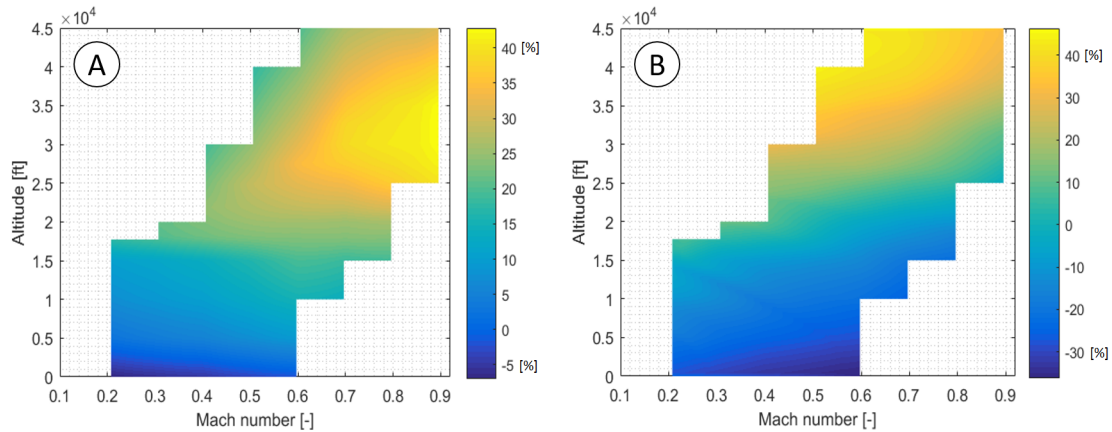


Figure 6.3: Percentage difference between maximum thrust (A) and maximum fuel flow (B) used for this thesis and the one used by Hendriks [1]

difference in fuel flow which results from the engine model used by Hendriks [1] and the one used in this work. On the left it can be seen that at lower altitudes the thrust is within 5% of each other. At higher altitudes and Mach numbers however the values diverge to where the one used for this work is close to 40% higher. On the right it can be seen that the maximum fuel flow models are within roughly -30 to 40% of one another. At high altitude the ones used for this work is approximately 40% higher which corresponds roughly to the rise in maximum thrust, albeit in different conditions. Around 20.000 to 25.000 feet the two models show close resemblance in their output. At low altitude Hendriks' model predicts higher maximum fuel flow up to 30%. Mach number seems to have a smaller influence on the difference in maximum fuel flow compared to maximum thrust than altitude does. It should be noted that Figure 6.3 shows the maximum values rather than an output comparison across all three input dimensions (velocity, altitude and thrust setting). Moreover, the optimal cruise conditions generated using this input seems to correspond closer to reality than those of Hendriks which seem rather low. Underestimation of available thrust at high altitudes could be one of the main reasons. This also gives confidence in the accuracy of the models and interpolation used here.

6.1.3 Step climb and steady horizontal flight

After inspection of the cruise and step algorithms under various conditions some interesting properties become apparent. As mentioned in Chapter 5 the step climb uses a difference in thrust (equal to required potential energy input for altitude gain) to determine the fuel cost associated with step climbs. What is interesting about this assumption is that the perfect energy conversion causes any changes in fuel efficiency (fuel required per unit thrust) can be exploited by the algorithm. Figure 6.4 shows two flights that cross a horizontal distance of 1000 km at FL260 at 300.000 kg in ISA. One flies a steady horizontal path and the other uses alternating step climbs and descents across the majority of the track. The top left graph shows their altitude throughout the flight and the bottom left shows their mass development. It is clear that even though the flight paths differ greatly, compared to the total mass they seem to remain the same weight. Instead of showing the absolute weight, the right image shows the difference between the oscillatory and steady horizontal case through the flight. It can be seen that at the initial step up the oscillatory version consumes more fuel, however the fuel it saves during the step down more than compensates for it. This leads to an eventual advantage of

6. Model Verification

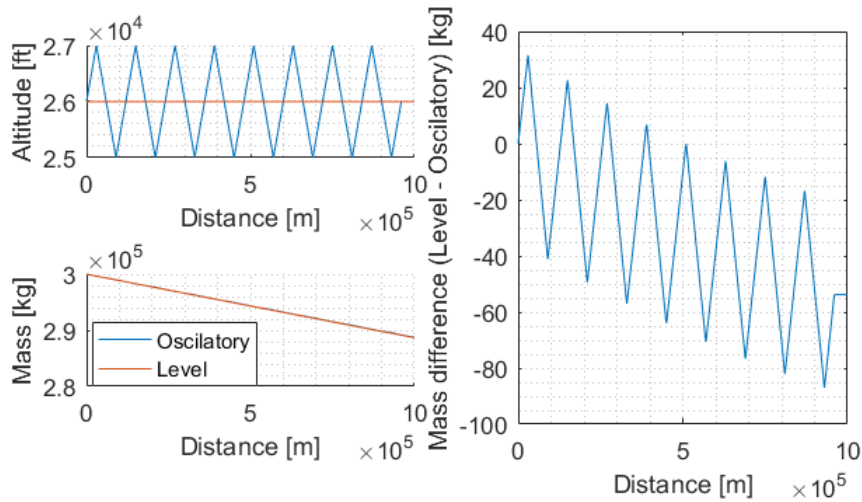


Figure 6.4: Fuel consumption of level cruise vs repeated step climbs in ISA at 26,000ft, 250m/s and 300,000kg

the oscillatory scenario compared to steady horizontal flight. A sequence of 8 oscillations over 1000km under the given conditions yields a 54 kg fuel advantage.

It seems unrealistic and counter intuitive that alternating steps are more fuel efficient than steady horizontal flight. What should be considered here is the following. Table 6.1 shows the output of three different scenarios. Steady horizontal flight, a 50 ft step climb and descent are simulated at 25,000 feet at 250 m/s and 300,000 kg in ISA. The scenarios cover a very small range of altitudes and masses which diminishes any other effect than that of the difference in required thrust. What is remarkable about these results is that even though all cover the same unit of time and horizontal distance, the climb consumes 1.53 kg more fuel than level flight and the descent 1.84 kg less. Since they both stem from the same thrust difference they are caused by non-linear behaviour in the engine efficiency. Even though the difference is small it is clear that if the two actions are combined it gives a reduction of $2 \cdot 17.2 - (18.7 + 15.4) = 0.3$ kg in 12 seconds of up-down flying compared to level flight. Obviously this ignores any dynamic behaviour in addition to relying on perfect energy conversion from surplus thrust to potential energy. Fortunately, since the simulations in this thesis do not contain large numbers of steps this effect is relatively small compared to that shown in Figure 6.4. In short, this behaviour is caused by assumptions in the model. Its impact on the flight plan and potential incorporation of dynamic behaviour should be considered for further research.

Table 6.1: Impact of step climb/descent on instantaneous fuel consumption compared to steady horizontal flight at 25,000ft, 250m/s, 300,000kg in ISA

Scenario	dt [s]	dh [ft]	ds [m]	Thrust [N]	ff [kg/s]	fuel [kg]	dThrust [N]	dff [kg/s]	dfuel [kg]
Level flight	6	0	1.50E+03	1.74E+05	2.87	17.2	0	0	0
50 ft climb	6	50	1.50E+03	2.04E+05	3.12	18.7	3.00E+04	0.254	1.53
50 ft descent	6	50	1.50E+03	1.44E+05	2.56	15.4	-3.00E+04	-0.308	-1.84

6.2 Simulation and integration

This section covers some key decisions made in simulation. It covers the generation of the cruise conditions, the optimal cruise conditions grid and grid for evaluating climb performance.

6.2.1 Optimal cruise condition generation

The generation of cruise conditions is done using a cost function and optimizer. Since the simulation and subsequent results rely heavily on the output of this process, the input parameters are all carefully weighed before making a final decision. As input for `fmincon` and the subsequent optimal profile, the following decisions have to be made. The tolerance of the decision variable (`TolX`), tolerance of the objective function (`TolFun`), starting point (`X0`) and the algorithm that is used (interior-point, trust-region-reflective, Sequential Quadratic Programming (SQP) or active-set). Next to that, to stay as close as possible to actual optimal conditions, the profile should be generated for a large number of aircraft masses.

In order to select the best combination of optimizer options, the performance of a large set of sample problems was evaluated. The option with both the most accurate and fast results was selected. Active-set and trust-region-reflective did not yield any usable result. Both interior point and SQP were extensively tested on various initial conditions and tolerances. The SQP algorithm was found to produce a more accurate results faster. Lower tolerances found unrealistic results, however from $1e-5$ for `TolFun` and $1e-8$ for `TolX` the results were deemed realistic. They continued to increase in accuracy up to $1e-12$ were they practically leveled off. The computation time however was found to be proportional to the accuracy in this last phase (therefore $1e-12$ takes hardly any longer than $1e-15$). This is why the decision was made to stick to a $1e-15$ for both `TolX` and `TolFun`. As for the number of steps of the aircraft mass, this relates linearly to the computation time. A resolution of 50 steps gives an interval of approximately 2 metric tons (0.6 to 0.9 % of aircraft weight). Increasing the resolution does not yield accuracy improvements that offset the required computation time. Therefore, and given the spatial resolution of the optimal cruise conditions grid, this number was deemed an appropriate interval.

As described in Chapter 5, the optimal conditions need to abide an operational envelope constraint. This constraint is defined by the minimum and maximum allowed velocities (CAS and Mach) and a minimum rate of climb that the aircraft should be able to reach. The "rate of climb envelope" is attained by a minimum surplus thrust that the engines should be able to provide to achieve the minimum work required to attain the target rate of climb. This effectively pushes the aircraft envelope down with respect to the absolute maximum altitude. The higher the required climb rate, the more the effective service ceiling is pushed down. Given that in case an aircraft is not able to achieve 500 feet per minute it should report this to ATC, this was chosen as absolute minimum service ceiling [93].

As shown in Figure 5.9 when the altitude constraint is added something interesting happens. As `fmincon` optimizes the cost associated with particular conditions it uses altitude and velocity to do so. When one of them is fixed - in this case altitude - a single parameter remains to minimize cost. This is the reason for the saw tooth pattern as seen in Figure 5.9. It can be shown that as the aircraft weight changes the optimal velocity also changes. Due to the relatively coarse grid of optimal conditions as used in simulation and the use of a natural

6. Model Verification

neighbor interpolation this effect is not apparent in the final simulation.

6.2.2 Cruise conditions grid

Generating the optimal cruise conditions is a computationally expensive process. Rather than making it an integrated part of the simulation (thereby greatly increasing simulation time), a grid of optimal cruise conditions is created. The routine evaluates both absolute and flight-level constrained optimal conditions at 50 latitudes, 120 longitudes and 50 aircraft weights. This is done for three different atmospheres (May 2017, February 2017 and February 2014) and both fuel and time optimal conditions. Of course the finer the grid, the closer these conditions resemble the actual case. The evaluation of 50 latitude x 120 longitude x 50 weight = 300.000 nodes takes approximately 100 hours of processing which is the highest resolution practically possible in the context of this thesis. Figures 6.5 and 6.6 show the optimal cruise altitude for fuel optimal flights for the minimum and maximum aircraft weight in the May 2017 NWP. As can be seen, the two resemble each other fairly closely, though of course the flight-level bound data is more discrete in nature.

When considering the operational envelope of commercial jet aircraft, cruise altitudes are typically between 30.000 and 40.000 feet, usually tending towards the top boundary. For the Boeing 747-400 aircraft as is the subject of this thesis this is also true. Validation on aircraft tracking websites (e.g. flightradar24.com) confirm that transatlantic flights by KLM mostly keep to altitudes between 32.000 and 38.000 feet. Relating this to the values seen in the cruise conditions grid, it can be found that the grid sufficiently approximates day-to-day operational practice. Moreover, the fact that aircraft never cruise at their Maximum Take-Off Weight (MTOW) and the results from Section 8.1 only confirm that the cruise conditions matrix provides the realism this thesis pursues. The same holds for the velocity matrices.

It is interesting to see that the cruise grid does not stick to a single pressure altitude for a given aircraft weight. In practice this leads to potential step descents along a flight profile. Although they are not uncommon in practice, most flights only feature step climbs. Closer inspection however notes that the fuel optimal conditions are governed by the local specific fuel flow (V/ff). Note that on a single pressure altitude, differences in temperature lead to difference in aerodynamic drag since $C_D = f(C_L, M)$ and $M = f(Thrust, V)$. This implies a change in required thrust for steady horizontal flight, which changes the fuel flow and in turn, the local specific fuel consumption. In some nodes this leads to a higher or lower cruise altitude. Therefore, even though cruise typically features step climbs, the cruise grid also has step descends due to temperature variance over pressure altitudes. In order to keep the complexity of the simulation within limits, the cruise conditions as dictated by the optimality matrices is kept as guideline for simulation of all flights rather than post processing it by smoothing or altering it in another way.

One of the main concerns with any grid based interpolation is to which extent the inter-node conditions are accurate. In most cases an easy way to improve inter-node accuracy is simply by increasing the resolution of the grid. As mentioned this is not an option, therefore what is left is to choose an appropriate interpolation scheme. The interpolation function provides the following options for 3D interpolation: nearest neighbor, linear, cubic and spline. Due to the discrete nature of the flight level changes any interpolation scheme that does not output a distinct flight level is undesirable. Moreover, due to the fact that most optimal conditions are

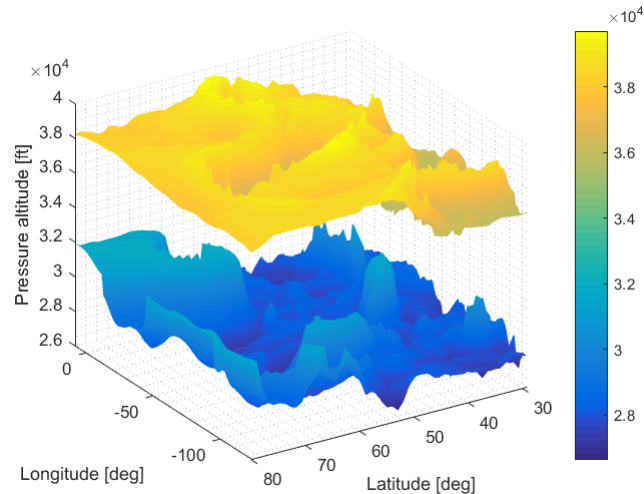


Figure 6.5: Unrestricted optimal cruise altitude in 2014 NWP of 252672 kg (top) and 362874 kg (bottom)

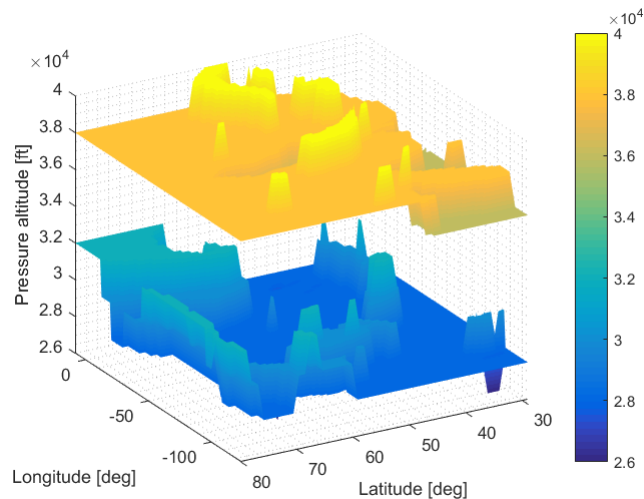


Figure 6.6: Flight level restricted optimal cruise altitude in 2014 NWP of 252672 kg (top) and 362874 kg (bottom)

at or close to the boundaries of the operational envelope there is a risk of outputting unfeasible inter-node conditions. Taking this into account, it was decided that the nearest neighbor interpolation is most suited, while avoiding unfeasible output. Due to careful selection of the grid parameters there is no need for extrapolation.

6.2.3 Climb phase interpolation

Similarly to the optimal cruise conditions, also the climb phase calculation is too computationally expensive to have as integrated part of the simulation. In order to avoid lengthy simulations as much as possible, a three dimensional climb grid was created. Each climb ends at 15.000 feet at scheduled CAS. Their difference lies in the TOC velocity, altitude and weight. Due to the backwards integration, at any point during cruise the corresponding climb distance needs to be estimated. This is possible using the climb matrix. The cruise phase therefore only ends when the corresponding climb exactly matches the predefined origin location of the flight. The required fuel and time can be found the same way. Figure 6.7 shows the trajectory,

6. Model Verification

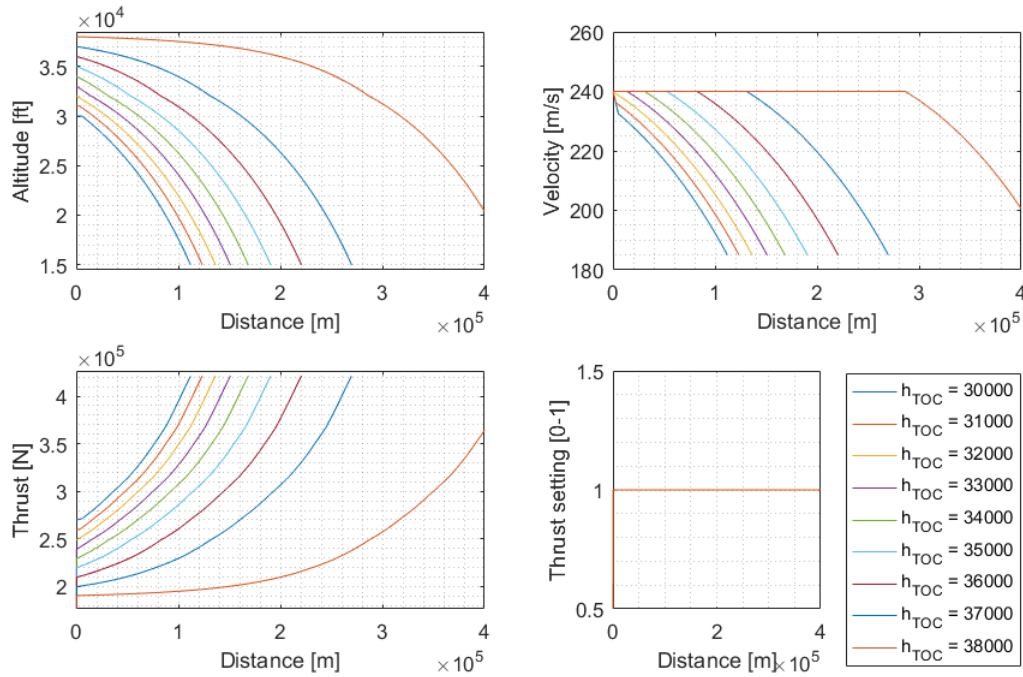


Figure 6.7: Overview of selected climb scenarios - TOC for all 240 m/s TAS and 317672 kg

velocity and performance during a set of climbs. It uses a TOC weight of approximately 318 metric tons and 240 m/s TAS. The altitude is changed in order to be able to see the different climb trajectories. It should be noted that these follow the climb velocity schedule. Of course cruise velocity rarely equals the climb scheduled velocity exactly. Therefore when the TOC velocity is higher than the climb schedule, a full thrust level acceleration is added to the climb and when it is lower the climb is continued at this lower TOC speed. The latter can be seen in the top right plot in Figure 6.7 from the flattened top of the velocity plot. The horizontal acceleration can be seen in the very leftmost part of the 30.000 feet plot. Close to a distance of zero the altitude is constant and velocity increases much faster than it did before the climb levelled off.

6.3 Contrail prediction model

This section covers verification of the contrail model. Figure 6.8 shows a comparison between the critical temperature and ambient temperature as determined by the contrail model for the February 2014 NWP (A) and those determined in ISA by Schumann (B) [4]. Since sample points across a wide range of geographic locations were selected and the atmosphere has natural variations there is some scattering in the left image. It can however be seen that both show the critical temperatures at low altitude between -30 and -40 degrees Celsius. They also show a similar linear progression to lower temperatures as altitude increases. The ambient temperature also shows a similar shape and location in both plots. Given their similarity and the verification of the NWP data in the previous section Figure 6.8 clearly shows that the conditions for contrail formation seem to agree with those seen in literature.

Chapter 5 explains how the contrail prediction model works. Figure 5.15 shows the locations at 250 hPa where persistent contrails form, would they be encountered during simulation. Of course there are some steps that lead up to these conditions. The first, contrail formation, is

6.3. Contrail prediction model

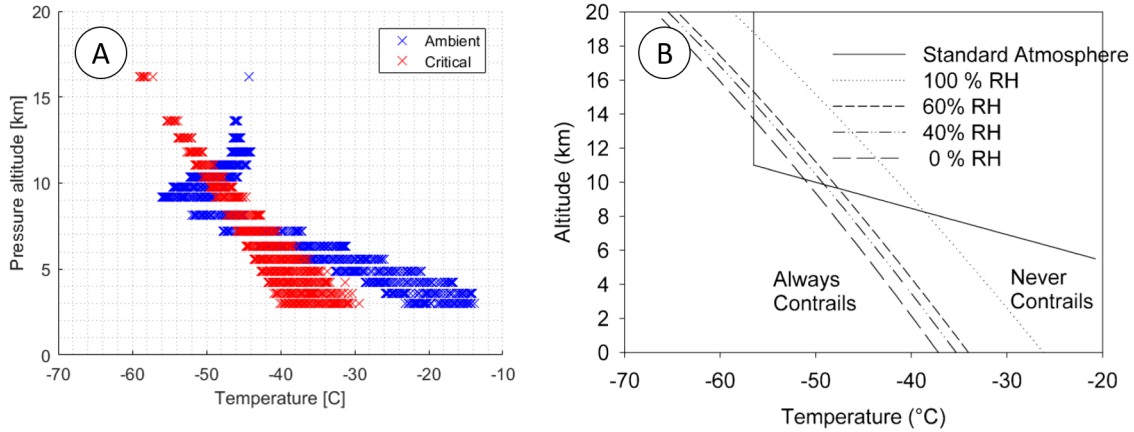


Figure 6.8: Critical temperature and ambient temperature in February 2014 NWP on the left (A) and ISA on the right [4] (B)

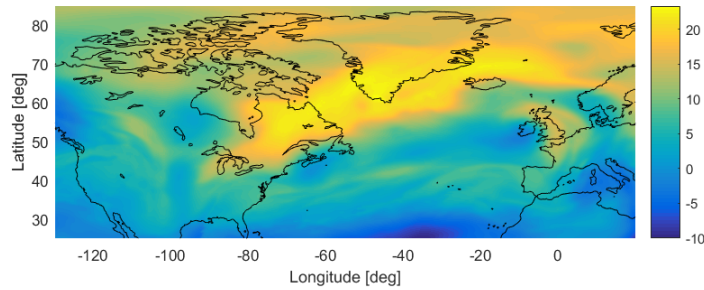


Figure 6.9: $T_{amb} - T_{crit}$ at 250hPa (34000ft)

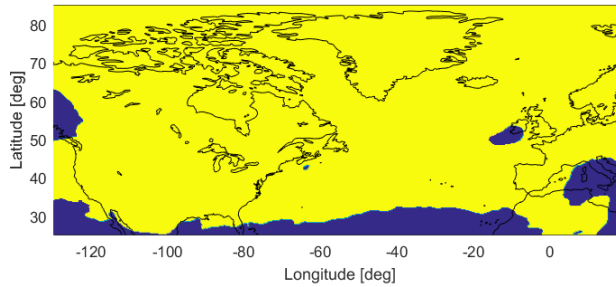


Figure 6.10: Contrail formation regions at 250hPa (34000ft)

dependent on the two temperatures T_{crit} and T_{amb} shown in Figure 6.8. The difference between these is depicted in Figure 6.9. As the Schmidt-Appleman criterion dictates, if the ambient temperature is below the critical temperature (positive value in Figure 6.9) contrails will form. Figure 6.10 shows the regions in which this criterion is met and contrails will form initially in yellow. It is clear that at this altitude, which coincides with the right altitude for formation in ISA, contrails form nearly everywhere. Observations confirm that during winter months it is very common to see initial condensation in the wake of aircraft. What is less common however is for them to persist.

The second step which is required for persistent contrails to occur is for initial contrails to persist. This is more open to interpretation since persistence is difficult to capture in a single

6. Model Verification

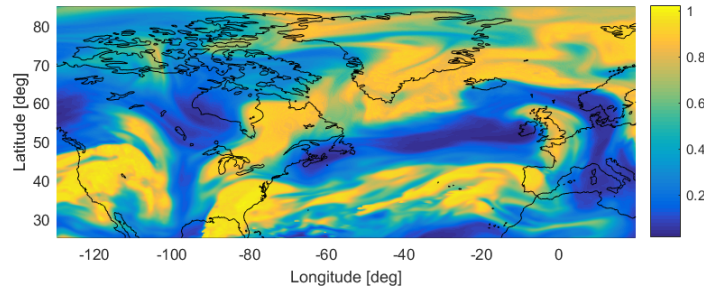


Figure 6.11: RH_i at 250hPa (34000ft)

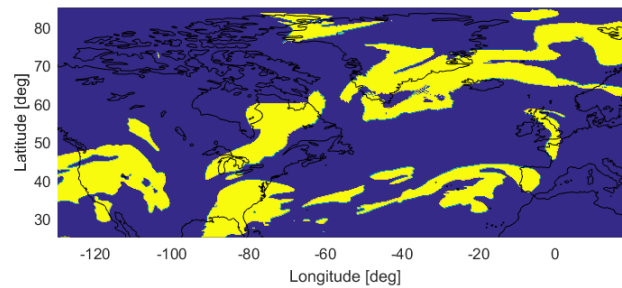


Figure 6.12: Contrail persistence regions at 250hPa (34000ft)

condition. Extensive assessment of temporal effects and optical density is necessary as a minimum. It is however clear that contrails only persist at high relative humidity. This makes sense as higher humidity (more saturation) will keep contrails from evaporating or may even lead to additional cloud formation as the contrails nucleate over-saturated regions. Figure 6.11 shows the relative humidity with respect to ice (RH_i) at 250 hPa. The higher this value, the more likely contrails will persist. Just like Hendriks did, it was decided that a single cutoff humidity best fits the needs of this thesis. The persistence criterion was set to 80% or higher RH_i as previously done by Schumann and Hendriks [4, 1]. Note that this is the relative humidity with respect to ice and needs conversion from relative humidity with respect to liquid water. Figure 6.12 shows the regions where any initial contrails will persist according to the criterion in yellow. Right away it can be seen that these regions occur far less often than those for formation. The majority of the area is blue rather than yellow which means formed contrails will quickly evaporate and their direct effect on the global climate is limited. The occurrence of persistent contrails at this altitude therefore are mainly dictated by persistence rather than formation.

Figure 6.13 shows the regions where initial contrails will persist for different criteria in yellow. This thesis assumes 80% which can be seen in the bottom left corner. It is both clear and obvious that with a higher relative humidity the share of locations where contrails persist decreases. At 90% there are hardly any spots across the Atlantic Ocean at this altitude where they persist. On the other hand, for 60% it can be seen that huge areas are yellow.

A general impression on the size and shape of persistent contrail regions can be obtained from figures throughout this report. What is clear from them is that the contrail regions are indeed very widespread but most contrail regions cover a large range of altitudes. Gierens suggests that ISSRs are often very thin at a few hundred meters from bottom to top and in the order

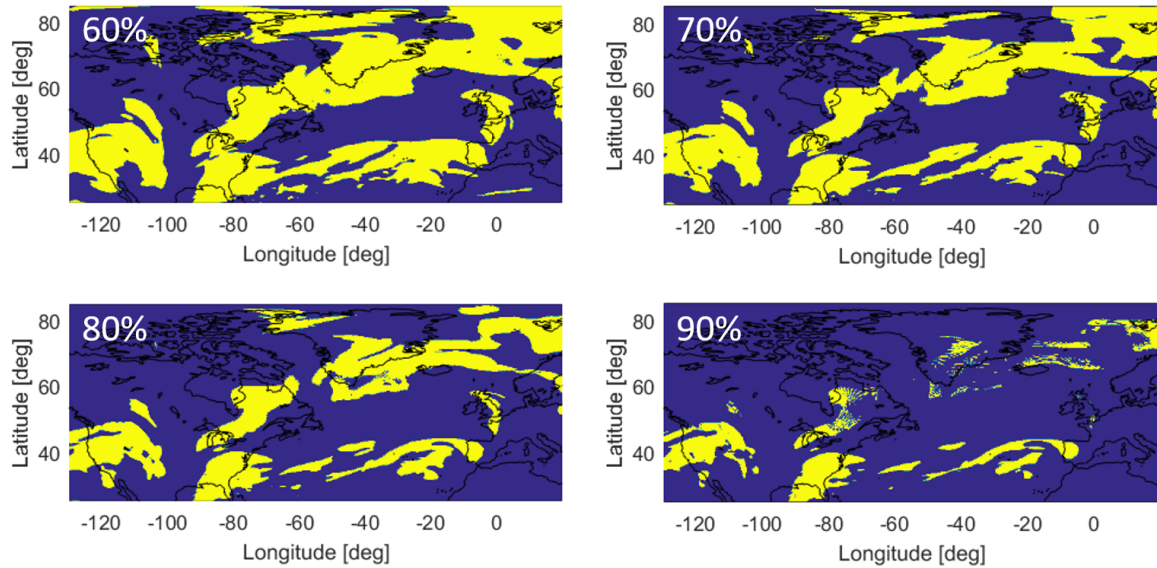


Figure 6.13: Contrail persistence regions at 250hPa (34000ft) for 60, 70, 80 and 90% RH_i in February 2014 NWP

of 150-200 km across [69]. Since they are often used as a proxy for persistent contrail regions it is natural to assume contrail regions have the same shape and size. These figures however show that the persistent contrail regions in this thesis are not the "pancakes" that allow for very simple mitigation by changing altitude by a few hundred meters.

6.4 Optimization method

Both verification of ground track selection and profile optimization are described in this section.

6.4.1 Ground track selection

As explained in Chapter 5 the ground track optimization uses Dijkstra's algorithm to find the optimal path. This algorithm is extensively documented and researched and is proven to find the optimal solution in a network given a topology and edge cost. Throughout generation of the results its implementation has proven to indeed produce the results as expected. This leaves the estimation of weight and flight level on each node and corresponding optimal cruise conditions as potential source of errors.

Figure 6.14 shows a set of ground tracks in the May 2017 NWP to Vancouver. The red line shows the non-mitigated ground track, which only uses estimated air distance as edge cost in the network. As β_{grnd} increases also expected contrail distance is added to the edge cost as described in Equation (5.28). It is clear that the larger the contrail cost parameter, the more avoidance action can be seen in the track. At $\beta_{grnd} = 10$ the ground track can be seen to completely avoid one of the regions (yellow areas). It should be noted that the contrail plot shows that of a single altitude (250hPa) whereas the edge cost takes into account estimated cruise altitude to determine the contrails encountered as discussed in Chapter 5.

6. Model Verification

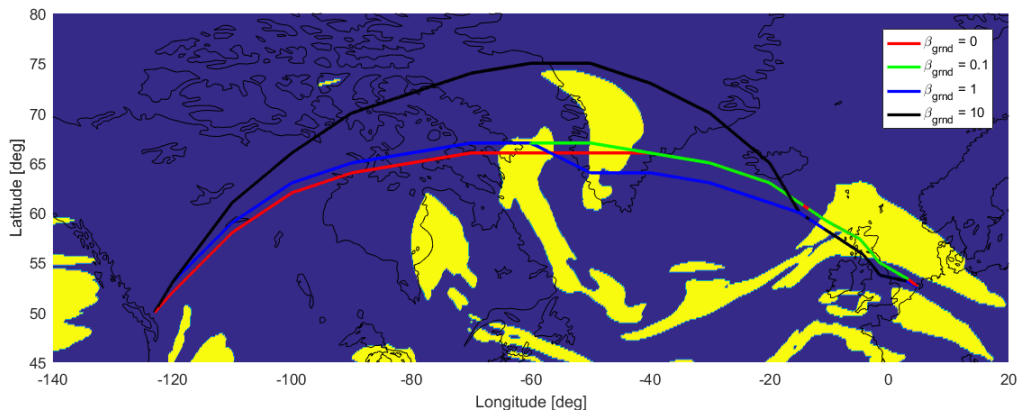


Figure 6.14: Fuel optimal ground tracks to Vancouver (CYVR) for β_{grnd} in May 2017 NWP - Persistent contrail regions shown at 250hPa

Since Dijkstra's algorithm merely optimizes a track for given edge cost, it cannot prevent errors in these weights themselves. One such source of errors is caused by the assumption of linear fuel flow as a function of distance to the destination. The estimated weight at each node might be off, which may lead to an actual cruise altitude to be a flight level higher or lower than predicted. Consequently, the actual contrail distance on that segment is different from the estimate which may in some cases cause increases in contrail distance as β_{grnd} increases. It should be noted however that from a practicality perspective this assumption is made. As this work aims to prove that contrail mitigation is possible at low fuel and time cost through flight planning, rather than pinpoint the absolute best trajectory at every point this is deemed appropriate.

A noteworthy variable in the ground track optimization is the interval at which wind and contrail distance is evaluated along each airway. Even though simulation of the ground track mitigation results is performed using a 1km interval, the input for Dijkstra's algorithm is pre-processed using a 5km resolution (ea. every 5km the wind and contrail conditions are evaluated and results summed to produce air distance and contrail distance). The reason for this decreased resolution is the total length of airways is too large for a 1km resolution to remain practical. Decreasing the resolution by a factor 5 reduces the computation time by the same factor while the contrail edge cost is now reduced to a multiple of 5km rather than 1km. Moreover, simulation of the ground track mitigation strategy itself is conducted in the 1km resolution. As can be seen in Section 8.2, occasional increases in contrail distance rather than decreases as β_{grnd} increases is caused by a combination of edge cost error and decreased resolution of input for Dijkstra's.

6.4.2 Profile optimization

The profile optimization routine is described in detail in Chapter 5. As mentioned there, each contrail region that is encountered is mitigated locally. At four locations (two fixed, two variable) the aircraft climbs, descends or stays level compared to the original profile. Depending on the fit of each member of a generation in the differential evolution process, a new set of solutions is generated and evaluated for fitness. Figure 6.15 shows the mitigated profiles to Washington D.C. in the February 2014 NWP for different β_{prof} . It can be seen that the five sections in which contrails are generated are not mitigated when $\beta_{prof} = 0$. Here the black

lines that indicated the mitigated profile are identical to the blue cruise phase track. As the contrail cost increases the changes to the profile become more pronounced. It can clearly be seen that the alterations are indeed mitigating contrail regions. What is also clear is that the assumption of local optimization may lead to impractical climbing and descending between neighboring regions. It should be noted however that given complex nature of contrail regions and computational effort involved it is outside the scope of this thesis to find a global contrail avoidance optimum. Of course future research could investigate this further, however local avoidance should suffice in order to approximate the effectiveness of contrail mitigation in this setting.

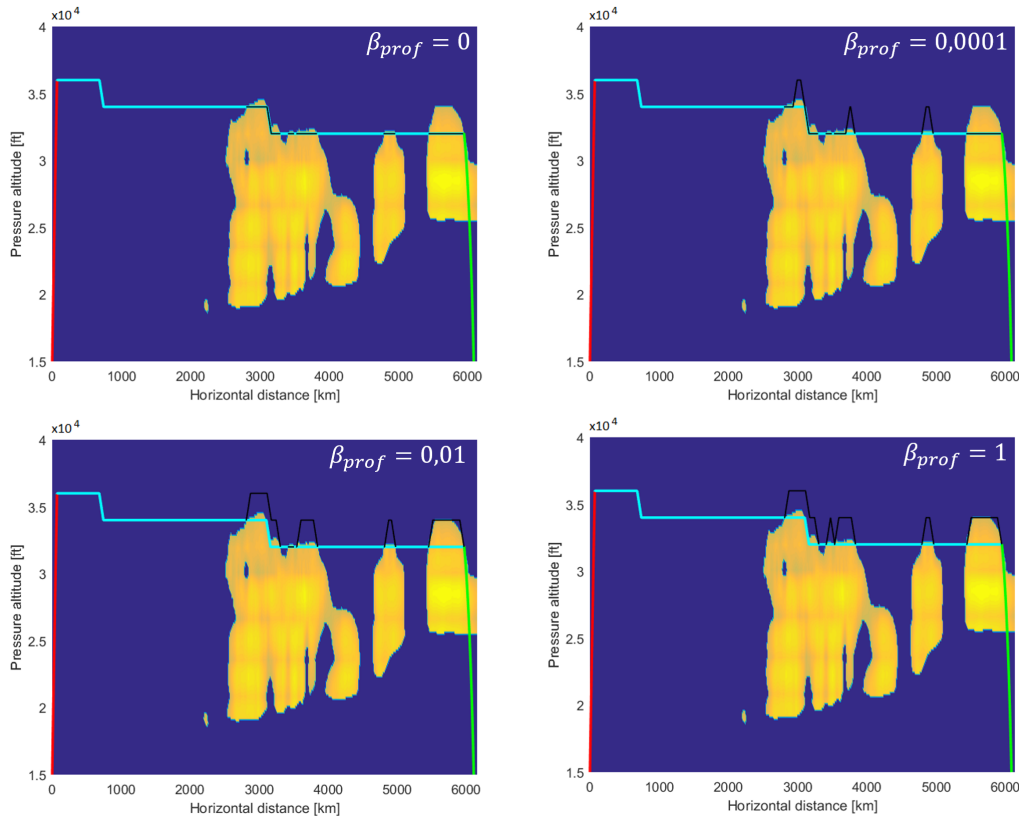


Figure 6.15: Fuel optimal flight profile with alterations (in black) to Washington D.C. (KIAD) for β_{prof} in Feb 2014 NWP

An extremely important issue in any optimization routine is to what extent the algorithm converges to an optimal solution. Especially given the fact that the model used in this thesis uses differential evolution for the profile mitigation, this should be considered carefully. To that end, the constraint for number of generations is lifted and the profile mitigation algorithm is performed for all destinations, all atmospheres, both fuel and time optimal and β_{prof} of $[10^{-5} 10^{-4} 10^{-3} 10^{-2} 10^{-1} 10^0 10^1]$. The results of each generation are stored and analyzed to produce the results as can be seen in Figure 6.16. On the left the normalized RMSE of the best result in each generation compared to the final converged value is shown. On the right the share of contrail regions that converges within a number of generations can be seen. It should be noted that in this context convergence is reached if the mean of the generation is within 0.1% of the best solution. Not a single case exceeds 211 generations to achieve this.

There are two main conclusions that can be drawn from Figure 6.16. The first is that after

6. Model Verification

50 or so generations, the best solution hardly ever improves as shown by a flat value of the normalized RMSE of the generation's best on the left. The second is that approximately 10% of regions have not met the convergence condition at the 40 generations mark and therefore requires further computation. With this knowledge a generation limit of 43 is deemed best in order to reduce computation time while retaining reliability and convergence in the solutions as much as possible (i.e. not spend energy on endless iterations when it is shown this adds little to the output). This is the number of generations required to have the normalized RMSE drop below 1%.

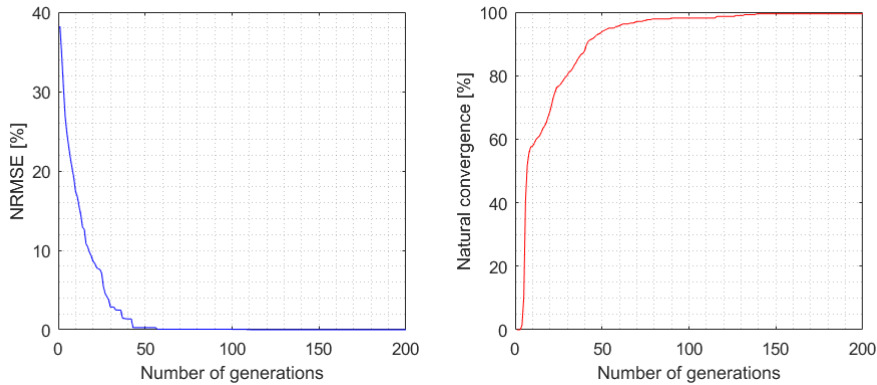


Figure 6.16: Normalized RMSE of generation best compared to final solution and share of local optimizations that converge within number of generations

Another important factor to consider in verification of the differential evolution algorithm is the population size. Along with a restriction on number of generations it governs much of the optimization behaviour. Based on three points where a distinct decision between three options is made, this gives a total of $3^3 = 27$ permutations for each profile if we ignore the variation in locations at which they are made. In order to sufficiently explore the solution space, the number of arbitrary profiles which is initially generated should be of ample size. However it should also not be too large as the population size relates linearly to computation time. Generally, differential evolution uses a population size between 50 and 200 [94]. Higher dimensional problems of course require a larger set, however given the low number of dimensions that is the case here a smaller set suffices. Testing of low dimensional sample problems confirms that in many cases a population of 50 is the best choice [94]. Taking into account the restriction of computation time it was decided to adopt this value in the differential evolution model.

CHAPTER 7

SCENARIOS

Before the results of any mitigation strategies are shown a baseline flight plan is presented. It starts with a single flight in ISA. More complexity is added by including the atmospheric conditions from the NWP first and later also wind and other destinations. The section concludes with an overview of standard flight plans against which the performance of other (contrail mitigated) flights can be tested.

After the baseline, the effect of ground track selection is evaluated. As explained in Chapter 5 the ground track selection algorithm uses a predefined edge cost over which the optimal track is selected. By including contrail cost into the network, Dijkstra's algorithm can also find an ideal track including contrails. Since these are based on estimates for weight and altitude, subsequent simulation of a flight along this ground track is required to give the final results from this type of mitigation strategy. By varying the ground track contrail cost parameter β_{grnd} , the impact of contrail length on the ground track can be changed. By doing so, rather than a mere binary scale for mitigation, also the results for partial mitigation can be evaluated.

Next to the ground track alterations, also flight profile optimization is proposed as potential mitigation strategy. On a single (non-mitigated) ground track the profile mitigation contrail cost parameter β_{prof} is changed. The relationship between a range of these values and contrail distance, fuel and time is presented.

In addition to using the two contrail mitigation strategies separately, also a combination of the two is evaluated. The ground track is changed using ground track contrail cost parameter β_{grnd} after which profiles for a number of profile mitigation cost parameters β_{prof} are generated. In doing so, a combination of the two parameters could be obtained which gives a better mitigation performance than one of the two achieves separately.

Please note that simulations are ran for a number of atmospheric conditions (May 2017, February 2017 and February 2014), on different operational parameters (fuel optimal and time optimal) and for different destinations (KIAD - Washington D.C., CYWG - Winnipeg and CYVR - Vancouver).

To be able to generalize the results as much as possible, the assumption of free track selection across the Atlantic Ocean is tested. This is done from cases where only ground tracks that follow the NATs of that day are allowed. Additionally a qualitative assessment of the step climb size, effect of changing the aircraft type and eastbound traffic is made.

CHAPTER 8

RESULTS

After elaborating on relevant literature in Chapters 2 to 4 and describing the model in detail in Chapter 5 and testing it in Chapter 6, in Chapter 8 the results from running various scenarios are presented.

The chapter is structured as follows. At first, the baseline flight plan is presented starting with the most simple cases and introducing complexities along the way in Section 8.1. Section 8.2 introduces cases where ground track alterations are used as a mitigation strategy. After this, Section 8.3 shows the results from profile-only contrail mitigation simulations. Section 8.4 goes on to explore the potential of a hybrid approach after which a contrail mitigation sensitivity analysis is performed as presented in Section 8.5. Finally the effect of changing various constraints and other simulation parameters is demonstrated in Section 8.6. A complete overview of numeric results is provided in the Appendix.

8.1 Baseline flight plan

The baseline flight plan is presented for three reasons. First, before any contrail mitigation strategy is applied the traditional flight plan needs to be determined. It comes natural that the result of that process is given prior to mitigation results. Second, by increasing the relative complexity of the scenarios that are presented it becomes easier to thoroughly understand the model and interpret results and implications thereof. Third, the changes in particularly fuel consumption and flight time as a result of contrail mitigation need to be placed in a wider context to be able to assess them. Among other things this chapter provides some insight into the effect of wind, origin-destination, difference in atmospheric conditions and cost index used for flights.

8.1.1 Baseline flight plan in ISA to Washington D.C.

The first step in evaluating a number of contrail mitigated trajectories is simulating a simplified model. Rather than right away using NWP data including wind, temperature and humidity initially only the ISA model is used. As can be seen in Figure 8.1 the ground track in this very closely resembles a great circle track, just like expected when wind is ignored. It can be seen that after departure from the Netherlands, the trajectory crosses over the UK and the North of Ireland. The aircraft then crosses over Newfoundland and enters US airspace where it follows the appropriate airways to Washington D.C. Using this track and the optimal flight profile for ISA conditions, the altitude and velocity along the flight are obtained and plotted as can be seen in Figure 8.2. As is typical for large commercial jet aircraft the cruise altitude

varies between FL300 and FL400 and increases as the aircraft loses weight. Due to decreasing temperature, which directly influences the speed of sound, the true airspeed decreases slightly. The Mach number stays close to 0.85 during the entire flight as it does in practice. A three dimensional visualization of the final trajectory can be seen in Figure 8.3. Additionally, the development of the aircraft mass and flight time is given as a function of the horizontal distance travelled as shown in Figure 8.4. As expected both are close to linear though closer inspection shows a slight effect of decreasing velocity on time and that of the mass on its derivative (fuel flow).

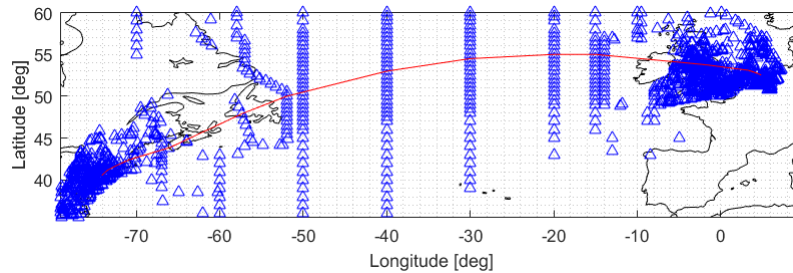


Figure 8.1: Fuel optimal ground track to Washington D.C. (KIAD) in ISA

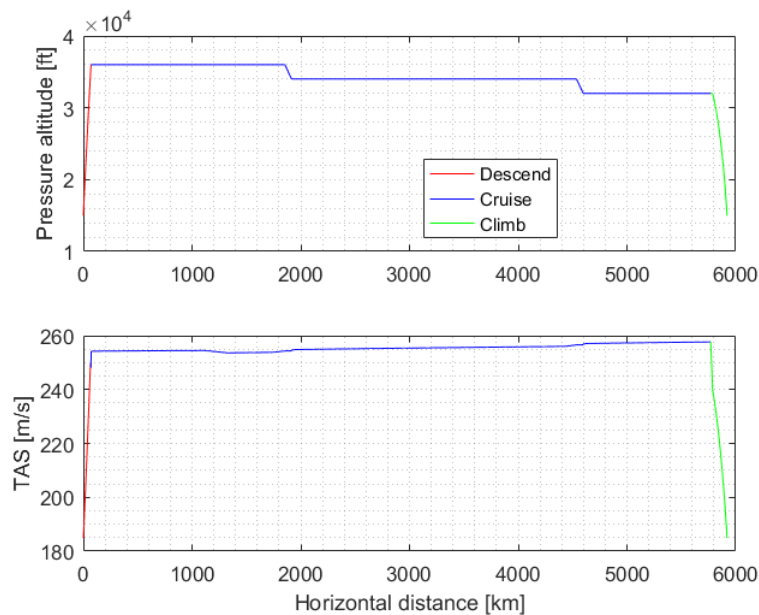


Figure 8.2: Fuel optimal flight profile to Washington D.C. (KIAD) in ISA

As discussed in Chapter 5 the model uses the cost index as one of the inputs. This value determines the relative cost of fuel and time in the cruise conditions cost optimization. A cost index of zero translates to a fuel optimal flight where time, and therefore speed, is not intrinsically valued. On the other hand at a large cost index, conditions correspond to a time optimal flight, where fuel cost is deemed irrelevant. Given the target of emulating a realistic flight planning situation and the fact that commercial tools do use it, this thesis should also include results obtained for other situations that fuel optimal. Given the difficulty of relating a particular value of cost index in the model to the ones used by airlines only the two extremes were used. Table 8.1 shows beginning and end states of mass, time and horizontal distance along with the difference between the two moments. It does so for both fuel optimal and time

8. Results

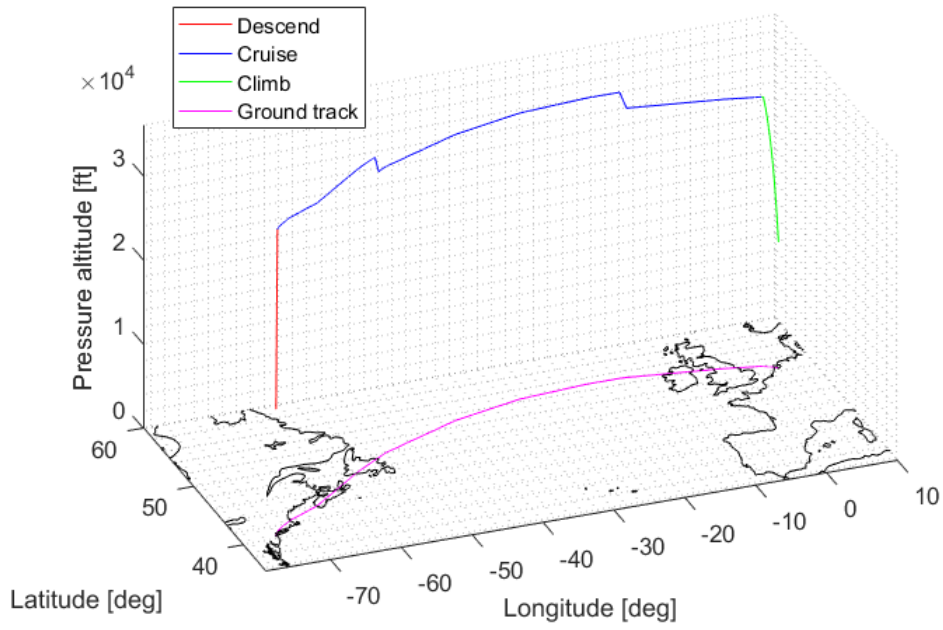


Figure 8.3: Fuel optimal three dimensional trajectory to Washington D.C. (KIAD) in ISA

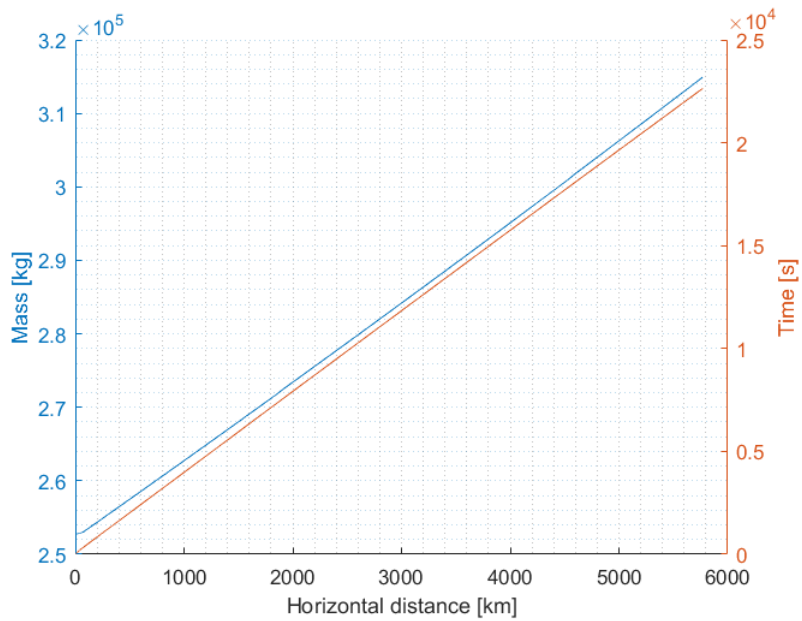


Figure 8.4: Mass and time development of fuel optimal flight to Washington D.C. (KIAD) in ISA as function of horizontal distance

optimal flights from the Netherlands to Washington D.C. in ISA. It should be noted that the time optimal flight follows the same ground track, however it remains at FL280 during the entire cruise phase of the flight while maintaining Mach 0.90 which is the maximum allowed Mach number. When considering Figure 6.1, it can be seen that these conditions correspond to the highest velocity in the flight envelope, where the boundaries for maximum CAS and Mach meet while respecting the 2000 ft allowed flight level interval.

As can be seen in Table 8.1 the fuel optimal flight consumes close to 65 metric tons of fuel and takes close to 6.5 hours to travel nearly 5900 km. It should be noted that this excludes any time and fuel for taxi, take-off and initial climb to 15000 feet, as well as descent from 15000 feet, landing and taxi at the destination airport. The time optimal case has as expected a higher fuel consumption at slightly over 72 metric tons though the flight time is decreased to just over 6 hours. For the given conditions, the difference between optimal fuel and optimal time is 7.2 metric tons of fuel and about 27 minutes of flight time.

Table 8.1: Results from non-mitigated fuel optimal and time optimal flights in ISA

	ISA - no wind - fuel optimal	ISA - no wind - time optimal	unit
m_{TO}	317,512	324,729	kg
m_{Land}	252,672	252,672	kg
t_{TO}	0	0	s
t_{Land}	23,227	21,610	s
s_{TO}	0	0	km
s_{Land}	5,897.366	5,897.366	km
dm	64,840	72,057	kg
dt	6h 27m 7s	6h 0m 10s	h:m:s
ds	5,897.366	5,897.366	km

8.1.2 Baseline flight plan in NWP without wind

Replacing the ISA model by NWP data changes a number of factors which can be seen in Figures 8.5 and 8.6. Most important for this thesis is the fact that contrail regions can only be mapped when temperature, pressure and humidity are known. Since ISA does not include humidity the NWP data gives insight into physical locations of regions where persistent contrails will form. These regions can be seen as the yellow areas in Figures 8.5 and 8.6. It is clear that for fuel optimal flight, contrails are generated whereas time optimal flights do not generate persistent contrails on this ground track. Secondly, changes of the previously mentioned properties in the horizontal plane mean that optimal conditions are not constant in this plane. As is discussed in Section 6.2.2 this may cause steps downward, which contradicts the standard situation where only step climbs are seen. This can be seen from the step at approximately 1700km in Figure 8.5. As discussed in Section 6.2.2, this is caused by temperature variations which change the local speed of sound and thus the Mach number. Since drag is a function of the Mach number this changes the required thrust, which changes fuel flow. In short, temperature changes lead to different cruise conditions which may lead to different optimal altitudes and velocities on the same pressure altitude. Furthermore, the ground track in both fuel and time optimal flight cases will be identical as the edge weights in the optimal path are either dependent on ground distance, local wind conditions and contrail formation conditions. As this scenario contains no wind effects or contrail mitigation, the edge weights are identical for time and fuel optimal cases. The profiles however are very different as can be seen in Figures 8.5 and 8.6. Fuel optimal flight follows the traditional increase in flight level as the aircraft loses

8. Results

weight (with exception of a single step down). The time optimal case adheres closely to the time optimal altitude of FL280 across the entire flight. At this altitude the maximum TAS is achieved while respecting CAS and Mach constraints. Table 8.2 shows the numeric results of non-mitigated fuel optimal and time optimal flights to Washington D.C. (KIAD) in the May 2017 NWP without wind.

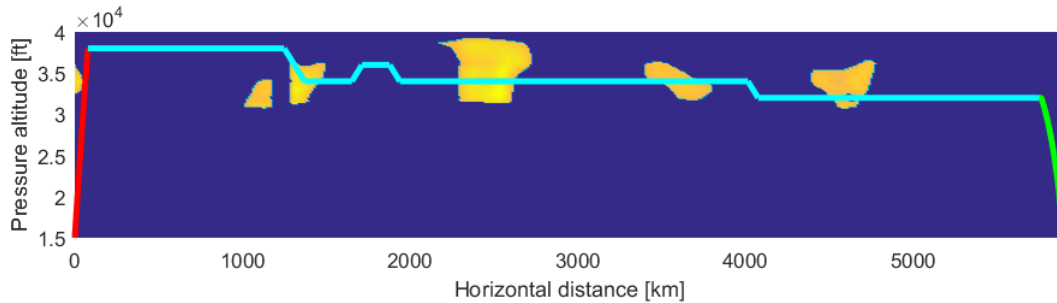


Figure 8.5: Fuel optimal flight to Washington D.C. (KIAD) in NWP May 2017 without wind

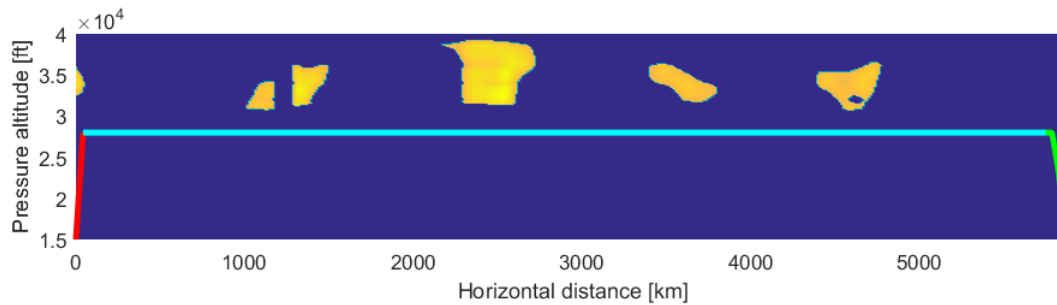


Figure 8.6: Time optimal flight to Washington D.C. (KIAD) in NWP May 2017 without wind

Table 8.2: Numeric results of non-mitigated fuel optimal and time optimal flights to Washington D.C. (KIAD) in May 2017 NWP without wind

	no wind - fuel optimal	no wind - time optimal	unit
m_{TO}	317,566	323,917	<i>kg</i>
m_{Land}	252,672	252,672	<i>kg</i>
t_{TO}	0	0	<i>s</i>
t_{Land}	23,307	21,709	<i>s</i>
s_{TO}	0	0	<i>km</i>
s_{Land}	5,897.366	5,897.365	<i>km</i>
dm	64,894	71,245	<i>kg</i>
dt	6h 28m 27s	6h 1m 49s	<i>h:m:s</i>
ds	5,897.366	5,897.365	<i>km</i>

8.1.3 Baseline flight plan in NWP with wind

After inclusion of the local atmospheric conditions, also the effect of wind is added to the model. Figure 8.7 shows the ground track of two fuel optimal flights to Washington D.C. with and without incorporation of the wind. It can clearly be seen that after leaving the European continent, the two lines diverge. The green line (no wind) follows the great circle arc as closely as possible given the network topology. The red line however (with wind) avoids an area of strong headwind by taking a more southerly route. The largest difference between these flights

therefore is the total distance travelled through the air.

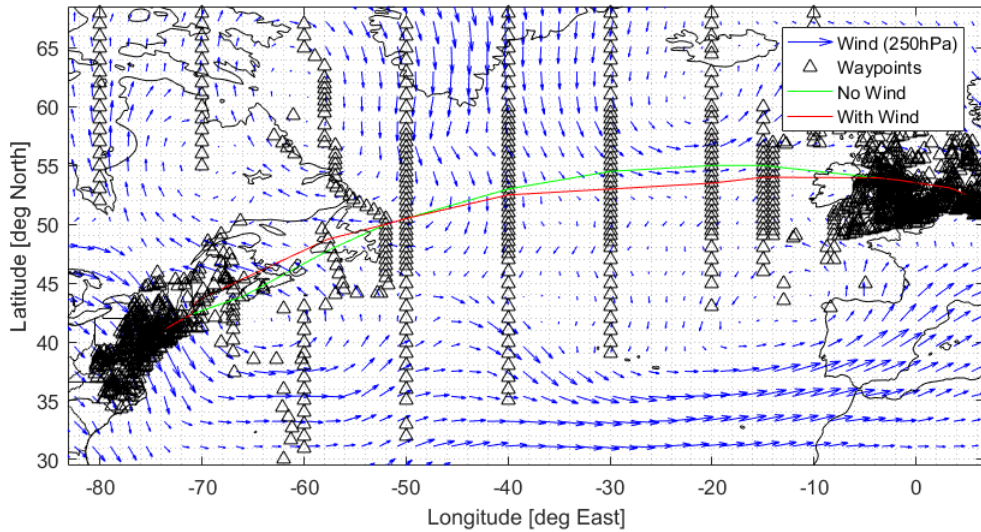


Figure 8.7: Ground track of fuel optimal flight in NWP May 2017 with and without wind

Table 8.3 shows the effect of wind on both fuel and time optimal flights in the May 2017 atmosphere. It can be seen that the smallest air distance for the fuel optimal flight is 5871 kilometers compared to a minimum a minimum ground distance of 5926 kilometers. Over the course of the flight with wind taken into account, the total flight time is 207 seconds shorter and the fuel consumption is 606 kg less. For the time optimal case the flight is effectively nearly 55 kilometers shorter, 195 seconds faster and consumes 647 kg less fuel. It should be noted that the "no wind" simulation differs from the results shown in Section 8.1.2. This is because the results as shown in this section differ only in the ground track. The minimum ground distance case therefore uses the ground track as if there was no wind, however during simulation the wind is incorporated. This was done to create a fair comparison between the ground distance optimal track and the air distance optimal track as shown in Table 8.3. Compare this to the previous section where wind is not considered at all during track generation or simulation.

Table 8.3: Comparison of numeric results of non-mitigated fuel optimal and time optimal flights to Washington D.C. (KIAD) in May 2017 NWP with wind and without wind

	Fuel optimal		Time optimal		unit
	Min ground distance	Min air distance	Min ground distance	Min air distance	
m_{TO}	317,911	317,302	324,409	323,762	kg
m_{Land}	252,672	252,672	252,672	252,672	kg
t_{TO}	0	0	0	0	s
t_{Land}	23,425	23,218	21,855	21,661	s
s_{TO}	0	0	0	0	km
s_{Land}	5,926.332	5,871.104	5,936.977	5,882.411	km
dm	65,239	64,630	71,737	71,090	kg
dt	6h 30m 25s	6h 26m 58s	6h 4m 15s	6h 1m 1s	h:m:s
ds	5,926.332	5,871.104	5,936.977	5,882.411	km

8. Results

8.1.4 Baseline flight plans to Winnipeg and Vancouver

The final step in demonstrating a complete baseline flight plan is inclusion of the alternative destinations. Besides Washington D.C. (KIAD), two other airports in North America have been selected. In order to fully explore trajectories along the more contrail prone northern routes, Winnipeg (CYWG) and Vancouver (CYVR) were selected as the second and third option. The largest difference compared to Washington D.C. is that these flights are longer in distance and time and follow a more northern trajectory. This means that more fuel is taken on board which leads to a lower cruise altitude during the first stage of the flight. Furthermore, the northern trajectories are more likely to encounter contrail regions. Table 8.4 shows the results of these flights.

Table 8.4: Comparison of numeric results of non-mitigated fuel optimal and time optimal flights to different destinations in May 2017 NWP including wind

	Fuel optimal			Time optimal			unit
	KIAD	CYWG	CYVR	KIAD	CYWG	CYVR	
m_{TO}	317,302	325,249	340,452	323,762	332,568	348,472	kg
m_{Land}	252,672	252,672	252,672	252,672	252,672	252,672	kg
t_{TO}	0	0	0	0	0	0	s
t_{Land}	23.218	25.938	31.015	21.661	24.273	28.912	s
s_{TO}	0	0	0	0	0	0	km
s_{Land}	5,871.104	6,613.080	7,931.614	5,882.411	6,594.946	7,837.486	km
dm	64,630	72,577	87,780	71,090	79,896	95,800	kg
dt	6h 26m 58s	7h 12m 17s	8h 36m 55s	6h 1m 1s	6h 44m 33s	8h 1m 52s	h:m:s
ds	5,871.104	6,613.080	7,931.614	5,882.412	6,594.946	7,837.486	km

8.2 Ground track selection

As mentioned, the ground track optimization uses the contrail distance and weighting parameter β_{grnd} on each edge along with the air distance to come up with a total cost. This contrail distance is of course based on an estimate for cruise altitude. Simulation of the flight along the optimal track as determined by Dijkstra's algorithm is necessary to determine the final contrail distance and aircraft state history. This section presents the results from these simulations.

8.2.1 Fuel optimal flights

Figure 8.8 shows the relation between β_{grnd} and contrail distance and fuel consumption for fuel optimal flights compared to the non-mitigated case. What is clear is that ground track alterations can indeed be used to mitigate contrails at the expense of some additional fuel (and flight time). At no point are more contrail generated than the corresponding baseline. At low values of β_{grnd} the mitigation effect is relatively low, though additional fuel burn here is also rather low. At higher values, larger portions of contrails can be mitigated and in some cases they are avoided completely while additional fuel consumption stays below 10 % for most flights. The discrete steps in the graph are caused by the distinct changes in ground track. Obviously the size of these steps and their location is dependent on local contrail region size and shape but regardless, a trend can clearly be seen that shows a trade off between contrail distance and fuel consumption as β_{grnd} increases. Mitigation results on fuel consumption are diminishing as they get closer to zero.

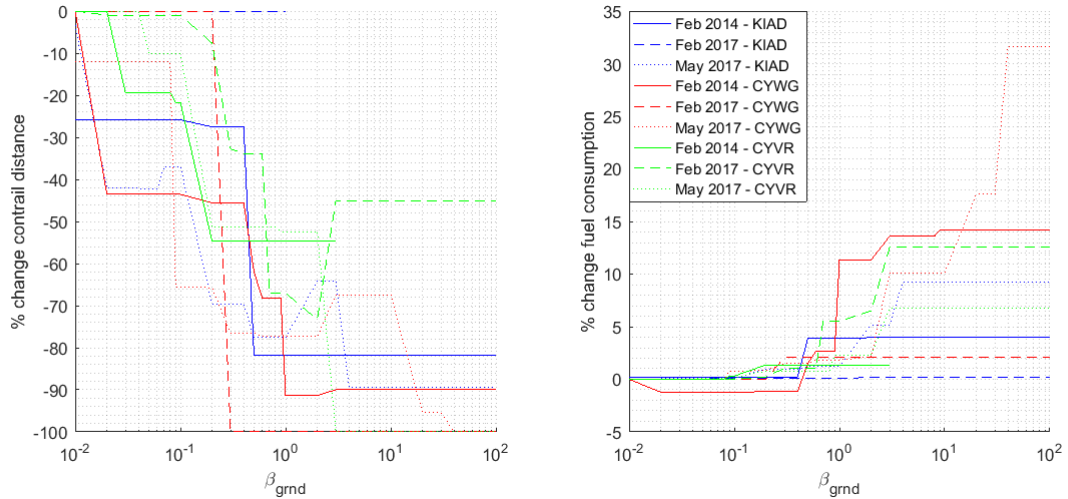


Figure 8.8: Fuel optimal flights: effect of β_{grnd} on contrail distance and fuel consumption

It can be seen from Figure 8.8 that ground track optimization cannot always mitigate contrails completely. A number of cases end with a constant, nonzero amount of contrails. The fuel optimal flight to Washington D.C. (KIAD) in the February 2014 NWP is an example of that, finishing at slightly over 80% mitigated. At the same time also no increase in fuel consumption occurs since the track stays the same.

What can also be seen is that for some flights, the contrails generated may increase as β_{grnd} increases. This is caused by the fact that the ground track is selected based on an early estimate of cruise conditions. The results in this chapter however follow from simulating a flight over that particular ground track. Increases in contrails generated for increasing β_{grnd} therefore are caused by estimation errors in the contrail portion of the edge weights in the ground track. The same holds for decreases in fuel consumption as this is based on the air distance encountered at the cruise altitude prediction. Air distance errors however should be extremely small as their deviation from the actual situation is much less prone to large errors. In other words, potential wind speed difference between two flight levels is much lower than contrail distance could be (e.g. if they were on the boundary of a contrail region).

8.2.2 Time optimal flights

Figure 8.9 shows the relation between β_{grnd} and contrail distance and flight time for time optimal flights compared to the non-mitigated case. It is clear that just like for fuel optimal flights, a contrail penalty can be used to alter ground tracks of time optimal flights in a way that mitigates contrails at the expense of flight time (and fuel consumption). The graph shows a similar progression of contrail mitigation as β_{grnd} increases. Compared to fuel optimal flights the mitigation potential is slightly higher though. At approximately $\beta_{grnd} = 1$, contrails can be seen to be mitigated more than 70% in most cases while additional flight time hardly exceeds a few percent. More mitigation however is relatively costly as a further increase to 90% mitigation results in a much larger 15-30% increase in flight time. Mitigation results on flight time are therefore diminishing as they get closer to zero.

8. Results

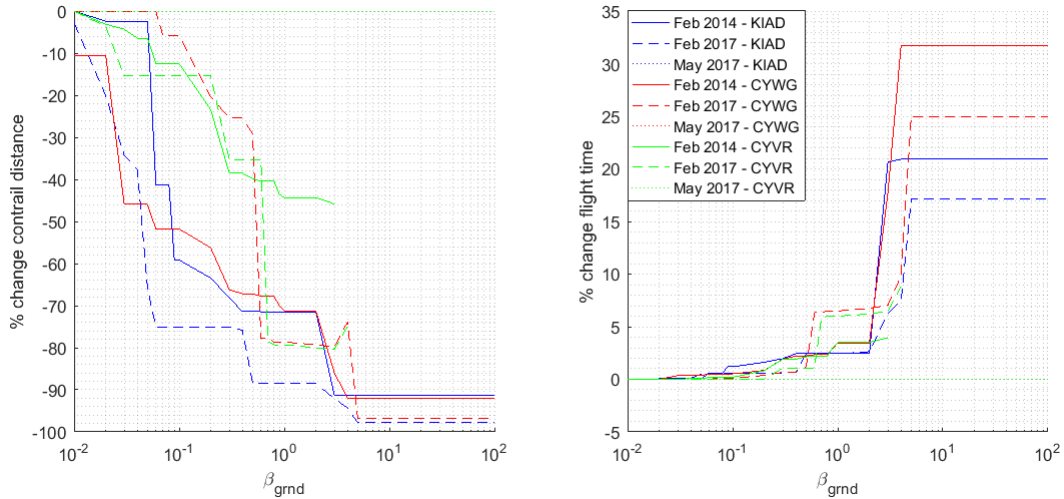


Figure 8.9: Time optimal flights: effect of β_{grnd} on contrail distance and flight time

It should be noted that in May 2017 NWP there are no persistent contrails generated at any stage of the flight. Also some conditions feature no data for higher values of β_{grnd} because the resulting flight path distance exceeds the aircraft range for the given conditions. This can be seen by the absence of dotted lines that would show the May 2017 data and early end of the green lines which would otherwise show the values of flight to Vancouver (CYVR) for higher values of β_{grnd} .

Based in Section 8.2, simulation of flights along contrail weighted ground tracks shows that ground track alterations can be used to mitigate contrails. Especially at low values of β_{grnd} large shares of contrails are mitigated at very low fuel and time cost. Higher values show additional fuel consumption below 10% for most fuel optimal flights. Time optimal flights show at most a few percent additional flight time at 70% contrails mitigated and 15-30% additional time at 90% contrails mitigated.

8.3 Altitude profile optimization

As explained in Section 5.7 the altitude profile optimization uses step climbs and descents to avoid contrails. The ground track is kept constant throughout. A differential evolution algorithm locally optimizes an objective function by changing a set of decision variables. The objective function features contrail distance, as well as extra fuel consumption and flight time. The decision variables are the the decisions (climb, hold or descend) taken at four distinct points and their locations. The locations of the first and last decision is not variable, as well as the decision at the final location. This ensures the flight ends at the same altitude compared to the original trajectory. This all results in five decision variables that determine the profile change for each contrail region as seen in Figure 5.17.

This section presents the results obtained from the profile optimization. Changes that are typically seen as the profile contrail cost parameter β_{prof} changes are shown in Figure 6.15. Resulting changes in contrails, fuel consumption and flight time are presented here.

Figure 8.10 shows the relation between β_{prof} and contrail distance and fuel consumption for

fuel optimal flights compared to the non-mitigated case. What can be found is a decrease of contrails generated at the expense of slightly higher fuel consumption and very small increase in flight time in fuel optimal cases. Time optimal flights can be seen to decrease their fuel consumption and increase in flight time as contrail distance generated decreases. From β_{prof} exceeding a value of approximately 0.05, its effect is practically constant in terms of contrails, fuel and time. As can be seen, the lines are not smooth but somewhat jagged, which can be explained by the stochastic nature of differential evolution and a hard limit for number of generations. Also due to the way the algorithms are constructed, some data cannot be compared fairly and is omitted from the average shown here. This also results in a less smooth curve.

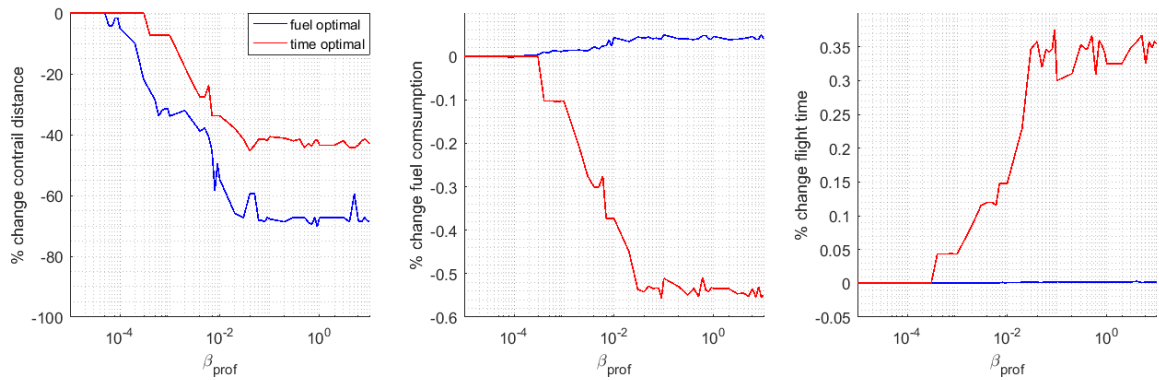


Figure 8.10: Average change in contrail distance, fuel consumption and flight time of fuel and time optimal flights as function of β_{prof}

One of the most striking observations in the graph is the scale used for fuel consumption and flight time, compared to the one for ground track mitigation. It can be seen that up to 70% of contrail for fuel optimal flights are mitigated at the expense of less than 0.1% additional fuel. In real terms this would correspond to in the order of 50kg additional fuel and an insignificant change of flight time. For time optimal flights it would imply 40% contrail savings at 0.55% less fuel and 0.35% additional time. This relates to up to 500kg fuel savings and 90 seconds of extra flight time. It is clear that these values are very promising, however it should be kept in mind that the simulation is ran assuming steady, horizontal flight. Step climbs are simulated with the assumption that all potential energy needed is provided by perfect conversion of surplus mechanical work ($F \cdot ds$) of the engines. In other words, the engines surplus thrust is converted one to one into potential energy. For practical reasons this is a useful assumption. In reality the change in fuel consumption as a result of profile changes is expected to be smaller than that of ground track changes, however it seems that this assumption has diminished the fuel cost of climbs even further. A further reason for this is the resolution of the optimal cruise grid. In some cases the simulation may encounter sub-optimal conditions in the normal cruise between nodes. Profile changes could in this case improve fuel consumption of a flight that is regarded as fuel optimal. As explained in Chapter 6 the maximum reasonable resolution is kept, however it is not perfect and sub-optimal conditions may occur, potentially leading to underestimation of fuel cost of profile mitigation trajectories.

It should be noted that time optimal flights find the altitude at which the maximum CAS and Mach number meet. Flying either higher or lower will result in a lower cruise speed and thus more flight time. A side effect when mitigating contrails however is that the lower cruise speed at mitigation altitudes results in lower fuel consumption. Therefore, deviating from the

8. Results

time optimal profile for contrail mitigation reasons decreases fuel consumption for the flight as well as increasing flight time rather than increasing fuel consumption as it does for most conventional flights.

The flight simulation uses an interpolation of the climb distance to determine when it is close to or at the TOC distance. The profile alterations use this same criterion, however if a step is required at the final node, this step is added after the stopping criterion for TOC was satisfied. An example of this can be seen in Figure 8.11. The result is that the flight is slightly longer or shorter and slightly misses its destination fix if the TOC is inside a contrail region. This is the case in the February 2014 NWP as can be seen from the data in Figure 8.10 where the flight to Washington D.C. (KIAD) is overshoot due to a profile alteration that goes over the non-mitigated profile and the one to Winnipeg (CYWG) is slightly undershot. Of course the fuel consumption of two profiles with different starting location cannot be compared fairly and thus are omitted from the data presented in Figure 8.10.

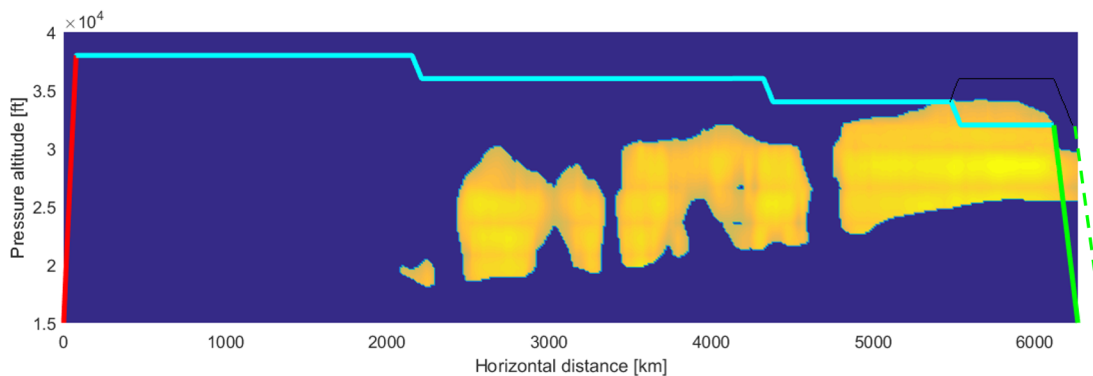


Figure 8.11: Origin overshoot due to TOC being inside contrail region as shown by the offset dashed climb phase (example of non-comparable output)

Section 8.3 shows the results of profile optimization for contrail mitigation. Although these are very case dependent it is clear that up to $\beta_{prof} = 0.05$ contrails are increasingly avoided. Fuel optimal flights shows an increased fuel consumption of less than 0.1% and negligible change in flight time. Time optimal flights are forced to reduce cruise speed which increases flight time up to 0.3% and reduced fuel consumption up to 0.55%. It should be noted that these results are generated based on a set of assumptions and limitations that may decrease the cost of a step climb and profile alterations compared to the every day operations. Regardless, it is clear that profile alterations are a much more efficient single strategy to mitigate contrails in most flights compared to ground track alterations.

8.4 Hybrid contrail mitigation

The results of separate ground track and profile mitigation strategies is shown in Sections 8.2 and 8.3. Since both restrict the freedom to alter the trajectory to a single plane, their results could be improved by combining the strategies. An optimal path that makes use of both ground track and profile alterations should perform better than either strategy by itself. Note that the results presented here are generated by sequential optimization of the ground track and profile. In essence, the results show a number of altitude profile mitigated trajectories performed on a set of optimal ground tracks.

For generation of the hybrid results, various combinations of β_{grnd} and β_{prof} need to be evaluated. In an ideal case this is matrix of results from the combinations of all β_{grnd} and β_{prof} as evaluated separately in Sections 8.2 and 8.3. Due to limited computational capacity however a subset of parameters need to be chosen. From empirical investigation it was found that the highest number of evaluations that is practically feasible is around 50. This results in a resolution of either 7x7, 6x8, 5x9 or 5x10 evaluations. In order to provide an equal number of samples from each type of weight the 7x7 square matrix option was chosen. From the relative impact of the contrail cost parameters as shown in Sections 8.2 and 8.3 the selection was made. Sections that are deemed as irrelevant because they add little information are disregarded for the hybrid optimization. An example of such a case are the values of β_{grnd} from 20 to 100 in Figures 8.8 and 8.9. In this region, nearly all lines remain flat which makes it much less interesting to investigate for the hybrid case. Due to the fact that the results for β_{grnd} are already known, the rest of the scale was divided into 7 sections. This gives a sample set of $\beta_{grnd} = [0 \ 0.01 \ 0.03 \ 0.1 \ 0.3 \ 1 \ 3 \ 10]$. Due to the use of a log scale, the halfway point between e.g. 1 and 10 is approximately 3 rather than 5 like it is in a linear scale. For the profile optimization part of hybrid optimization a similar selection process yields a sample set of $\beta_{prof} = [0 \ 10^{-5} \ 10^{-4} \ 10^{-3} \ 10^{-2} \ 10^{-1} \ 10^0 \ 10^1]$.

Figure 8.12 shows the change in contrail distance for a range of β_{grnd} and β_{prof} . On the left the results for fuel optimal flights can be found and the right hand side shows time optimal flights. As is clear from the high peaks, a very small value for both contrail cost parameters results in no change in contrail distance. As these increase however the contrails that are generated are mitigated to a comparable degree. As expected, in most cases a combination of both gives an improvement on the result of only a single cost parameter. It can be seen that their impact is dependent on the other, as demonstrated by the small impact of β_{prof} at high β_{grnd} . The logical conclusion is that the combination with the best mitigation return on fuel and time should be selected in potential future application.

What is also clear from Figure 8.12 is that the average effect of both cost parameters levels off. A strong decline in the mitigating effect can be seen after β_{grnd} exceeds approximately 1, and β_{prof} exceeds 0.1 for both fuel and time optimal flights. Furthermore, the mitigating effect for both is similar in magnitude. Time optimal flights can however be observed to get close to generating absolutely no contrails using only a single mitigation action, whereas fuel optimal flights need a combination to achieve this. It should be noted that the results here are average results and underlying cases that do not yield valid results are omitted. Examples are extremely long (unfeasible) routes on high β_{grnd} tracks to Vancouver (CYVR) and trajectories that do not generate any contrails to begin with (time optimal in May 2017 NWP).

8. Results

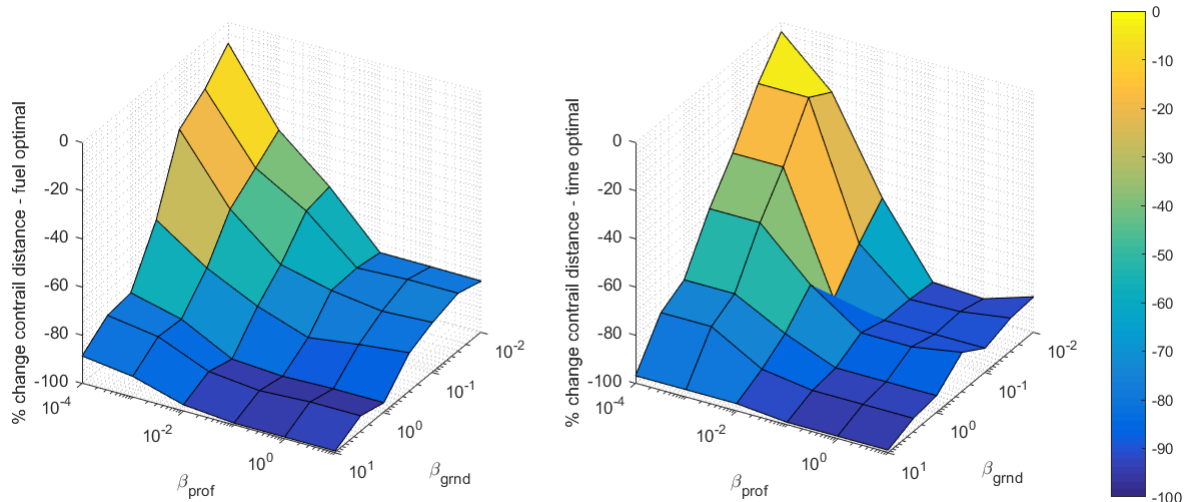


Figure 8.12: Average change in contrail distance of fuel optimal (left) and time optimal (right) flights for various β_{grnd} and β_{prof}

Figure 8.13 shows the average change in fuel consumption of fuel optimal flights (left) and average change in flight time for time optimal flights (right) as function of β_{grnd} and β_{prof} . In order to obtain a clear view of the surface, the orientation of the x and y axes are different compared to Figure 8.12. What is clear is that both fuel and flight time changes very little with β_{prof} compared to β_{grnd} . This is confirmed by observations from Sections 8.2 and 8.3 where changes in profile results in much smaller fuel and time changes compared to track alterations. Changes of hybrid results are of the same magnitude for both. It can however be seen that for time optimal flights at low β_{grnd} , increasing β_{prof} leads to small but visible changes in flight time. Changes in fuel consumption due to profile changes are too small to be visible compared to those of track alterations in the hybrid plot. Again, it is expected that the change of both fuel and time for profile alterations is smaller than that of profile alterations, however due to some assumptions and computation constraints this effect is magnified.

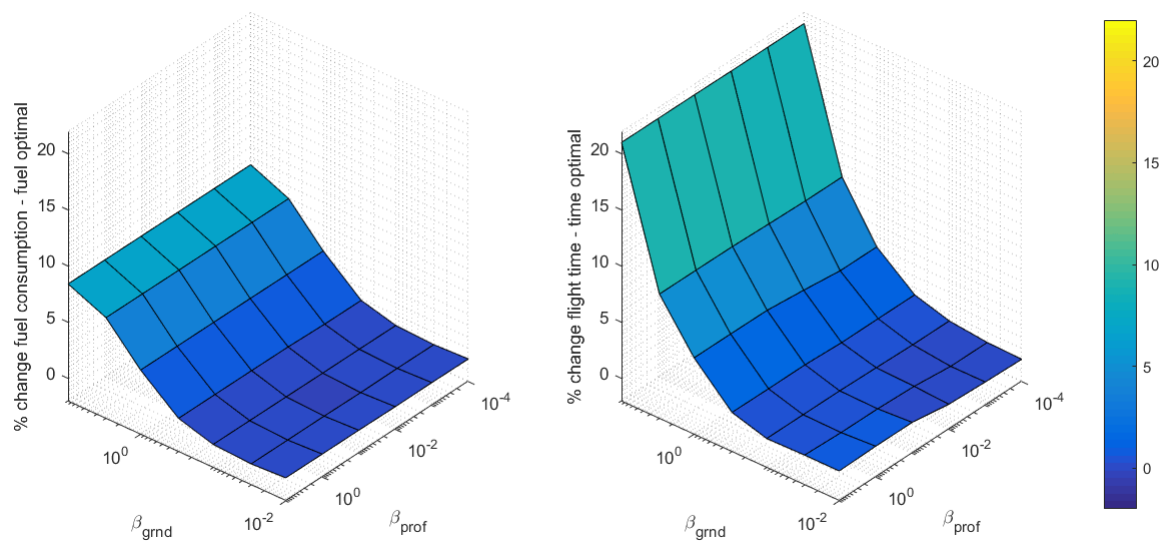


Figure 8.13: Average change in fuel consumption of fuel optimal flights (left) and flight time of time optimal flights (right) for various β_{grnd} and β_{prof}

When considering all of Section 8.4 the following can be said. Hybrid mitigation shows characteristics of both ground and profile mitigation strategies, however it outperforms the individual strategies as expected. While results are very case dependent it is clear that a majority of contrails can be mitigated at very low additional fuel and flight time. Given the large difference in the cost of ground track alterations compared to profile optimization as seen in Figure 8.13 the emphasis should be on the latter.

8.5 Sensitivity of contrail mitigation

Sections 8.2 to 8.4 show the change in contrails, fuel consumption and flight time for various contrail cost parameters. The main question that this thesis aims to answer however is what amount of fuel and flight time is associated with a certain amount of contrail mitigation. This section aims to assess this question by presenting sensitivity analyses of both separate contrail cost parameters and the hybrid case.

8.5.1 Ground track selection sensitivity

Figure 8.14 shows the sensitivity of contrail distance compared to fuel and flight time for ground track mitigated flights. It can be clearly seen that as more contrails are mitigated, this costs more fuel and flight time to achieve. It can also be seen that nearly half of all contrails can be mitigated against 2-3% additional fuel and flight time. A hypothetical trend line could show a more generalized version of what is reasonable to expect given the scenarios tested. The exact value is of course very dependent on the case and some cases even show 80% contrails mitigated against less than 2% additional fuel and time. These values seem to correspond to the results found in literature as mentioned in Chapter 2.

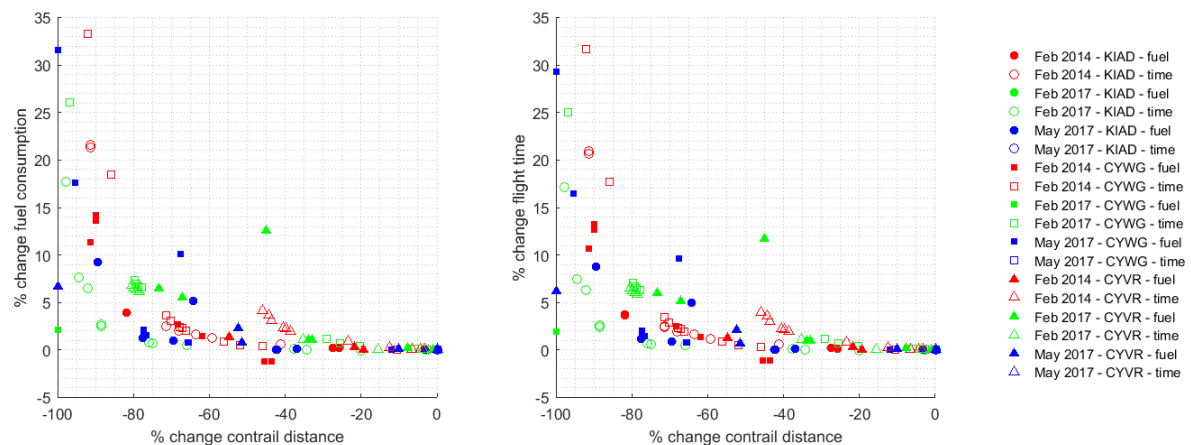


Figure 8.14: Sensitivity of ground track contrail mitigation on fuel and flight time

8.5.2 Altitude profile optimization sensitivity

Profile alterations have a very different effect on fuel consumption and flight time for time optimal flights compared to fuel optimal. Therefore, the results of these two flight conditions are presented separately.

Figure 8.15 shows the sensitivity of contrail distance compared to fuel and flight time for profile mitigated fuel optimal flights. This relation is not as clear as the one shown for ground

8. Results

track selection, however it can be seen that increasing contrail mitigation requires additional fuel and flight time. The values however are very case dependent for previously mentioned reasons, those being optimal cruise grid inter-node conditions, the assumption of steady horizontal flight and perfect conversion between surplus work from the engines to potential energy and vice versa. These are combined with the complex shape of contrail regions, constraints on decision variables and evaluations of objective function and the use of a meta-heuristic optimization method to obtain the results as shown. Regardless, a trend of increasing fuel and flight time for mitigating contrails can be seen. Additionally, it is shown that the relative cost of profile mitigation is smaller compared to track alterations, although the exact quantity is difficult to predict accurately.

One of the things that can be seen in Figure 8.15 is an improvement of fuel consumption for the flight to Vancouver (CYVR) in February 2014 NWP. If the baseline truly represents the most optimal flight, this should of course not be possible, however given the resolution of the cruise conditions grid, it was found that in this case, a profile alteration found better cruise conditions compared to the one dictated by the grid. On the other hand, the flight to Winnipeg (CYWG) in February 2017 NWP shows a sharp increase in fuel and does not move past 50% contrails mitigated. In the end, it is mostly the size and shape of the contrail region that determines how much mitigation is possible for a given flight.

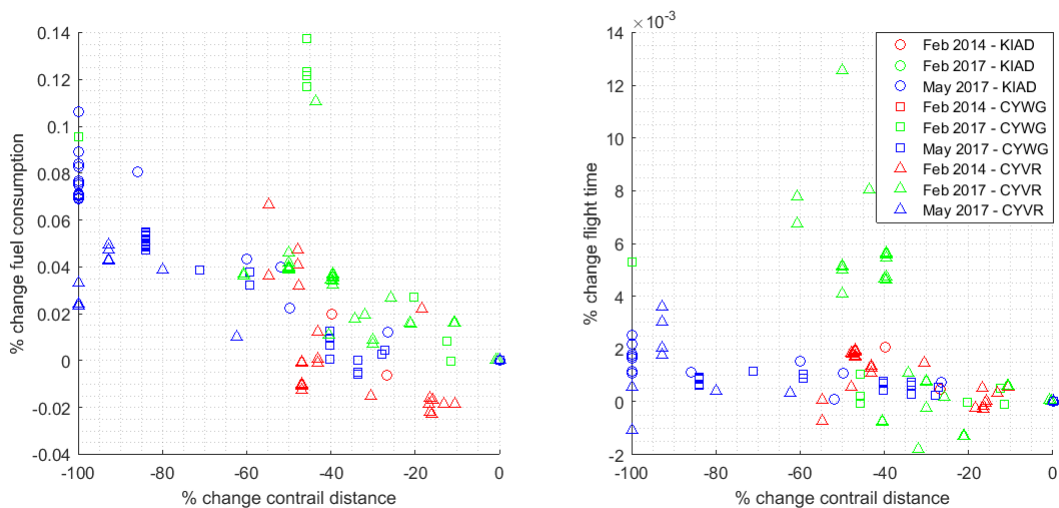


Figure 8.15: Sensitivity of profile based contrail mitigation on fuel and flight time for fuel optimal flights

Figure 8.16 shows the sensitivity of contrail distance compared to fuel and flight time for profile mitigated time optimal flights. Compared to fuel optimal flights it is much less colorful for two reasons. Time optimal flights in the May 2017 NWP encounter no contrail regions and therefore cannot be mitigated. On top of that, all time optimal flights in the February 2014 NWP have their TOC inside a contrail regions. This leads to an unfair comparison of data as they overshoot the origin as shown in Figure 8.11. This leaves the data as seen in the figure. It shows a counter intuitive relation between contrail mitigation and fuel consumption. As explained in Section 8.3, deviation from the time optimal altitude results in a decrease in cruise speed with corresponding decrease in fuel consumption and increase in flight time. Time optimal flights therefore can reduce fuel consumption up to 1.3% while reducing over 80% of contrails. Flight time in this case is however increases 0.5-0.7% depending on the destination.

Again, this is solely based on atmospheric conditions of a single moment in time compared to multiple for fuel optimal results.

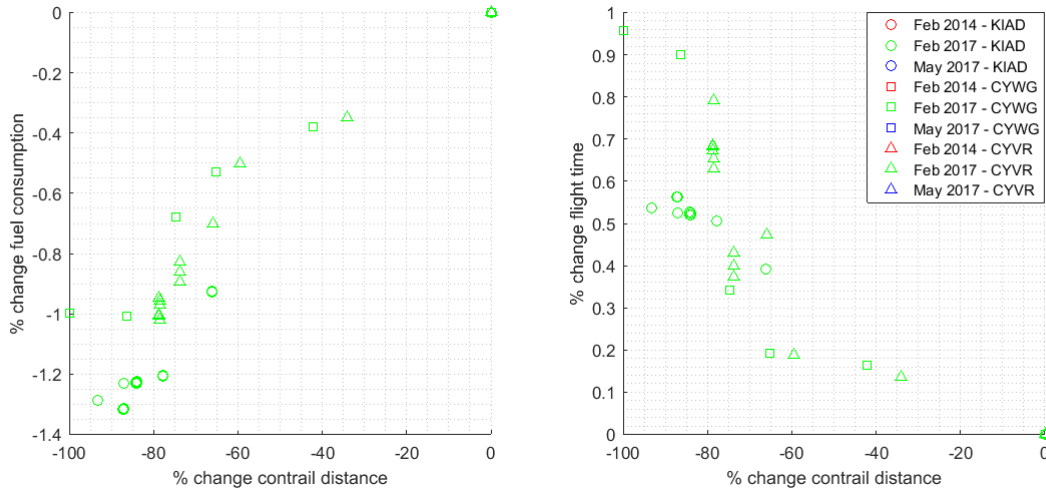


Figure 8.16: Sensitivity of profile based contrail mitigation on fuel and flight time for time optimal flights

8.5.3 Hybrid contrail mitigation sensitivity

Figure 8.17 shows the sensitivity of contrail distance compared to fuel and flight time for hybrid mitigated fuel optimal flights. On the left the change in fuel consumption for fuel optimal flights is shown and on the right the change in flight time for time optimal flights. When comparing these results to those of the two separate mitigation strategies, it is clear that the hybrid case contains features of both. Again results are very case dependent, however what is clear is that at least 50% of contrails can be mitigated at less than 2% additional fuel which improves on the ground track selection only strategy. For higher mitigation percentages the results are much more diverse and may range from close to 0 to 14% fuel at over 80% contrail mitigation. As for time optimal flights there are similar conclusions to be made. A large part (40-60%) of contrails can be mitigated while flight time increases at most a few percent. For higher contrail mitigation (over 80%) this may increase to more than 20% additional flight time.

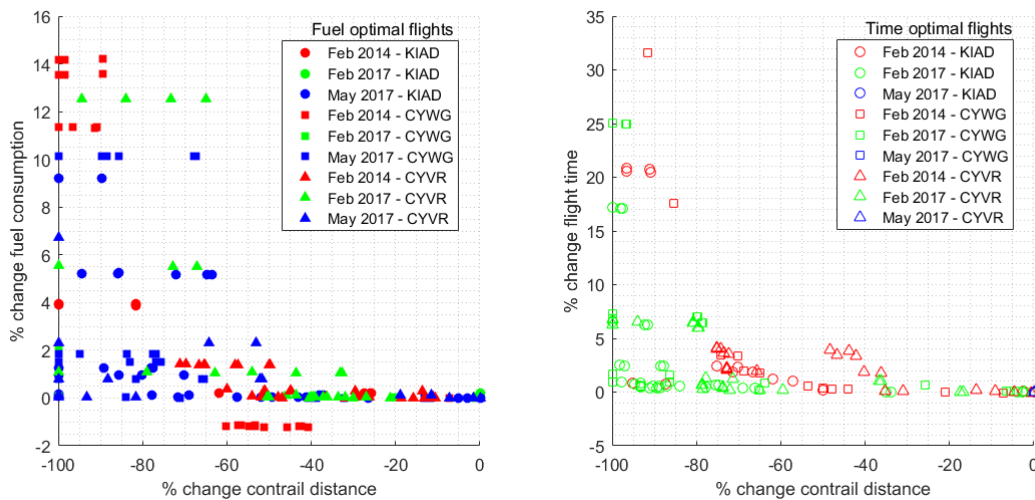


Figure 8.17: Sensitivity of hybrid contrail mitigation on fuel consumption and flight time

8. Results

It can be observed that in one case the fuel optimal flight is improved upon in terms of fuel consumption when mitigating contrails. Just like mentioned in for the profile mitigation sensitivity this is a consequence of the resolution of the optimal cruise conditions grid. Between nodes this may lead to sub-optimal conditions compared to actual optimal altitude and velocity. Given the restrictions imposed by (computation) time and complexity this was deemed acceptable.

Summarizing, by means of ground track alterations nearly half of all contrails can be mitigated against 2-3% additional fuel and flight time. Profile mitigation shows a different image for fuel optimal flights compared to time optimal. For fuel optimal flights there is a trend of increasing fuel consumption up to 0.1% with decreasing contrail distance, albeit very case dependent. For time optimal flights the case is reversed. Due to operational constraints any profile alteration leads to a lower cruise velocity which comes with increases in flight time and reduced fuel consumption. Over 80% of contrails can be mitigated while reducing fuel approximately 1.2% and increasing flight time by 0.4-0.8%. For hybrid mitigation results are also very case dependent. What is clear is that at least 50% of contrails can be mitigated at less than 2% additional fuel which exceeds ground track selection only strategy (i.e. hybrid outperforms a single dimension strategy).

8.6 Alternative scenarios and constraints

Chapter 8 presents the results that are generated from simulation and optimization of a set of scenarios. These aim to provide a representative set and conclusions that are also generalizable to some extent. In order to add to this purpose, some additional factors are explored that help bring the insights to a higher level. This section goes into the effect of fixing the North Atlantic Tracks, size of the step climb, changing aircraft type and flying eastbound rather than westbound.

8.6.1 Fixed North Atlantic Tracks

The majority of this thesis assumes the ability to freely determine a ground track across the Atlantic Ocean. In practice however the NAT system is still in use which restricts lateral movement. Since the tracks at the time of the February 2014 NWP are not available only the other two days are considered. The westbound tracks are processed and their track from entering to exiting the NAT is fixed.

Since this constraint is set on the track and not on profile alterations it is assumed that the effectiveness of this mitigation strategy is not influenced. It may be that given a slightly different track compared to the "free" cases as presented in the rest of this thesis the contrail regions that are encountered are different, however there is no difference in how they are mitigated by means of profile alterations. Therefore it is interesting to see how much track alterations can be used to mitigate profile when NATs are fixed.

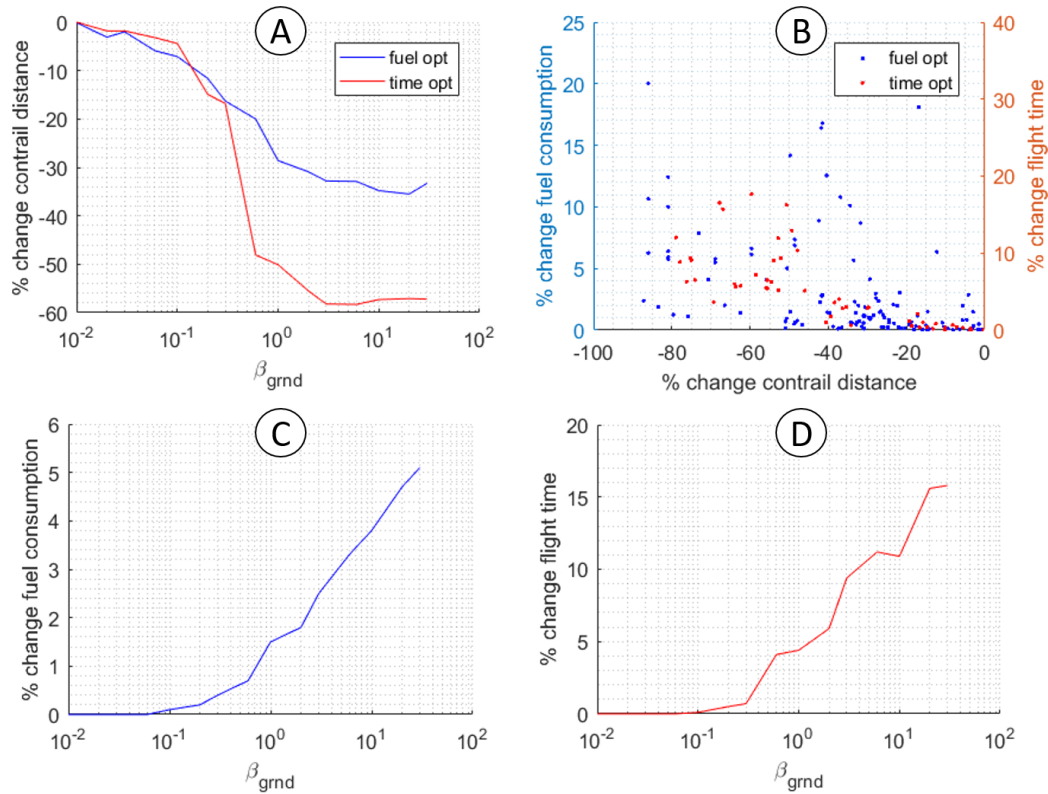


Figure 8.18: Results from ground track alterations given fixed NATs - A) contrail mitigation vs β_{grnd} , B) sensitivity of ground track alterations of fixed NAT routes for fuel consumption of fuel optimal flights on left y-axis and flight time for time optimal flights on right y-axis, C) additional fuel consumption vs β_{grnd} of fuel optimal flights, D) additional flight time vs β_{grnd} of time optimal flights

Figure 8.18 shows the results of contrail mitigation for the case where the ground track is fixed during the NAT sections of the flight. On the top left (A) it can be seen that as β_{grnd} increases the average amount of contrails generated decreases to approximately 30-35% for time optimal flights and 55-60% for fuel optimal flights. It is no surprise that if a large part of the track is fixed, the mitigation potential is smaller than the free ground track alterations. The lines level off at approximately the same order of magnitude β_{grnd} compared to the free cases. It can be seen that just as with the original ground track alterations a small increase of contrail distance with increasing β_{grnd} . This is caused by the same estimation errors and sample size changes as mentioned before. The response of both fuel and time optimal flights in terms of fuel consumption and flight time changes can be found in the bottom figures (C and D). These are again averages and indicate a trend rather than absolute values corresponding to specific cases. The top right graph in Figure 8.18 (B) shows the sensitivity of contrail distance compared to fuel consumption (blue marks and left y-axis) and flight time (red marks and right y-axis). It can be seen that the results are very widely spread. Compared to the free case there is a much less clear advantage to ground track alterations for contrail mitigation. In some instances contrails can be decreased by 70% at 1-2% fuel consumption and 4% flight time, though this is very case dependent. When sticking to the NATs it can be said that approximately 20% of contrails can be mitigated against less than 1% fuel and time, but beyond that point cannot easily be generalized and should be looked at case by case.

8. Results

8.6.2 500 ft step climb

Commercial aircraft in cruise phase fly at a certain pressure altitude. When multiple streams of traffic are near or cross each other often the flight levels (intervals of 1000 feet vertically) are divided between them to maintain separation while making efficient use of airspace. Most commonly aircraft on airways are obligated to fly at alternating flight levels which lead to most aircraft cruising horizontally (pressure altitude) with a few 2000 ft step climbs between. This is also the case which is assumed in the majority of this thesis. However, with ever improving CNS systems other options may also become a reality in the future. If for example reduced separation allows for 500 ft step climbs this may impact contrail mitigation as well.

The way the profile mitigation algorithm is set up makes it difficult to quantify the impact of changing from 2000ft steps to 500ft. What can be done is to assess the impact more qualitatively. From the profile mitigation cases that ran, roughly 30-50% of cases show sections that could benefit from the decreased step climb. These are areas at which the step as performed is excessive compared to the effort that is actually required (e.g. 2000ft step climb where 400ft would suffice to exit the contrail region). It can however be seen in many figures throughout this report that the contrail regions cover a large altitude range. Small changes in altitude are therefore only effective in case the trajectory is inside but close to the top or bottom of a contrail region. This specific case seems to occur in the results but only for a minority of flights. Obviously, staying closer to the optimal conditions should help decrease fuel consumption due to mitigation manoeuvres. As changes due to the 2000ft steps are already below a tenth of a percent (note assumptions that may have impacted this value significantly) reducing the step will draw this value closer and closer to zero. Moreover, the actual profile can also be closer to the optimal continuous profile. As the size of the step decreases the trajectory approximates free flight for which Hendriks has performed analyses [1]. In short, the smaller the steps, the better the result, albeit with diminishing returns and increased workload for pilots and ATC in the current situation.

8.6.3 Other aircraft types

Besides the aircraft used for simulation in this thesis there are many other types used for commercial aviation across the globe. Of course these have characteristics that may change the contrail that they generate. As can be found from the extensive model description in Chapter 5 the most important factors in contrail generation is the critical temperature for contrail formation, local temperature and local humidity. In essence, changing aircraft type could change the critical temperature by changing the slope of the ideal mixing line (G) or local conditions due to changes in horizontal and vertical trajectory of the aircraft.

The slope of the ideal mixing line G is influenced mainly by increases in engine efficiency. This efficiency parameter η can be found in the denominator in Equation (2.1). With increasing efficiency the conditions under which contrails form occur at more places in the atmosphere as can be seen in Figure 8.19. As is clear from the difference between the top left and bottom right cases, increasing efficiency also increases the total distance along which contrails are formed for practically any flight in this atmosphere.

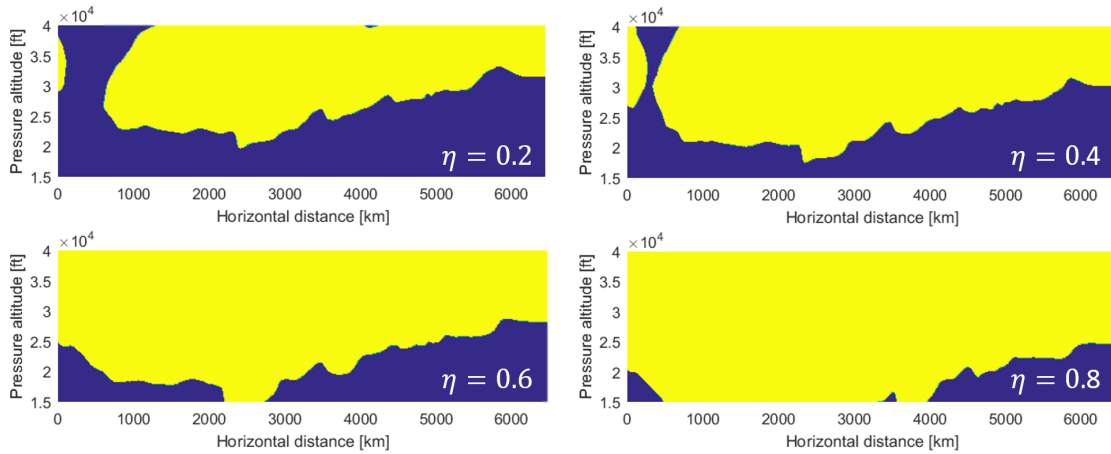


Figure 8.19: Contrail formation areas (yellow) encountered by flights to Winnipeg (CYWG) for different engine efficiency

Figure 8.20 shows the regions where persistent contrails form whereas Figure 8.19 merely shows formation regions. The difference between the two is determined by the humidity threshold at which contrails persist. Obviously this greatly impacts the size of contrail regions, though just like in Figure 8.19 it can be seen in Figure 8.20 that with increasing efficiency, the share of persistent contrail regions increases, albeit mainly on the lower end of each individual region. Schumann confirms this by reporting observations of an altitude range along which efficient aircraft do create condensation trails where less efficient ones do not [95]. It should be noted that this thesis assumes a 35% efficiency and the maximum value of 80% shown in the figures does not correspond to any reasonably achievable value for commercial jet engines now or in the near future.

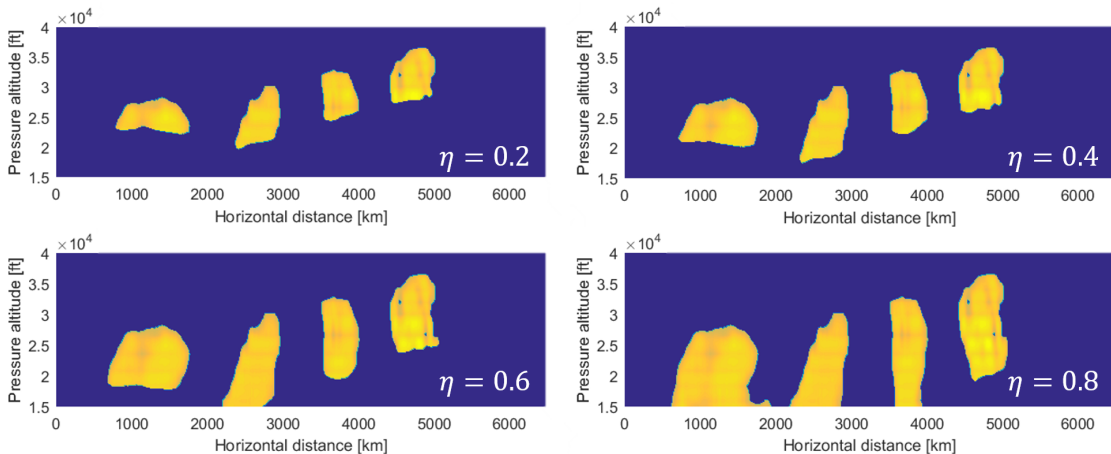


Figure 8.20: Persistent contrail regions (yellow) encountered by flights to Winnipeg (CYWG) for different engine efficiency

Besides through difference in contrail formation criteria, another way the contrail distance could change with changing aircraft type is due to different trajectory. Figure 8.21 shows contrail regions (yellow) that are encountered along a flight to Washington D.C. in the three different atmospheric conditions. It shows horizontal flight levels from 30.000 to 40.000 feet. Aircraft that spend the majority of their cruise above 34.000 feet generate hardly any contrails in the February 2014 and 2017 atmospheres. In the May 2017 atmosphere it can be seen that contrails are generated at higher altitudes though below 30.000 feet they are not. If the results

8. Results

of these plots could be generalized one could argue that high altitude flight is favorable in the winter months and when the summer comes, it may be favorable to fly at lower altitudes. Moreover, air traffic above approximately 39.000 feet does not generate contrails at any stage of the cruise. Smaller jet aircraft are an example of such flights as they typically cruise at higher altitudes with private jets commonly exceeding 41.000 feet.

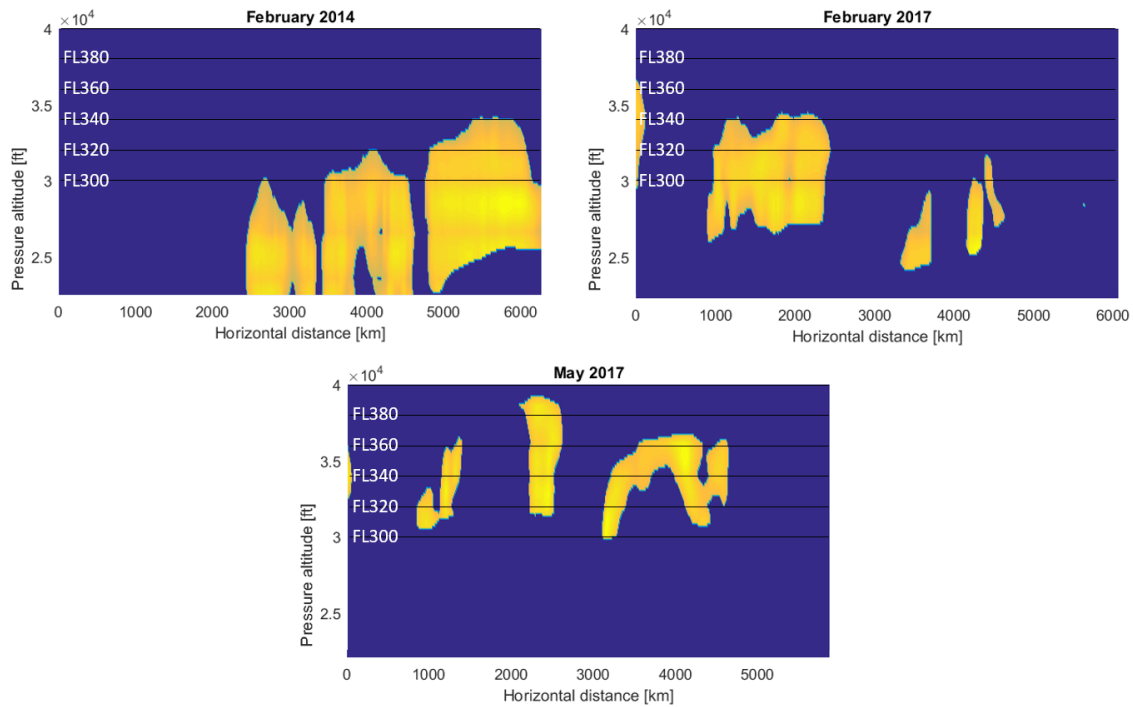


Figure 8.21: Contrail regions (yellow) encountered by flights to Washington D.C. (KIAD) for three different atmospheres including flight levels

8.6.4 Eastbound flights

The results as shown in this work are based on westbound flights only. In reality however air traffic goes both ways between Europe and the US. Another variation that is worth investigating therefore is what would change for an eastbound flight compared to westbound. As the aircraft and atmospheric conditions are identical the most important difference is the route that the aircraft takes from origin to destination. Due to wind patterns in the global atmosphere the ground track is distinctly different between the two directions. Similar effects can be seen in traffic that crosses the Pacific Ocean (e.g. between Tokyo and Los Angeles). Due to the computational burden involved with it, no simulation of eastbound traffic is conducted but rather a qualitative assessment is made. As indicated in Figure 8.22, westbound traffic generally takes a more northerly route which avoids the jet stream whereas eastbound flights try to take advantage of it and take a more southerly track. Validation from historic records of the North Atlantic Tracks and actual flight paths confirms this. What can be seen from Figure 8.22 is that in the February 2014 case eastbound traffic is much less likely to encounter persistent contrail regions. In the other two cases, the results are much less obvious. No large difference in contrail distance can be found between the two directions. Obviously the sample set here is too small to draw statistically relevant conclusions, however, it does demonstrate a case where westbound traffic would contribute to much more total contrail distance compared to eastbound. There is no evidence of the reverse thus the logical conclusion could be that it

seems that either there is no large difference or eastbound flights are (slightly) less prone to persistent contrail formation. Further research could help provide insight into this.

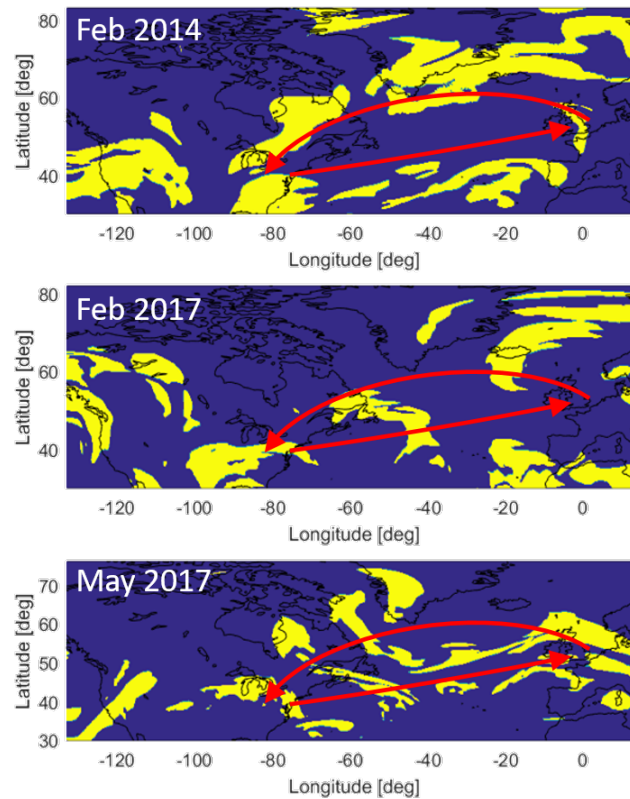


Figure 8.22: Persistent contrail regions (yellow) at 250hPa (34000ft) in Feb 2014, Feb 2017 and May 2017 NWP including generalized ground tracks

In summary, when assessing how the results would change when alternative scenarios are considered the following can be said. If the North Atlantic Track system was adhered to rather than allowing free ground track selection contrail mitigation is still possible. The effect however would be diminished for ground track alterations. For profile alterations there would be no change. When the size of the step changes is decreased both the performance of the baseline track increases as it is closer to the continuous optimum and excessive mitigating action can be decreased. Situations exist where profile alterations have an interest in a smaller step change at e.g. the top edge of a contrail region. Hence additional fuel consumption is expected to be reduced albeit with diminishing returns as the step size decreases. For other aircraft types increases in engine efficiency has a negative effect on contrail distance and aircraft that fly at higher altitudes appear to generate less contrails in winter. Lastly, there is no hard evidence to show more or less persistent contrail distance when comparing eastbound to westbound traffic. It does seem more likely that westbound flights are prone to more persistent contrail generation compared to eastbound than the reverse.

CHAPTER 9

DISCUSSION

As mentioned in Chapter 2 literature reports contrail mitigation potential through altitude changes in three categories. First, a global cruise altitude reduction is shown to have an almost linear relation between lowering cruise altitude and contrail reduction [35]. Contrails were found to decrease by 1% with every 133ft (40m) altitude reduction until 6000 ft (1830m) with a reduction of 45%. Second, temporal and local cruise altitude reduction is shown to have a similar effect. Temporal revision of maximum flight level above Central Europe suggested an increase of 4% fuel consumption as a consequence and increased air traffic controller workload [45]. The third category is perhaps the most interesting to consider in the context of this thesis. It covers studies where contrails were mitigated on an individual flight basis. These are elaborated on here.

Mannstein shows that a general reduction of flight altitude of at least 6000 ft would be necessary to avoid 50% of contrails [5]. If selective changes were used instead, an altitude change of less than 2000 ft leads to 50% reduction of contrails. It should be noted that this work uses ISSR occurrence as a proxy for contrail regions. The use of the Schmidt-Appleman criterion along with relative humidity as predictor for persistent contrail formation seems like a more accurate option. Based on the shape of contrail regions in this work and that of ISSRs as reported in literature it seems like the results from Mannstein would be diminished somewhat.

Soler uses a four dimensional trajectory planning algorithm to guide the aircraft through a network of fixes while performing step climbs and descents [6]. Because it does not assume free flight it stays closer to real world situations. The problem is initially formulated as a multi phase mixed integer optimal control problem and after various manipulations solved by a branch-and-bound algorithm. Results for continental US flights show increased fuel consumption in the order of 3% when taking into account contrail cost compared to purely operational cost optimization. These results seem to correspond to those obtained in this work. Since both use lateral and altitude changes in a realistic flight planning context, it seems that they compliment each other.

Sridhar also considers individual flights above the continental US for contrail mitigation [7]. Analysis of 12 city pairs shows that contrail time can be reduced by 70% at the expense of 2% additional fuel. Altitude optimization is shown to increase the effectiveness of the mitigation action considerably compared to without it while it also yields a positive result. This confirms the observation that ground track alterations are a potential strategy, however a combination of both is ideal. Both the conclusions and the order of magnitude of numerical results of this

work seems to agree with Sridhar. It should however be noted that the fuel consumption from altitude changes in this work is underestimated and therefore not comparable.

Klima investigates rerouting of 581 flights connecting 14 city pairs and 628 international flights over the North Atlantic between 15 city pairs [8]. It is shown that compared to the actual flights a 65-80% reduction of contrails is possible while reducing the total operating cost by 5-7%. This shows that actual flights can be improved upon while also reducing contrails. Compared to the customized fuel optimal route, 55-85% of the contrails can be mitigated while increasing fuel by 2.5-3.5% and flight time by 0.5-1%. Again, these statements seem to confirm some results as seen in this report. Current operations can be improved upon and sub-optimal conditions are commonplace in reality. Flight time changes are much lower though positive when a majority share of contrails are mitigated. Additional fuel is in the order of a few percent just like other research has shown.

Campbell uses mixed integer linear programming to reroute a single flight above the continental US [9]. A conical cost grid including adjustable persistent contrail cost parameter was used to steer the aircraft. At 50% of contrails mitigated, fuel burn increases 1.48% and no contrails were generated at a fuel cost of 6.18%. The use of a single flight to generate results could of course skew results. Compared to Campbell, the use of multiple scenarios extends the validity of results compared to this report but also shows the dependence on the case at hand. 100% reduction may not be feasible for each situation as can be found in this report. Partial mitigation on the other hand shows similar order of magnitude results.

Hendriks explores the potential of contrail mitigation through free four dimensional trajectory optimization [1]. He develops a tool that optimizes flights for fuel and flight time while mitigating the formation of persistent contrails. He uses a Gauss Pseudospectral Optimization Software (GPOPS) package and NWP data by the Canadian GDPS. Scenarios are performed using a similar domain, aircraft and weather data compared to this work. Hendriks shows that 90% of the induced contrails can be mitigated against an increased fuel consumption of less than 1.5%. Due to these promising results the question arises whether they hold in a practical context in this thesis. Flight planning was selected as the tool to assess this. Compared to Hendriks' results, the results in this work show less potential. It is however expected that a free flight situation should provide more ideal results. What can be said is that even though potential is reduced by the use of flight planning and practical constraints, both reports confirm that it is relatively easy to mitigate the majority of contrails at very low fuel and time cost. In his work Hendriks compares his own to comparable work by means of a summary table. This table was adopted and supplemented with the results from this work and can be seen below [1].

9. Discussion

Literature comparison	This study	Hendriks	Sridhar	Kaiser	Noppel
Meteorologic data Source (type) Resolution (points) Resolution (km x km) Including wind	NWP (global) 750x1500x15 (lat,lon,alt) 25x25km (hor) Yes	NWP (global) 750x1500x15 (lat,lon,alt) 25x25km (hor) Yes	RUC (global) 37 (alt) 40x40km (hor) Yes	Radiosonde (local) 5 points along route Yes	MetOffice (global) 432x325x19 (lat,lon,alt) No
Contrail model Contrail parameter Contrail model	Schmidt-Appleman + RHi Binary occurrence criterion	Schmidt-Appleman + RHi Probability per grid cell	RHi Radial penalty functions	Schmidt-Appleman + RHi Probability per point	Schmidt-Appleman Parametrized
Method Route Traffic data from Altitude Ground trajectory Contrail factor Objective Performance model	Multiple long transatlantic Multiple days Pre-processed optimal grid ATS contrained optimal Contrail length Min fuel, time Mixed	Single long (AMS-KIAD) Individual flights Free flight Free flight Contrail time Min fuel, time or DOC Enhanced performance model	Multiple (12 US city pairs) Single day (May 24, 2007) En-route fixed Free flight Contrail time Min fuel Parametrization SFC(z)	Single short (AMS-LOWS) Individual flight Ceiling limit ATS route (fixed) Contrail length Max specific range Enhanced performance model	Single long (LND-JFK) 1 year (2005) Free flight Free flight Contrail length Min fuel [Unknown]
Optimization Optimization method	Mixed (Dijkstra, SQP and Differential Evolution)	Dynamic optimization Gaus Pseudospectral Method	Nonlinear optimal control	Finite element method	Simplex optimization
Results Sensitivity Analysis Tradeoff level	Yes Contrail vs fuel and time	Yes RF/Contrail vs fuel, time and DOC	Yes Contrail vs fuel and time	No RF/Env. cost vs fuel	No Contrail vs fuel
Conclusion In numbers	-70% Con = +0-3% Fuel HEAVY CASE DEPENDENCY	-90% Con = +1.5% Fuel	-100% Con = +0-4.3% time -83% Con = +2.5% fuel	-100% Con = +2.5% Fuel (fixed alt) -100% Con = +1.5% Fuel (dh allowed)	-78% Con = +0.8% Fuel

CHAPTER 10

CONCLUSION

This thesis aims to help assess and move towards the potential use of flight planning in commercial operations in order to reduce the environmental impact of persistent condensation trails that are generated. The objective is to assess the fuel and time cost associated with mitigating the environmental impact of contrails caused by flights from Europe to North America by developing a realistic flight planning tool that includes a measure of the contrails generated and using it to optimize a set of characteristic flights. In doing so, relevant literature was studied and tools for flight planning, contrail prediction and implementation of mitigation strategies were created. Subsequently a set of scenarios was simulated and the results analyzed.

Experts have shown that global warming is a real and significant problem. Compared to carbon dioxide, the contribution of contrails to global warming is much less studied. As they form and persist, contrails change the local energy balance of the atmosphere, leading to a net warming effect. Therefore just like for carbon dioxide, reducing contrails where possible should help reduce anthropogenic global warming. Contrails have been studied since early in the 20th century. Their formation criterion was formulated by Schmidt [2] and Appleman [3] and later combined by Schumann [4] in 1996. Overall it is clear that technology or different fuel (additives) are not a feasible mitigation option. Operational avoidance is seen as the best option in reducing contrail climate effects [50] mainly in the form of altitude changes. Research generally shows that the majority of contrails can be mitigated at the expense of 2-3% additional fuel [6, 7, 8, 9]. Previous work to this thesis shows potential for 90% contrail mitigation at less than 1.5% additional fuel in free flight conditions [1]. The impact on flight time is generally much smaller (at most 1%) due to the use of altitude changes more than lateral movement or velocity changes. Most current studies however remained rather separated from real life operations. Their conclusions rely heavily on unrealistic conditions and ignore practical constraints which is why this thesis focuses on the use of realistic flight planning to assess potential for contrail mitigation.

The method used to generate the results as shown in Chapter 8 is the following. A flight planning tool was created using publicly available route structure with additional freedom where the NAT system traditionally is. Based on this two dimensional network and an estimate of local cruise conditions a ground track is selected. Along this ground track the flight is simulated in steady horizontal flight using step climbs to keep to a 2000ft interval of predetermined optimal cruise conditions. The distance of contrails that are generated along the flight are added and recorded. For mitigation there are three methods used. The first is by including the cost of contrails in the cost associated with a particular edge in the network and subsequent

10. Conclusion

diversion by the ground path finding algorithm. The second is by adjusting the altitude profile along each region that is encountered during a flight. The third option combines lateral and profile alterations to form a hybrid strategy.

Cases were evaluated for three different atmospheric data sets. NWP data from the Canadian GDPS was collected for the 12th of February 2014, 14th of February 2017 and 11th of May 2017. Both fuel optimal and time optimal flights for a B747 aircraft were simulated from the Netherlands to Washington D.C. (KIAD), Winnipeg (CYWG) and Vancouver (CYVR). After baseline flights were established for all, mitigation by means of ground track selection, altitude profile alterations and a combination of both was conducted.

Simulation of flights along contrail weighted ground tracks shows that ground track alterations can be used to mitigate contrails. Especially at low values of β_{grnd} large shares of contrails are mitigated at very low fuel and time cost. Higher values show additional fuel consumption below 10% for most fuel optimal flights. Time optimal flights show at most a few percent additional flight time at 70% contrails mitigated and 15-30% additional time at 90% contrails mitigated.

The results for profile alterations are very case dependent. It is clear that up to $\beta_{prof} = 0.05$ contrails are increasingly avoided. Fuel optimal flights show an increased fuel consumption of less than 0.1% and negligible change in flight time. Time optimal flights are forced to reduce cruise speed which increases flight time up to 0.3% and reduced fuel consumption up to 0.55%. It should be noted that these results are generated based on a set of assumptions and limitations that may decrease the cost of a step climb and profile alterations compared to the every day operations. Regardless, it is clear that profile alterations are a much more efficient single strategy to mitigate contrails in most flights compared to ground track alterations.

Hybrid mitigation shows characteristics of both ground and altitude profile mitigation strategies, however it outperforms the individual strategies as expected. While results are very case dependent it is clear that a majority of contrails can be mitigated at very low additional fuel and flight time. Given the large difference in the cost of ground track alterations compared to profile optimization the emphasis should be on the latter.

When assessing how the results would change when alternative scenarios are considered the following can be said. If the North Atlantic Track system was adhered to rather than allowing free ground track selection contrail mitigation is still possible. The effect however would be diminished for ground track alterations. For profile alterations there would be no change. When the size of the step changes is decreased both the performance of the baseline track increases as it is closer to the continuous optimum and excessive mitigating action can be decreased. Situations exist where profile alterations have an interest in a smaller step change at e.g. the top edge of a contrail region. Hence additional fuel consumption is reduced albeit with diminishing returns as the step size decreases. For other aircraft types increases in engine efficiency has a negative effect on contrail distance and aircraft that fly at higher altitudes appear to generate less contrails in winter. There is no strong evidence to suggest large differences in contrail distance in eastbound compared to westbound traffic. It does seem more likely that westbound flights are prone to more persistent contrail generation compared to eastbound than the reverse.

In short, by means of ground track alterations nearly half of all contrails can be mitigated against 2-3% additional fuel and flight time. Profile mitigation shows a different image for fuel optimal flights compared to time optimal. For fuel optimal flights there is a trend of increasing fuel consumption up to 0.1% with decreasing contrail distance, albeit very case dependent. For time optimal flights the case is reversed. Due to operational constraints any profile alteration leads to a lower cruise velocity which comes with increases in flight time and reduced fuel consumption. Over 80% of contrails can be mitigated while reducing fuel approximately 1.2% and increasing flight time by 0.4-0.8%. For hybrid mitigation results are also very case dependent. What is clear is that at least 50% of contrails can be mitigated at less than 2% additional fuel which exceeds ground track selection only strategy (i.e. hybrid outperforms a single dimension strategy).

The results have confirmed the hypothesis that large shares of contrails can be mitigated against a few percent additional fuel consumption and flight time. Compared to literature the mitigation potential shows similar results. Compared to Hendriks [1] the results show more additional fuel for ground track selection strategy and less for profile alterations. It should be noted that the profile alterations strategy should be further investigated using full three dimensional flight dynamics to account for the dynamic non-steady-horizontal effects that occur in climbing flight. Assumptions here were made to reduce computation time to within acceptable boundaries.

For future research a lot of recommendations can be made, however the most relevant and critical ones are mentioned here. First of all, since flight planning seems like a great tool for contrail mitigation future research that assesses its potential should use/emulate current or future commercial tools as much as possible. A great way this could be done by cooperation with providers of these tools and services. As this research provides more insight into operational feasibility significant steps towards regulating policy and other incentives can be made. Second, while this thesis uses contrail distance as mitigation objective this is not the ultimate goal of the trajectory alterations. It is the environmental impact that ultimately should be minimized, which means taking into account not only instantaneous contrails but also their time impact, interaction with other types of clouds, changes in other exhaust sources like carbon dioxide, secondary effects etc. In an ideal world it would be the total climate impact that is minimized along with optimizing some monetary value in flight planning tools. On a more realistic level future research should pay attention to accurate input data for weather, aircraft behaviour and rules imposed by ATC and regulating bodies. Moreover, this thesis covers only a single aircraft on three flights across the Atlantic Ocean. Given the heavy dependency on atmospheric conditions it is advised to further explore mitigation potential for different moments in time (e.g. due to diurnal or annual cycles). As climate change is a global issue, other parts of the globe and aircraft should be considered for analysis. Also if computational resources allow for it, flight and atmospheric dynamics as well as instantaneous optimization of the objective function should provide better results compared to preprocessed optimal conditions and separate horizontal and vertical track selection.

REFERENCES

- [1] Hendriks, T., *Contrail Mitigation by means of 4D Aircraft Trajectory Optimisation*, Ph.D. thesis, TU Delft, Delft University of Technology, 2015. II, 1, 2, 17, 43, 44, 45, 51, 52, 53, 60, 84, 89, 91, 93, 106
- [2] Schmidt, E., “Die Entstehung von Eisnebel aus den Auspuffgasen von Flugmotoren,” *Schriften der Deutschen Akademie der Luftfahrtforschung*, Vol. 44, 1941, pp. 1–15. 1, 3, 4, 91
- [3] Appleman, H., “The formation of exhaust condensation trails by jet aircraft,” *Bull. Amer. Meteor. Soc.*, Vol. 34, No. 1, 1953, pp. 14–20. 1, 3, 4, 10, 91
- [4] Schumann, U., “On conditions for contrail formation from aircraft exhausts,” *Meteorologische Zeitschrift*, Vol. 5, No. 1, 1996, pp. 4–23. 1, 3, 4, 5, 6, 44, 45, 58, 59, 60, 91, 107
- [5] Mannstein, H., Spichtinger, P., and Gierens, K., “A note on how to avoid contrail cirrus,” *Transportation Research Part D: Transport and Environment*, Vol. 10, No. 5, 2005, pp. 421 – 426. 1, 9, 17, 18, 88, 106
- [6] Soler, M., Zou, B., and Hansen, M., “Flight trajectory design in the presence of contrails: Application of a multiphase mixed-integer optimal control approach,” *Transportation Research Part C: Emerging Technologies*, Vol. 48, 2014, pp. 172–194. 1, 17, 88, 91
- [7] Sridhar, B., Ng, H., and Chen, N., “Aircraft trajectory optimization and contrails avoidance in the presence of winds,” *Journal of Guidance, Control, and Dynamics*, Vol. 34, No. 5, 2011, pp. 1577–1584. 1, 17, 88, 91
- [8] Klima, K., *Assessment of a global contrail modeling method and operational strategies for contrail mitigation*, Ph.D. thesis, Massachusetts Institute of Technology, 2005. 1, 17, 89, 91
- [9] Campbell, S., Neogi, N., and Bragg, M., “An operational strategy for persistent contrail mitigation,” *9th AIAA Aviation Technology, Integration, and Operations Conference, Hilton Head, South Carolina*, 2009, pp. 1–14. 1, 17, 89, 91
- [10] Schumann, U., “A contrail cirrus prediction model,” *Geoscientific Model Development*, Vol. 5, 2012, pp. 543–580. 1, 9, 15
- [11] Travis, D. J., Carleton, A. M., and Changnon, S. A., “An Empirical Model to Predict Widespread Occurrences of Contrails,” *Journal of Applied Meteorology*, Vol. 36, No. 9, 1997, pp. 1211–1220. 2, 9, 10

- [12] Duda, D. P. and Minnis, P., “Basic Diagnosis and Prediction of Persistent Contrail Occurrence Using High-Resolution Numerical Weather Analyses/Forecasts and Logistic Regression. Part I: Effects of Random Error,” *Journal of Applied Meteorology and Climatology*, Vol. 48, No. 9, 2009, pp. 1780–1789. 2, 9
- [13] Schumann, U., “Formation, properties and climatic effects of contrails,” *Comptes rendus - Physique*, Vol. 6, No. 4-5, 2005, pp. 549–565. 3
- [14] Ettenreich, R., “Wolkenbildung über einer Feuersbrunst und an Flugzeugabgasen,” *Meteorol. Z*, Vol. 36, 1919, pp. 355–356. 3
- [15] Schrader, M., “Calculations of Aircraft Contrail Formation Critical Temperatures,” *Journal of Applied Meteorology*, Vol. 36, No. 12, 1997, pp. 1725–1729. 4, 7, 8, 106
- [16] Cavcar, M., “The International Standard Atmosphere (ISA),” Tech. rep., Anadolu University, 2014. 5, 40
- [17] National Center for Biotechnology Information, U.S. National Library of Medicine, “PubChem,” <http://pubchem.ncbi.nlm.nih.gov>, Accessed: August 2, 2016. 5
- [18] The Engineering ToolBox, “Engineering Toolbox: Air - Molecular Mass,” <http://www.engineeringtoolbox.com/molecular-mass-air-d.679.html>, Accessed: August 2, 2016. 5
- [19] Booker, H., *Environmental impact of stratospheric flight : biological and climatic effects of aircraft emissions in the stratosphere*, National Academy of Sciences, Washington, 1975. 5
- [20] Air BP - A specialized aviation division of The British Petroleum Company, “Handbook of Products,” 2000. 5
- [21] Noppel, F. and Singh, R., “Overview on contrail and cirrus cloud avoidance technology,” *Journal of Aircraft*, Vol. 44, No. 5, 2007, pp. 1721–1726. 7, 16, 17, 106
- [22] Brewer, A., “Condensation trails,” *Weather*, Vol. 1, No. 2, 1946, pp. 34–40. 7
- [23] Ferris, P., “The formation and forecasting of condensation trails behind modern aircraft,” *Meteorological Applications*, Vol. 3, No. 4, 1996, pp. 301–306. 7
- [24] Jensen, E., “Environmental conditions required for contrail formation and persistence,” *Journal of Geophysical Research: Atmospheres*, Vol. 103, No. D4, 1998, pp. 3929–3936. 7, 8
- [25] Gao, H., *Aircraft cruise phase altitude optimization considering contrail avoidance*, Master’s thesis, Massachusetts Institute of Technology, 2013. 7
- [26] Sonntag, D., “Advancements in the field of hygrometry,” *Meteorologische Zeitschrift*, Vol. 3, No. 2, 1994, pp. 51–66. 8, 44
- [27] Murphy, D.M. and Koop, T., “Review of the vapour pressures of ice and supercooled water for atmospheric applications,” *Quarterly Journal of the Royal Meteorological Society*, Vol. 131, No. 608, 2005, pp. 1539–1565. 8
- [28] Paoli, R. and Shariff, K., “Contrail modeling and simulation,” *Annual Review of Fluid Mechanics*, Vol. 48, 2016, pp. 393–427. 9

REFERENCES

- [29] Gerz, T., Dürbeck, T., and Konopka, P., “Transport and effective diffusion of aircraft emissions,” *Journal of Geophysical Research: Atmospheres*, Vol. 103, No. D20, 1998, pp. 25905–25913. 9
- [30] Bjornson, B. M., “SAC contrail formation study,” Tech. rep., DTIC Document, 1992. 10
- [31] Jackson, A., Newton, B., Hahn, D., and Bussey, A., “Statistical contrail forecasting,” *Journal of Applied Meteorology*, Vol. 40, No. 2, 2001, pp. 269–279. 10
- [32] Rädcl, G. and Shine, K. P., “Radiative forcing by persistent contrails and its dependence on cruise altitudes,” *Journal of Geophysical Research: Atmospheres*, Vol. 113, No. D7, 2008. 10
- [33] Ponater, M., Marquart, S., and Sausen, R., “Contrails in a comprehensive global climate model: Parameterization and radiative forcing results,” *Journal of Geophysical Research: Atmospheres*, Vol. 107, No. D13, 2002. 10, 15
- [34] Marquart, S., Ponater, M., Mager, F., and Sausen, R., “Future development of contrail cover, optical depth, and radiative forcing: Impacts of increasing air traffic and climate change,” *Journal of Climate*, Vol. 16, No. 17, 2003, pp. 2890–2904. 10, 16
- [35] Fichter, C., Marquart, S., Sausen, R., and Lee, D. S., “The impact of cruise altitude on contrails and related radiative forcing,” *Meteorologische Zeitschrift*, Vol. 14, No. 4, 2005, pp. 563–572. 10, 17, 88
- [36] Sausen, R., Gierens, K., Ponater, M., and Schumann, U., “A Diagnostic Study of the Global Distribution of Contrails Part I: Present Day Climate,” *Theoretical and Applied Climatology*, Vol. 61, No. 3-4, 1998, pp. 127–141. 10, 11
- [37] Mannstein, H., Meyer, R., and Wendling, P., “Operational detection of contrails from NOAA-AVHRR-data,” *International Journal of Remote Sensing*, Vol. 20, No. 8, 1999, pp. 1641–1660. 11
- [38] Pultau, V., *Literature study of climate effects of contrails caused by aircraft emissions*, Koninklijk Nederlands Meteorologisch Instituut, De Bilt, 1998. 11
- [39] Mannstein, H., Leiter, C., Meyer, R., Wendling, P., Minnis, P., and Palikonda, R., “Regional contrail coverage estimated from AVHRR data,” *Proceedings of the Meteorological Satellite Data User’s Conference*, 2000, pp. 578–585. 11
- [40] Mannstein, H. and Schumann, U., “Aircraft induced contrail cirrus over Europe,” *Meteorologische Zeitschrift*, Vol. 14, No. 4, 2005, pp. 549–554. 11
- [41] Stubenrauch, C. J. and Schumann, U., “Impact of air traffic on cirrus coverage,” *Geophysical research letters*, Vol. 32, No. 14, 2005. 11
- [42] Gierens, K., Sausen, R., and Schumann, U., “A diagnostic study of the global distribution of contrails part II: Future air traffic scenarios,” *Theoretical and Applied Climatology*, Vol. 63, No. 1-2, 1999, pp. 1–9. 11
- [43] Bakan, S., Betancor, M., Gayler, V., and Grassl, H., “Contrail frequency over Europe from NOAA-satellite images,” *Annales Geophysicae*, Vol. 12, No. 10-11, 1994, pp. 962–968. 11
- [44] Noppel, F., *Contrail and cirrus cloud avoidance technology*, Ph.D. thesis, Cranfield University - School of Mechanical Engineering, 2007. 11

- [45] Williams, V., Noland, R. B., and Toumi, R., “Reducing the climate change impacts of aviation by restricting cruise altitudes,” *Transportation Research Part D: Transport and Environment*, Vol. 7, No. 6, 2002, pp. 451–464. 11, 17, 88
- [46] Penner, J., *Aviation and the global atmosphere : a special report of IPCC Working Groups I and III in collaboration with the Scientific Assessment Panel to the Montreal Protocol on Substances that Deplete the Ozone Layer*, Cambridge University Press, Cambridge, 1999. 12, 14, 16, 18
- [47] Sausen, R., Isaksen, I., Grewe, V., Hauglustaine, D., Lee, D. S., Myhre, G., Köhler, M. O., Pitari, G., Schumann, U., Stordal, F., et al., “Aviation radiative forcing in 2000: An update on IPCC (1999),” *Meteorologische Zeitschrift*, Vol. 14, No. 4, 2005, pp. 555–561. 12, 16
- [48] Lee, D., Pitari, G., Grewe, V., Gierens, K., Penner, J., Petzold, A., Prather, M., Schumann, U., Bais, A., Bernsten, T., et al., “Transport impacts on atmosphere and climate: Aviation,” *Atmospheric Environment*, Vol. 44, No. 37, 2010, pp. 4678–4734. 12
- [49] Scheelhaase, J. D. and Grimme, W. G., “Emissions trading for international aviation—an estimation of the economic impact on selected European airlines,” *Journal of Air Transport Management*, Vol. 13, No. 5, 2007, pp. 253–263. 12, 15
- [50] Lee, D. S., Fahey, D. W., Forster, P. M., Newton, P. J., Wit, R. C., Lim, L. L., Owen, B., and Sausen, R., “Aviation and global climate change in the 21st century,” *Atmospheric Environment*, Vol. 43, No. 22, 2009, pp. 3520–3537. 13, 16, 18, 19, 91, 106
- [51] IATA, “Annual Review 2016,” Tech. rep., International Air Transport Association (IATA), 2016. 13
- [52] Jiang, H., “Key Findings on Airplane Economic Life,” Tech. rep., Boeing, 2013. 13
- [53] ICAO, “Annual Report of the ICAO Council: 2014,” Tech. rep., International Civil Aviation Organization (ICAO), 2014. 14, 106
- [54] ICAO, “Study on Financial Situation of Airports and Air Navigation Services 2003,” Tech. rep., International Civil Aviation Organization (ICAO), 2003. 14, 106
- [55] ICAO, “FINANCIAL SITUATION OF AIRPORTS AND AIR NAVIGATION SERVICES 2005,” Tech. rep., International Civil Aviation Organization (ICAO), 2007. 14, 106
- [56] DataBank, W., “World Development Indicators - Air transport, passengers carried,” Tech. rep., The World Bank, 2007. 14, 106
- [57] European Commission, “Reducing emissions from aviation,” http://ec.europa.eu/clima/policies/transport/aviation/index_en.htm, Accessed: October 12, 2016. 14
- [58] European Commission, “The EU Emissions Trading System (EU ETS),” Tech. rep., European Union, 2013. 14
- [59] Anger, A., “Including aviation in the European emissions trading scheme: impacts on the industry, CO₂ emissions and macroeconomic activity in the EU,” *Journal of Air Transport Management*, Vol. 16, No. 2, 2010, pp. 100–105. 15
- [60] Minnis, P., Schumann, U., Doelling, D. R., Gierens, K. M., and Fahey, D. W., “Global distribution of contrail radiative forcing,” *Geophysical Research Letters*, Vol. 26, No. 13, 1999, pp. 1853–1856. 15, 16

REFERENCES

- [61] Gierens, K. M., Lim, L., and Eleftheratos, K., “A review of various strategies for contrail avoidance,” *Open Atmospheric Science Journal*, Vol. 2, 2008, pp. 1–7. 15, 16
- [62] Meerkötter, R., Schumann, U., Doelling, D., Minnis, P., Nakajima, T., and Tsushima, Y., “Radiative forcing by contrails,” *Annales Geophysicae*, Vol. 17, No. 8, 1999, pp. 1080–1094. 15, 16
- [63] Frömming, C., Ponater, M., Burkhardt, U., Stenke, A., Pechtl, S., and Sausen, R., “Sensitivity of contrail coverage and contrail radiative forcing to selected key parameters,” *Atmospheric environment*, Vol. 45, No. 7, 2011, pp. 1483–1490. 15
- [64] Espinoza, H. R., “Simple parameterizations of the radiative properties of cloud layers: a review,” *Atmospheric research*, Vol. 35, No. 2, 1995, pp. 113–125. 15
- [65] Minnis, P., Ayers, J. K., Palikonda, R., and Phan, D., “Contrails, cirrus trends, and climate,” *Journal of Climate*, Vol. 17, No. 8, 2004, pp. 1671–1685. 16
- [66] Burkhardt, U. and Kärcher, B., “Global radiative forcing from contrail cirrus,” *Nature climate change*, Vol. 1, No. 1, 2011, pp. 54–58. 16
- [67] Stuber, N., Forster, P., Rädcl, G., and Shine, K., “The importance of the diurnal and annual cycle of air traffic for contrail radiative forcing,” *Nature*, Vol. 441, No. 7095, 2006, pp. 864–867. 16
- [68] Gierens, K., “Are fuel additives a viable contrail mitigation option?” *Atmospheric Environment*, Vol. 41, No. 21, 2007, pp. 4548–4552. 16
- [69] Gierens, K., Spichtinger, P., and Schumann, U., “Ice supersaturation,” *Atmospheric Physics*, Springer, 2012, pp. 135–150. 17, 61
- [70] Dickson, N., Gierens, K., Rogers, H., and Jones, R., “Vertical spatial scales of ice supersaturation and probability of ice supersaturated layers in low resolution profiles of relative humidity,” *Proceedings of the International Conference on Transport, Atmosphere and Climate (TAC-2)*, Aachen and Maastricht, 2009, pp. 22–25. 17
- [71] Gierens, K. and Spichtinger, P., “On the size distribution of ice-supersaturated regions in the upper troposphere and lowermost stratosphere,” *Annales Geophysicae*, Vol. 18, No. 4, 2000, pp. 499–504. 17
- [72] Williams, V., Noland, R. B., and Toumi, R., “Air transport cruise altitude restrictions to minimize contrail formation,” *Climate Policy*, Vol. 3, No. 3, 2003, pp. 207–219. 17
- [73] Deuber, O., Sigrun, M., Robert, S., Michael, P., and Ling, L., “A physical metric-based framework for evaluating the climate trade-off between CO₂ and contrails—The case of lowering aircraft flight trajectories,” *Environmental science & policy*, Vol. 25, 2013, pp. 176–185. 18, 19, 20
- [74] Fuglestedt, J. S., Shine, K. P., Berntsen, T., Cook, J., Lee, D., Stenke, A., Skeie, R. B., Velders, G., and Waitz, I., “Transport impacts on atmosphere and climate: Metrics,” *Atmospheric Environment*, Vol. 44, No. 37, 2010, pp. 4648–4677. 19
- [75] Houghton, J. T., *Climate change 1995: The science of climate change: contribution of working group I to the second assessment report of the Intergovernmental Panel on Climate Change*, Vol. 2, Cambridge University Press, 1996. 19

- [76] Shine, K. P., Fuglestedt, J. S., Hailemariam, K., and Stuber, N., “Alternatives to the global warming potential for comparing climate impacts of emissions of greenhouse gases,” *Climatic Change*, Vol. 68, No. 3, 2005, pp. 281–302. 19
- [77] Gillett, N. P. and Matthews, H. D., “Accounting for carbon cycle feedbacks in a comparison of the global warming effects of greenhouse gases,” *Environmental Research Letters*, Vol. 5, No. 3, 2010, pp. 034011. 20
- [78] Deuber, O., Luderer, G., and Edenhofer, O., “Physico-economic evaluation of climate metrics: A conceptual framework,” *Environmental science & policy*, Vol. 29, 2013, pp. 37–45. 20
- [79] Belobaba, P., *The global airline industry*, Wiley, Chichester, U.K, 2009. 22, 23, 106
- [80] Rumler, W., Günther, T., Weißhaar, U., and Fricke, H., “Flight profile variations due to the spreading practice of cost index based flight planning,” *4th International Conference on Research in Air Transportation, Budapest*, 2010, pp. 209—216. 22
- [81] United States - Federal Aviation Administration, “Appendix A. ICAO FLIGHT PLANS,” <http://tfmlearning.fly.faa.gov/Publications/atpubs/FSS/AppendixA.htm>, Accessed: September 1, 2017. 23, 106
- [82] United States - Department of Defence - Flight Information Publication H3-H4, “Extract (via PhotoShopPro) from DoD Flight Information Publication Enroute High Altitude Caribbean and South America,” https://commons.wikimedia.org/wiki/File:IFR_high_altitude_en_route_chart_-_Brasilia_-_UW2,_UZ6_airways.jpg, Accessed: September 11, 2017. 24, 106
- [83] Airlinesoftware.net, “Digital Solutions Directory,” <https://www.airlinesoftware.net/>, Accessed: October 19, 2016. 22, 24
- [84] Weitz, L., “Derivation of a Point-Mass Aircraft Model used for Fast-Time Simulation,” Tech. rep., MITRE, 2015. 39
- [85] Government of Canada - Department of Environment and natural resources, “25km resolution numerical data of the Global Deterministic Forecast System (GDPS) model - grib2 format,” https://weather.gc.ca/grib/grib2_glb_25km_e.html, Accessed: February 14, 2017 and May 11, 2017. 42, 43, 106
- [86] Xu, K.-M. and Krueger, S. K., “Evaluation of cloudiness parameterizations using a cumulus ensemble model,” *Monthly weather review*, Vol. 119, No. 2, 1991, pp. 342–367. 45
- [87] Houck, C. R., Joines, J., and Kay, M. G., “A genetic algorithm for function optimization: a Matlab implementation,” *NCSU-IE TR*, Vol. 95, No. 09, 1995. 47
- [88] Vesterstrom, J. and Thomsen, R., “A comparative study of differential evolution, particle swarm optimization, and evolutionary algorithms on numerical benchmark problems,” *Evolutionary Computation, 2004. CEC2004. Congress on*, Vol. 2, IEEE, 2004, pp. 1980–1987. 47, 48
- [89] Whitley, D., “A genetic algorithm tutorial,” *Statistics and computing*, Vol. 4, No. 2, 1994, pp. 65–85. 47

REFERENCES

- [90] Fleetwood, K., “An introduction to differential evolution,” *In Proceedings of Mathematics and Statistics of Complex Systems (MASCOS) One Day Symposium, 26th November, Brisbane, Australia*, Mathematics and Statistics of Complex Systems (MASCOS), 2004, pp. 785–791. 48
- [91] Storn, R. and Price, K., *Differential evolution—a simple and efficient adaptive scheme for global optimization over continuous spaces*, Vol. 3, ICSI Berkeley, 1995. 48
- [92] Ho-Huu, V., Nguyen-Thoi, T., Vo-Duy, T., and Nguyen-Trang, T., “An adaptive elitist differential evolution for optimization of truss structures with discrete design variables,” *Computers & Structures*, Vol. 165, 2016, pp. 59–75. 48
- [93] Federal Aviation Administration, “Aeronautical Information Manual - Official Guide to Basic Flight Information and ATC Procedures,” https://www.faa.gov/air_traffic/publications/media/AIM_Basic_4-03-14.pdf, Accessed: July 4, 2017. 55
- [94] Piotrowski, A. P., “Review of differential evolution population size,” *Swarm and Evolutionary Computation*, Vol. 32, 2017, pp. 1–24. 64
- [95] Schumann, U., “Influence of propulsion efficiency on contrail formation,” *Aerospace science and technology*, Vol. 4, No. 6, 2000, pp. 391–401. 85

NOMENCLATURE

Greek Symbols

Symbol	Description	Units
β_{grnd}	Contrail penalty for ground track changes	—
β_{prof}	Contrail penalty for altitude profile changes	—
Δ	Difference between situations	—
δ	Air pressure ratio	—
ϵ	Ratio of molar masses	—
η	Propulsive efficiency	—
γ	Climb angle, wind triangle angle, ratio of specific heat	$deg, deg, -$
λ	Climate sensitivity parameter	—
ρ	Air density	kg/m^3

Roman Symbols

Symbol	Description	Units
a	Speed of sound	m/s
atm	Atmospheric input	Feb 2014 / Feb 2017 / May 2017
C	Heat capacity of the system	JK^{-1}
C_D	Drag coefficient	—
C_{fuel}	Non-dimensional fuel cost	—
C_{time}	Non-dimensional time cost	—
CI	Cost index	—
C_L	Lift coefficient	—
c_p	Specific heat capacity	$Jkg^{-1}K^{-1}$
ct	Contrail distance	m
D	Drag force	N

NOMENCLATURE

$dest$	Flight destination	KIAD / CYWG / CYVR
E	Energy	J
EI_{H_2O}	Emission index of water vapour	$kgkg^{-1}$
e_L	Vapour saturation pressure	N/m^2
F	Force	N
$f_{1,2,3,4}$	Altitude change in 2000ft interval	ft
ff	Fuel flow	kg/s
G	Slope of ideal mixing line	$Jkg^{-1}K^{-1}$
g	Gravitational constant	$9.81m/s^2$
h	Altitude	m
L	Lift force	N
M	Mach number	–
m_{land}	Landing weight	kg
$mode$	Aircraft optimal flight mode	fuel/time
m_{TO}	Take-off weight	kg
p	Pressure	N/m^2
p_0	Surface pressure in ISA	N/m^2
p_{11km}	Pressure at 11km altitude in ISA	N/m^2
$p_{partial}$	Partial vapour pressure	N/m^2
p_{sat}	Saturation vapour pressure	N/m^2
Q	Specific combustion heat	$MJkg^{-1}$
R	Specific gas constant	$287.04Jkg^{-1}K^{-1}$
RF	Radiative forcing	W/m^2
RH_i	Relative humidity with respect to ice	–
RH_w	Relative humidity with respect to water	–
S	Surface area	m^2
s	Horizontal distance	m
$s_{1,2,3,4}$	Horizontal location of decision	m
SH	Specific humidity	$kgkg^{-1}$
s_{land}	Horizontal distance at landing	m
s_{TO}	Horizontal distance at take-off	m

t	Time	s
T_0	Surface temperature in ISA	$^{\circ}K$
T_{11km}	Temperature at 11km altitude in ISA	$^{\circ}K$
T_{amb}	Ambient temperature	$^{\circ}K$
T_c	Critical temperature at 100% relative humidity	$^{\circ}K$
T_{cf}	Generalized critical temperature	$^{\circ}K$
t_{land}	Time at landing	s
T_{LC}	See T_{cf}	$^{\circ}K$
T_{LM}	See T_c	$^{\circ}K$
t_{TO}	Time at take-off	s
U	See RH_w	—
V	Velocity	m/s
V_{air}	Velocity with respect to air	m/s
V_{ground}	Velocity with respect to ground	m/s
V_{wind}	Velocity of wind with respect to ground	m/s
x	Horizontal location	m

LIST OF ABBREVIATIONS

- AIP** Aeronautical Information Publication. 24, 28, 30
- ANSP** Air Navigation Service Provider. 28, 30
- ATC** Air Traffic Control. II, 2, 27, 30, 34–36, 55, 84, 93
- ATO** Air Transport & Operations. 47
- BADA** Base of Aircraft Data. 24
- CAA** Civil Aviation Authority. 28
- CAEP** Committee on Aviation Environmental Protection. 14
- CAS** Calibrated Airspeed. 36, 39, 51, 52, 55, 57, 69, 70, 75, 106
- CNS** Communication, Navigation and Surveillance. 14, 21, 28–30, 84
- CoCiP** Contrail Cirrus Prediction. 9
- CYVR** Vancouver. 62, 65, 72, 74, 77, 80, 92, 107
- CYWG** Winnipeg. 65, 72, 76, 80, 85, 92, 108
- DLR** Deutschen Zentrums für Luft- und Raumfahrt. 9
- EDI** Economic Damage Index. 20
- ETS** Emissions Trading System. 14, 19, 20
- FAA** Federal Aviation Administration. 21, 28, 30
- GDP** Global Damage Potential. 18, 20
- GDPS** Global Deterministic Forecast System. 42, 43, 89, 92, 99, 106
- GTP** Global Temperature (Change) Potential. 18–20
- GWP** Global Warming Potential. 18–20
- ICAO** International Civil Aviation Organization. 14
- ILS** Instrument Landing System. 21
- IPCC** Intergovernmental Panel on Climate Change. 12, 16, 18, 19

- ISA** International Standard Atmosphere. 5, 6, 33, 37, 40–42, 52–54, 58, 59, 65–69, 106, 107, 109
- ISSR** Ice Super Saturated Region. 9, 17, 18, 60, 88, 106
- KIAD** Washington D.C.. 33–35, 47, 63, 65, 67, 68, 70–73, 76, 86, 92, 106–109
- KPI** Key Performance Indicator. 14
- LVNL** Luchtverkeersleiding Nederland. 28
- MGTP** Mean Global Temperature Potential. 18–20
- MTOW** Maximum Take-Off Weight. 35, 56
- NAR** North American Route. 30
- NAT** North Atlantic Track. V, 29, 30, 65, 82, 83, 86, 87, 91, 108
- NAT-OTS** North Atlantic Organized Track System. 28–30
- NDB** Non Directional Beacon. 22
- NWP** Numeric Weather Prediction. 37, 39, 40, 42, 43, 45, 51, 52, 56–59, 61–63, 65, 66, 69–74, 76, 77, 80, 82, 87, 89, 92, 106–109
- RAD** Route Availability Document. 24
- RMSE** Root Mean Square Error. 42, 63, 64, 107
- SID** Standard Instrument Departure. 22, 24
- SQP** Sequential Quadratic Programming. 35, 55
- STAR** Standard Terminal Arrival Route. 22, 24
- TAS** True Airspeed. 36, 58, 70
- TOC** Top of Climb. 57, 58, 76, 80, 107
- UK** United Kingdom. 28, 30, 66
- UN** United Nations. 14
- US** United States. 11, 17, 21, 28, 30, 41, 66, 86, 88, 89
- VOR** VHF Omni Directional Radio Range. 22

LIST OF FIGURES

2.1	Contrail formation conditions	5
2.2	Persistence of contrails [21]	7
2.3	Illustration of contrail persistence by Schrader [15]	8
3.1	Overview of aviation emissions and their impact on climate change and damages [50]	13
3.2	Worldwide annual number of scheduled pax [53, 54, 55, 56]	14
3.3	Probability of flying in ISSR after various altitude change policies [5]	18
4.1	Typical flight phases [79]	23
4.2	Example flight plan [81]	23
4.3	Example airway structure above Brazil [82]	24
5.1	Schematic representation of flight planning algorithm	26
5.2	Free body diagram of forces acting on point mass and resulting acceleration	27
5.3	Upper ATS routes above the UK and Netherlands	28
5.4	Upper ATS routes above North-Eastern United States	29
5.5	Complete Europe to United States network topology used for simulation	31
5.6	Wind triangle method	33
5.7	Mass and cruise altitude estimates for NL to Washington D.C. (KIAD) flight	34
5.8	Ground track from NL to Washington D.C. (KIAD) in wind field at 250 hPa	35
5.9	Altitude profile of unbound optimum, flight level constrained and flight level + Mach number constrained at $CI = 0$	37
5.10	Drag polar used to model aerodynamic behaviour	38
5.11	Max thrust in Newton and fuel flow in kg/s used to model engine characteristics	39
5.12	Horizontal (left) and vertical (right) resolution of Canadian GDPS NWP data	42
5.13	Canada GDPS NWP accuracy development with respect to prediction horizon [85]	43
5.14	Comparison of ISA and 2014 and 2017 Canada GDPS NWP data at Spijkerboor fix	43
5.15	Persistent contrail formation regions (yellow) at 250hPa (34000ft)	46
5.16	Ground track alterations NL to Washington DC (KIAD) at given values of β_{ground}	47
5.17	Hypothetical situations (blue) with potential profile alterations (red)	49
5.18	Mitigation profile generation on flight passing through two contrail regions	50
6.1	Steady horizontal flight unit cost at m_{land} in ISA with CAS and Mach constraints and fuel optimal (A) and time optimal (B) cases in May 2017 NWP	52
6.2	Absolute percentage difference between drag coefficient (C_D) in this thesis and the one used by Hendriks [1]	52
6.3	Percentage difference between maximum thrust (A) and maximum fuel flow (B) used for this thesis and the one used by Hendriks [1]	53

6.4	Fuel consumption of level cruise vs repeated step climbs in ISA at 26.000ft, 250m/s and 300.000kg	54
6.5	Unrestricted optimal cruise altitude in 2014 NWP of 252672 kg (top) and 362874 kg (bottom)	57
6.6	Flight level restricted optimal cruise altitude in 2014 NWP of 252672 kg (top) and 362874 kg (bottom)	57
6.7	Overview of selected climb scenarios - TOC for all 240 m/s TAS and 317672 kg . .	58
6.8	Critical temperature and ambient temperature in February 2014 NWP on the left (A) and ISA on the right [4] (B)	59
6.9	$T_{amb} - T_{crit}$ at 250hPa (34000ft)	59
6.10	Contrail formation regions at 250hPa (34000ft)	59
6.11	RH_i at 250hPa (34000ft)	60
6.12	Contrail persistence regions at 250hPa (34000ft)	60
6.13	Contrail persistence regions at 250hPa (34000ft) for 60, 70, 80 and 90% RH_i in February 2014 NWP	61
6.14	Fuel optimal ground tracks to Vancouver (CYVR) for β_{grnd} in May 2017 NWP - Persistent contrail regions shown at 250hPa	62
6.15	Fuel optimal flight profile with alterations (in black) to Washington D.C. (KIAD) for β_{prof} in Feb 2014 NWP	63
6.16	Normalized RMSE of generation best compared to final solution and share of local optimizations that converge within number of generations	64
8.1	Fuel optimal ground track to Washington D.C. (KIAD) in ISA	67
8.2	Fuel optimal flight profile to Washington D.C. (KIAD) in ISA	67
8.3	Fuel optimal three dimensional trajectory to Washington D.C. (KIAD) in ISA . .	68
8.4	Mass and time development of fuel optimal flight to Washington D.C. (KIAD) in ISA as function of horizontal distance	68
8.5	Fuel optimal flight to Washington D.C. (KIAD) in NWP May 2017 without wind .	70
8.6	Time optimal flight to Washington D.C. (KIAD) in NWP May 2017 without wind	70
8.7	Ground track of fuel optimal flight in NWP May 2017 with and without wind . . .	71
8.8	Fuel optimal flights: effect of β_{grnd} on contrail distance and fuel consumption . . .	73
8.9	Time optimal flights: effect of β_{grnd} on contrail distance and flight time	74
8.10	Average change in contrail distance, fuel consumption and flight time of fuel and time optimal flights as function of β_{prof}	75
8.11	Origin overshoot due to TOC being inside contrail region as shown by the offset dashed climb phase (example of non-comparable output)	76
8.12	Average change in contrail distance of fuel optimal (left) and time optimal (right) flights for various β_{grnd} and β_{prof}	78
8.13	Average change in fuel consumption of fuel optimal flights (left) and flight time of time optimal flights (right) for various β_{grnd} and β_{prof}	78
8.14	Sensitivity of ground track contrail mitigation on fuel and flight time	79
8.15	Sensitivity of profile based contrail mitigation on fuel and flight time for fuel optimal flights	80
8.16	Sensitivity of profile based contrail mitigation on fuel and flight time for time optimal flights	81
8.17	Sensitivity of hybrid contrail mitigation on fuel consumption and flight time . . .	81

LIST OF FIGURES

8.18 Results from ground track alterations given fixed NATs - A) contrail mitigation vs β_{grnd} , B) sensitivity of ground track alterations of fixed NAT routes for fuel consumption of fuel optimal flights on left y-axis and flight time for time optimal flights on right y-axis, C) additional fuel consumption vs β_{grnd} of fuel optimal flights, D) additional flight time vs β_{grnd} of time optimal flights	83
8.19 Contrail formation areas (yellow) encountered by flights to Winnipeg (CYWG) for different engine efficiency	85
8.20 Persistent contrail regions (yellow) encountered by flights to Winnipeg (CYWG) for different engine efficiency	85
8.21 Contrail regions (yellow) encountered by flights to Washington D.C. (KIAD) for three different atmospheres including flight levels	86
8.22 Persistent contrail regions (yellow) at 250hPa (34000ft) in Feb 2014, Feb 2017 and May 2017 NWP including generalized ground tracks	87

LIST OF TABLES

- 4.1 Overview of selected flight planning software 24
- 6.1 Impact of step climb/descent on instantaneous fuel consumption compared to steady horizontal flight at 25.000ft, 250m/s, 300.000kg in ISA 54
- 8.1 Results from non-mitigated fuel optimal and time optimal flights in ISA 69
- 8.2 Numeric results of non-mitigated fuel optimal and time optimal flights to Washington D.C. (KIAD) in May 2017 NWP without wind 70
- 8.3 Comparison of numeric results of non-mitigated fuel optimal and time optimal flights to Washington D.C. (KIAD) in May 2017 NWP with wind and without wind . . . 71
- 8.4 Comparison of numeric results of non-mitigated fuel optimal and time optimal flights to different destinations in May 2017 NWP including wind 72

APPENDIX A

NUMERIC RESULTS - BASELINE

β_{grnd}	β_{prof}	Dest	Atm	Mode	dm [kg]	ds [m]	dt [h:m:s]	ct _{tot} [m]	% dm	% ds	% dt	% CT
0	0	KIAD	ISA	fuel opt	64,840	5,897,366	6h 27m 7s	-	-	-	-	-
0	0	CYWG	ISA	fuel opt	71,560	6,485,112	7h 5m 10s	-	-	-	-	-
0	0	CYVR	ISA	fuel opt	84,862	7,632,200	8h 19m 21s	-	-	-	-	-
0	0	KIAD	Feb-14	fuel opt	70,435	6,264,467	7h 0m 9s	654,729	-	-	-	-
0	0	CYWG	Feb-14	fuel opt	77,564	6,839,002	7h 40m 39s	2,238,395	-	-	-	-
0	0	CYVR	Feb-14	fuel opt	88,254	7,766,065	8h 40m 7s	1,550,551	-	-	-	-
0	0	KIAD	Feb-17	fuel opt	67,195	6,062,762	6h 41m 29s	0	-	-	-	-
0	0	CYWG	Feb-17	fuel opt	71,749	6,471,289	7h 7m 41s	515,195	-	-	-	-
0	0	CYVR	Feb-17	fuel opt	86,867	7,739,677	8h 32m 6s	1,145,812	-	-	-	-
0	0	KIAD	May-17	fuel opt	64,630	5,871,104	6h 26m 58s	1,165,000	-	-	-	-
0	0	CYWG	May-17	fuel opt	72,577	6,613,080	7h 12m 17s	1,360,000	-	-	-	-
0	0	CYVR	May-17	fuel opt	87,780	7,931,614	8h 36m 55s	1,037,044	-	-	-	-
0	0	KIAD	ISA	time opt	72,057	5,897,366	6h 0m 10s	-	-	-	-	-
0	0	CYWG	ISA	time opt	79,430	6,485,112	6h 35m 52s	-	-	-	-	-
0	0	CYVR	ISA	time opt	93,992	7,632,200	7h 45m 33s	-	-	-	-	-
0	0	KIAD	Feb-14	time opt	74,108	5,937,317	6h 16m 15s	2,315,000	-	-	-	-
0	0	CYWG	Feb-14	time opt	85,065	6,777,028	7h 10m 9s	2,940,000	-	-	-	-
0	0	CYVR	Feb-14	time opt	97,849	7,786,731	8h 12m 9s	2,700,000	-	-	-	-
0	0	KIAD	Feb-17	time opt	72,513	5,922,568	6h 8m 16s	1,975,000	-	-	-	-
0	0	CYWG	Feb-17	time opt	80,129	6,481,044	6h 45m 48s	1,325,000	-	-	-	-
0	0	CYVR	Feb-17	time opt	95,609	7,725,148	8h 1m 8s	1,395,000	-	-	-	-
0	0	KIAD	May-17	time opt	71,090	5,882,411	6h 1m 1s	0	-	-	-	-
0	0	CYWG	May-17	time opt	79,896	6,594,946	6h 44m 33s	0	-	-	-	-
0	0	CYVR	May-17	time opt	95,800	7,837,486	8h 1m 52s	0	-	-	-	-

APPENDIX B

NUMERIC RESULTS - GROUND TRACK

B. Numeric results - Ground track

β_{grnd}	β_{prof}	Dest	Atm	Mode	dm [kg]	ds [m]	dt [h:m:s]	ct _{tot} [m]	% dm	% ds	% dt	% CT
0	0	KIAD	Feb-14	fuel opt	70,437	6,264,467	7h 0m 9s	655,770	0.0000%	0.0000%	0.0000%	0.0%
0.01	0	KIAD	Feb-14	fuel opt	70,569	6,265,300	7h 0m 51s	486,194	0.1879%	0.0133%	0.1666%	-25.9%
0.02	0	KIAD	Feb-14	fuel opt	70,569	6,265,300	7h 0m 51s	486,194	0.1879%	0.0133%	0.1666%	-25.9%
0.03	0	KIAD	Feb-14	fuel opt	70,569	6,265,300	7h 0m 51s	486,194	0.1879%	0.0133%	0.1666%	-25.9%
0.04	0	KIAD	Feb-14	fuel opt	70,569	6,265,300	7h 0m 51s	486,194	0.1879%	0.0133%	0.1666%	-25.9%
0.05	0	KIAD	Feb-14	fuel opt	70,569	6,265,300	7h 0m 51s	486,194	0.1879%	0.0133%	0.1666%	-25.9%
0.06	0	KIAD	Feb-14	fuel opt	70,569	6,265,300	7h 0m 51s	486,194	0.1879%	0.0133%	0.1666%	-25.9%
0.07	0	KIAD	Feb-14	fuel opt	70,569	6,265,300	7h 0m 51s	486,194	0.1879%	0.0133%	0.1666%	-25.9%
0.08	0	KIAD	Feb-14	fuel opt	70,569	6,265,300	7h 0m 51s	486,194	0.1879%	0.0133%	0.1666%	-25.9%
0.09	0	KIAD	Feb-14	fuel opt	70,569	6,265,300	7h 0m 51s	486,194	0.1879%	0.0133%	0.1666%	-25.9%
0.1	0	KIAD	Feb-14	fuel opt	70,569	6,265,300	7h 0m 51s	486,194	0.1879%	0.0133%	0.1666%	-25.9%
0.2	0	KIAD	Feb-14	fuel opt	70,588	6,266,822	7h 0m 57s	475,194	0.2143%	0.0376%	0.1914%	-27.5%
0.3	0	KIAD	Feb-14	fuel opt	70,588	6,266,822	7h 0m 57s	475,194	0.2143%	0.0376%	0.1914%	-27.5%
0.4	0	KIAD	Feb-14	fuel opt	70,588	6,266,822	7h 0m 57s	475,194	0.2143%	0.0376%	0.1914%	-27.5%
0.5	0	KIAD	Feb-14	fuel opt	73,175	6,465,484	7h 15m 32s	119,895	3.8868%	3.2088%	3.6638%	-81.7%
0.6	0	KIAD	Feb-14	fuel opt	73,175	6,465,484	7h 15m 32s	119,895	3.8868%	3.2088%	3.6638%	-81.7%
0.7	0	KIAD	Feb-14	fuel opt	73,175	6,465,484	7h 15m 32s	119,895	3.8868%	3.2088%	3.6638%	-81.7%
0.8	0	KIAD	Feb-14	fuel opt	73,175	6,465,484	7h 15m 32s	119,895	3.8868%	3.2088%	3.6638%	-81.7%
0.9	0	KIAD	Feb-14	fuel opt	73,175	6,465,484	7h 15m 32s	119,895	3.8868%	3.2088%	3.6638%	-81.7%
1	0	KIAD	Feb-14	fuel opt	73,229	6,471,104	7h 15m 51s	119,896	3.9638%	3.2986%	3.7359%	-81.7%
2	0	KIAD	Feb-14	fuel opt	73,229	6,471,104	7h 15m 51s	119,896	3.9638%	3.2986%	3.7359%	-81.7%
3	0	KIAD	Feb-14	fuel opt	73,229	6,471,104	7h 15m 51s	119,896	3.9638%	3.2986%	3.7359%	-81.7%
4	0	KIAD	Feb-14	fuel opt	73,229	6,471,104	7h 15m 51s	119,896	3.9638%	3.2986%	3.7359%	-81.7%
5	0	KIAD	Feb-14	fuel opt	73,229	6,471,104	7h 15m 51s	119,896	3.9638%	3.2986%	3.7359%	-81.7%
6	0	KIAD	Feb-14	fuel opt	73,229	6,471,104	7h 15m 51s	119,896	3.9638%	3.2986%	3.7359%	-81.7%
7	0	KIAD	Feb-14	fuel opt	73,229	6,471,104	7h 15m 51s	119,896	3.9638%	3.2986%	3.7359%	-81.7%
8	0	KIAD	Feb-14	fuel opt	73,229	6,471,104	7h 15m 51s	119,896	3.9638%	3.2986%	3.7359%	-81.7%
9	0	KIAD	Feb-14	fuel opt	73,229	6,471,104	7h 15m 51s	119,896	3.9638%	3.2986%	3.7359%	-81.7%
10	0	KIAD	Feb-14	fuel opt	73,229	6,471,104	7h 15m 51s	119,896	3.9638%	3.2986%	3.7359%	-81.7%
20	0	KIAD	Feb-14	fuel opt	73,229	6,471,104	7h 15m 51s	119,896	3.9638%	3.2986%	3.7359%	-81.7%
30	0	KIAD	Feb-14	fuel opt	73,229	6,471,104	7h 15m 51s	119,896	3.9638%	3.2986%	3.7359%	-81.7%
40	0	KIAD	Feb-14	fuel opt	73,229	6,471,104	7h 15m 51s	119,896	3.9638%	3.2986%	3.7359%	-81.7%
50	0	KIAD	Feb-14	fuel opt	73,229	6,471,104	7h 15m 51s	119,896	3.9638%	3.2986%	3.7359%	-81.7%
60	0	KIAD	Feb-14	fuel opt	73,229	6,471,104	7h 15m 51s	119,896	3.9638%	3.2986%	3.7359%	-81.7%
70	0	KIAD	Feb-14	fuel opt	73,229	6,471,104	7h 15m 51s	119,896	3.9638%	3.2986%	3.7359%	-81.7%
80	0	KIAD	Feb-14	fuel opt	73,229	6,471,104	7h 15m 51s	119,896	3.9638%	3.2986%	3.7359%	-81.7%
90	0	KIAD	Feb-14	fuel opt	73,229	6,471,104	7h 15m 51s	119,896	3.9638%	3.2986%	3.7359%	-81.7%
100	0	KIAD	Feb-14	fuel opt	73,229	6,471,104	7h 15m 51s	119,896	3.9638%	3.2986%	3.7359%	-81.7%
0	0	CYWG	Feb-14	fuel opt	77,555	6,837,999	7h 40m 35s	2,348,628	0.0000%	0.0000%	0.0000%	0.0%
0.01	0	CYWG	Feb-14	fuel opt	77,555	6,837,999	7h 40m 35s	2,348,628	0.0000%	0.0000%	0.0000%	0.0%
0.02	0	CYWG	Feb-14	fuel opt	76,602	6,771,409	7h 35m 25s	1,325,949	-1.2287%	-0.9738%	-1.1215%	-43.5%
0.03	0	CYWG	Feb-14	fuel opt	76,602	6,771,409	7h 35m 25s	1,325,949	-1.2287%	-0.9738%	-1.1215%	-43.5%
0.04	0	CYWG	Feb-14	fuel opt	76,602	6,771,409	7h 35m 25s	1,325,949	-1.2287%	-0.9738%	-1.1215%	-43.5%
0.05	0	CYWG	Feb-14	fuel opt	76,602	6,771,409	7h 35m 25s	1,325,949	-1.2287%	-0.9738%	-1.1215%	-43.5%
0.06	0	CYWG	Feb-14	fuel opt	76,602	6,771,409	7h 35m 25s	1,325,949	-1.2287%	-0.9738%	-1.1215%	-43.5%
0.07	0	CYWG	Feb-14	fuel opt	76,602	6,771,409	7h 35m 25s	1,325,949	-1.2287%	-0.9738%	-1.1215%	-43.5%
0.08	0	CYWG	Feb-14	fuel opt	76,602	6,771,409	7h 35m 25s	1,325,949	-1.2287%	-0.9738%	-1.1215%	-43.5%
0.09	0	CYWG	Feb-14	fuel opt	76,602	6,771,409	7h 35m 25s	1,325,949	-1.2287%	-0.9738%	-1.1215%	-43.5%
0.1	0	CYWG	Feb-14	fuel opt	76,602	6,771,409	7h 35m 25s	1,325,949	-1.2287%	-0.9738%	-1.1215%	-43.5%
0.2	0	CYWG	Feb-14	fuel opt	76,650	6,776,869	7h 35m 41s	1,277,949	-1.1676%	-0.8940%	-1.0644%	-45.6%
0.3	0	CYWG	Feb-14	fuel opt	76,650	6,776,869	7h 35m 41s	1,277,949	-1.1676%	-0.8940%	-1.0644%	-45.6%
0.4	0	CYWG	Feb-14	fuel opt	76,650	6,776,869	7h 35m 41s	1,277,949	-1.1676%	-0.8940%	-1.0644%	-45.6%
0.5	0	CYWG	Feb-14	fuel opt	78,724	6,936,487	7h 47m 4s	894,567	1.5076%	1.4403%	1.4069%	-61.9%
0.6	0	CYWG	Feb-14	fuel opt	79,636	7,034,519	7h 52m 18s	746,530	2.6834%	2.8739%	2.5423%	-68.2%
0.7	0	CYWG	Feb-14	fuel opt	79,636	7,034,519	7h 52m 18s	746,530	2.6834%	2.8739%	2.5423%	-68.2%
0.8	0	CYWG	Feb-14	fuel opt	79,636	7,034,519	7h 52m 18s	746,530	2.6834%	2.8739%	2.5423%	-68.2%
0.9	0	CYWG	Feb-14	fuel opt	79,636	7,034,519	7h 52m 18s	746,530	2.6834%	2.8739%	2.5423%	-68.2%
1	0	CYWG	Feb-14	fuel opt	86,356	7,583,977	8h 29m 34s	203,601	11.3476%	10.9093%	10.6335%	-91.3%
2	0	CYWG	Feb-14	fuel opt	86,356	7,583,977	8h 29m 34s	203,601	11.3476%	10.9093%	10.6335%	-91.3%
3	0	CYWG	Feb-14	fuel opt	88,093	7,725,277	8h 39m 2s	235,000	13.5872%	12.9757%	12.6903%	-90.0%
4	0	CYWG	Feb-14	fuel opt	88,093	7,725,277	8h 39m 2s	235,000	13.5872%	12.9757%	12.6903%	-90.0%
5	0	CYWG	Feb-14	fuel opt	88,093	7,725,277	8h 39m 2s	235,000	13.5872%	12.9757%	12.6903%	-90.0%
6	0	CYWG	Feb-14	fuel opt	88,093	7,725,277	8h 39m 2s	235,000	13.5872%	12.9757%	12.6903%	-90.0%
7	0	CYWG	Feb-14	fuel opt	88,093	7,725,277	8h 39m 2s	235,000	13.5872%	12.9757%	12.6903%	-90.0%
8	0	CYWG	Feb-14	fuel opt	88,093	7,725,277	8h 39m 2s	235,000	13.5872%	12.9757%	12.6903%	-90.0%
9	0	CYWG	Feb-14	fuel opt	88,576	7,766,087	8h 41m 42s	235,000	14.2108%	13.5725%	13.2690%	-90.0%
10	0	CYWG	Feb-14	fuel opt	88,576	7,766,087	8h 41m 42s	235,000	14.2108%	13.5725%	13.2690%	-90.0%
20	0	CYWG	Feb-14	fuel opt	88,576	7,766,087	8h 41m 42s	235,000	14.2108%	13.5725%	13.2690%	-90.0%
30	0	CYWG	Feb-14	fuel opt	88,576	7,766,087	8h 41m 42s	235,000	14.2108%	13.5725%	13.2690%	-90.0%
40	0	CYWG	Feb-14	fuel opt	88,576	7,766,087	8h 41m 42s	235,000	14.2108%	13.5725%	13.2690%	-90.0%
50	0	CYWG	Feb-14	fuel opt	88,576	7,766,087	8h 41m 42s	235,000	14.2108%	13.5725%	13.2690%	-90.0%
60	0	CYWG	Feb-14	fuel opt	88,576	7,766,087	8h 41m 42s	235,000	14.2108%	13.5725%	13.2690%	-90.0%
70	0	CYWG	Feb-14	fuel opt	88,576	7,766,087	8h 41m 42s	235,000	14.2108%	13.5725%	13.2690%	-90.0%
80	0	CYWG	Feb-14	fuel opt	88,576	7,766,087	8h 41m 42s	235,000	14.2108%	13.5725%	13.2690%	-90.0%
90	0	CYWG	Feb-14	fuel opt	88,576	7,766,087	8h 41m 42s	235,000	14.2108%	13.5725%	13.2690%	-90.0%
100	0	CYWG	Feb-14	fuel opt	88,576	7,766,087	8h 41m 42s	235,000	14.2108%	13.5725%	13.2690%	-90.0%

B. Numeric results - Ground track

β_{grnd}	β_{prof}	Dest	Atm	Mode	dm [kg]	ds [m]	dt [h:m:s]	ct _{tot} [m]	% dm	% ds	% dt	% CT
0	0	CYWG	Feb-17	fuel opt	71,752	6,471,289	7h 7m 41s	509,193	0.0000%	0.0000%	0.0000%	0.0%
0.01	0	CYWG	Feb-17	fuel opt	71,752	6,471,289	7h 7m 41s	509,193	0.0000%	0.0000%	0.0000%	0.0%
0.02	0	CYWG	Feb-17	fuel opt	71,752	6,471,289	7h 7m 41s	509,193	0.0000%	0.0000%	0.0000%	0.0%
0.03	0	CYWG	Feb-17	fuel opt	71,752	6,471,289	7h 7m 41s	509,193	0.0000%	0.0000%	0.0000%	0.0%
0.04	0	CYWG	Feb-17	fuel opt	71,752	6,471,289	7h 7m 41s	509,193	0.0000%	0.0000%	0.0000%	0.0%
0.05	0	CYWG	Feb-17	fuel opt	71,752	6,471,289	7h 7m 41s	509,193	0.0000%	0.0000%	0.0000%	0.0%
0.06	0	CYWG	Feb-17	fuel opt	71,752	6,471,289	7h 7m 41s	509,193	0.0000%	0.0000%	0.0000%	0.0%
0.07	0	CYWG	Feb-17	fuel opt	71,752	6,471,289	7h 7m 41s	509,193	0.0000%	0.0000%	0.0000%	0.0%
0.08	0	CYWG	Feb-17	fuel opt	71,752	6,471,289	7h 7m 41s	509,193	0.0000%	0.0000%	0.0000%	0.0%
0.09	0	CYWG	Feb-17	fuel opt	71,752	6,471,289	7h 7m 41s	509,193	0.0000%	0.0000%	0.0000%	0.0%
0.1	0	CYWG	Feb-17	fuel opt	71,752	6,471,289	7h 7m 41s	509,193	0.0000%	0.0000%	0.0000%	0.0%
0.2	0	CYWG	Feb-17	fuel opt	71,752	6,471,289	7h 7m 41s	509,193	0.0000%	0.0000%	0.0000%	0.0%
0.3	0	CYWG	Feb-17	fuel opt	73,261	6,600,968	7h 16m 3s	0	2.1029%	2.0039%	1.9572%	-100.0%
0.4	0	CYWG	Feb-17	fuel opt	73,261	6,600,968	7h 16m 3s	0	2.1029%	2.0039%	1.9572%	-100.0%
0.5	0	CYWG	Feb-17	fuel opt	73,261	6,600,968	7h 16m 3s	0	2.1029%	2.0039%	1.9572%	-100.0%
0.6	0	CYWG	Feb-17	fuel opt	73,261	6,600,968	7h 16m 3s	0	2.1029%	2.0039%	1.9572%	-100.0%
0.7	0	CYWG	Feb-17	fuel opt	73,261	6,600,968	7h 16m 3s	0	2.1029%	2.0039%	1.9572%	-100.0%
0.8	0	CYWG	Feb-17	fuel opt	73,261	6,600,968	7h 16m 3s	0	2.1029%	2.0039%	1.9572%	-100.0%
0.9	0	CYWG	Feb-17	fuel opt	73,261	6,600,968	7h 16m 3s	0	2.1029%	2.0039%	1.9572%	-100.0%
1	0	CYWG	Feb-17	fuel opt	73,261	6,600,968	7h 16m 3s	0	2.1029%	2.0039%	1.9572%	-100.0%
2	0	CYWG	Feb-17	fuel opt	73,261	6,600,968	7h 16m 3s	0	2.1029%	2.0039%	1.9572%	-100.0%
3	0	CYWG	Feb-17	fuel opt	73,261	6,600,968	7h 16m 3s	0	2.1029%	2.0039%	1.9572%	-100.0%
4	0	CYWG	Feb-17	fuel opt	73,261	6,600,968	7h 16m 3s	0	2.1029%	2.0039%	1.9572%	-100.0%
5	0	CYWG	Feb-17	fuel opt	73,261	6,600,968	7h 16m 3s	0	2.1029%	2.0039%	1.9572%	-100.0%
6	0	CYWG	Feb-17	fuel opt	73,261	6,600,968	7h 16m 3s	0	2.1029%	2.0039%	1.9572%	-100.0%
7	0	CYWG	Feb-17	fuel opt	73,261	6,600,968	7h 16m 3s	0	2.1029%	2.0039%	1.9572%	-100.0%
8	0	CYWG	Feb-17	fuel opt	73,261	6,600,968	7h 16m 3s	0	2.1029%	2.0039%	1.9572%	-100.0%
9	0	CYWG	Feb-17	fuel opt	73,261	6,600,968	7h 16m 3s	0	2.1029%	2.0039%	1.9572%	-100.0%
10	0	CYWG	Feb-17	fuel opt	73,261	6,600,968	7h 16m 3s	0	2.1029%	2.0039%	1.9572%	-100.0%
20	0	CYWG	Feb-17	fuel opt	73,261	6,600,968	7h 16m 3s	0	2.1029%	2.0039%	1.9572%	-100.0%
30	0	CYWG	Feb-17	fuel opt	73,261	6,600,968	7h 16m 3s	0	2.1029%	2.0039%	1.9572%	-100.0%
40	0	CYWG	Feb-17	fuel opt	73,261	6,600,968	7h 16m 3s	0	2.1029%	2.0039%	1.9572%	-100.0%
50	0	CYWG	Feb-17	fuel opt	73,261	6,600,968	7h 16m 3s	0	2.1029%	2.0039%	1.9572%	-100.0%
60	0	CYWG	Feb-17	fuel opt	73,261	6,600,968	7h 16m 3s	0	2.1029%	2.0039%	1.9572%	-100.0%
70	0	CYWG	Feb-17	fuel opt	73,261	6,600,968	7h 16m 3s	0	2.1029%	2.0039%	1.9572%	-100.0%
80	0	CYWG	Feb-17	fuel opt	73,261	6,600,968	7h 16m 3s	0	2.1029%	2.0039%	1.9572%	-100.0%
90	0	CYWG	Feb-17	fuel opt	73,261	6,600,968	7h 16m 3s	0	2.1029%	2.0039%	1.9572%	-100.0%
100	0	CYWG	Feb-17	fuel opt	73,261	6,600,968	7h 16m 3s	0	2.1029%	2.0039%	1.9572%	-100.0%
0	0	CYVR	Feb-17	fuel opt	86,870	7,739,677	8h 32m 5s	1,141,802	0.0000%	0.0000%	0.0000%	0.0%
0.01	0	CYVR	Feb-17	fuel opt	86,870	7,739,677	8h 32m 5s	1,141,802	0.0000%	0.0000%	0.0000%	0.0%
0.02	0	CYVR	Feb-17	fuel opt	86,883	7,740,377	8h 32m 8s	1,130,767	0.0148%	0.0090%	0.0069%	-1.0%
0.03	0	CYVR	Feb-17	fuel opt	86,883	7,740,377	8h 32m 8s	1,130,767	0.0148%	0.0090%	0.0069%	-1.0%
0.04	0	CYVR	Feb-17	fuel opt	86,883	7,740,377	8h 32m 8s	1,130,767	0.0148%	0.0090%	0.0069%	-1.0%
0.05	0	CYVR	Feb-17	fuel opt	86,883	7,740,377	8h 32m 8s	1,130,767	0.0148%	0.0090%	0.0069%	-1.0%
0.06	0	CYVR	Feb-17	fuel opt	86,883	7,740,377	8h 32m 8s	1,130,767	0.0148%	0.0090%	0.0069%	-1.0%
0.07	0	CYVR	Feb-17	fuel opt	86,883	7,740,377	8h 32m 8s	1,130,767	0.0148%	0.0090%	0.0069%	-1.0%
0.08	0	CYVR	Feb-17	fuel opt	86,883	7,740,377	8h 32m 8s	1,130,767	0.0148%	0.0090%	0.0069%	-1.0%
0.09	0	CYVR	Feb-17	fuel opt	86,883	7,740,377	8h 32m 8s	1,130,767	0.0148%	0.0090%	0.0069%	-1.0%
0.1	0	CYVR	Feb-17	fuel opt	86,883	7,740,377	8h 32m 8s	1,130,767	0.0148%	0.0090%	0.0069%	-1.0%
0.2	0	CYVR	Feb-17	fuel opt	87,076	7,758,235	8h 33m 4s	1,054,803	0.2380%	0.2398%	0.1904%	-7.6%
0.3	0	CYVR	Feb-17	fuel opt	87,780	7,820,234	8h 37m 2s	767,495	1.0476%	1.0408%	0.9662%	-32.8%
0.4	0	CYVR	Feb-17	fuel opt	87,819	7,823,475	8h 37m 15s	755,495	1.0923%	1.0827%	1.0083%	-33.8%
0.5	0	CYVR	Feb-17	fuel opt	87,819	7,823,475	8h 37m 15s	755,495	1.0923%	1.0827%	1.0083%	-33.8%
0.6	0	CYVR	Feb-17	fuel opt	87,819	7,823,475	8h 37m 15s	755,495	1.0923%	1.0827%	1.0083%	-33.8%
0.7	0	CYVR	Feb-17	fuel opt	91,667	8,147,440	8h 58m 32s	376,193	5.5228%	5.2685%	5.1627%	-67.1%
0.8	0	CYVR	Feb-17	fuel opt	91,667	8,147,440	8h 58m 32s	376,193	5.5228%	5.2685%	5.1627%	-67.1%
0.9	0	CYVR	Feb-17	fuel opt	91,667	8,147,440	8h 58m 32s	376,193	5.5228%	5.2685%	5.1627%	-67.1%
1	0	CYVR	Feb-17	fuel opt	91,667	8,147,440	8h 58m 32s	376,193	5.5228%	5.2685%	5.1627%	-67.1%
2	0	CYVR	Feb-17	fuel opt	92,513	8,218,480	9h 3m 7s	305,118	6.4959%	6.1863%	6.0585%	-73.3%
3	0	CYVR	Feb-17	fuel opt	97,765	8,650,620	9h 31m 55s	627,446	12.5427%	11.7698%	11.6834%	-45.0%
4	0	CYVR	Feb-17	fuel opt	97,765	8,650,620	9h 31m 55s	627,446	12.5427%	11.7698%	11.6834%	-45.0%
5	0	CYVR	Feb-17	fuel opt	97,765	8,650,620	9h 31m 55s	627,446	12.5427%	11.7698%	11.6834%	-45.0%
6	0	CYVR	Feb-17	fuel opt	97,765	8,650,620	9h 31m 55s	627,446	12.5427%	11.7698%	11.6834%	-45.0%
7	0	CYVR	Feb-17	fuel opt	97,765	8,650,620	9h 31m 55s	627,446	12.5427%	11.7698%	11.6834%	-45.0%
8	0	CYVR	Feb-17	fuel opt	97,765	8,650,620	9h 31m 55s	627,446	12.5427%	11.7698%	11.6834%	-45.0%
9	0	CYVR	Feb-17	fuel opt	97,765	8,650,620	9h 31m 55s	627,446	12.5427%	11.7698%	11.6834%	-45.0%
10	0	CYVR	Feb-17	fuel opt	97,765	8,650,620	9h 31m 55s	627,446	12.5427%	11.7698%	11.6834%	-45.0%
20	0	CYVR	Feb-17	fuel opt	97,765	8,650,620	9h 31m 55s	627,446	12.5427%	11.7698%	11.6834%	-45.0%
30	0	CYVR	Feb-17	fuel opt	97,765	8,650,620	9h 31m 55s	627,446	12.5427%	11.7698%	11.6834%	-45.0%
40	0	CYVR	Feb-17	fuel opt	97,765	8,650,620	9h 31m 55s	627,446	12.5427%	11.7698%	11.6834%	-45.0%
50	0	CYVR	Feb-17	fuel opt	97,765	8,650,620	9h 31m 55s	627,446	12.5427%	11.7698%	11.6834%	-45.0%
60	0	CYVR	Feb-17	fuel opt	97,765	8,650,620	9h 31m 55s	627,446	12.5427%	11.7698%	11.6834%	-45.0%
70	0	CYVR	Feb-17	fuel opt	97,765	8,650,620	9h 31m 55s	627,446	12.5427%	11.7698%	11.6834%	-45.0%
80	0	CYVR	Feb-17	fuel opt	97,765	8,650,620	9h 31m 55s	627,446	12.5427%	11.7698%	11.6834%	-45.0%
90	0	CYVR	Feb-17	fuel opt	97,765	8,650,620	9h 31m 55s	627,446	12.5427%	11.7698%	11.6834%	-45.0%
100	0	CYVR	Feb-17	fuel opt	97,765	8,650,620	9h 31m 55s	627,446	12.5427%	11.7698%	11.6834%	-45.0%

β_{grnd}	β_{prof}	Dest	Atm	Mode	dm [kg]	ds [m]	dt [h:m:s]	ct_{tot} [m]	% dm	% ds	% dt	% CT
0	0	KIAD	May-17	fuel opt	64,632	5,871,104	6h 26m 58s	1,144,000	0.0000%	0.0000%	0.0000%	0.0%
0.01	0	KIAD	May-17	fuel opt	64,638	5,871,146	6h 26m 59s	1,106,000	0.0086%	0.0007%	0.0056%	-3.3%
0.02	0	KIAD	May-17	fuel opt	64,665	5,873,644	6h 27m 9s	662,000	0.0514%	0.0433%	0.0472%	-42.1%
0.03	0	KIAD	May-17	fuel opt	64,665	5,873,644	6h 27m 9s	662,000	0.0514%	0.0433%	0.0472%	-42.1%
0.04	0	KIAD	May-17	fuel opt	64,665	5,873,644	6h 27m 9s	662,000	0.0514%	0.0433%	0.0472%	-42.1%
0.05	0	KIAD	May-17	fuel opt	64,671	5,874,174	6h 27m 10s	660,000	0.0596%	0.0523%	0.0549%	-42.3%
0.06	0	KIAD	May-17	fuel opt	64,671	5,874,174	6h 27m 10s	660,000	0.0596%	0.0523%	0.0549%	-42.3%
0.07	0	KIAD	May-17	fuel opt	64,711	5,880,182	6h 27m 20s	721,193	0.1217%	0.1546%	0.0975%	-37.0%
0.08	0	KIAD	May-17	fuel opt	64,711	5,880,182	6h 27m 20s	721,193	0.1217%	0.1546%	0.0975%	-37.0%
0.09	0	KIAD	May-17	fuel opt	64,711	5,880,182	6h 27m 20s	721,193	0.1217%	0.1546%	0.0975%	-37.0%
0.1	0	KIAD	May-17	fuel opt	64,711	5,880,182	6h 27m 20s	721,193	0.1217%	0.1546%	0.0975%	-37.0%
0.2	0	KIAD	May-17	fuel opt	65,251	5,929,684	6h 30m 35s	348,565	0.9570%	0.9978%	0.9363%	-69.5%
0.3	0	KIAD	May-17	fuel opt	65,251	5,929,684	6h 30m 35s	348,565	0.9570%	0.9978%	0.9363%	-69.5%
0.4	0	KIAD	May-17	fuel opt	65,251	5,929,684	6h 30m 35s	348,565	0.9570%	0.9978%	0.9363%	-69.5%
0.5	0	KIAD	May-17	fuel opt	65,433	5,947,674	6h 31m 38s	256,494	1.2391%	1.3042%	1.2058%	-77.6%
0.6	0	KIAD	May-17	fuel opt	65,433	5,947,674	6h 31m 38s	256,494	1.2391%	1.3042%	1.2058%	-77.6%
0.7	0	KIAD	May-17	fuel opt	65,433	5,947,674	6h 31m 38s	256,494	1.2391%	1.3042%	1.2058%	-77.6%
0.8	0	KIAD	May-17	fuel opt	65,433	5,947,674	6h 31m 38s	256,494	1.2391%	1.3042%	1.2058%	-77.6%
0.9	0	KIAD	May-17	fuel opt	65,433	5,947,674	6h 31m 38s	256,494	1.2391%	1.3042%	1.2058%	-77.6%
1	0	KIAD	May-17	fuel opt	65,433	5,947,674	6h 31m 38s	256,494	1.2391%	1.3042%	1.2058%	-77.6%
2	0	KIAD	May-17	fuel opt	67,980	6,179,691	6h 46m 17s	410,000	5.1799%	5.2560%	4.9951%	-64.2%
3	0	KIAD	May-17	fuel opt	67,980	6,179,691	6h 46m 17s	410,000	5.1799%	5.2560%	4.9951%	-64.2%
4	0	KIAD	May-17	fuel opt	70,590	6,382,891	7h 1m 5s	120,639	9.2180%	8.7171%	8.8164%	-89.5%
5	0	KIAD	May-17	fuel opt	70,590	6,382,891	7h 1m 5s	120,639	9.2180%	8.7171%	8.8164%	-89.5%
6	0	KIAD	May-17	fuel opt	70,590	6,382,891	7h 1m 5s	120,639	9.2180%	8.7171%	8.8164%	-89.5%
7	0	KIAD	May-17	fuel opt	70,590	6,382,891	7h 1m 5s	120,639	9.2180%	8.7171%	8.8164%	-89.5%
8	0	KIAD	May-17	fuel opt	70,590	6,382,891	7h 1m 5s	120,639	9.2180%	8.7171%	8.8164%	-89.5%
9	0	KIAD	May-17	fuel opt	70,590	6,382,891	7h 1m 5s	120,639	9.2180%	8.7171%	8.8164%	-89.5%
10	0	KIAD	May-17	fuel opt	70,590	6,382,891	7h 1m 5s	120,639	9.2180%	8.7171%	8.8164%	-89.5%
20	0	KIAD	May-17	fuel opt	70,590	6,382,891	7h 1m 5s	120,639	9.2180%	8.7171%	8.8164%	-89.5%
30	0	KIAD	May-17	fuel opt	70,590	6,382,891	7h 1m 5s	120,639	9.2180%	8.7171%	8.8164%	-89.5%
40	0	KIAD	May-17	fuel opt	70,590	6,382,891	7h 1m 5s	120,639	9.2180%	8.7171%	8.8164%	-89.5%
50	0	KIAD	May-17	fuel opt	70,590	6,382,891	7h 1m 5s	120,639	9.2180%	8.7171%	8.8164%	-89.5%
60	0	KIAD	May-17	fuel opt	70,590	6,382,891	7h 1m 5s	120,639	9.2180%	8.7171%	8.8164%	-89.5%
70	0	KIAD	May-17	fuel opt	70,590	6,382,891	7h 1m 5s	120,639	9.2180%	8.7171%	8.8164%	-89.5%
80	0	KIAD	May-17	fuel opt	70,590	6,382,891	7h 1m 5s	120,639	9.2180%	8.7171%	8.8164%	-89.5%
90	0	KIAD	May-17	fuel opt	70,590	6,382,891	7h 1m 5s	120,639	9.2180%	8.7171%	8.8164%	-89.5%
100	0	KIAD	May-17	fuel opt	70,590	6,382,891	7h 1m 5s	120,639	9.2180%	8.7171%	8.8164%	-89.5%
0	0	CYWG	May-17	fuel opt	72,582	6,613,080	7h 12m 17s	1,343,000	0.0000%	0.0000%	0.0000%	0.0%
0.01	0	CYWG	May-17	fuel opt	72,582	6,613,255	7h 12m 17s	1,182,000	-0.0002%	0.0026%	0.0000%	-12.0%
0.02	0	CYWG	May-17	fuel opt	72,582	6,613,255	7h 12m 17s	1,182,000	-0.0002%	0.0026%	0.0000%	-12.0%
0.03	0	CYWG	May-17	fuel opt	72,582	6,613,255	7h 12m 17s	1,182,000	-0.0002%	0.0026%	0.0000%	-12.0%
0.04	0	CYWG	May-17	fuel opt	72,582	6,613,255	7h 12m 17s	1,182,000	-0.0002%	0.0026%	0.0000%	-12.0%
0.05	0	CYWG	May-17	fuel opt	72,582	6,613,255	7h 12m 17s	1,182,000	-0.0002%	0.0026%	0.0000%	-12.0%
0.06	0	CYWG	May-17	fuel opt	72,582	6,613,255	7h 12m 17s	1,182,000	-0.0002%	0.0026%	0.0000%	-12.0%
0.07	0	CYWG	May-17	fuel opt	72,582	6,613,255	7h 12m 17s	1,182,000	-0.0002%	0.0026%	0.0000%	-12.0%
0.08	0	CYWG	May-17	fuel opt	72,582	6,613,255	7h 12m 17s	1,182,000	-0.0002%	0.0026%	0.0000%	-12.0%
0.09	0	CYWG	May-17	fuel opt	73,161	6,665,746	7h 15m 37s	463,000	0.7973%	0.7964%	0.7697%	-65.5%
0.1	0	CYWG	May-17	fuel opt	73,161	6,665,746	7h 15m 37s	463,000	0.7973%	0.7964%	0.7697%	-65.5%
0.2	0	CYWG	May-17	fuel opt	73,177	6,667,106	7h 15m 42s	460,000	0.8190%	0.8170%	0.7904%	-65.7%
0.3	0	CYWG	May-17	fuel opt	73,683	6,707,026	7h 18m 37s	315,000	1.5163%	1.4206%	1.4617%	-76.5%
0.4	0	CYWG	May-17	fuel opt	73,683	6,707,026	7h 18m 37s	315,000	1.5163%	1.4206%	1.4617%	-76.5%
0.5	0	CYWG	May-17	fuel opt	73,683	6,707,026	7h 18m 37s	315,000	1.5163%	1.4206%	1.4617%	-76.5%
0.6	0	CYWG	May-17	fuel opt	73,911	6,726,331	7h 19m 53s	305,000	1.8311%	1.7125%	1.7575%	-77.3%
0.7	0	CYWG	May-17	fuel opt	73,911	6,726,331	7h 19m 53s	305,000	1.8311%	1.7125%	1.7575%	-77.3%
0.8	0	CYWG	May-17	fuel opt	73,911	6,726,331	7h 19m 53s	305,000	1.8311%	1.7125%	1.7575%	-77.3%
0.9	0	CYWG	May-17	fuel opt	73,911	6,726,331	7h 19m 53s	305,000	1.8311%	1.7125%	1.7575%	-77.3%
1	0	CYWG	May-17	fuel opt	73,911	6,726,331	7h 19m 53s	305,000	1.8311%	1.7125%	1.7575%	-77.3%
2	0	CYWG	May-17	fuel opt	74,142	6,746,991	7h 21m 12s	304,000	2.1487%	2.0249%	2.0623%	-77.4%
3	0	CYWG	May-17	fuel opt	79,938	7,241,571	7h 53m 47s	437,000	10.1349%	9.5038%	9.5992%	-67.5%
4	0	CYWG	May-17	fuel opt	79,938	7,241,571	7h 53m 47s	437,000	10.1349%	9.5038%	9.5992%	-67.5%
5	0	CYWG	May-17	fuel opt	79,938	7,241,571	7h 53m 47s	437,000	10.1349%	9.5038%	9.5992%	-67.5%
6	0	CYWG	May-17	fuel opt	79,938	7,241,571	7h 53m 47s	437,000	10.1349%	9.5038%	9.5992%	-67.5%
7	0	CYWG	May-17	fuel opt	79,938	7,241,571	7h 53m 47s	437,000	10.1349%	9.5038%	9.5992%	-67.5%
8	0	CYWG	May-17	fuel opt	79,938	7,241,571	7h 53m 47s	437,000	10.1349%	9.5038%	9.5992%	-67.5%
9	0	CYWG	May-17	fuel opt	79,938	7,241,571	7h 53m 47s	437,000	10.1349%	9.5038%	9.5992%	-67.5%
10	0	CYWG	May-17	fuel opt	79,938	7,241,571	7h 53m 47s	437,000	10.1349%	9.5038%	9.5992%	-67.5%
20	0	CYWG	May-17	fuel opt	85,341	7,737,791	8h 23m 34s	62,000	17.5781%	17.0074%	16.4872%	-95.4%
30	0	CYWG	May-17	fuel opt	85,341	7,737,791	8h 23m 34s	62,000	17.5781%	17.0074%	16.4872%	-95.4%
40	0	CYWG	May-17	fuel opt	95,526	8,552,071	9h 19m 7s	0	31.6100%	29.3205%	29.3367%	-100.0%
50	0	CYWG	May-17	fuel opt	95,526	8,552,071	9h 19m 7s	0	31.6100%	29.3205%	29.3367%	-100.0%
60	0	CYWG	May-17	fuel opt	95,526	8,552,071	9h 19m 7s	0	31.6100%	29.3205%	29.3367%	-100.0%
70	0	CYWG	May-17	fuel opt	95,526	8,552,071	9h 19m 7s	0	31.6100%	29.3205%	29.3367%	-100.0%
80	0	CYWG	May-17	fuel opt	95,526	8,552,071	9h 19m 7s	0	31.6100%	29.3205%	29.3367%	-100.0%
90	0	CYWG	May-17	fuel opt	95,526	8,552,071	9h 19m 7s	0	31.6100%	29.3205%	29.3367%	-100.0%
100	0	CYWG	May-17	fuel opt	95,526	8,552,071	9h 19m 7s	0	31.6100%	29.3205%	29.3367%	-100.0%

B. Numeric results - Ground track

β_{grnd}	β_{prof}	Dest	Atm	Mode	dm [kg]	ds [m]	dt [h:m:s]	ct _{tot} [m]	% dm	% ds	% dt	% CT
0	0	CYVR	May-17	fuel opt	87,783	7,931,614	8h 36m 55s	1,022,041	0.0000%	0.0000%	0.0000%	0.0%
0.01	0	CYVR	May-17	fuel opt	87,783	7,931,614	8h 36m 55s	1,022,041	0.0000%	0.0000%	0.0000%	0.0%
0.02	0	CYVR	May-17	fuel opt	87,783	7,931,614	8h 36m 55s	1,022,041	0.0000%	0.0000%	0.0000%	0.0%
0.03	0	CYVR	May-17	fuel opt	87,783	7,931,614	8h 36m 55s	1,022,041	0.0000%	0.0000%	0.0000%	0.0%
0.04	0	CYVR	May-17	fuel opt	87,783	7,931,614	8h 36m 55s	1,022,041	0.0000%	0.0000%	0.0000%	0.0%
0.05	0	CYVR	May-17	fuel opt	87,894	7,938,204	8h 37m 30s	917,986	0.1266%	0.0831%	0.1130%	-10.2%
0.06	0	CYVR	May-17	fuel opt	87,894	7,938,204	8h 37m 30s	917,986	0.1266%	0.0831%	0.1130%	-10.2%
0.07	0	CYVR	May-17	fuel opt	87,894	7,938,204	8h 37m 30s	917,986	0.1266%	0.0831%	0.1130%	-10.2%
0.08	0	CYVR	May-17	fuel opt	87,894	7,938,204	8h 37m 30s	917,986	0.1266%	0.0831%	0.1130%	-10.2%
0.09	0	CYVR	May-17	fuel opt	87,894	7,938,204	8h 37m 30s	917,986	0.1266%	0.0831%	0.1130%	-10.2%
0.1	0	CYVR	May-17	fuel opt	87,894	7,938,204	8h 37m 30s	917,986	0.1266%	0.0831%	0.1130%	-10.2%
0.2	0	CYVR	May-17	fuel opt	88,481	7,990,746	8h 40m 41s	497,057	0.7950%	0.7455%	0.7309%	-51.4%
0.3	0	CYVR	May-17	fuel opt	88,481	7,990,746	8h 40m 41s	497,057	0.7950%	0.7455%	0.7309%	-51.4%
0.4	0	CYVR	May-17	fuel opt	88,481	7,990,746	8h 40m 41s	497,057	0.7950%	0.7455%	0.7309%	-51.4%
0.5	0	CYVR	May-17	fuel opt	88,481	7,990,746	8h 40m 41s	497,057	0.7950%	0.7455%	0.7309%	-51.4%
0.6	0	CYVR	May-17	fuel opt	88,481	7,990,746	8h 40m 41s	497,057	0.7950%	0.7455%	0.7309%	-51.4%
0.7	0	CYVR	May-17	fuel opt	88,481	7,990,746	8h 40m 41s	497,057	0.7950%	0.7455%	0.7309%	-51.4%
0.8	0	CYVR	May-17	fuel opt	88,481	7,990,746	8h 40m 41s	497,057	0.7950%	0.7455%	0.7309%	-51.4%
0.9	0	CYVR	May-17	fuel opt	89,799	8,104,466	8h 47m 56s	486,605	2.2973%	2.1793%	2.1325%	-52.4%
1	0	CYVR	May-17	fuel opt	89,799	8,104,466	8h 47m 56s	486,605	2.2973%	2.1793%	2.1325%	-52.4%
2	0	CYVR	May-17	fuel opt	89,799	8,104,466	8h 47m 56s	486,605	2.2973%	2.1793%	2.1325%	-52.4%
3	0	CYVR	May-17	fuel opt	93,680	8,419,506	9h 9m 14s	0	6.7185%	6.1512%	6.2529%	-100.0%
4	0	CYVR	May-17	fuel opt	93,680	8,419,506	9h 9m 14s	0	6.7185%	6.1512%	6.2529%	-100.0%
5	0	CYVR	May-17	fuel opt	93,680	8,419,506	9h 9m 14s	0	6.7185%	6.1512%	6.2529%	-100.0%
6	0	CYVR	May-17	fuel opt	93,680	8,419,506	9h 9m 14s	0	6.7185%	6.1512%	6.2529%	-100.0%
7	0	CYVR	May-17	fuel opt	93,680	8,419,506	9h 9m 14s	0	6.7185%	6.1512%	6.2529%	-100.0%
8	0	CYVR	May-17	fuel opt	93,680	8,419,506	9h 9m 14s	0	6.7185%	6.1512%	6.2529%	-100.0%
9	0	CYVR	May-17	fuel opt	93,680	8,419,506	9h 9m 14s	0	6.7185%	6.1512%	6.2529%	-100.0%
10	0	CYVR	May-17	fuel opt	93,680	8,419,506	9h 9m 14s	0	6.7185%	6.1512%	6.2529%	-100.0%
20	0	CYVR	May-17	fuel opt	93,680	8,419,506	9h 9m 14s	0	6.7185%	6.1512%	6.2529%	-100.0%
30	0	CYVR	May-17	fuel opt	93,680	8,419,506	9h 9m 14s	0	6.7185%	6.1512%	6.2529%	-100.0%
40	0	CYVR	May-17	fuel opt	93,680	8,419,506	9h 9m 14s	0	6.7185%	6.1512%	6.2529%	-100.0%
50	0	CYVR	May-17	fuel opt	93,680	8,419,506	9h 9m 14s	0	6.7185%	6.1512%	6.2529%	-100.0%
60	0	CYVR	May-17	fuel opt	93,680	8,419,506	9h 9m 14s	0	6.7185%	6.1512%	6.2529%	-100.0%
70	0	CYVR	May-17	fuel opt	93,680	8,419,506	9h 9m 14s	0	6.7185%	6.1512%	6.2529%	-100.0%
80	0	CYVR	May-17	fuel opt	93,680	8,419,506	9h 9m 14s	0	6.7185%	6.1512%	6.2529%	-100.0%
90	0	CYVR	May-17	fuel opt	93,680	8,419,506	9h 9m 14s	0	6.7185%	6.1512%	6.2529%	-100.0%
100	0	CYVR	May-17	fuel opt	93,680	8,419,506	9h 9m 14s	0	6.7185%	6.1512%	6.2529%	-100.0%
0	0	KIAD	Feb-14	time opt	74,023	5,929,677	6h 15m 46s	2,424,057	0.0000%	0.0000%	0.0000%	0.0%
0.01	0	KIAD	Feb-14	time opt	74,023	5,929,677	6h 15m 46s	2,424,057	0.0000%	0.0000%	0.0000%	0.0%
0.02	0	KIAD	Feb-14	time opt	74,052	5,933,817	6h 15m 57s	2,365,197	0.0388%	0.0698%	0.0489%	-2.4%
0.03	0	KIAD	Feb-14	time opt	74,052	5,933,817	6h 15m 57s	2,365,197	0.0388%	0.0698%	0.0489%	-2.4%
0.04	0	KIAD	Feb-14	time opt	74,052	5,933,817	6h 15m 57s	2,365,197	0.0388%	0.0698%	0.0489%	-2.4%
0.05	0	KIAD	Feb-14	time opt	74,052	5,933,817	6h 15m 57s	2,365,197	0.0388%	0.0698%	0.0489%	-2.4%
0.06	0	KIAD	Feb-14	time opt	74,473	5,980,693	6h 18m 5s	1,424,073	0.6085%	0.8604%	0.6153%	-41.3%
0.07	0	KIAD	Feb-14	time opt	74,473	5,980,693	6h 18m 5s	1,424,073	0.6085%	0.8604%	0.6153%	-41.3%
0.08	0	KIAD	Feb-14	time opt	74,473	5,980,693	6h 18m 5s	1,424,073	0.6085%	0.8604%	0.6153%	-41.3%
0.09	0	KIAD	Feb-14	time opt	74,940	6,018,623	6h 20m 16s	990,003	1.2393%	1.5000%	1.1989%	-59.2%
0.1	0	KIAD	Feb-14	time opt	74,940	6,018,623	6h 20m 16s	990,003	1.2393%	1.5000%	1.1989%	-59.2%
0.2	0	KIAD	Feb-14	time opt	75,253	6,046,915	6h 21m 51s	885,295	1.6621%	1.9771%	1.6175%	-63.5%
0.3	0	KIAD	Feb-14	time opt	75,511	6,068,225	6h 23m 8s	771,605	2.0102%	2.3365%	1.9616%	-68.2%
0.4	0	KIAD	Feb-14	time opt	75,874	6,097,525	6h 24m 54s	692,905	2.5003%	2.8306%	2.4302%	-71.4%
0.5	0	KIAD	Feb-14	time opt	75,874	6,097,525	6h 24m 54s	692,905	2.5003%	2.8306%	2.4302%	-71.4%
0.6	0	KIAD	Feb-14	time opt	75,906	6,100,165	6h 25m 1s	692,545	2.5442%	2.8752%	2.4626%	-71.4%
0.7	0	KIAD	Feb-14	time opt	75,906	6,100,165	6h 25m 1s	692,545	2.5442%	2.8752%	2.4626%	-71.4%
0.8	0	KIAD	Feb-14	time opt	75,906	6,100,165	6h 25m 1s	692,545	2.5442%	2.8752%	2.4626%	-71.4%
0.9	0	KIAD	Feb-14	time opt	75,906	6,100,165	6h 25m 1s	692,545	2.5442%	2.8752%	2.4626%	-71.4%
1	0	KIAD	Feb-14	time opt	75,906	6,100,165	6h 25m 1s	692,545	2.5442%	2.8752%	2.4626%	-71.4%
2	0	KIAD	Feb-14	time opt	75,906	6,100,165	6h 25m 1s	692,545	2.5442%	2.8752%	2.4626%	-71.4%
3	0	KIAD	Feb-14	time opt	89,838	7,172,740	7h 33m 19s	209,120	21.3651%	20.9634%	20.6350%	-91.4%
4	0	KIAD	Feb-14	time opt	90,046	7,189,540	7h 34m 22s	208,920	21.6463%	21.2467%	20.9156%	-91.4%
5	0	KIAD	Feb-14	time opt	90,046	7,189,540	7h 34m 22s	208,920	21.6463%	21.2467%	20.9156%	-91.4%
6	0	KIAD	Feb-14	time opt	90,046	7,189,540	7h 34m 22s	208,920	21.6463%	21.2467%	20.9156%	-91.4%
7	0	KIAD	Feb-14	time opt	90,046	7,189,540	7h 34m 22s	208,920	21.6463%	21.2467%	20.9156%	-91.4%
8	0	KIAD	Feb-14	time opt	90,046	7,189,540	7h 34m 22s	208,920	21.6463%	21.2467%	20.9156%	-91.4%
9	0	KIAD	Feb-14	time opt	90,046	7,189,540	7h 34m 22s	208,920	21.6463%	21.2467%	20.9156%	-91.4%
10	0	KIAD	Feb-14	time opt	90,046	7,189,540	7h 34m 22s	208,920	21.6463%	21.2467%	20.9156%	-91.4%
20	0	KIAD	Feb-14	time opt	90,046	7,189,540	7h 34m 22s	208,920	21.6463%	21.2467%	20.9156%	-91.4%
30	0	KIAD	Feb-14	time opt	90,046	7,189,540	7h 34m 22s	208,920	21.6463%	21.2467%	20.9156%	-91.4%
40	0	KIAD	Feb-14	time opt	90,046	7,189,540	7h 34m 22s	208,920	21.6463%	21.2467%	20.9156%	-91.4%
50	0	KIAD	Feb-14	time opt	90,046	7,189,540	7h 34m 22s	208,920	21.6463%	21.2467%	20.9156%	-91.4%
60	0	KIAD	Feb-14	time opt	90,046	7,189,540	7h 34m 22s	208,920	21.6463%	21.2467%	20.9156%	-91.4%
70	0	KIAD	Feb-14	time opt	90,046	7,189,540	7h 34m 22s	208,920	21.6463%	21.2467%	20.9156%	-91.4%
80	0	KIAD	Feb-14	time opt	90,046	7,189,540	7h 34m 22s	208,920	21.6463%	21.2467%	20.9156%	-91.4%
90	0	KIAD	Feb-14	time opt	90,046	7,189,540	7h 34m 22s	208,920	21.6463%	21.2467%	20.9156%	-91.4%
100	0	KIAD	Feb-14	time opt	90,046	7,189,540	7h 34m 22s	208,920	21.6463%	21.2467%	20.9156%	-91.4%

β_{grnd}	β_{prof}	Dest	Atm	Mode	dm [kg]	ds [m]	dt [h:m:s]	ct _{tot} [m]	% dm	% ds	% dt	% CT
0	0	CYWG	Feb-14	time opt	84,972	6,769,079	7h 9m 39s	3,048,250	0.0000%	0.0000%	0.0000%	0.0%
0.01	0	CYWG	Feb-14	time opt	84,974	6,770,462	7h 9m 42s	2,726,633	0.0024%	0.0204%	0.0100%	-10.6%
0.02	0	CYWG	Feb-14	time opt	84,974	6,770,462	7h 9m 42s	2,726,633	0.0024%	0.0204%	0.0100%	-10.6%
0.03	0	CYWG	Feb-14	time opt	85,292	6,796,563	7h 11m 12s	1,647,734	0.3765%	0.4060%	0.3595%	-45.9%
0.04	0	CYWG	Feb-14	time opt	85,292	6,796,563	7h 11m 12s	1,647,734	0.3765%	0.4060%	0.3595%	-45.9%
0.05	0	CYWG	Feb-14	time opt	85,292	6,796,563	7h 11m 12s	1,647,734	0.3765%	0.4060%	0.3595%	-45.9%
0.06	0	CYWG	Feb-14	time opt	85,428	6,807,353	7h 11m 53s	1,469,524	0.5370%	0.5654%	0.5197%	-51.8%
0.07	0	CYWG	Feb-14	time opt	85,428	6,807,353	7h 11m 53s	1,469,524	0.5370%	0.5654%	0.5197%	-51.8%
0.08	0	CYWG	Feb-14	time opt	85,428	6,807,353	7h 11m 53s	1,469,524	0.5370%	0.5654%	0.5197%	-51.8%
0.09	0	CYWG	Feb-14	time opt	85,428	6,807,353	7h 11m 53s	1,469,524	0.5370%	0.5654%	0.5197%	-51.8%
0.1	0	CYWG	Feb-14	time opt	85,428	6,807,353	7h 11m 53s	1,469,524	0.5370%	0.5654%	0.5197%	-51.8%
0.2	0	CYWG	Feb-14	time opt	85,714	6,830,593	7h 13m 16s	1,332,764	0.8733%	0.9088%	0.8434%	-56.3%
0.3	0	CYWG	Feb-14	time opt	86,661	6,905,110	7h 17m 54s	1,030,281	1.9876%	2.0096%	1.9187%	-66.2%
0.4	0	CYWG	Feb-14	time opt	86,933	6,925,740	7h 19m 14s	1,000,911	2.3077%	2.3144%	2.2310%	-67.2%
0.5	0	CYWG	Feb-14	time opt	86,933	6,925,740	7h 19m 14s	1,000,911	2.3077%	2.3144%	2.2310%	-67.2%
0.6	0	CYWG	Feb-14	time opt	87,030	6,933,379	7h 19m 43s	982,550	2.4225%	2.4272%	2.3419%	-67.8%
0.7	0	CYWG	Feb-14	time opt	87,030	6,933,379	7h 19m 43s	982,550	2.4225%	2.4272%	2.3419%	-67.8%
0.8	0	CYWG	Feb-14	time opt	87,030	6,933,379	7h 19m 43s	982,550	2.4225%	2.4272%	2.3419%	-67.8%
0.9	0	CYWG	Feb-14	time opt	87,547	6,977,599	7h 22m 12s	910,771	3.0302%	3.0805%	2.9223%	-70.1%
1	0	CYWG	Feb-14	time opt	88,035	7,015,429	7h 24m 35s	875,601	3.6048%	3.6393%	3.4752%	-71.3%
2	0	CYWG	Feb-14	time opt	88,035	7,015,429	7h 24m 35s	875,601	3.6048%	3.6393%	3.4752%	-71.3%
3	0	CYWG	Feb-14	time opt	100,691	7,979,054	8h 25m 56s	427,225	18.4994%	17.8750%	17.7542%	-86.0%
4	0	CYWG	Feb-14	time opt	113,295	8,930,784	9h 25m 51s	245,956	33.3321%	31.9350%	31.7007%	-91.9%
5	0	CYWG	Feb-14	time opt	113,295	8,930,784	9h 25m 51s	245,956	33.3321%	31.9350%	31.7007%	-91.9%
6	0	CYWG	Feb-14	time opt	113,295	8,930,784	9h 25m 51s	245,956	33.3321%	31.9350%	31.7007%	-91.9%
7	0	CYWG	Feb-14	time opt	113,295	8,930,784	9h 25m 51s	245,956	33.3321%	31.9350%	31.7007%	-91.9%
8	0	CYWG	Feb-14	time opt	113,295	8,930,784	9h 25m 51s	245,956	33.3321%	31.9350%	31.7007%	-91.9%
9	0	CYWG	Feb-14	time opt	113,295	8,930,784	9h 25m 51s	245,956	33.3321%	31.9350%	31.7007%	-91.9%
10	0	CYWG	Feb-14	time opt	113,295	8,930,784	9h 25m 51s	245,956	33.3321%	31.9350%	31.7007%	-91.9%
20	0	CYWG	Feb-14	time opt	113,295	8,930,784	9h 25m 51s	245,956	33.3321%	31.9350%	31.7007%	-91.9%
30	0	CYWG	Feb-14	time opt	113,295	8,930,784	9h 25m 51s	245,956	33.3321%	31.9350%	31.7007%	-91.9%
40	0	CYWG	Feb-14	time opt	113,295	8,930,784	9h 25m 51s	245,956	33.3321%	31.9350%	31.7007%	-91.9%
50	0	CYWG	Feb-14	time opt	113,295	8,930,784	9h 25m 51s	245,956	33.3321%	31.9350%	31.7007%	-91.9%
60	0	CYWG	Feb-14	time opt	113,295	8,930,784	9h 25m 51s	245,956	33.3321%	31.9350%	31.7007%	-91.9%
70	0	CYWG	Feb-14	time opt	113,295	8,930,784	9h 25m 51s	245,956	33.3321%	31.9350%	31.7007%	-91.9%
80	0	CYWG	Feb-14	time opt	113,295	8,930,784	9h 25m 51s	245,956	33.3321%	31.9350%	31.7007%	-91.9%
90	0	CYWG	Feb-14	time opt	113,295	8,930,784	9h 25m 51s	245,956	33.3321%	31.9350%	31.7007%	-91.9%
100	0	CYWG	Feb-14	time opt	113,295	8,930,784	9h 25m 51s	245,956	33.3321%	31.9350%	31.7007%	-91.9%
0	0	CYVR	Feb-14	time opt	97,735	7,777,291	8h 11m 33s	2,806,544	0.0000%	0.0000%	0.0000%	0.0%
0.01	0	CYVR	Feb-14	time opt	97,735	7,777,291	8h 11m 33s	2,806,544	0.0000%	0.0000%	0.0000%	0.0%
0.02	0	CYVR	Feb-14	time opt	97,758	7,778,451	8h 11m 40s	2,718,704	0.0230%	0.0149%	0.0248%	-3.1%
0.03	0	CYVR	Feb-14	time opt	97,759	7,778,991	8h 11m 41s	2,685,244	0.0246%	0.0219%	0.0255%	-4.3%
0.04	0	CYVR	Feb-14	time opt	97,795	7,781,471	8h 11m 51s	2,625,724	0.0611%	0.0537%	0.0602%	-6.4%
0.05	0	CYVR	Feb-14	time opt	97,795	7,781,471	8h 11m 51s	2,625,724	0.0611%	0.0537%	0.0602%	-6.4%
0.06	0	CYVR	Feb-14	time opt	97,928	7,791,011	8h 12m 29s	2,455,264	0.1966%	0.1764%	0.1897%	-12.5%
0.07	0	CYVR	Feb-14	time opt	97,928	7,791,011	8h 12m 29s	2,455,264	0.1966%	0.1764%	0.1897%	-12.5%
0.08	0	CYVR	Feb-14	time opt	97,928	7,791,011	8h 12m 29s	2,455,264	0.1966%	0.1764%	0.1897%	-12.5%
0.09	0	CYVR	Feb-14	time opt	97,928	7,791,011	8h 12m 29s	2,455,264	0.1966%	0.1764%	0.1897%	-12.5%
0.1	0	CYVR	Feb-14	time opt	97,928	7,791,011	8h 12m 29s	2,455,264	0.1966%	0.1764%	0.1897%	-12.5%
0.2	0	CYVR	Feb-14	time opt	98,575	7,840,341	8h 15m 37s	2,148,594	0.8589%	0.8107%	0.8286%	-23.4%
0.3	0	CYVR	Feb-14	time opt	99,673	7,924,810	8h 20m 54s	1,725,063	1.9830%	1.8968%	1.9025%	-38.5%
0.4	0	CYVR	Feb-14	time opt	99,673	7,924,810	8h 20m 54s	1,725,063	1.9830%	1.8968%	1.9025%	-38.5%
0.5	0	CYVR	Feb-14	time opt	99,926	7,943,750	8h 22m 4s	1,690,003	2.2411%	2.1403%	2.1395%	-39.8%
0.6	0	CYVR	Feb-14	time opt	100,025	7,951,389	8h 22m 33s	1,671,642	2.3424%	2.2385%	2.2365%	-40.4%
0.7	0	CYVR	Feb-14	time opt	100,025	7,951,389	8h 22m 33s	1,671,642	2.3424%	2.2385%	2.2365%	-40.4%
0.8	0	CYVR	Feb-14	time opt	100,025	7,951,389	8h 22m 33s	1,671,642	2.3424%	2.2385%	2.2365%	-40.4%
0.9	0	CYVR	Feb-14	time opt	100,787	8,010,979	8h 26m 15s	1,583,232	3.1225%	3.0047%	2.9914%	-43.6%
1	0	CYVR	Feb-14	time opt	101,317	8,051,229	8h 28m 48s	1,562,482	3.6650%	3.5223%	3.5085%	-44.3%
2	0	CYVR	Feb-14	time opt	101,317	8,051,229	8h 28m 48s	1,562,482	3.6650%	3.5223%	3.5085%	-44.3%
3	0	CYVR	Feb-14	time opt	101,785	8,086,569	8h 31m 2s	1,519,822	4.1439%	3.9767%	3.9645%	-45.8%
4	0	CYVR	Feb-14	time opt	-	-	-	-	-	-	-	-
5	0	CYVR	Feb-14	time opt	-	-	-	-	-	-	-	-
6	0	CYVR	Feb-14	time opt	-	-	-	-	-	-	-	-
7	0	CYVR	Feb-14	time opt	-	-	-	-	-	-	-	-
8	0	CYVR	Feb-14	time opt	-	-	-	-	-	-	-	-
9	0	CYVR	Feb-14	time opt	-	-	-	-	-	-	-	-
10	0	CYVR	Feb-14	time opt	-	-	-	-	-	-	-	-
20	0	CYVR	Feb-14	time opt	-	-	-	-	-	-	-	-
30	0	CYVR	Feb-14	time opt	-	-	-	-	-	-	-	-
40	0	CYVR	Feb-14	time opt	-	-	-	-	-	-	-	-
50	0	CYVR	Feb-14	time opt	-	-	-	-	-	-	-	-
60	0	CYVR	Feb-14	time opt	-	-	-	-	-	-	-	-
70	0	CYVR	Feb-14	time opt	-	-	-	-	-	-	-	-
80	0	CYVR	Feb-14	time opt	-	-	-	-	-	-	-	-
90	0	CYVR	Feb-14	time opt	-	-	-	-	-	-	-	-
100	0	CYVR	Feb-14	time opt	-	-	-	-	-	-	-	-

B. Numeric results - Ground track

β_{grnd}	β_{prof}	Dest	Atm	Mode	dm [kg]	ds [m]	dt [h:m:s]	ct _{tot} [m]	% dm	% ds	% dt	% CT
0	0	KIAD	Feb-17	time opt	72,515	5,922,568	6h 8m 16s	1,951,000	0.0000%	0.0000%	0.0000%	0.0%
0.01	0	KIAD	Feb-17	time opt	72,515	5,922,868	6h 8m 16s	1,897,000	0.0003%	0.0051%	0.0008%	-2.8%
0.02	0	KIAD	Feb-17	time opt	72,500	5,925,938	6h 8m 12s	1,559,000	-0.0211%	0.0589%	-0.0174%	-20.1%
0.03	0	KIAD	Feb-17	time opt	72,552	5,934,968	6h 8m 22s	1,282,000	0.0508%	0.2094%	0.0286%	-34.3%
0.04	0	KIAD	Feb-17	time opt	72,610	5,936,668	6h 8m 40s	1,218,000	0.1311%	0.2381%	0.1084%	-37.6%
0.05	0	KIAD	Feb-17	time opt	72,881	5,962,988	6h 10m 2s	664,000	0.5046%	0.6825%	0.4828%	-66.0%
0.06	0	KIAD	Feb-17	time opt	72,999	5,971,778	6h 10m 32s	487,000	0.6677%	0.8309%	0.6165%	-75.0%
0.07	0	KIAD	Feb-17	time opt	72,999	5,971,778	6h 10m 32s	487,000	0.6677%	0.8309%	0.6165%	-75.0%
0.08	0	KIAD	Feb-17	time opt	72,999	5,971,778	6h 10m 32s	487,000	0.6677%	0.8309%	0.6165%	-75.0%
0.09	0	KIAD	Feb-17	time opt	72,999	5,971,778	6h 10m 32s	487,000	0.6677%	0.8309%	0.6165%	-75.0%
0.1	0	KIAD	Feb-17	time opt	72,999	5,971,778	6h 10m 32s	487,000	0.6677%	0.8309%	0.6165%	-75.0%
0.2	0	KIAD	Feb-17	time opt	72,999	5,971,778	6h 10m 32s	487,000	0.6677%	0.8309%	0.6165%	-75.0%
0.3	0	KIAD	Feb-17	time opt	72,999	5,971,778	6h 10m 32s	487,000	0.6677%	0.8309%	0.6165%	-75.0%
0.4	0	KIAD	Feb-17	time opt	73,066	5,977,518	6h 10m 52s	471,000	0.7597%	0.9278%	0.7075%	-75.9%
0.5	0	KIAD	Feb-17	time opt	74,348	6,083,926	6h 17m 13s	227,000	2.5279%	2.7245%	2.4329%	-88.4%
0.6	0	KIAD	Feb-17	time opt	74,348	6,083,926	6h 17m 13s	227,000	2.5279%	2.7245%	2.4329%	-88.4%
0.7	0	KIAD	Feb-17	time opt	74,348	6,083,926	6h 17m 13s	227,000	2.5279%	2.7245%	2.4329%	-88.4%
0.8	0	KIAD	Feb-17	time opt	74,348	6,083,926	6h 17m 13s	227,000	2.5279%	2.7245%	2.4329%	-88.4%
0.9	0	KIAD	Feb-17	time opt	74,348	6,083,926	6h 17m 13s	227,000	2.5279%	2.7245%	2.4329%	-88.4%
1	0	KIAD	Feb-17	time opt	74,348	6,083,926	6h 17m 13s	227,000	2.5279%	2.7245%	2.4329%	-88.4%
2	0	KIAD	Feb-17	time opt	74,503	6,096,526	6h 17m 56s	225,000	2.7412%	2.9372%	2.6272%	-88.5%
3	0	KIAD	Feb-17	time opt	77,213	6,315,486	6h 31m 23s	154,000	6.4780%	6.6343%	6.2789%	-92.1%
4	0	KIAD	Feb-17	time opt	78,083	6,385,916	6h 35m 39s	111,000	7.6775%	7.8234%	7.4363%	-94.3%
5	0	KIAD	Feb-17	time opt	85,362	6,960,300	7h 11m 20s	42,000	17.7164%	17.5217%	17.1282%	-97.8%
6	0	KIAD	Feb-17	time opt	85,362	6,960,300	7h 11m 20s	42,000	17.7164%	17.5217%	17.1282%	-97.8%
7	0	KIAD	Feb-17	time opt	85,362	6,960,300	7h 11m 20s	42,000	17.7164%	17.5217%	17.1282%	-97.8%
8	0	KIAD	Feb-17	time opt	85,362	6,960,300	7h 11m 20s	42,000	17.7164%	17.5217%	17.1282%	-97.8%
9	0	KIAD	Feb-17	time opt	85,362	6,960,300	7h 11m 20s	42,000	17.7164%	17.5217%	17.1282%	-97.8%
10	0	KIAD	Feb-17	time opt	85,362	6,960,300	7h 11m 20s	42,000	17.7164%	17.5217%	17.1282%	-97.8%
20	0	KIAD	Feb-17	time opt	85,362	6,960,300	7h 11m 20s	42,000	17.7164%	17.5217%	17.1282%	-97.8%
30	0	KIAD	Feb-17	time opt	85,362	6,960,300	7h 11m 20s	42,000	17.7164%	17.5217%	17.1282%	-97.8%
40	0	KIAD	Feb-17	time opt	85,362	6,960,300	7h 11m 20s	42,000	17.7164%	17.5217%	17.1282%	-97.8%
50	0	KIAD	Feb-17	time opt	85,362	6,960,300	7h 11m 20s	42,000	17.7164%	17.5217%	17.1282%	-97.8%
60	0	KIAD	Feb-17	time opt	85,362	6,960,300	7h 11m 20s	42,000	17.7164%	17.5217%	17.1282%	-97.8%
70	0	KIAD	Feb-17	time opt	85,362	6,960,300	7h 11m 20s	42,000	17.7164%	17.5217%	17.1282%	-97.8%
80	0	KIAD	Feb-17	time opt	85,362	6,960,300	7h 11m 20s	42,000	17.7164%	17.5217%	17.1282%	-97.8%
90	0	KIAD	Feb-17	time opt	85,362	6,960,300	7h 11m 20s	42,000	17.7164%	17.5217%	17.1282%	-97.8%
100	0	KIAD	Feb-17	time opt	85,362	6,960,300	7h 11m 20s	42,000	17.7164%	17.5217%	17.1282%	-97.8%
0	0	CYWG	Feb-17	time opt	80,132	6,481,044	6h 45m 48s	1,317,000	0.0000%	0.0000%	0.0000%	0.0%
0.01	0	CYWG	Feb-17	time opt	80,132	6,481,044	6h 45m 48s	1,317,000	0.0000%	0.0000%	0.0000%	0.0%
0.02	0	CYWG	Feb-17	time opt	80,132	6,481,044	6h 45m 48s	1,317,000	0.0000%	0.0000%	0.0000%	0.0%
0.03	0	CYWG	Feb-17	time opt	80,132	6,481,044	6h 45m 48s	1,317,000	0.0000%	0.0000%	0.0000%	0.0%
0.04	0	CYWG	Feb-17	time opt	80,132	6,481,044	6h 45m 48s	1,317,000	0.0000%	0.0000%	0.0000%	0.0%
0.05	0	CYWG	Feb-17	time opt	80,132	6,481,044	6h 45m 48s	1,317,000	0.0000%	0.0000%	0.0000%	0.0%
0.06	0	CYWG	Feb-17	time opt	80,132	6,481,044	6h 45m 48s	1,317,000	0.0000%	0.0000%	0.0000%	0.0%
0.07	0	CYWG	Feb-17	time opt	80,209	6,487,384	6h 46m 12s	1,240,000	0.0968%	0.0978%	0.0989%	-5.8%
0.08	0	CYWG	Feb-17	time opt	80,209	6,487,384	6h 46m 12s	1,240,000	0.0968%	0.0978%	0.0989%	-5.8%
0.09	0	CYWG	Feb-17	time opt	80,209	6,487,384	6h 46m 12s	1,240,000	0.0968%	0.0978%	0.0989%	-5.8%
0.1	0	CYWG	Feb-17	time opt	80,209	6,487,384	6h 46m 12s	1,240,000	0.0968%	0.0978%	0.0989%	-5.8%
0.2	0	CYWG	Feb-17	time opt	80,435	6,507,434	6h 47m 18s	1,048,000	0.3781%	0.4072%	0.3704%	-20.4%
0.3	0	CYWG	Feb-17	time opt	80,684	6,527,944	6h 48m 32s	982,000	0.6900%	0.7236%	0.6752%	-25.4%
0.4	0	CYWG	Feb-17	time opt	80,684	6,527,944	6h 48m 32s	982,000	0.6900%	0.7236%	0.6752%	-25.4%
0.5	0	CYWG	Feb-17	time opt	81,110	6,563,448	6h 50m 37s	934,000	1.2216%	1.2715%	1.1880%	-29.1%
0.6	0	CYWG	Feb-17	time opt	85,391	6,887,249	7h 11m 31s	293,000	6.5633%	6.2676%	6.3374%	-77.8%
0.7	0	CYWG	Feb-17	time opt	85,391	6,887,249	7h 11m 31s	293,000	6.5633%	6.2676%	6.3374%	-77.8%
0.8	0	CYWG	Feb-17	time opt	85,518	6,896,839	7h 12m 8s	281,000	6.7221%	6.4156%	6.4907%	-78.7%
0.9	0	CYWG	Feb-17	time opt	85,518	6,896,839	7h 12m 8s	281,000	6.7221%	6.4156%	6.4907%	-78.7%
1	0	CYWG	Feb-17	time opt	85,518	6,896,839	7h 12m 8s	281,000	6.7221%	6.4156%	6.4907%	-78.7%
2	0	CYWG	Feb-17	time opt	85,718	6,912,019	7h 13m 7s	273,000	6.9715%	6.6498%	6.7303%	-79.3%
3	0	CYWG	Feb-17	time opt	85,989	6,932,669	7h 14m 26s	266,000	7.3096%	6.9684%	7.0546%	-79.8%
4	0	CYWG	Feb-17	time opt	88,298	7,110,179	7h 25m 39s	344,000	10.1919%	9.7073%	9.8185%	-73.9%
5	0	CYWG	Feb-17	time opt	101,046	8,096,909	8h 27m 13s	43,000	26.0997%	24.9322%	24.9902%	-96.7%
6	0	CYWG	Feb-17	time opt	101,046	8,096,909	8h 27m 13s	43,000	26.0997%	24.9322%	24.9902%	-96.7%
7	0	CYWG	Feb-17	time opt	101,046	8,096,909	8h 27m 13s	43,000	26.0997%	24.9322%	24.9902%	-96.7%
8	0	CYWG	Feb-17	time opt	101,046	8,096,909	8h 27m 13s	43,000	26.0997%	24.9322%	24.9902%	-96.7%
9	0	CYWG	Feb-17	time opt	101,046	8,096,909	8h 27m 13s	43,000	26.0997%	24.9322%	24.9902%	-96.7%
10	0	CYWG	Feb-17	time opt	101,046	8,096,909	8h 27m 13s	43,000	26.0997%	24.9322%	24.9902%	-96.7%
20	0	CYWG	Feb-17	time opt	101,046	8,096,909	8h 27m 13s	43,000	26.0997%	24.9322%	24.9902%	-96.7%
30	0	CYWG	Feb-17	time opt	101,046	8,096,909	8h 27m 13s	43,000	26.0997%	24.9322%	24.9902%	-96.7%
40	0	CYWG	Feb-17	time opt	101,046	8,096,909	8h 27m 13s	43,000	26.0997%	24.9322%	24.9902%	-96.7%
50	0	CYWG	Feb-17	time opt	101,046	8,096,909	8h 27m 13s	43,000	26.0997%	24.9322%	24.9902%	-96.7%
60	0	CYWG	Feb-17	time opt	101,046	8,096,909	8h 27m 13s	43,000	26.0997%	24.9322%	24.9902%	-96.7%
70	0	CYWG	Feb-17	time opt	101,046	8,096,909	8h 27m 13s	43,000	26.0997%	24.9322%	24.9902%	-96.7%
80	0	CYWG	Feb-17	time opt	101,046	8,096,909	8h 27m 13s	43,000	26.0997%	24.9322%	24.9902%	-96.7%
90	0	CYWG	Feb-17	time opt	101,046	8,096,909	8h 27m 13s	43,000	26.0997%	24.9322%	24.9902%	-96.7%
100	0	CYWG	Feb-17	time opt	101,046	8,096,909	8h 27m 13s	43,000	26.0997%	24.9322%	24.9902%	-96.7%

β_{grnd}	β_{prof}	Dest	Atm	Mode	dm [kg]	ds [m]	dt [h:m:s]	ct _{tot} [m]	% dm	% ds	% dt	% CT
0	0	CYVR	Feb-17	time opt	95,610	7,725,148	8h 1m 8s	1,364,000	0.0000%	0.0000%	0.0000%	0.0%
0.01	0	CYVR	Feb-17	time opt	95,610	7,725,148	8h 1m 8s	1,364,000	0.0000%	0.0000%	0.0000%	0.0%
0.02	0	CYVR	Feb-17	time opt	95,616	7,725,608	8h 1m 9s	1,314,000	0.0070%	0.0060%	0.0035%	-3.7%
0.03	0	CYVR	Feb-17	time opt	95,629	7,727,058	8h 1m 13s	1,153,000	0.0197%	0.0247%	0.0174%	-15.5%
0.04	0	CYVR	Feb-17	time opt	95,629	7,727,058	8h 1m 13s	1,153,000	0.0197%	0.0247%	0.0174%	-15.5%
0.05	0	CYVR	Feb-17	time opt	95,629	7,727,058	8h 1m 13s	1,153,000	0.0197%	0.0247%	0.0174%	-15.5%
0.06	0	CYVR	Feb-17	time opt	95,629	7,727,058	8h 1m 13s	1,153,000	0.0197%	0.0247%	0.0174%	-15.5%
0.07	0	CYVR	Feb-17	time opt	95,629	7,727,058	8h 1m 13s	1,153,000	0.0197%	0.0247%	0.0174%	-15.5%
0.08	0	CYVR	Feb-17	time opt	95,629	7,727,058	8h 1m 13s	1,153,000	0.0197%	0.0247%	0.0174%	-15.5%
0.09	0	CYVR	Feb-17	time opt	95,629	7,727,058	8h 1m 13s	1,153,000	0.0197%	0.0247%	0.0174%	-15.5%
0.1	0	CYVR	Feb-17	time opt	95,629	7,727,058	8h 1m 13s	1,153,000	0.0197%	0.0247%	0.0174%	-15.5%
0.2	0	CYVR	Feb-17	time opt	95,629	7,727,058	8h 1m 13s	1,153,000	0.0197%	0.0247%	0.0174%	-15.5%
0.3	0	CYVR	Feb-17	time opt	96,684	7,807,408	8h 6m 17s	882,000	1.1237%	1.0648%	1.0705%	-35.3%
0.4	0	CYVR	Feb-17	time opt	96,684	7,807,408	8h 6m 17s	882,000	1.1237%	1.0648%	1.0705%	-35.3%
0.5	0	CYVR	Feb-17	time opt	96,684	7,807,408	8h 6m 17s	882,000	1.1237%	1.0648%	1.0705%	-35.3%
0.6	0	CYVR	Feb-17	time opt	96,684	7,807,408	8h 6m 17s	882,000	1.1237%	1.0648%	1.0705%	-35.3%
0.7	0	CYVR	Feb-17	time opt	101,497	8,166,649	8h 29m 23s	293,000	6.1574%	5.7151%	5.8706%	-78.5%
0.8	0	CYVR	Feb-17	time opt	101,626	8,176,239	8h 30m 0s	282,000	6.2929%	5.8393%	5.9998%	-79.3%
0.9	0	CYVR	Feb-17	time opt	101,626	8,176,239	8h 30m 0s	282,000	6.2929%	5.8393%	5.9998%	-79.3%
1	0	CYVR	Feb-17	time opt	101,626	8,176,239	8h 30m 0s	282,000	6.2929%	5.8393%	5.9998%	-79.3%
2	0	CYVR	Feb-17	time opt	101,830	8,191,419	8h 30m 58s	273,000	6.5057%	6.0358%	6.2020%	-80.0%
3	0	CYVR	Feb-17	time opt	102,106	8,212,069	8h 32m 17s	267,000	6.7941%	6.3031%	6.4755%	-80.4%
4	0	CYVR	Feb-17	time opt	104,458	8,389,579	8h 43m 30s	343,000	9.2541%	8.6009%	8.8072%	-74.9%
5	0	CYVR	Feb-17	time opt	-	-	-	-	-	-	-	-
6	0	CYVR	Feb-17	time opt	-	-	-	-	-	-	-	-
7	0	CYVR	Feb-17	time opt	-	-	-	-	-	-	-	-
8	0	CYVR	Feb-17	time opt	-	-	-	-	-	-	-	-
9	0	CYVR	Feb-17	time opt	-	-	-	-	-	-	-	-
10	0	CYVR	Feb-17	time opt	-	-	-	-	-	-	-	-
20	0	CYVR	Feb-17	time opt	-	-	-	-	-	-	-	-
30	0	CYVR	Feb-17	time opt	-	-	-	-	-	-	-	-
40	0	CYVR	Feb-17	time opt	-	-	-	-	-	-	-	-
50	0	CYVR	Feb-17	time opt	-	-	-	-	-	-	-	-
60	0	CYVR	Feb-17	time opt	-	-	-	-	-	-	-	-
70	0	CYVR	Feb-17	time opt	-	-	-	-	-	-	-	-
80	0	CYVR	Feb-17	time opt	-	-	-	-	-	-	-	-
90	0	CYVR	Feb-17	time opt	-	-	-	-	-	-	-	-
100	0	CYVR	Feb-17	time opt	-	-	-	-	-	-	-	-
0	0	KIAD	May-17	time opt	71,091	5,882,411	6h 1m 1s	0	0.0000%	0.0000%	0.0000%	0.0%
0.01	0	KIAD	May-17	time opt	71,091	5,882,411	6h 1m 1s	0	0.0000%	0.0000%	0.0000%	0.0%
0.02	0	KIAD	May-17	time opt	71,091	5,882,411	6h 1m 1s	0	0.0000%	0.0000%	0.0000%	0.0%
0.03	0	KIAD	May-17	time opt	71,091	5,882,411	6h 1m 1s	0	0.0000%	0.0000%	0.0000%	0.0%
0.04	0	KIAD	May-17	time opt	71,091	5,882,411	6h 1m 1s	0	0.0000%	0.0000%	0.0000%	0.0%
0.05	0	KIAD	May-17	time opt	71,091	5,882,411	6h 1m 1s	0	0.0000%	0.0000%	0.0000%	0.0%
0.06	0	KIAD	May-17	time opt	71,091	5,882,411	6h 1m 1s	0	0.0000%	0.0000%	0.0000%	0.0%
0.07	0	KIAD	May-17	time opt	71,091	5,882,411	6h 1m 1s	0	0.0000%	0.0000%	0.0000%	0.0%
0.08	0	KIAD	May-17	time opt	71,091	5,882,411	6h 1m 1s	0	0.0000%	0.0000%	0.0000%	0.0%
0.09	0	KIAD	May-17	time opt	71,091	5,882,411	6h 1m 1s	0	0.0000%	0.0000%	0.0000%	0.0%
0.1	0	KIAD	May-17	time opt	71,091	5,882,411	6h 1m 1s	0	0.0000%	0.0000%	0.0000%	0.0%
0.2	0	KIAD	May-17	time opt	71,091	5,882,411	6h 1m 1s	0	0.0000%	0.0000%	0.0000%	0.0%
0.3	0	KIAD	May-17	time opt	71,091	5,882,411	6h 1m 1s	0	0.0000%	0.0000%	0.0000%	0.0%
0.4	0	KIAD	May-17	time opt	71,091	5,882,411	6h 1m 1s	0	0.0000%	0.0000%	0.0000%	0.0%
0.5	0	KIAD	May-17	time opt	71,091	5,882,411	6h 1m 1s	0	0.0000%	0.0000%	0.0000%	0.0%
0.6	0	KIAD	May-17	time opt	71,091	5,882,411	6h 1m 1s	0	0.0000%	0.0000%	0.0000%	0.0%
0.7	0	KIAD	May-17	time opt	71,091	5,882,411	6h 1m 1s	0	0.0000%	0.0000%	0.0000%	0.0%
0.8	0	KIAD	May-17	time opt	71,091	5,882,411	6h 1m 1s	0	0.0000%	0.0000%	0.0000%	0.0%
0.9	0	KIAD	May-17	time opt	71,091	5,882,411	6h 1m 1s	0	0.0000%	0.0000%	0.0000%	0.0%
1	0	KIAD	May-17	time opt	71,091	5,882,411	6h 1m 1s	0	0.0000%	0.0000%	0.0000%	0.0%
2	0	KIAD	May-17	time opt	71,091	5,882,411	6h 1m 1s	0	0.0000%	0.0000%	0.0000%	0.0%
3	0	KIAD	May-17	time opt	71,091	5,882,411	6h 1m 1s	0	0.0000%	0.0000%	0.0000%	0.0%
4	0	KIAD	May-17	time opt	71,091	5,882,411	6h 1m 1s	0	0.0000%	0.0000%	0.0000%	0.0%
5	0	KIAD	May-17	time opt	71,091	5,882,411	6h 1m 1s	0	0.0000%	0.0000%	0.0000%	0.0%
6	0	KIAD	May-17	time opt	71,091	5,882,411	6h 1m 1s	0	0.0000%	0.0000%	0.0000%	0.0%
7	0	KIAD	May-17	time opt	71,091	5,882,411	6h 1m 1s	0	0.0000%	0.0000%	0.0000%	0.0%
8	0	KIAD	May-17	time opt	71,091	5,882,411	6h 1m 1s	0	0.0000%	0.0000%	0.0000%	0.0%
9	0	KIAD	May-17	time opt	71,091	5,882,411	6h 1m 1s	0	0.0000%	0.0000%	0.0000%	0.0%
10	0	KIAD	May-17	time opt	71,091	5,882,411	6h 1m 1s	0	0.0000%	0.0000%	0.0000%	0.0%
20	0	KIAD	May-17	time opt	71,091	5,882,411	6h 1m 1s	0	0.0000%	0.0000%	0.0000%	0.0%
30	0	KIAD	May-17	time opt	71,091	5,882,411	6h 1m 1s	0	0.0000%	0.0000%	0.0000%	0.0%
40	0	KIAD	May-17	time opt	71,091	5,882,411	6h 1m 1s	0	0.0000%	0.0000%	0.0000%	0.0%
50	0	KIAD	May-17	time opt	71,091	5,882,411	6h 1m 1s	0	0.0000%	0.0000%	0.0000%	0.0%
60	0	KIAD	May-17	time opt	71,091	5,882,411	6h 1m 1s	0	0.0000%	0.0000%	0.0000%	0.0%
70	0	KIAD	May-17	time opt	71,091	5,882,411	6h 1m 1s	0	0.0000%	0.0000%	0.0000%	0.0%
80	0	KIAD	May-17	time opt	71,091	5,882,411	6h 1m 1s	0	0.0000%	0.0000%	0.0000%	0.0%
90	0	KIAD	May-17	time opt	71,091	5,882,411	6h 1m 1s	0	0.0000%	0.0000%	0.0000%	0.0%
100	0	KIAD	May-17	time opt	71,091	5,882,411	6h 1m 1s	0	0.0000%	0.0000%	0.0000%	0.0%

C. Numeric results - Altitude profile

β_{grnd}	β_{prof}	Dest	Atm	Mode	dm [kg]	ds [m]	dt [h:m:s]	ct _{tot} [m]	% dm	% ds	% dt	% CT
0	1.0E-05	CYWG	Feb-14	fuel opt	77,564	6,839,002	7h 40m 39s	2,238,395	0.0000%	0.0000%	0.0000%	0.0%
0	2.0E-05	CYWG	Feb-14	fuel opt	77,564	6,839,002	7h 40m 39s	2,238,395	0.0000%	0.0000%	0.0000%	0.0%
0	3.0E-05	CYWG	Feb-14	fuel opt	77,564	6,839,002	7h 40m 39s	2,238,395	0.0000%	0.0000%	0.0000%	0.0%
0	4.0E-05	CYWG	Feb-14	fuel opt	77,564	6,839,002	7h 40m 39s	2,238,395	0.0000%	0.0000%	0.0000%	0.0%
0	5.0E-05	CYWG	Feb-14	fuel opt	77,564	6,839,002	7h 40m 39s	2,238,395	0.0000%	0.0000%	0.0000%	0.0%
0	6.0E-05	CYWG	Feb-14	fuel opt	77,564	6,839,023	7h 40m 39s	2,233,418	-0.0002%	0.0003%	0.0006%	-0.2%
0	7.0E-05	CYWG	Feb-14	fuel opt	77,564	6,839,023	7h 40m 39s	2,233,418	-0.0002%	0.0003%	0.0006%	-0.2%
0	8.0E-05	CYWG	Feb-14	fuel opt	77,564	6,839,002	7h 40m 39s	2,238,395	0.0000%	0.0000%	0.0000%	0.0%
0	9.0E-05	CYWG	Feb-14	fuel opt	77,564	6,839,022	7h 40m 39s	2,233,416	-0.0001%	0.0003%	0.0005%	-0.2%
0	1.0E-04	CYWG	Feb-14	fuel opt	77,577	6,839,034	7h 40m 39s	2,078,679	0.0173%	0.0005%	0.0011%	-7.1%
0	2.0E-04	CYWG	Feb-14	fuel opt	77,577	6,839,034	7h 40m 39s	2,078,679	0.0173%	0.0005%	0.0011%	-7.1%
0	3.0E-04	CYWG	Feb-14	fuel opt	77,577	6,839,034	7h 40m 39s	2,078,679	0.0173%	0.0005%	0.0011%	-7.1%
0	4.0E-04	CYWG	Feb-14	fuel opt	77,554	6,836,632	7h 40m 30s	1,888,696	-0.0133%	-0.0347%	-0.0329%	-15.6%
0	5.0E-04	CYWG	Feb-14	fuel opt	77,554	6,836,632	7h 40m 30s	1,888,696	-0.0133%	-0.0347%	-0.0329%	-15.6%
0	6.0E-04	CYWG	Feb-14	fuel opt	77,554	6,836,632	7h 40m 30s	1,888,696	-0.0133%	-0.0347%	-0.0329%	-15.6%
0	7.0E-04	CYWG	Feb-14	fuel opt	77,554	6,836,632	7h 40m 30s	1,888,696	-0.0133%	-0.0347%	-0.0329%	-15.6%
0	8.0E-04	CYWG	Feb-14	fuel opt	77,554	6,836,632	7h 40m 30s	1,888,696	-0.0133%	-0.0347%	-0.0329%	-15.6%
0	9.0E-04	CYWG	Feb-14	fuel opt	77,554	6,836,688	7h 40m 30s	1,883,752	-0.0126%	-0.0338%	-0.0320%	-15.8%
0	1.0E-03	CYWG	Feb-14	fuel opt	77,554	6,836,666	7h 40m 30s	1,888,730	-0.0124%	-0.0341%	-0.0326%	-15.6%
0	2.0E-03	CYWG	Feb-14	fuel opt	77,554	6,836,666	7h 40m 30s	1,888,730	-0.0124%	-0.0341%	-0.0326%	-15.6%
0	3.0E-03	CYWG	Feb-14	fuel opt	77,554	6,836,632	7h 40m 30s	1,888,696	-0.0133%	-0.0347%	-0.0329%	-15.6%
0	4.0E-03	CYWG	Feb-14	fuel opt	77,554	6,836,666	7h 40m 30s	1,888,730	-0.0124%	-0.0341%	-0.0326%	-15.6%
0	5.0E-03	CYWG	Feb-14	fuel opt	77,554	6,836,666	7h 40m 30s	1,888,730	-0.0124%	-0.0341%	-0.0326%	-15.6%
0	6.0E-03	CYWG	Feb-14	fuel opt	77,554	6,836,666	7h 40m 30s	1,888,730	-0.0124%	-0.0341%	-0.0326%	-15.6%
0	7.0E-03	CYWG	Feb-14	fuel opt	77,554	6,836,666	7h 40m 30s	1,888,730	-0.0124%	-0.0341%	-0.0326%	-15.6%
0	8.0E-03	CYWG	Feb-14	fuel opt	77,675	6,841,680	7h 40m 50s	1,423,439	0.1431%	0.0392%	0.0400%	-36.4%
0	9.0E-03	CYWG	Feb-14	fuel opt	77,590	6,838,921	7h 40m 39s	1,810,875	0.0334%	-0.0012%	0.0014%	-19.1%
0	1.0E-02	CYWG	Feb-14	fuel opt	76,931	6,778,405	7h 36m 37s	1,471,199	-0.8166%	-0.8860%	-0.8753%	-34.3%
0	2.0E-02	CYWG	Feb-14	fuel opt	77,677	6,838,403	7h 40m 37s	1,406,137	0.1454%	-0.0088%	-0.0074%	-37.2%
0	3.0E-02	CYWG	Feb-14	fuel opt	77,686	6,841,778	7h 40m 51s	1,369,681	0.1577%	0.0406%	0.0415%	-38.8%
0	4.0E-02	CYWG	Feb-14	fuel opt	77,003	6,782,823	7h 36m 55s	1,350,565	-0.7238%	-0.8214%	-0.8106%	-39.7%
0	5.0E-02	CYWG	Feb-14	fuel opt	76,973	6,780,672	7h 36m 46s	1,369,681	-0.7622%	-0.8529%	-0.8421%	-38.8%
0	6.0E-02	CYWG	Feb-14	fuel opt	77,864	6,840,695	7h 40m 46s	972,511	0.3871%	0.0248%	0.0233%	-56.6%
0	7.0E-02	CYWG	Feb-14	fuel opt	77,002	6,782,818	7h 36m 55s	1,350,562	-0.7252%	-0.8215%	-0.8106%	-39.7%
0	8.0E-02	CYWG	Feb-14	fuel opt	76,981	6,777,756	7h 36m 35s	1,286,578	-0.7523%	-0.8955%	-0.8843%	-42.5%
0	9.0E-02	CYWG	Feb-14	fuel opt	76,981	6,777,737	7h 36m 35s	1,281,569	-0.7519%	-0.8958%	-0.8842%	-42.7%
0	1.0E-01	CYWG	Feb-14	fuel opt	77,790	6,842,879	7h 40m 55s	1,428,213	0.2919%	0.0567%	0.0582%	-36.2%
0	2.0E-01	CYWG	Feb-14	fuel opt	76,980	6,777,749	7h 36m 35s	1,281,570	-0.7527%	-0.8956%	-0.8843%	-42.7%
0	3.0E-01	CYWG	Feb-14	fuel opt	76,981	6,777,750	7h 36m 35s	1,286,581	-0.7513%	-0.8956%	-0.8842%	-42.5%
0	4.0E-01	CYWG	Feb-14	fuel opt	77,809	6,843,365	7h 40m 57s	1,303,692	0.3159%	0.0638%	0.0652%	-41.8%
0	5.0E-01	CYWG	Feb-14	fuel opt	77,809	6,843,365	7h 40m 57s	1,303,692	0.3159%	0.0638%	0.0652%	-41.8%
0	6.0E-01	CYWG	Feb-14	fuel opt	77,862	6,840,601	7h 40m 45s	1,152,469	0.3846%	0.0234%	0.0233%	-48.5%
0	7.0E-01	CYWG	Feb-14	fuel opt	77,861	6,840,601	7h 40m 45s	1,147,467	0.3833%	0.0234%	0.0233%	-48.7%
0	8.0E-01	CYWG	Feb-14	fuel opt	77,861	6,840,601	7h 40m 45s	1,147,467	0.3833%	0.0234%	0.0233%	-48.7%
0	9.0E-01	CYWG	Feb-14	fuel opt	76,969	6,764,408	7h 35m 41s	1,147,467	-0.7675%	-1.0907%	-1.0784%	-48.7%
0	1.0E+00	CYWG	Feb-14	fuel opt	76,976	6,772,219	7h 36m 13s	1,303,692	-0.7578%	-0.9765%	-0.9637%	-41.8%
0	2.0E+00	CYWG	Feb-14	fuel opt	77,010	6,768,931	7h 35m 59s	1,266,988	-0.7140%	-1.0246%	-1.0127%	-43.4%
0	3.0E+00	CYWG	Feb-14	fuel opt	77,862	6,840,601	7h 40m 45s	1,152,469	0.3846%	0.0234%	0.0233%	-48.5%
0	4.0E+00	CYWG	Feb-14	fuel opt	77,862	6,840,601	7h 40m 45s	1,152,469	0.3846%	0.0234%	0.0233%	-48.5%
0	5.0E+00	CYWG	Feb-14	fuel opt	76,968	6,777,714	7h 36m 35s	1,350,442	-0.7688%	-0.8961%	-0.8844%	-39.7%
0	6.0E+00	CYWG	Feb-14	fuel opt	77,782	6,840,976	7h 40m 48s	1,287,502	0.2814%	0.0289%	0.0307%	-42.5%
0	7.0E+00	CYWG	Feb-14	fuel opt	77,862	6,840,601	7h 40m 45s	1,152,469	0.3846%	0.0234%	0.0233%	-48.5%
0	8.0E+00	CYWG	Feb-14	fuel opt	77,862	6,840,601	7h 40m 45s	1,152,469	0.3846%	0.0234%	0.0233%	-48.5%
0	9.0E+00	CYWG	Feb-14	fuel opt	77,864	6,840,695	7h 40m 46s	972,511	0.3871%	0.0248%	0.0233%	-56.6%
0	1.0E+01	CYWG	Feb-14	fuel opt	77,861	6,840,601	7h 40m 45s	1,147,467	0.3833%	0.0234%	0.0233%	-48.7%

β_{grnd}	β_{prof}	Dest	Atm	Mode	dm [kg]	ds [m]	dt [h:m:s]	ct _{tot} [m]	% dm	% ds	% dt	% CT
0	1.0E-05	CYVR	Feb-14	fuel opt	88,254	7,766,065	8h 40m 7s	1,550,551	0.0000%	0.0000%	0.0000%	0.0%
0	2.0E-05	CYVR	Feb-14	fuel opt	88,254	7,766,065	8h 40m 7s	1,550,551	0.0000%	0.0000%	0.0000%	0.0%
0	3.0E-05	CYVR	Feb-14	fuel opt	88,254	7,766,065	8h 40m 7s	1,550,551	0.0000%	0.0000%	0.0000%	0.0%
0	4.0E-05	CYVR	Feb-14	fuel opt	88,254	7,766,065	8h 40m 7s	1,550,551	0.0000%	0.0000%	0.0000%	0.0%
0	5.0E-05	CYVR	Feb-14	fuel opt	88,254	7,766,065	8h 40m 7s	1,550,551	0.0000%	0.0000%	0.0000%	0.0%
0	6.0E-05	CYVR	Feb-14	fuel opt	88,237	7,766,065	8h 40m 7s	1,345,551	-0.0187%	0.0000%	0.0003%	-13.2%
0	7.0E-05	CYVR	Feb-14	fuel opt	88,237	7,766,065	8h 40m 7s	1,345,551	-0.0187%	0.0000%	0.0003%	-13.2%
0	8.0E-05	CYVR	Feb-14	fuel opt	88,237	7,766,065	8h 40m 7s	1,345,551	-0.0187%	0.0000%	0.0003%	-13.2%
0	9.0E-05	CYVR	Feb-14	fuel opt	88,237	7,766,065	8h 40m 7s	1,345,551	-0.0187%	0.0000%	0.0003%	-13.2%
0	1.0E-04	CYVR	Feb-14	fuel opt	88,237	7,766,065	8h 40m 7s	1,345,551	-0.0187%	0.0000%	0.0003%	-13.2%
0	2.0E-04	CYVR	Feb-14	fuel opt	88,239	7,766,065	8h 40m 7s	1,305,653	-0.0170%	0.0000%	0.0000%	-15.8%
0	3.0E-04	CYVR	Feb-14	fuel opt	88,237	7,766,065	8h 40m 7s	1,345,551	-0.0187%	0.0000%	0.0003%	-13.2%
0	4.0E-04	CYVR	Feb-14	fuel opt	88,237	7,766,065	8h 40m 7s	1,345,551	-0.0187%	0.0000%	0.0003%	-13.2%
0	5.0E-04	CYVR	Feb-14	fuel opt	88,237	7,766,065	8h 40m 7s	1,345,551	-0.0187%	0.0000%	0.0003%	-13.2%
0	6.0E-04	CYVR	Feb-14	fuel opt	88,237	7,766,065	8h 40m 7s	1,345,551	-0.0187%	0.0000%	0.0003%	-13.2%
0	7.0E-04	CYVR	Feb-14	fuel opt	88,237	7,766,065	8h 40m 7s	1,345,551	-0.0187%	0.0000%	0.0003%	-13.2%
0	8.0E-04	CYVR	Feb-14	fuel opt	88,237	7,766,065	8h 40m 7s	1,345,551	-0.0187%	0.0000%	0.0003%	-13.2%
0	9.0E-04	CYVR	Feb-14	fuel opt	88,237	7,766,065	8h 40m 7s	1,345,551	-0.0187%	0.0000%	0.0003%	-13.2%
0	1.0E-03	CYVR	Feb-14	fuel opt	88,239	7,766,065	8h 40m 7s	1,305,653	-0.0170%	0.0000%	0.0000%	-15.8%
0	2.0E-03	CYVR	Feb-14	fuel opt	88,237	7,766,065	8h 40m 7s	1,385,716	-0.0186%	0.0000%	0.0005%	-10.6%
0	3.0E-03	CYVR	Feb-14	fuel opt	88,237	7,766,065	8h 40m 7s	1,385,716	-0.0186%	0.0000%	0.0005%	-10.6%
0	4.0E-03	CYVR	Feb-14	fuel opt	88,273	7,766,065	8h 40m 7s	1,265,142	0.0218%	0.0000%	-0.0003%	-18.4%
0	5.0E-03	CYVR	Feb-14	fuel opt	88,237	7,766,065	8h 40m 7s	1,290,447	-0.0184%	0.0000%	0.0005%	-16.8%
0	6.0E-03	CYVR	Feb-14	fuel opt	88,273	7,766,065	8h 40m 7s	1,265,142	0.0218%	0.0000%	-0.0003%	-18.4%
0	7.0E-03	CYVR	Feb-14	fuel opt	88,233	7,766,065	8h 40m 7s	1,303,296	-0.0231%	0.0000%	-0.0001%	-15.9%
0	8.0E-03	CYVR	Feb-14	fuel opt	88,239	7,766,065	8h 40m 7s	1,295,533	-0.0159%	0.0000%	-0.0002%	-16.4%
0	9.0E-03	CYVR	Feb-14	fuel opt	88,234	7,766,065	8h 40m 7s	1,293,174	-0.0220%	0.0000%	-0.0003%	-16.6%
0	1.0E-02	CYVR	Feb-14	fuel opt	88,240	7,766,065	8h 40m 7s	1,078,866	-0.0153%	0.0000%	0.0015%	-30.4%
0	2.0E-02	CYVR	Feb-14	fuel opt	88,242	7,766,065	8h 40m 7s	824,841	-0.0127%	0.0000%	0.0017%	-46.8%
0	3.0E-02	CYVR	Feb-14	fuel opt	88,282	7,766,065	8h 40m 7s	811,882	0.0320%	0.0000%	0.0018%	-47.6%
0	4.0E-02	CYVR	Feb-14	fuel opt	88,242	7,766,065	8h 40m 7s	824,841	-0.0127%	0.0000%	0.0017%	-46.8%
0	5.0E-02	CYVR	Feb-14	fuel opt	88,242	7,766,065	8h 40m 7s	824,841	-0.0127%	0.0000%	0.0017%	-46.8%
0	6.0E-02	CYVR	Feb-14	fuel opt	88,253	7,766,065	8h 40m 7s	883,681	-0.0010%	0.0000%	0.0013%	-43.0%
0	7.0E-02	CYVR	Feb-14	fuel opt	88,254	7,766,065	8h 40m 7s	883,664	0.0008%	0.0000%	0.0013%	-43.0%
0	8.0E-02	CYVR	Feb-14	fuel opt	88,244	7,766,065	8h 40m 7s	824,822	-0.0110%	0.0000%	0.0019%	-46.8%
0	9.0E-02	CYVR	Feb-14	fuel opt	88,253	7,766,065	8h 40m 7s	824,823	-0.0009%	0.0000%	0.0017%	-46.8%
0	1.0E-01	CYVR	Feb-14	fuel opt	88,244	7,766,065	8h 40m 7s	824,822	-0.0110%	0.0000%	0.0019%	-46.8%
0	2.0E-01	CYVR	Feb-14	fuel opt	88,244	7,766,065	8h 40m 7s	824,822	-0.0109%	0.0000%	0.0019%	-46.8%
0	3.0E-01	CYVR	Feb-14	fuel opt	88,244	7,766,065	8h 40m 7s	824,825	-0.0103%	0.0000%	0.0019%	-46.8%
0	4.0E-01	CYVR	Feb-14	fuel opt	88,244	7,766,065	8h 40m 7s	824,822	-0.0109%	0.0000%	0.0019%	-46.8%
0	5.0E-01	CYVR	Feb-14	fuel opt	88,253	7,766,065	8h 40m 7s	824,822	-0.0007%	0.0000%	0.0017%	-46.8%
0	6.0E-01	CYVR	Feb-14	fuel opt	88,295	7,766,065	8h 40m 7s	806,876	0.0473%	0.0000%	0.0005%	-48.0%
0	7.0E-01	CYVR	Feb-14	fuel opt	88,264	7,766,065	8h 40m 7s	883,653	0.0122%	0.0000%	0.0011%	-43.0%
0	8.0E-01	CYVR	Feb-14	fuel opt	88,244	7,766,065	8h 40m 7s	824,822	-0.0110%	0.0000%	0.0019%	-46.8%
0	9.0E-01	CYVR	Feb-14	fuel opt	88,244	7,766,065	8h 40m 7s	824,822	-0.0109%	0.0000%	0.0019%	-46.8%
0	1.0E+00	CYVR	Feb-14	fuel opt	88,290	7,766,065	8h 40m 7s	806,876	0.0409%	0.0000%	0.0018%	-48.0%
0	2.0E+00	CYVR	Feb-14	fuel opt	88,244	7,766,065	8h 40m 7s	824,822	-0.0107%	0.0000%	0.0019%	-46.8%
0	3.0E+00	CYVR	Feb-14	fuel opt	88,244	7,766,065	8h 40m 7s	824,822	-0.0109%	0.0000%	0.0019%	-46.8%
0	4.0E+00	CYVR	Feb-14	fuel opt	88,244	7,766,065	8h 40m 7s	824,822	-0.0109%	0.0000%	0.0019%	-46.8%
0	5.0E+00	CYVR	Feb-14	fuel opt	88,245	7,766,065	8h 40m 7s	824,828	-0.0099%	0.0000%	0.0019%	-46.8%
0	6.0E+00	CYVR	Feb-14	fuel opt	88,285	7,766,065	8h 40m 7s	700,892	0.0361%	0.0000%	0.0001%	-54.8%
0	7.0E+00	CYVR	Feb-14	fuel opt	88,244	7,766,065	8h 40m 7s	824,825	-0.0103%	0.0000%	0.0019%	-46.8%
0	8.0E+00	CYVR	Feb-14	fuel opt	88,244	7,766,065	8h 40m 7s	824,822	-0.0107%	0.0000%	0.0019%	-46.8%
0	9.0E+00	CYVR	Feb-14	fuel opt	88,312	7,766,065	8h 40m 7s	701,835	0.0665%	0.0000%	-0.0007%	-54.7%
0	1.0E+01	CYVR	Feb-14	fuel opt	88,244	7,766,065	8h 40m 7s	824,822	-0.0107%	0.0000%	0.0019%	-46.8%

C. Numeric results - Altitude profile

β_{grnd}	β_{prof}	Dest	Atm	Mode	dm [kg]	ds [m]	dt [h:m:s]	ct _{tot} [m]	% dm	% ds	% dt	% CT
0	1.0E-05	CYVR	Feb-17	fuel opt	86,867	7,739,677	8h 32m 6s	1,145,812	0.0000%	0.0000%	0.0000%	0.0%
0	2.0E-05	CYVR	Feb-17	fuel opt	86,867	7,739,677	8h 32m 6s	1,145,812	0.0000%	0.0000%	0.0000%	0.0%
0	3.0E-05	CYVR	Feb-17	fuel opt	86,867	7,739,677	8h 32m 6s	1,145,812	0.0000%	0.0000%	0.0000%	0.0%
0	4.0E-05	CYVR	Feb-17	fuel opt	86,867	7,739,677	8h 32m 6s	1,145,812	0.0000%	0.0000%	0.0000%	0.0%
0	5.0E-05	CYVR	Feb-17	fuel opt	86,867	7,739,677	8h 32m 6s	1,145,812	0.0000%	0.0000%	0.0000%	0.0%
0	6.0E-05	CYVR	Feb-17	fuel opt	86,881	7,739,677	8h 32m 5s	905,947	0.0156%	0.0000%	-0.0013%	-20.9%
0	7.0E-05	CYVR	Feb-17	fuel opt	86,881	7,739,677	8h 32m 5s	905,947	0.0156%	0.0000%	-0.0013%	-20.9%
0	8.0E-05	CYVR	Feb-17	fuel opt	86,867	7,739,677	8h 32m 6s	1,145,812	0.0000%	0.0000%	0.0000%	0.0%
0	9.0E-05	CYVR	Feb-17	fuel opt	86,867	7,739,677	8h 32m 6s	1,145,812	0.0000%	0.0000%	0.0000%	0.0%
0	1.0E-04	CYVR	Feb-17	fuel opt	86,868	7,739,677	8h 32m 6s	1,140,817	0.0002%	0.0000%	0.0000%	-0.4%
0	2.0E-04	CYVR	Feb-17	fuel opt	86,868	7,739,677	8h 32m 6s	1,135,876	0.0002%	0.0000%	0.0001%	-0.9%
0	3.0E-04	CYVR	Feb-17	fuel opt	86,881	7,739,677	8h 32m 6s	1,020,847	0.0161%	0.0000%	0.0006%	-10.9%
0	4.0E-04	CYVR	Feb-17	fuel opt	86,881	7,739,677	8h 32m 5s	900,953	0.0158%	0.0000%	-0.0013%	-21.4%
0	5.0E-04	CYVR	Feb-17	fuel opt	86,881	7,739,677	8h 32m 6s	1,025,841	0.0160%	0.0000%	0.0006%	-10.5%
0	6.0E-04	CYVR	Feb-17	fuel opt	86,881	7,739,677	8h 32m 5s	900,953	0.0158%	0.0000%	-0.0013%	-21.4%
0	7.0E-04	CYVR	Feb-17	fuel opt	86,891	7,739,677	8h 32m 6s	851,410	0.0267%	0.0000%	0.0002%	-25.7%
0	8.0E-04	CYVR	Feb-17	fuel opt	86,881	7,739,677	8h 32m 5s	900,953	0.0158%	0.0000%	-0.0013%	-21.4%
0	9.0E-04	CYVR	Feb-17	fuel opt	86,881	7,739,677	8h 32m 5s	900,953	0.0158%	0.0000%	-0.0013%	-21.4%
0	1.0E-03	CYVR	Feb-17	fuel opt	86,884	7,739,677	8h 32m 5s	780,679	0.0195%	0.0000%	-0.0018%	-31.9%
0	2.0E-03	CYVR	Feb-17	fuel opt	86,881	7,739,677	8h 32m 5s	900,953	0.0158%	0.0000%	-0.0013%	-21.4%
0	3.0E-03	CYVR	Feb-17	fuel opt	86,877	7,739,677	8h 32m 5s	680,679	0.0108%	0.0000%	-0.0008%	-40.6%
0	4.0E-03	CYVR	Feb-17	fuel opt	86,877	7,739,677	8h 32m 5s	680,679	0.0108%	0.0000%	-0.0008%	-40.6%
0	5.0E-03	CYVR	Feb-17	fuel opt	86,883	7,739,677	8h 32m 6s	751,410	0.0179%	0.0000%	0.0011%	-34.4%
0	6.0E-03	CYVR	Feb-17	fuel opt	86,874	7,739,677	8h 32m 6s	800,953	0.0071%	0.0000%	-0.0002%	-30.1%
0	7.0E-03	CYVR	Feb-17	fuel opt	86,875	7,739,677	8h 32m 6s	800,855	0.0089%	0.0000%	0.0007%	-30.1%
0	8.0E-03	CYVR	Feb-17	fuel opt	86,874	7,739,677	8h 32m 6s	800,953	0.0071%	0.0000%	-0.0002%	-30.1%
0	9.0E-03	CYVR	Feb-17	fuel opt	86,877	7,739,677	8h 32m 5s	680,679	0.0108%	0.0000%	-0.0008%	-40.6%
0	1.0E-02	CYVR	Feb-17	fuel opt	86,874	7,739,677	8h 32m 6s	800,953	0.0071%	0.0000%	-0.0002%	-30.1%
0	2.0E-02	CYVR	Feb-17	fuel opt	86,875	7,739,677	8h 32m 6s	800,843	0.0086%	0.0000%	0.0008%	-30.1%
0	3.0E-02	CYVR	Feb-17	fuel opt	86,897	7,739,677	8h 32m 7s	692,719	0.0340%	0.0000%	0.0047%	-39.5%
0	4.0E-02	CYVR	Feb-17	fuel opt	86,899	7,739,677	8h 32m 7s	692,652	0.0358%	0.0000%	0.0056%	-39.5%
0	5.0E-02	CYVR	Feb-17	fuel opt	86,898	7,739,677	8h 32m 7s	692,785	0.0350%	0.0000%	0.0046%	-39.5%
0	6.0E-02	CYVR	Feb-17	fuel opt	86,901	7,739,677	8h 32m 7s	572,510	0.0388%	0.0000%	0.0041%	-50.0%
0	7.0E-02	CYVR	Feb-17	fuel opt	86,904	7,739,677	8h 32m 7s	572,450	0.0418%	0.0000%	0.0050%	-50.0%
0	8.0E-02	CYVR	Feb-17	fuel opt	86,902	7,739,677	8h 32m 7s	572,376	0.0396%	0.0000%	0.0051%	-50.0%
0	9.0E-02	CYVR	Feb-17	fuel opt	86,898	7,739,677	8h 32m 7s	692,785	0.0350%	0.0000%	0.0046%	-39.5%
0	1.0E-01	CYVR	Feb-17	fuel opt	86,963	7,739,677	8h 32m 8s	647,354	0.1105%	0.0000%	0.0080%	-43.5%
0	2.0E-01	CYVR	Feb-17	fuel opt	86,902	7,739,677	8h 32m 7s	572,394	0.0401%	0.0000%	0.0051%	-50.0%
0	3.0E-01	CYVR	Feb-17	fuel opt	86,897	7,739,677	8h 32m 7s	692,719	0.0340%	0.0000%	0.0047%	-39.5%
0	4.0E-01	CYVR	Feb-17	fuel opt	86,898	7,739,677	8h 32m 7s	692,785	0.0350%	0.0000%	0.0046%	-39.5%
0	5.0E-01	CYVR	Feb-17	fuel opt	86,899	7,739,677	8h 32m 7s	692,687	0.0369%	0.0000%	0.0056%	-39.5%
0	6.0E-01	CYVR	Feb-17	fuel opt	86,901	7,739,677	8h 32m 7s	572,510	0.0388%	0.0000%	0.0041%	-50.0%
0	7.0E-01	CYVR	Feb-17	fuel opt	86,899	7,739,677	8h 32m 8s	451,298	0.0361%	0.0000%	0.0067%	-60.6%
0	8.0E-01	CYVR	Feb-17	fuel opt	86,899	7,739,677	8h 32m 7s	692,669	0.0364%	0.0000%	0.0056%	-39.5%
0	9.0E-01	CYVR	Feb-17	fuel opt	86,899	7,739,677	8h 32m 8s	451,165	0.0369%	0.0000%	0.0078%	-60.6%
0	1.0E+00	CYVR	Feb-17	fuel opt	86,898	7,739,677	8h 32m 7s	692,785	0.0350%	0.0000%	0.0046%	-39.5%
0	2.0E+00	CYVR	Feb-17	fuel opt	86,898	7,739,677	8h 32m 7s	692,785	0.0350%	0.0000%	0.0046%	-39.5%
0	3.0E+00	CYVR	Feb-17	fuel opt	86,898	7,739,677	8h 32m 7s	692,785	0.0350%	0.0000%	0.0046%	-39.5%
0	4.0E+00	CYVR	Feb-17	fuel opt	86,907	7,739,677	8h 32m 9s	572,490	0.0459%	0.0000%	0.0125%	-50.0%
0	5.0E+00	CYVR	Feb-17	fuel opt	86,897	7,739,677	8h 32m 7s	687,748	0.0345%	0.0000%	0.0046%	-40.0%
0	6.0E+00	CYVR	Feb-17	fuel opt	86,896	7,739,677	8h 32m 7s	692,614	0.0324%	0.0000%	0.0055%	-39.6%
0	7.0E+00	CYVR	Feb-17	fuel opt	86,901	7,739,677	8h 32m 7s	572,362	0.0391%	0.0000%	0.0051%	-50.0%
0	8.0E+00	CYVR	Feb-17	fuel opt	86,898	7,739,677	8h 32m 7s	692,785	0.0350%	0.0000%	0.0046%	-39.5%
0	9.0E+00	CYVR	Feb-17	fuel opt	86,896	7,739,677	8h 32m 7s	692,614	0.0324%	0.0000%	0.0055%	-39.6%
0	1.0E+01	CYVR	Feb-17	fuel opt	86,901	7,739,677	8h 32m 7s	572,362	0.0391%	0.0000%	0.0051%	-50.0%

C. Numeric results - Altitude profile

β_{grnd}	β_{prof}	Dest	Atm	Mode	dm [kg]	ds [m]	dt [h:m:s]	ct _{tot} [m]	% dm	% ds	% dt	% CT
0	1.0E-05	CYWG	May-17	fuel opt	72,577	6,613,080	7h 12m 17s	1,360,000	0.0000%	0.0000%	0.0000%	0.0%
0	2.0E-05	CYWG	May-17	fuel opt	72,577	6,613,080	7h 12m 17s	1,360,000	0.0000%	0.0000%	0.0000%	0.0%
0	3.0E-05	CYWG	May-17	fuel opt	72,577	6,613,080	7h 12m 17s	1,360,000	0.0000%	0.0000%	0.0000%	0.0%
0	4.0E-05	CYWG	May-17	fuel opt	72,577	6,613,080	7h 12m 17s	1,360,000	0.0000%	0.0000%	0.0000%	0.0%
0	5.0E-05	CYWG	May-17	fuel opt	72,577	6,613,080	7h 12m 17s	1,360,000	0.0000%	0.0000%	0.0000%	0.0%
0	6.0E-05	CYWG	May-17	fuel opt	72,577	6,613,080	7h 12m 17s	1,360,000	0.0000%	0.0000%	0.0000%	0.0%
0	7.0E-05	CYWG	May-17	fuel opt	72,577	6,613,080	7h 12m 17s	1,360,000	0.0000%	0.0000%	0.0000%	0.0%
0	8.0E-05	CYWG	May-17	fuel opt	72,577	6,613,080	7h 12m 17s	1,360,000	0.0000%	0.0000%	0.0000%	0.0%
0	9.0E-05	CYWG	May-17	fuel opt	72,577	6,613,080	7h 12m 17s	1,360,000	0.0000%	0.0000%	0.0000%	0.0%
0	1.0E-04	CYWG	May-17	fuel opt	72,577	6,613,080	7h 12m 17s	1,360,000	0.0000%	0.0000%	0.0000%	0.0%
0	2.0E-04	CYWG	May-17	fuel opt	72,577	6,613,080	7h 12m 17s	1,360,000	0.0000%	0.0000%	0.0000%	0.0%
0	3.0E-04	CYWG	May-17	fuel opt	72,579	6,613,080	7h 12m 18s	981,119	0.0026%	0.0000%	0.0002%	-27.9%
0	4.0E-04	CYWG	May-17	fuel opt	72,581	6,613,080	7h 12m 18s	991,577	0.0046%	0.0000%	0.0005%	-27.1%
0	5.0E-04	CYWG	May-17	fuel opt	72,573	6,613,080	7h 12m 18s	902,050	-0.0056%	0.0000%	0.0006%	-33.7%
0	6.0E-04	CYWG	May-17	fuel opt	72,585	6,613,080	7h 12m 18s	812,783	0.0098%	0.0000%	0.0004%	-40.2%
0	7.0E-04	CYWG	May-17	fuel opt	72,574	6,613,080	7h 12m 18s	902,049	-0.0048%	0.0000%	0.0006%	-33.7%
0	8.0E-04	CYWG	May-17	fuel opt	72,577	6,613,080	7h 12m 18s	902,032	0.0000%	0.0000%	0.0007%	-33.7%
0	9.0E-04	CYWG	May-17	fuel opt	72,573	6,613,080	7h 12m 18s	901,864	-0.0059%	0.0000%	0.0003%	-33.7%
0	1.0E-03	CYWG	May-17	fuel opt	72,582	6,613,080	7h 12m 18s	812,729	0.0065%	0.0000%	0.0008%	-40.2%
0	2.0E-03	CYWG	May-17	fuel opt	72,587	6,613,080	7h 12m 18s	812,696	0.0126%	0.0000%	0.0007%	-40.2%
0	3.0E-03	CYWG	May-17	fuel opt	72,578	6,613,080	7h 12m 18s	812,746	0.0006%	0.0000%	0.0007%	-40.2%
0	4.0E-03	CYWG	May-17	fuel opt	72,605	6,613,080	7h 12m 18s	553,812	0.0377%	0.0000%	0.0009%	-59.3%
0	5.0E-03	CYWG	May-17	fuel opt	72,601	6,613,080	7h 12m 18s	553,814	0.0324%	0.0000%	0.0011%	-59.3%
0	6.0E-03	CYWG	May-17	fuel opt	72,617	6,613,080	7h 12m 18s	218,117	0.0543%	0.0000%	0.0009%	-84.0%
0	7.0E-03	CYWG	May-17	fuel opt	72,606	6,613,080	7h 12m 18s	393,886	0.0389%	0.0000%	0.0012%	-71.0%
0	8.0E-03	CYWG	May-17	fuel opt	72,613	6,613,080	7h 12m 18s	218,117	0.0489%	0.0000%	0.0009%	-84.0%
0	9.0E-03	CYWG	May-17	fuel opt	72,613	6,613,080	7h 12m 18s	218,133	0.0486%	0.0000%	0.0006%	-84.0%
0	1.0E-02	CYWG	May-17	fuel opt	72,613	6,613,080	7h 12m 18s	218,133	0.0490%	0.0000%	0.0006%	-84.0%
0	2.0E-02	CYWG	May-17	fuel opt	72,612	6,613,080	7h 12m 18s	218,134	0.0473%	0.0000%	0.0007%	-84.0%
0	3.0E-02	CYWG	May-17	fuel opt	72,612	6,613,080	7h 12m 18s	218,134	0.0473%	0.0000%	0.0007%	-84.0%
0	4.0E-02	CYWG	May-17	fuel opt	72,613	6,613,080	7h 12m 18s	218,133	0.0490%	0.0000%	0.0006%	-84.0%
0	5.0E-02	CYWG	May-17	fuel opt	72,613	6,613,080	7h 12m 18s	218,117	0.0489%	0.0000%	0.0009%	-84.0%
0	6.0E-02	CYWG	May-17	fuel opt	72,613	6,613,080	7h 12m 18s	218,117	0.0486%	0.0000%	0.0009%	-84.0%
0	7.0E-02	CYWG	May-17	fuel opt	72,613	6,613,080	7h 12m 18s	218,133	0.0490%	0.0000%	0.0006%	-84.0%
0	8.0E-02	CYWG	May-17	fuel opt	72,613	6,613,080	7h 12m 18s	218,118	0.0491%	0.0000%	0.0009%	-84.0%
0	9.0E-02	CYWG	May-17	fuel opt	72,613	6,613,080	7h 12m 18s	218,117	0.0494%	0.0000%	0.0009%	-84.0%
0	1.0E-01	CYWG	May-17	fuel opt	72,613	6,613,080	7h 12m 18s	218,133	0.0490%	0.0000%	0.0006%	-84.0%
0	2.0E+01	CYWG	May-17	fuel opt	72,614	6,613,080	7h 12m 18s	218,117	0.0498%	0.0000%	0.0009%	-84.0%
0	3.0E+01	CYWG	May-17	fuel opt	72,617	6,613,080	7h 12m 18s	218,117	0.0550%	0.0000%	0.0009%	-84.0%
0	4.0E+01	CYWG	May-17	fuel opt	72,616	6,613,080	7h 12m 18s	218,117	0.0535%	0.0000%	0.0009%	-84.0%
0	5.0E+01	CYWG	May-17	fuel opt	72,614	6,613,080	7h 12m 18s	218,117	0.0498%	0.0000%	0.0009%	-84.0%
0	6.0E+01	CYWG	May-17	fuel opt	72,613	6,613,080	7h 12m 18s	218,117	0.0489%	0.0000%	0.0009%	-84.0%
0	7.0E+01	CYWG	May-17	fuel opt	72,616	6,613,080	7h 12m 18s	218,117	0.0536%	0.0000%	0.0009%	-84.0%
0	8.0E+01	CYWG	May-17	fuel opt	72,615	6,613,080	7h 12m 18s	218,117	0.0517%	0.0000%	0.0009%	-84.0%
0	9.0E+01	CYWG	May-17	fuel opt	72,613	6,613,080	7h 12m 18s	218,133	0.0486%	0.0000%	0.0006%	-84.0%
0	1.0E+00	CYWG	May-17	fuel opt	72,613	6,613,080	7h 12m 18s	218,117	0.0489%	0.0000%	0.0009%	-84.0%
0	2.0E+00	CYWG	May-17	fuel opt	72,614	6,613,080	7h 12m 18s	218,117	0.0498%	0.0000%	0.0009%	-84.0%
0	3.0E+00	CYWG	May-17	fuel opt	72,613	6,613,080	7h 12m 18s	218,117	0.0489%	0.0000%	0.0009%	-84.0%
0	4.0E+00	CYWG	May-17	fuel opt	72,615	6,613,080	7h 12m 18s	218,117	0.0512%	0.0000%	0.0009%	-84.0%
0	5.0E+00	CYWG	May-17	fuel opt	72,614	6,613,080	7h 12m 18s	218,117	0.0498%	0.0000%	0.0009%	-84.0%
0	6.0E+00	CYWG	May-17	fuel opt	72,615	6,613,080	7h 12m 18s	218,117	0.0517%	0.0000%	0.0009%	-84.0%
0	7.0E+00	CYWG	May-17	fuel opt	72,613	6,613,080	7h 12m 18s	218,133	0.0488%	0.0000%	0.0006%	-84.0%
0	8.0E+00	CYWG	May-17	fuel opt	72,616	6,613,080	7h 12m 18s	218,117	0.0531%	0.0000%	0.0009%	-84.0%
0	9.0E+00	CYWG	May-17	fuel opt	72,613	6,613,080	7h 12m 18s	218,133	0.0486%	0.0000%	0.0006%	-84.0%
0	1.0E+01	CYWG	May-17	fuel opt	72,617	6,613,080	7h 12m 18s	218,133	0.0551%	0.0000%	0.0007%	-84.0%

C. Numeric results - Altitude profile

β_{grnd}	β_{prof}	Dest	Atm	Mode	dm [kg]	ds [m]	dt [h:m:s]	ct _{tot} [m]	% dm	% ds	% dt	% CT
0	1.0E-05	KIAD	Feb-14	time opt	74,108	5,937,317	6h 16m 15s	2,315,000	0.0000%	0.0000%	0.0000%	0.0%
0	2.0E-05	KIAD	Feb-14	time opt	74,108	5,937,317	6h 16m 15s	2,315,000	0.0000%	0.0000%	0.0000%	0.0%
0	3.0E-05	KIAD	Feb-14	time opt	74,108	5,937,317	6h 16m 15s	2,315,000	0.0000%	0.0000%	0.0000%	0.0%
0	4.0E-05	KIAD	Feb-14	time opt	74,108	5,937,317	6h 16m 15s	2,315,000	0.0000%	0.0000%	0.0000%	0.0%
0	5.0E-05	KIAD	Feb-14	time opt	74,108	5,937,317	6h 16m 15s	2,315,000	0.0000%	0.0000%	0.0000%	0.0%
0	6.0E-05	KIAD	Feb-14	time opt	74,108	5,937,317	6h 16m 15s	2,315,000	0.0000%	0.0000%	0.0000%	0.0%
0	7.0E-05	KIAD	Feb-14	time opt	74,108	5,937,317	6h 16m 15s	2,315,000	0.0000%	0.0000%	0.0000%	0.0%
0	8.0E-05	KIAD	Feb-14	time opt	74,108	5,937,317	6h 16m 15s	2,315,000	0.0000%	0.0000%	0.0000%	0.0%
0	9.0E-05	KIAD	Feb-14	time opt	74,108	5,937,317	6h 16m 15s	2,315,000	0.0000%	0.0000%	0.0000%	0.0%
0	1.0E-04	KIAD	Feb-14	time opt	74,108	5,937,317	6h 16m 15s	2,315,000	0.0000%	0.0000%	0.0000%	0.0%
0	2.0E-04	KIAD	Feb-14	time opt	74,108	5,937,317	6h 16m 15s	2,315,000	0.0000%	0.0000%	0.0000%	0.0%
0	3.0E-04	KIAD	Feb-14	time opt	74,108	5,937,317	6h 16m 15s	2,315,000	0.0000%	0.0000%	0.0000%	0.0%
0	4.0E-04	KIAD	Feb-14	time opt	74,108	5,937,317	6h 16m 15s	2,315,000	0.0000%	0.0000%	0.0000%	0.0%
0	5.0E-04	KIAD	Feb-14	time opt	74,108	5,937,317	6h 16m 15s	2,315,000	0.0000%	0.0000%	0.0000%	0.0%
0	6.0E-04	KIAD	Feb-14	time opt	74,108	5,937,317	6h 16m 15s	2,315,000	0.0000%	0.0000%	0.0000%	0.0%
0	7.0E-04	KIAD	Feb-14	time opt	74,108	5,937,317	6h 16m 15s	2,315,000	0.0000%	0.0000%	0.0000%	0.0%
0	8.0E-04	KIAD	Feb-14	time opt	74,108	5,937,317	6h 16m 15s	2,315,000	0.0000%	0.0000%	0.0000%	0.0%
0	9.0E-04	KIAD	Feb-14	time opt	74,108	5,937,317	6h 16m 15s	2,315,000	0.0000%	0.0000%	0.0000%	0.0%
0	1.0E-03	KIAD	Feb-14	time opt	74,108	5,937,317	6h 16m 15s	2,315,000	0.0000%	0.0000%	0.0000%	0.0%
0	2.0E-03	KIAD	Feb-14	time opt	73,709	5,936,952	6h 16m 53s	1,160,000	-0.5383%	-0.0062%	0.1662%	-49.9%
0	3.0E-03	KIAD	Feb-14	time opt	73,709	5,936,952	6h 16m 53s	1,160,000	-0.5383%	-0.0062%	0.1662%	-49.9%
0	4.0E-03	KIAD	Feb-14	time opt	74,754	6,056,939	6h 26m 17s	683,336	0.8710%	2.0147%	2.6631%	-70.5%
0	5.0E-03	KIAD	Feb-14	time opt	73,709	5,936,952	6h 16m 53s	1,160,000	-0.5383%	-0.0062%	0.1662%	-49.9%
0	6.0E-03	KIAD	Feb-14	time opt	74,754	6,056,939	6h 26m 17s	683,336	0.8710%	2.0147%	2.6631%	-70.5%
0	7.0E-03	KIAD	Feb-14	time opt	73,257	5,929,677	6h 19m 27s	115,000	-1.1491%	-0.1287%	0.8490%	-95.0%
0	8.0E-03	KIAD	Feb-14	time opt	74,729	6,056,837	6h 26m 20s	688,336	0.8378%	2.0130%	2.6759%	-70.3%
0	9.0E-03	KIAD	Feb-14	time opt	74,754	6,056,939	6h 26m 17s	683,336	0.8710%	2.0147%	2.6631%	-70.5%
0	1.0E-02	KIAD	Feb-14	time opt	74,729	6,056,837	6h 26m 20s	688,336	0.8378%	2.0130%	2.6759%	-70.3%
0	2.0E-02	KIAD	Feb-14	time opt	73,233	5,929,677	6h 19m 30s	115,000	-1.1806%	-0.1287%	0.8635%	-95.0%
0	3.0E-02	KIAD	Feb-14	time opt	73,254	5,929,677	6h 19m 26s	115,000	-1.1525%	-0.1287%	0.8427%	-95.0%
0	4.0E-02	KIAD	Feb-14	time opt	73,229	5,929,677	6h 19m 30s	115,000	-1.1864%	-0.1287%	0.8632%	-95.0%
0	5.0E-02	KIAD	Feb-14	time opt	73,229	5,929,677	6h 19m 30s	115,000	-1.1864%	-0.1287%	0.8632%	-95.0%
0	6.0E-02	KIAD	Feb-14	time opt	73,292	5,929,677	6h 19m 28s	115,000	-1.1015%	-0.1287%	0.8521%	-95.0%
0	7.0E-02	KIAD	Feb-14	time opt	73,229	5,929,677	6h 19m 30s	115,000	-1.1864%	-0.1287%	0.8632%	-95.0%
0	8.0E-02	KIAD	Feb-14	time opt	73,254	5,929,677	6h 19m 26s	115,000	-1.1525%	-0.1287%	0.8427%	-95.0%
0	9.0E-02	KIAD	Feb-14	time opt	73,229	5,929,677	6h 19m 30s	115,000	-1.1864%	-0.1287%	0.8632%	-95.0%
0	1.0E-01	KIAD	Feb-14	time opt	73,257	5,929,677	6h 19m 27s	115,000	-1.1493%	-0.1287%	0.8491%	-95.0%
0	2.0E-01	KIAD	Feb-14	time opt	73,229	5,929,677	6h 19m 30s	115,000	-1.1864%	-0.1287%	0.8632%	-95.0%
0	3.0E-01	KIAD	Feb-14	time opt	73,254	5,929,677	6h 19m 26s	115,000	-1.1525%	-0.1287%	0.8427%	-95.0%
0	4.0E-01	KIAD	Feb-14	time opt	73,229	5,929,677	6h 19m 30s	115,000	-1.1864%	-0.1287%	0.8632%	-95.0%
0	5.0E-01	KIAD	Feb-14	time opt	73,257	5,929,677	6h 19m 27s	115,000	-1.1491%	-0.1287%	0.8490%	-95.0%
0	6.0E-01	KIAD	Feb-14	time opt	73,233	5,929,677	6h 19m 30s	115,000	-1.1806%	-0.1287%	0.8635%	-95.0%
0	7.0E-01	KIAD	Feb-14	time opt	73,225	5,929,677	6h 19m 16s	295,816	-1.1922%	-0.1287%	0.8017%	-87.2%
0	8.0E-01	KIAD	Feb-14	time opt	73,257	5,929,677	6h 19m 27s	115,000	-1.1491%	-0.1287%	0.8490%	-95.0%
0	9.0E-01	KIAD	Feb-14	time opt	73,229	5,929,677	6h 19m 30s	115,000	-1.1864%	-0.1287%	0.8632%	-95.0%
0	1.0E+00	KIAD	Feb-14	time opt	73,229	5,929,677	6h 19m 30s	115,000	-1.1864%	-0.1287%	0.8632%	-95.0%
0	2.0E+00	KIAD	Feb-14	time opt	73,229	5,929,677	6h 19m 30s	115,000	-1.1864%	-0.1287%	0.8632%	-95.0%
0	3.0E+00	KIAD	Feb-14	time opt	73,220	5,929,677	6h 19m 16s	295,816	-1.1980%	-0.1287%	0.8014%	-87.2%
0	4.0E+00	KIAD	Feb-14	time opt	73,229	5,929,677	6h 19m 30s	115,000	-1.1864%	-0.1287%	0.8632%	-95.0%
0	5.0E+00	KIAD	Feb-14	time opt	73,229	5,929,677	6h 19m 30s	115,000	-1.1864%	-0.1287%	0.8632%	-95.0%
0	6.0E+00	KIAD	Feb-14	time opt	73,283	5,929,677	6h 19m 28s	115,000	-1.1137%	-0.1287%	0.8526%	-95.0%
0	7.0E+00	KIAD	Feb-14	time opt	73,257	5,929,677	6h 19m 27s	115,000	-1.1493%	-0.1287%	0.8491%	-95.0%
0	8.0E+00	KIAD	Feb-14	time opt	73,229	5,929,677	6h 19m 30s	115,000	-1.1864%	-0.1287%	0.8632%	-95.0%
0	9.0E+00	KIAD	Feb-14	time opt	73,249	5,929,677	6h 19m 28s	115,000	-1.1592%	-0.1287%	0.8512%	-95.0%
0	1.0E+01	KIAD	Feb-14	time opt	73,229	5,929,677	6h 19m 30s	115,000	-1.1864%	-0.1287%	0.8632%	-95.0%

β_{grnd}	β_{prof}	Dest	Atm	Mode	dm [kg]	ds [m]	dt [h:m:s]	ct _{tot} [m]	% dm	% ds	% dt	% CT
0	1.0E-05	CYWG	Feb-14	time opt	85,065	6,777,028	7h 10m 9s	2,940,000	0.0000%	0.0000%	0.0000%	0.0%
0	2.0E-05	CYWG	Feb-14	time opt	85,065	6,777,028	7h 10m 9s	2,940,000	0.0000%	0.0000%	0.0000%	0.0%
0	3.0E-05	CYWG	Feb-14	time opt	85,065	6,777,028	7h 10m 9s	2,940,000	0.0000%	0.0000%	0.0000%	0.0%
0	4.0E-05	CYWG	Feb-14	time opt	85,065	6,777,028	7h 10m 9s	2,940,000	0.0000%	0.0000%	0.0000%	0.0%
0	5.0E-05	CYWG	Feb-14	time opt	85,065	6,777,028	7h 10m 9s	2,940,000	0.0000%	0.0000%	0.0000%	0.0%
0	6.0E-05	CYWG	Feb-14	time opt	85,065	6,777,028	7h 10m 9s	2,940,000	0.0000%	0.0000%	0.0000%	0.0%
0	7.0E-05	CYWG	Feb-14	time opt	85,065	6,777,028	7h 10m 9s	2,940,000	0.0000%	0.0000%	0.0000%	0.0%
0	8.0E-05	CYWG	Feb-14	time opt	85,065	6,777,028	7h 10m 9s	2,940,000	0.0000%	0.0000%	0.0000%	0.0%
0	9.0E-05	CYWG	Feb-14	time opt	85,065	6,777,028	7h 10m 9s	2,940,000	0.0000%	0.0000%	0.0000%	0.0%
0	1.0E-04	CYWG	Feb-14	time opt	85,065	6,777,028	7h 10m 9s	2,940,000	0.0000%	0.0000%	0.0000%	0.0%
0	2.0E-04	CYWG	Feb-14	time opt	85,065	6,777,028	7h 10m 9s	2,940,000	0.0000%	0.0000%	0.0000%	0.0%
0	3.0E-04	CYWG	Feb-14	time opt	85,065	6,777,028	7h 10m 9s	2,940,000	0.0000%	0.0000%	0.0000%	0.0%
0	4.0E-04	CYWG	Feb-14	time opt	85,065	6,777,028	7h 10m 9s	2,940,000	0.0000%	0.0000%	0.0000%	0.0%
0	5.0E-04	CYWG	Feb-14	time opt	85,065	6,777,028	7h 10m 9s	2,940,000	0.0000%	0.0000%	0.0000%	0.0%
0	6.0E-04	CYWG	Feb-14	time opt	85,065	6,777,028	7h 10m 9s	2,940,000	0.0000%	0.0000%	0.0000%	0.0%
0	7.0E-04	CYWG	Feb-14	time opt	85,065	6,777,028	7h 10m 9s	2,940,000	0.0000%	0.0000%	0.0000%	0.0%
0	8.0E-04	CYWG	Feb-14	time opt	85,065	6,777,028	7h 10m 9s	2,940,000	0.0000%	0.0000%	0.0000%	0.0%
0	9.0E-04	CYWG	Feb-14	time opt	85,065	6,777,028	7h 10m 9s	2,940,000	0.0000%	0.0000%	0.0000%	0.0%
0	1.0E-03	CYWG	Feb-14	time opt	85,065	6,777,028	7h 10m 9s	2,940,000	0.0000%	0.0000%	0.0000%	0.0%
0	2.0E-03	CYWG	Feb-14	time opt	85,065	6,777,028	7h 10m 9s	2,940,000	0.0000%	0.0000%	0.0000%	0.0%
0	3.0E-03	CYWG	Feb-14	time opt	85,633	6,896,350	7h 20m 42s	1,872,163	0.6680%	1.7607%	2.4530%	-36.3%
0	4.0E-03	CYWG	Feb-14	time opt	85,444	6,897,719	7h 21m 49s	1,610,230	0.4462%	1.7809%	2.7117%	-45.2%
0	5.0E-03	CYWG	Feb-14	time opt	86,298	6,956,116	7h 28m 2s	1,260,014	1.4498%	2.6426%	4.1549%	-57.1%
0	6.0E-03	CYWG	Feb-14	time opt	85,444	6,897,719	7h 21m 49s	1,610,230	0.4462%	1.7809%	2.7117%	-45.2%
0	7.0E-03	CYWG	Feb-14	time opt	86,298	6,956,116	7h 28m 2s	1,260,014	1.4498%	2.6426%	4.1549%	-57.1%
0	8.0E-03	CYWG	Feb-14	time opt	85,444	6,897,719	7h 21m 49s	1,610,230	0.4462%	1.7809%	2.7117%	-45.2%
0	9.0E-03	CYWG	Feb-14	time opt	86,137	6,952,903	7h 27m 52s	1,331,421	1.2601%	2.5952%	4.1157%	-54.7%
0	1.0E-02	CYWG	Feb-14	time opt	85,919	6,955,512	7h 28m 59s	1,126,356	1.0049%	2.6337%	4.3775%	-61.7%
0	2.0E-02	CYWG	Feb-14	time opt	85,854	6,954,151	7h 29m 16s	1,134,769	0.9279%	2.6136%	4.4420%	-61.4%
0	3.0E-02	CYWG	Feb-14	time opt	85,970	6,954,230	7h 28m 60s	1,167,010	1.0639%	2.6147%	4.3801%	-60.3%
0	4.0E-02	CYWG	Feb-14	time opt	85,969	6,954,244	7h 28m 60s	1,167,025	1.0637%	2.6149%	4.3796%	-60.3%
0	5.0E-02	CYWG	Feb-14	time opt	85,900	6,955,668	7h 29m 31s	963,081	0.9816%	2.6360%	4.5026%	-67.2%
0	6.0E-02	CYWG	Feb-14	time opt	85,901	6,955,648	7h 29m 32s	963,060	0.9827%	2.6357%	4.5037%	-67.2%
0	7.0E-02	CYWG	Feb-14	time opt	85,916	6,955,279	7h 29m 42s	962,682	1.0008%	2.6302%	4.5446%	-67.3%
0	8.0E-02	CYWG	Feb-14	time opt	85,886	6,953,624	7h 29m 22s	1,144,023	0.9651%	2.6058%	4.4662%	-61.1%
0	9.0E-02	CYWG	Feb-14	time opt	85,897	6,955,627	7h 29m 33s	958,043	0.9784%	2.6354%	4.5075%	-67.4%
0	1.0E-01	CYWG	Feb-14	time opt	85,901	6,955,660	7h 29m 30s	963,072	0.9834%	2.6358%	4.4982%	-67.2%
0	2.0E-01	CYWG	Feb-14	time opt	85,900	6,955,115	7h 29m 20s	962,532	0.9818%	2.6278%	4.4569%	-67.3%
0	3.0E-01	CYWG	Feb-14	time opt	85,922	6,955,271	7h 29m 33s	962,670	1.0081%	2.6301%	4.5072%	-67.3%
0	4.0E-01	CYWG	Feb-14	time opt	85,916	6,955,279	7h 29m 42s	962,682	1.0008%	2.6302%	4.5446%	-67.3%
0	5.0E-01	CYWG	Feb-14	time opt	85,920	6,955,284	7h 29m 36s	962,684	1.0060%	2.6303%	4.5209%	-67.3%
0	6.0E-01	CYWG	Feb-14	time opt	85,857	6,953,428	7h 28m 56s	1,143,850	0.9314%	2.6029%	4.3665%	-61.1%
0	7.0E-01	CYWG	Feb-14	time opt	85,916	6,955,279	7h 29m 42s	962,682	1.0008%	2.6302%	4.5446%	-67.3%
0	8.0E-01	CYWG	Feb-14	time opt	85,886	6,953,624	7h 29m 22s	1,144,023	0.9651%	2.6058%	4.4662%	-61.1%
0	9.0E-01	CYWG	Feb-14	time opt	85,883	6,953,624	7h 29m 22s	1,139,025	0.9625%	2.6058%	4.4675%	-61.3%
0	1.0E+00	CYWG	Feb-14	time opt	85,906	6,955,617	7h 29m 33s	963,026	0.9895%	2.6352%	4.5089%	-67.2%
0	2.0E+00	CYWG	Feb-14	time opt	85,910	6,955,612	7h 29m 31s	963,018	0.9938%	2.6351%	4.5023%	-67.2%
0	3.0E+00	CYWG	Feb-14	time opt	85,916	6,955,279	7h 29m 42s	962,682	1.0008%	2.6302%	4.5446%	-67.3%
0	4.0E+00	CYWG	Feb-14	time opt	85,916	6,955,279	7h 29m 42s	962,682	1.0008%	2.6302%	4.5446%	-67.3%
0	5.0E+00	CYWG	Feb-14	time opt	85,886	6,953,624	7h 29m 22s	1,144,023	0.9651%	2.6058%	4.4662%	-61.1%
0	6.0E+00	CYWG	Feb-14	time opt	85,905	6,955,618	7h 29m 33s	963,028	0.9874%	2.6352%	4.5075%	-67.2%
0	7.0E+00	CYWG	Feb-14	time opt	85,916	6,955,279	7h 29m 42s	962,682	1.0008%	2.6302%	4.5446%	-67.3%
0	8.0E+00	CYWG	Feb-14	time opt	85,916	6,955,279	7h 29m 42s	962,682	1.0008%	2.6302%	4.5446%	-67.3%
0	9.0E+00	CYWG	Feb-14	time opt	85,886	6,953,624	7h 29m 22s	1,144,023	0.9651%	2.6058%	4.4662%	-61.1%
0	1.0E+01	CYWG	Feb-14	time opt	85,876	6,953,962	7h 29m 13s	1,144,367	0.9538%	2.6108%	4.4306%	-61.1%

C. Numeric results - Altitude profile

β_{grnd}	β_{prof}	Dest	Atm	Mode	dm [kg]	ds [m]	dt [h:m:s]	ct _{tot} [m]	% dm	% ds	% dt	% CT
0	1.0E-05	CYVR	Feb-14	time opt	97,849	7,786,731	8h 12m 9s	2,700,000	0.0000%	0.0000%	0.0000%	0.0%
0	2.0E-05	CYVR	Feb-14	time opt	97,849	7,786,731	8h 12m 9s	2,700,000	0.0000%	0.0000%	0.0000%	0.0%
0	3.0E-05	CYVR	Feb-14	time opt	97,849	7,786,731	8h 12m 9s	2,700,000	0.0000%	0.0000%	0.0000%	0.0%
0	4.0E-05	CYVR	Feb-14	time opt	97,849	7,786,731	8h 12m 9s	2,700,000	0.0000%	0.0000%	0.0000%	0.0%
0	5.0E-05	CYVR	Feb-14	time opt	97,849	7,786,731	8h 12m 9s	2,700,000	0.0000%	0.0000%	0.0000%	0.0%
0	6.0E-05	CYVR	Feb-14	time opt	97,849	7,786,731	8h 12m 9s	2,700,000	0.0000%	0.0000%	0.0000%	0.0%
0	7.0E-05	CYVR	Feb-14	time opt	97,849	7,786,731	8h 12m 9s	2,700,000	0.0000%	0.0000%	0.0000%	0.0%
0	8.0E-05	CYVR	Feb-14	time opt	97,849	7,786,731	8h 12m 9s	2,700,000	0.0000%	0.0000%	0.0000%	0.0%
0	9.0E-05	CYVR	Feb-14	time opt	97,849	7,786,731	8h 12m 9s	2,700,000	0.0000%	0.0000%	0.0000%	0.0%
0	1.0E-04	CYVR	Feb-14	time opt	97,849	7,786,731	8h 12m 9s	2,700,000	0.0000%	0.0000%	0.0000%	0.0%
0	2.0E-04	CYVR	Feb-14	time opt	97,849	7,786,731	8h 12m 9s	2,700,000	0.0000%	0.0000%	0.0000%	0.0%
0	3.0E-04	CYVR	Feb-14	time opt	97,849	7,786,731	8h 12m 9s	2,700,000	0.0000%	0.0000%	0.0000%	0.0%
0	4.0E-04	CYVR	Feb-14	time opt	97,849	7,786,731	8h 12m 9s	2,700,000	0.0000%	0.0000%	0.0000%	0.0%
0	5.0E-04	CYVR	Feb-14	time opt	97,849	7,786,731	8h 12m 9s	2,700,000	0.0000%	0.0000%	0.0000%	0.0%
0	6.0E-04	CYVR	Feb-14	time opt	97,849	7,786,731	8h 12m 9s	2,700,000	0.0000%	0.0000%	0.0000%	0.0%
0	7.0E-04	CYVR	Feb-14	time opt	97,849	7,786,731	8h 12m 9s	2,700,000	0.0000%	0.0000%	0.0000%	0.0%
0	8.0E-04	CYVR	Feb-14	time opt	97,849	7,786,731	8h 12m 9s	2,700,000	0.0000%	0.0000%	0.0000%	0.0%
0	9.0E-04	CYVR	Feb-14	time opt	97,849	7,786,731	8h 12m 9s	2,700,000	0.0000%	0.0000%	0.0000%	0.0%
0	1.0E-03	CYVR	Feb-14	time opt	97,849	7,786,731	8h 12m 9s	2,700,000	0.0000%	0.0000%	0.0000%	0.0%
0	2.0E-03	CYVR	Feb-14	time opt	97,849	7,786,731	8h 12m 9s	2,700,000	0.0000%	0.0000%	0.0000%	0.0%
0	3.0E-03	CYVR	Feb-14	time opt	97,421	7,782,597	8h 12m 23s	1,863,833	-0.4384%	-0.0531%	0.0502%	-31.0%
0	4.0E-03	CYVR	Feb-14	time opt	97,421	7,782,597	8h 12m 23s	1,863,833	-0.4384%	-0.0531%	0.0502%	-31.0%
0	5.0E-03	CYVR	Feb-14	time opt	97,263	7,784,346	8h 14m 17s	1,962,478	-0.5992%	-0.0306%	0.4360%	-27.3%
0	6.0E-03	CYVR	Feb-14	time opt	97,421	7,782,597	8h 12m 23s	1,863,833	-0.4384%	-0.0531%	0.0502%	-31.0%
0	7.0E-03	CYVR	Feb-14	time opt	97,421	7,782,597	8h 12m 23s	1,863,833	-0.4384%	-0.0531%	0.0502%	-31.0%
0	8.0E-03	CYVR	Feb-14	time opt	97,421	7,782,597	8h 12m 23s	1,863,833	-0.4384%	-0.0531%	0.0502%	-31.0%
0	9.0E-03	CYVR	Feb-14	time opt	98,637	7,907,323	8h 21m 38s	1,586,990	0.8052%	1.5487%	1.9268%	-41.2%
0	1.0E-02	CYVR	Feb-14	time opt	97,421	7,782,597	8h 12m 23s	1,863,833	-0.4384%	-0.0531%	0.0502%	-31.0%
0	2.0E-02	CYVR	Feb-14	time opt	98,218	7,904,838	8h 22m 28s	1,386,527	0.3762%	1.5168%	2.0986%	-48.6%
0	3.0E-02	CYVR	Feb-14	time opt	98,204	7,905,600	8h 22m 39s	1,339,311	0.3622%	1.5266%	2.1336%	-50.4%
0	4.0E-02	CYVR	Feb-14	time opt	98,257	7,906,272	8h 22m 38s	1,281,061	0.4165%	1.5352%	2.1297%	-52.6%
0	5.0E-02	CYVR	Feb-14	time opt	98,257	7,906,279	8h 22m 37s	1,281,069	0.4165%	1.5353%	2.1285%	-52.6%
0	6.0E-02	CYVR	Feb-14	time opt	98,278	7,904,706	8h 22m 8s	1,339,170	0.4379%	1.5151%	2.0303%	-50.4%
0	7.0E-02	CYVR	Feb-14	time opt	98,331	7,905,403	8h 22m 6s	1,275,944	0.4925%	1.5240%	2.0217%	-52.7%
0	8.0E-02	CYVR	Feb-14	time opt	98,256	7,906,132	8h 22m 46s	1,280,922	0.4158%	1.5334%	2.1587%	-52.6%
0	9.0E-02	CYVR	Feb-14	time opt	98,256	7,906,129	8h 22m 46s	1,280,919	0.4159%	1.5334%	2.1594%	-52.6%
0	1.0E-01	CYVR	Feb-14	time opt	98,203	7,905,441	8h 22m 49s	1,339,153	0.3615%	1.5245%	2.1674%	-50.4%
0	2.0E-01	CYVR	Feb-14	time opt	98,327	7,905,167	8h 22m 33s	1,275,714	0.4875%	1.5210%	2.1140%	-52.8%
0	3.0E-01	CYVR	Feb-14	time opt	98,206	7,905,393	8h 23m 14s	1,338,966	0.3640%	1.5239%	2.2515%	-50.4%
0	4.0E-01	CYVR	Feb-14	time opt	98,332	7,905,164	8h 22m 33s	1,275,714	0.4934%	1.5210%	2.1130%	-52.8%
0	5.0E-01	CYVR	Feb-14	time opt	98,198	7,905,244	8h 23m 13s	1,338,961	0.3562%	1.5220%	2.2508%	-50.4%
0	6.0E-01	CYVR	Feb-14	time opt	98,253	7,905,916	8h 23m 12s	1,280,713	0.4124%	1.5306%	2.2466%	-52.6%
0	7.0E-01	CYVR	Feb-14	time opt	98,198	7,905,244	8h 23m 13s	1,338,961	0.3562%	1.5220%	2.2508%	-50.4%
0	8.0E-01	CYVR	Feb-14	time opt	98,198	7,905,244	8h 23m 13s	1,338,961	0.3562%	1.5220%	2.2508%	-50.4%
0	9.0E-01	CYVR	Feb-14	time opt	98,198	7,905,244	8h 23m 13s	1,338,961	0.3562%	1.5220%	2.2508%	-50.4%
0	1.0E+00	CYVR	Feb-14	time opt	98,252	7,905,917	8h 23m 12s	1,280,713	0.4115%	1.5306%	2.2467%	-52.6%
0	2.0E+00	CYVR	Feb-14	time opt	98,199	7,905,245	8h 23m 13s	1,338,961	0.3573%	1.5220%	2.2506%	-50.4%
0	3.0E+00	CYVR	Feb-14	time opt	98,327	7,905,167	8h 22m 33s	1,275,714	0.4875%	1.5210%	2.1140%	-52.8%
0	4.0E+00	CYVR	Feb-14	time opt	98,216	7,905,418	8h 23m 13s	1,339,118	0.3746%	1.5242%	2.2509%	-50.4%
0	5.0E+00	CYVR	Feb-14	time opt	98,255	7,905,916	8h 23m 12s	1,280,713	0.4143%	1.5306%	2.2462%	-52.6%
0	6.0E+00	CYVR	Feb-14	time opt	98,181	7,905,221	8h 23m 14s	1,338,961	0.3386%	1.5217%	2.2539%	-50.4%
0	7.0E+00	CYVR	Feb-14	time opt	98,254	7,905,916	8h 23m 12s	1,280,713	0.4134%	1.5306%	2.2464%	-52.6%
0	8.0E+00	CYVR	Feb-14	time opt	98,153	7,904,924	8h 23m 15s	1,338,961	0.3098%	1.5179%	2.2558%	-50.4%
0	9.0E+00	CYVR	Feb-14	time opt	98,200	7,905,675	8h 23m 15s	1,280,665	0.3579%	1.5275%	2.2553%	-52.6%
0	1.0E+01	CYVR	Feb-14	time opt	98,192	7,905,524	8h 23m 14s	1,280,659	0.3500%	1.5256%	2.2545%	-52.6%

β_{grnd}	β_{prof}	Dest	Atm	Mode	dm [kg]	ds [m]	dt [h:m:s]	ct _{tot} [m]	% dm	% ds	% dt	% CT
0	1.0E-05	KIAD	Feb-17	time opt	72,513	5,922,568	6h 8m 16s	1,975,000	0.0000%	0.0000%	0.0000%	0.0%
0	2.0E-05	KIAD	Feb-17	time opt	72,513	5,922,568	6h 8m 16s	1,975,000	0.0000%	0.0000%	0.0000%	0.0%
0	3.0E-05	KIAD	Feb-17	time opt	72,513	5,922,568	6h 8m 16s	1,975,000	0.0000%	0.0000%	0.0000%	0.0%
0	4.0E-05	KIAD	Feb-17	time opt	72,513	5,922,568	6h 8m 16s	1,975,000	0.0000%	0.0000%	0.0000%	0.0%
0	5.0E-05	KIAD	Feb-17	time opt	72,513	5,922,568	6h 8m 16s	1,975,000	0.0000%	0.0000%	0.0000%	0.0%
0	6.0E-05	KIAD	Feb-17	time opt	72,513	5,922,568	6h 8m 16s	1,975,000	0.0000%	0.0000%	0.0000%	0.0%
0	7.0E-05	KIAD	Feb-17	time opt	72,513	5,922,568	6h 8m 16s	1,975,000	0.0000%	0.0000%	0.0000%	0.0%
0	8.0E-05	KIAD	Feb-17	time opt	72,513	5,922,568	6h 8m 16s	1,975,000	0.0000%	0.0000%	0.0000%	0.0%
0	9.0E-05	KIAD	Feb-17	time opt	72,513	5,922,568	6h 8m 16s	1,975,000	0.0000%	0.0000%	0.0000%	0.0%
0	1.0E-04	KIAD	Feb-17	time opt	72,513	5,922,568	6h 8m 16s	1,975,000	0.0000%	0.0000%	0.0000%	0.0%
0	2.0E-04	KIAD	Feb-17	time opt	72,513	5,922,568	6h 8m 16s	1,975,000	0.0000%	0.0000%	0.0000%	0.0%
0	3.0E-04	KIAD	Feb-17	time opt	72,513	5,922,568	6h 8m 16s	1,975,000	0.0000%	0.0000%	0.0000%	0.0%
0	4.0E-04	KIAD	Feb-17	time opt	71,842	5,922,568	6h 9m 42s	670,000	-0.9255%	0.0000%	0.3915%	-66.1%
0	5.0E-04	KIAD	Feb-17	time opt	71,842	5,922,568	6h 9m 42s	670,000	-0.9255%	0.0000%	0.3915%	-66.1%
0	6.0E-04	KIAD	Feb-17	time opt	71,842	5,922,568	6h 9m 42s	670,000	-0.9255%	0.0000%	0.3915%	-66.1%
0	7.0E-04	KIAD	Feb-17	time opt	71,840	5,922,568	6h 9m 43s	670,000	-0.9289%	0.0000%	0.3929%	-66.1%
0	8.0E-04	KIAD	Feb-17	time opt	71,840	5,922,568	6h 9m 43s	670,000	-0.9289%	0.0000%	0.3929%	-66.1%
0	9.0E-04	KIAD	Feb-17	time opt	71,842	5,922,568	6h 9m 42s	670,000	-0.9255%	0.0000%	0.3915%	-66.1%
0	1.0E-03	KIAD	Feb-17	time opt	71,840	5,922,568	6h 9m 43s	670,000	-0.9289%	0.0000%	0.3929%	-66.1%
0	2.0E-03	KIAD	Feb-17	time opt	71,842	5,922,568	6h 9m 42s	670,000	-0.9255%	0.0000%	0.3915%	-66.1%
0	3.0E-03	KIAD	Feb-17	time opt	71,840	5,922,568	6h 9m 43s	670,000	-0.9289%	0.0000%	0.3929%	-66.1%
0	4.0E-03	KIAD	Feb-17	time opt	71,842	5,922,568	6h 9m 42s	670,000	-0.9255%	0.0000%	0.3915%	-66.1%
0	5.0E-03	KIAD	Feb-17	time opt	71,842	5,922,568	6h 9m 42s	670,000	-0.9255%	0.0000%	0.3915%	-66.1%
0	6.0E-03	KIAD	Feb-17	time opt	71,842	5,922,568	6h 9m 42s	670,000	-0.9255%	0.0000%	0.3915%	-66.1%
0	7.0E-03	KIAD	Feb-17	time opt	71,638	5,922,568	6h 10m 8s	437,203	-1.2067%	0.0000%	0.5069%	-77.9%
0	8.0E-03	KIAD	Feb-17	time opt	71,641	5,922,568	6h 10m 7s	437,203	-1.2033%	0.0000%	0.5054%	-77.9%
0	9.0E-03	KIAD	Feb-17	time opt	71,641	5,922,568	6h 10m 7s	437,203	-1.2033%	0.0000%	0.5054%	-77.9%
0	1.0E-02	KIAD	Feb-17	time opt	71,641	5,922,568	6h 10m 7s	437,203	-1.2033%	0.0000%	0.5054%	-77.9%
0	2.0E-02	KIAD	Feb-17	time opt	71,561	5,922,568	6h 10m 20s	255,809	-1.3132%	0.0000%	0.5622%	-87.0%
0	3.0E-02	KIAD	Feb-17	time opt	71,620	5,922,568	6h 10m 12s	309,723	-1.2319%	0.0000%	0.5269%	-84.3%
0	4.0E-02	KIAD	Feb-17	time opt	71,580	5,922,568	6h 10m 15s	132,203	-1.2870%	0.0000%	0.5380%	-93.3%
0	5.0E-02	KIAD	Feb-17	time opt	71,561	5,922,568	6h 10m 20s	255,809	-1.3132%	0.0000%	0.5622%	-87.0%
0	6.0E-02	KIAD	Feb-17	time opt	71,622	5,922,568	6h 10m 12s	314,727	-1.2289%	0.0000%	0.5253%	-84.1%
0	7.0E-02	KIAD	Feb-17	time opt	71,620	5,922,568	6h 10m 12s	309,723	-1.2319%	0.0000%	0.5269%	-84.3%
0	8.0E-02	KIAD	Feb-17	time opt	71,622	5,922,568	6h 10m 12s	314,727	-1.2289%	0.0000%	0.5253%	-84.1%
0	9.0E-02	KIAD	Feb-17	time opt	71,561	5,922,568	6h 10m 20s	255,809	-1.3132%	0.0000%	0.5622%	-87.0%
0	1.0E-01	KIAD	Feb-17	time opt	71,622	5,922,568	6h 10m 12s	314,727	-1.2289%	0.0000%	0.5253%	-84.1%
0	2.0E-01	KIAD	Feb-17	time opt	71,561	5,922,568	6h 10m 20s	255,809	-1.3132%	0.0000%	0.5622%	-87.0%
0	3.0E-01	KIAD	Feb-17	time opt	71,559	5,922,568	6h 10m 20s	250,807	-1.3167%	0.0000%	0.5636%	-87.3%
0	4.0E-01	KIAD	Feb-17	time opt	71,625	5,922,568	6h 10m 11s	314,723	-1.2258%	0.0000%	0.5205%	-84.1%
0	5.0E-01	KIAD	Feb-17	time opt	71,561	5,922,568	6h 10m 20s	255,809	-1.3132%	0.0000%	0.5622%	-87.0%
0	6.0E-01	KIAD	Feb-17	time opt	71,625	5,922,568	6h 10m 11s	314,723	-1.2254%	0.0000%	0.5198%	-84.1%
0	7.0E-01	KIAD	Feb-17	time opt	71,625	5,922,568	6h 10m 11s	314,723	-1.2254%	0.0000%	0.5198%	-84.1%
0	8.0E-01	KIAD	Feb-17	time opt	71,622	5,922,568	6h 10m 12s	255,857	-1.2295%	0.0000%	0.5261%	-87.0%
0	9.0E-01	KIAD	Feb-17	time opt	71,623	5,922,568	6h 10m 11s	309,718	-1.2284%	0.0000%	0.5213%	-84.3%
0	1.0E+00	KIAD	Feb-17	time opt	71,561	5,922,568	6h 10m 20s	255,809	-1.3132%	0.0000%	0.5622%	-87.0%
0	2.0E+00	KIAD	Feb-17	time opt	71,559	5,922,568	6h 10m 20s	255,809	-1.3165%	0.0000%	0.5637%	-87.0%
0	3.0E+00	KIAD	Feb-17	time opt	71,561	5,922,568	6h 10m 20s	255,809	-1.3132%	0.0000%	0.5622%	-87.0%
0	4.0E+00	KIAD	Feb-17	time opt	71,561	5,922,568	6h 10m 20s	255,809	-1.3132%	0.0000%	0.5622%	-87.0%
0	5.0E+00	KIAD	Feb-17	time opt	71,561	5,922,568	6h 10m 20s	255,809	-1.3132%	0.0000%	0.5622%	-87.0%
0	6.0E+00	KIAD	Feb-17	time opt	71,561	5,922,568	6h 10m 20s	255,809	-1.3132%	0.0000%	0.5622%	-87.0%
0	7.0E+00	KIAD	Feb-17	time opt	71,561	5,922,568	6h 10m 20s	255,809	-1.3132%	0.0000%	0.5622%	-87.0%
0	8.0E+00	KIAD	Feb-17	time opt	71,625	5,922,568	6h 10m 11s	314,723	-1.2254%	0.0000%	0.5198%	-84.1%
0	9.0E+00	KIAD	Feb-17	time opt	71,561	5,922,568	6h 10m 20s	255,809	-1.3132%	0.0000%	0.5622%	-87.0%
0	1.0E+01	KIAD	Feb-17	time opt	71,580	5,922,568	6h 10m 15s	132,203	-1.2870%	0.0000%	0.5380%	-93.3%

β_{grnd}	β_{prof}	Dest	Atm	Mode	dm [kg]	ds [m]	dt [h:m:s]	ct _{tot} [m]	% dm	% ds	% dt	% CT
0	1.0E-05	CYVR	Feb-17	time opt	95,609	7,725,148	8h 1m 8s	1,395,000	0.0000%	0.0000%	0.0000%	0.0%
0	2.0E-05	CYVR	Feb-17	time opt	95,609	7,725,148	8h 1m 8s	1,395,000	0.0000%	0.0000%	0.0000%	0.0%
0	3.0E-05	CYVR	Feb-17	time opt	95,609	7,725,148	8h 1m 8s	1,395,000	0.0000%	0.0000%	0.0000%	0.0%
0	4.0E-05	CYVR	Feb-17	time opt	95,609	7,725,148	8h 1m 8s	1,395,000	0.0000%	0.0000%	0.0000%	0.0%
0	5.0E-05	CYVR	Feb-17	time opt	95,609	7,725,148	8h 1m 8s	1,395,000	0.0000%	0.0000%	0.0000%	0.0%
0	6.0E-05	CYVR	Feb-17	time opt	95,609	7,725,148	8h 1m 8s	1,395,000	0.0000%	0.0000%	0.0000%	0.0%
0	7.0E-05	CYVR	Feb-17	time opt	95,609	7,725,148	8h 1m 8s	1,395,000	0.0000%	0.0000%	0.0000%	0.0%
0	8.0E-05	CYVR	Feb-17	time opt	95,609	7,725,148	8h 1m 8s	1,395,000	0.0000%	0.0000%	0.0000%	0.0%
0	9.0E-05	CYVR	Feb-17	time opt	95,609	7,725,148	8h 1m 8s	1,395,000	0.0000%	0.0000%	0.0000%	0.0%
0	1.0E-04	CYVR	Feb-17	time opt	95,609	7,725,148	8h 1m 8s	1,395,000	0.0000%	0.0000%	0.0000%	0.0%
0	2.0E-04	CYVR	Feb-17	time opt	95,609	7,725,148	8h 1m 8s	1,395,000	0.0000%	0.0000%	0.0000%	0.0%
0	3.0E-04	CYVR	Feb-17	time opt	95,609	7,725,148	8h 1m 8s	1,395,000	0.0000%	0.0000%	0.0000%	0.0%
0	4.0E-04	CYVR	Feb-17	time opt	95,609	7,725,148	8h 1m 8s	1,395,000	0.0000%	0.0000%	0.0000%	0.0%
0	5.0E-04	CYVR	Feb-17	time opt	95,609	7,725,148	8h 1m 8s	1,395,000	0.0000%	0.0000%	0.0000%	0.0%
0	6.0E-04	CYVR	Feb-17	time opt	95,609	7,725,148	8h 1m 8s	1,395,000	0.0000%	0.0000%	0.0000%	0.0%
0	7.0E-04	CYVR	Feb-17	time opt	95,609	7,725,148	8h 1m 8s	1,395,000	0.0000%	0.0000%	0.0000%	0.0%
0	8.0E-04	CYVR	Feb-17	time opt	95,609	7,725,148	8h 1m 8s	1,395,000	0.0000%	0.0000%	0.0000%	0.0%
0	9.0E-04	CYVR	Feb-17	time opt	95,609	7,725,148	8h 1m 8s	1,395,000	0.0000%	0.0000%	0.0000%	0.0%
0	1.0E-03	CYVR	Feb-17	time opt	95,609	7,725,148	8h 1m 8s	1,395,000	0.0000%	0.0000%	0.0000%	0.0%
0	2.0E-03	CYVR	Feb-17	time opt	95,276	7,725,148	8h 1m 47s	918,194	-0.3476%	0.0000%	0.1359%	-34.2%
0	3.0E-03	CYVR	Feb-17	time opt	95,276	7,725,148	8h 1m 47s	918,194	-0.3476%	0.0000%	0.1359%	-34.2%
0	4.0E-03	CYVR	Feb-17	time opt	95,276	7,725,148	8h 1m 47s	918,194	-0.3476%	0.0000%	0.1359%	-34.2%
0	5.0E-03	CYVR	Feb-17	time opt	95,276	7,725,148	8h 1m 47s	918,194	-0.3476%	0.0000%	0.1359%	-34.2%
0	6.0E-03	CYVR	Feb-17	time opt	95,276	7,725,148	8h 1m 47s	918,194	-0.3476%	0.0000%	0.1359%	-34.2%
0	7.0E-03	CYVR	Feb-17	time opt	95,128	7,725,148	8h 2m 2s	565,000	-0.5026%	0.0000%	0.1879%	-59.5%
0	8.0E-03	CYVR	Feb-17	time opt	95,128	7,725,148	8h 2m 2s	565,000	-0.5026%	0.0000%	0.1879%	-59.5%
0	9.0E-03	CYVR	Feb-17	time opt	95,128	7,725,148	8h 2m 2s	565,000	-0.5026%	0.0000%	0.1879%	-59.5%
0	1.0E-02	CYVR	Feb-17	time opt	95,128	7,725,148	8h 2m 2s	565,000	-0.5026%	0.0000%	0.1879%	-59.5%
0	2.0E-02	CYVR	Feb-17	time opt	94,939	7,725,148	8h 3m 24s	475,000	-0.7008%	0.0000%	0.4726%	-65.9%
0	3.0E-02	CYVR	Feb-17	time opt	94,680	7,725,148	8h 4m 16s	298,441	-0.9715%	0.0000%	0.6521%	-78.6%
0	4.0E-02	CYVR	Feb-17	time opt	94,680	7,725,148	8h 4m 16s	298,441	-0.9715%	0.0000%	0.6521%	-78.6%
0	5.0E-02	CYVR	Feb-17	time opt	94,786	7,725,148	8h 3m 3s	366,637	-0.8602%	0.0000%	0.3987%	-73.7%
0	6.0E-02	CYVR	Feb-17	time opt	94,680	7,725,148	8h 4m 16s	298,441	-0.9714%	0.0000%	0.6521%	-78.6%
0	7.0E-02	CYVR	Feb-17	time opt	94,692	7,725,148	8h 4m 9s	298,440	-0.9589%	0.0000%	0.6288%	-78.6%
0	8.0E-02	CYVR	Feb-17	time opt	94,680	7,725,148	8h 4m 16s	298,441	-0.9714%	0.0000%	0.6521%	-78.6%
0	9.0E-02	CYVR	Feb-17	time opt	94,633	7,725,148	8h 4m 57s	298,441	-1.0205%	0.0000%	0.7919%	-78.6%
0	1.0E-01	CYVR	Feb-17	time opt	94,818	7,725,148	8h 2m 56s	366,713	-0.8276%	0.0000%	0.3732%	-73.7%
0	2.0E-01	CYVR	Feb-17	time opt	94,786	7,725,148	8h 3m 3s	366,637	-0.8602%	0.0000%	0.3987%	-73.7%
0	3.0E-01	CYVR	Feb-17	time opt	94,680	7,725,148	8h 4m 16s	298,441	-0.9715%	0.0000%	0.6521%	-78.6%
0	4.0E-01	CYVR	Feb-17	time opt	94,680	7,725,148	8h 4m 16s	298,441	-0.9714%	0.0000%	0.6521%	-78.6%
0	5.0E-01	CYVR	Feb-17	time opt	94,645	7,725,148	8h 4m 25s	296,387	-1.0083%	0.0000%	0.6823%	-78.8%
0	6.0E-01	CYVR	Feb-17	time opt	94,818	7,725,148	8h 2m 56s	366,713	-0.8276%	0.0000%	0.3732%	-73.7%
0	7.0E-01	CYVR	Feb-17	time opt	94,645	7,725,148	8h 4m 25s	296,387	-1.0083%	0.0000%	0.6823%	-78.8%
0	8.0E-01	CYVR	Feb-17	time opt	94,646	7,725,148	8h 4m 25s	296,385	-1.0075%	0.0000%	0.6828%	-78.8%
0	9.0E-01	CYVR	Feb-17	time opt	94,692	7,725,148	8h 4m 9s	298,440	-0.9590%	0.0000%	0.6288%	-78.6%
0	1.0E+00	CYVR	Feb-17	time opt	94,753	7,725,148	8h 3m 12s	364,583	-0.8953%	0.0000%	0.4300%	-73.9%
0	2.0E+00	CYVR	Feb-17	time opt	94,754	7,725,148	8h 3m 12s	364,583	-0.8945%	0.0000%	0.4306%	-73.9%
0	3.0E+00	CYVR	Feb-17	time opt	94,692	7,725,148	8h 4m 9s	298,440	-0.9590%	0.0000%	0.6288%	-78.6%
0	4.0E+00	CYVR	Feb-17	time opt	94,692	7,725,148	8h 4m 9s	298,440	-0.9590%	0.0000%	0.6288%	-78.6%
0	5.0E+00	CYVR	Feb-17	time opt	94,646	7,725,148	8h 4m 25s	296,384	-1.0067%	0.0000%	0.6834%	-78.8%
0	6.0E+00	CYVR	Feb-17	time opt	94,753	7,725,148	8h 3m 12s	364,583	-0.8953%	0.0000%	0.4300%	-73.9%
0	7.0E+00	CYVR	Feb-17	time opt	94,649	7,725,148	8h 4m 26s	296,384	-1.0043%	0.0000%	0.6851%	-78.8%
0	8.0E+00	CYVR	Feb-17	time opt	94,704	7,725,148	8h 4m 22s	296,384	-0.9465%	0.0000%	0.6728%	-78.8%
0	9.0E+00	CYVR	Feb-17	time opt	94,649	7,725,148	8h 4m 26s	296,384	-1.0042%	0.0000%	0.6850%	-78.8%
0	1.0E+01	CYVR	Feb-17	time opt	94,649	7,725,148	8h 4m 26s	296,384	-1.0042%	0.0000%	0.6850%	-78.8%

APPENDIX D

NUMERIC RESULTS - HYBRID MITIGATION

β_{grnd}	β_{prof}	Dest	Atm	Mode	dm [kg]	ds [m]	dt [h:m:s]	ct _{tot} [m]	% dm	% ds	% dt	% CT
0	0	KIAD	Feb-14	fuel opt	70,435	6,264,467	7h 0m 9s	654,729	0.0000%	0.0000%	0.0000%	0.0%
0	0.0001	KIAD	Feb-14	fuel opt	70,435	6,264,467	7h 0m 9s	654,729	0.0000%	0.0000%	0.0000%	0.0%
0	0.001	KIAD	Feb-14	fuel opt	70,449	6,264,467	7h 0m 9s	394,785	0.0197%	0.0000%	0.0021%	-39.7%
0	0.01	KIAD	Feb-14	fuel opt	70,770	6,291,059	7h 1m 56s	124,886	0.4759%	0.4245%	0.4247%	-80.9%
0	0.1	KIAD	Feb-14	fuel opt	70,770	6,291,059	7h 1m 56s	124,886	0.4759%	0.4245%	0.4247%	-80.9%
0	1	KIAD	Feb-14	fuel opt	70,770	6,291,059	7h 1m 56s	124,886	0.4759%	0.4245%	0.4247%	-80.9%
0	10	KIAD	Feb-14	fuel opt	70,770	6,291,059	7h 1m 56s	124,886	0.4759%	0.4245%	0.4247%	-80.9%
0.01	0	KIAD	Feb-14	fuel opt	70,569	6,265,300	7h 0m 51s	486,194	0.1908%	0.0133%	0.1661%	-25.7%
0.01	0.0001	KIAD	Feb-14	fuel opt	70,567	6,265,300	7h 0m 51s	485,179	0.1872%	0.0133%	0.1662%	-25.9%
0.01	0.001	KIAD	Feb-14	fuel opt	70,574	6,265,300	7h 0m 51s	250,000	0.1980%	0.0133%	0.1680%	-61.8%
0.01	0.01	KIAD	Feb-14	fuel opt	70,946	6,296,725	7h 2m 57s	0	0.7254%	0.5149%	0.6671%	-100.0%
0.01	0.1	KIAD	Feb-14	fuel opt	70,946	6,296,724	7h 2m 57s	0	0.7262%	0.5149%	0.6671%	-100.0%
0.01	1	KIAD	Feb-14	fuel opt	70,946	6,296,725	7h 2m 57s	0	0.7254%	0.5149%	0.6671%	-100.0%
0.01	10	KIAD	Feb-14	fuel opt	70,946	6,296,725	7h 2m 57s	0	0.7254%	0.5149%	0.6671%	-100.0%
0.03	0	KIAD	Feb-14	fuel opt	70,569	6,265,300	7h 0m 51s	486,194	0.1908%	0.0133%	0.1661%	-25.7%
0.03	0.0001	KIAD	Feb-14	fuel opt	70,567	6,265,300	7h 0m 51s	485,179	0.1872%	0.0133%	0.1662%	-25.9%
0.03	0.001	KIAD	Feb-14	fuel opt	70,574	6,265,300	7h 0m 51s	250,000	0.1980%	0.0133%	0.1680%	-61.8%
0.03	0.01	KIAD	Feb-14	fuel opt	70,946	6,296,725	7h 2m 57s	0	0.7254%	0.5149%	0.6671%	-100.0%
0.03	0.1	KIAD	Feb-14	fuel opt	70,947	6,296,723	7h 2m 57s	0	0.7268%	0.5149%	0.6671%	-100.0%
0.03	1	KIAD	Feb-14	fuel opt	70,946	6,296,725	7h 2m 57s	0	0.7254%	0.5149%	0.6671%	-100.0%
0.03	10	KIAD	Feb-14	fuel opt	70,946	6,296,725	7h 2m 57s	0	0.7256%	0.5149%	0.6671%	-100.0%
0.1	0	KIAD	Feb-14	fuel opt	70,569	6,265,300	7h 0m 51s	486,194	0.1908%	0.0133%	0.1661%	-25.7%
0.1	0.0001	KIAD	Feb-14	fuel opt	70,567	6,265,300	7h 0m 51s	485,179	0.1872%	0.0133%	0.1662%	-25.9%
0.1	0.001	KIAD	Feb-14	fuel opt	70,574	6,265,300	7h 0m 51s	250,000	0.1980%	0.0133%	0.1680%	-61.8%
0.1	0.01	KIAD	Feb-14	fuel opt	70,946	6,296,725	7h 2m 57s	0	0.7256%	0.5149%	0.6671%	-100.0%
0.1	0.1	KIAD	Feb-14	fuel opt	70,947	6,296,723	7h 2m 57s	0	0.7268%	0.5149%	0.6671%	-100.0%
0.1	1	KIAD	Feb-14	fuel opt	70,946	6,296,725	7h 2m 57s	0	0.7256%	0.5149%	0.6671%	-100.0%
0.1	10	KIAD	Feb-14	fuel opt	70,946	6,296,725	7h 2m 57s	0	0.7256%	0.5149%	0.6671%	-100.0%
0.3	0	KIAD	Feb-14	fuel opt	70,588	6,266,822	7h 0m 57s	475,194	0.2171%	0.0376%	0.1908%	-27.4%
0.3	0.0001	KIAD	Feb-14	fuel opt	70,585	6,266,822	7h 0m 57s	475,179	0.2135%	0.0376%	0.1909%	-27.4%
0.3	0.001	KIAD	Feb-14	fuel opt	70,592	6,266,822	7h 0m 58s	250,000	0.2235%	0.0376%	0.1928%	-61.8%
0.3	0.01	KIAD	Feb-14	fuel opt	70,826	6,286,559	7h 2m 16s	0	0.5546%	0.3527%	0.5060%	-100.0%
0.3	0.1	KIAD	Feb-14	fuel opt	70,826	6,286,559	7h 2m 16s	0	0.5546%	0.3527%	0.5060%	-100.0%
0.3	1	KIAD	Feb-14	fuel opt	70,826	6,286,559	7h 2m 16s	0	0.5546%	0.3527%	0.5060%	-100.0%
0.3	10	KIAD	Feb-14	fuel opt	70,826	6,286,566	7h 2m 16s	0	0.5551%	0.3528%	0.5061%	-100.0%
1	0	KIAD	Feb-14	fuel opt	73,175	6,465,484	7h 15m 32s	119,895	3.8897%	3.2088%	3.6633%	-81.7%
1	0.0001	KIAD	Feb-14	fuel opt	73,178	6,465,484	7h 15m 32s	0	3.8944%	3.2088%	3.6631%	-100.0%
1	0.001	KIAD	Feb-14	fuel opt	73,172	6,465,484	7h 15m 32s	119,896	3.8859%	3.2088%	3.6633%	-81.7%
1	0.01	KIAD	Feb-14	fuel opt	73,178	6,465,484	7h 15m 32s	0	3.8944%	3.2088%	3.6631%	-100.0%
1	0.1	KIAD	Feb-14	fuel opt	73,178	6,465,484	7h 15m 32s	0	3.8944%	3.2088%	3.6631%	-100.0%
1	1	KIAD	Feb-14	fuel opt	73,178	6,465,484	7h 15m 32s	0	3.8944%	3.2088%	3.6631%	-100.0%
1	10	KIAD	Feb-14	fuel opt	73,178	6,465,484	7h 15m 32s	0	3.8944%	3.2088%	3.6631%	-100.0%
3	0	KIAD	Feb-14	fuel opt	73,229	6,471,104	7h 15m 51s	119,896	3.9667%	3.2986%	3.7354%	-81.7%
3	0.0001	KIAD	Feb-14	fuel opt	73,232	6,471,104	7h 15m 51s	0	3.9715%	3.2986%	3.7352%	-100.0%
3	0.001	KIAD	Feb-14	fuel opt	73,226	6,471,104	7h 15m 51s	119,897	3.9630%	3.2986%	3.7355%	-81.7%
3	0.01	KIAD	Feb-14	fuel opt	73,232	6,471,104	7h 15m 51s	0	3.9715%	3.2986%	3.7352%	-100.0%
3	0.1	KIAD	Feb-14	fuel opt	73,232	6,471,104	7h 15m 51s	0	3.9715%	3.2986%	3.7352%	-100.0%
3	1	KIAD	Feb-14	fuel opt	73,232	6,471,104	7h 15m 51s	0	3.9715%	3.2986%	3.7352%	-100.0%
3	10	KIAD	Feb-14	fuel opt	73,232	6,471,104	7h 15m 51s	0	3.9715%	3.2986%	3.7352%	-100.0%
10	0	KIAD	Feb-14	fuel opt	73,229	6,471,104	7h 15m 51s	119,896	3.9667%	3.2986%	3.7354%	-81.7%
10	0.0001	KIAD	Feb-14	fuel opt	73,232	6,471,104	7h 15m 51s	0	3.9715%	3.2986%	3.7352%	-100.0%
10	0.001	KIAD	Feb-14	fuel opt	73,226	6,471,104	7h 15m 51s	119,897	3.9630%	3.2986%	3.7355%	-81.7%
10	0.01	KIAD	Feb-14	fuel opt	73,232	6,471,104	7h 15m 51s	0	3.9715%	3.2986%	3.7352%	-100.0%
10	0.1	KIAD	Feb-14	fuel opt	73,232	6,471,104	7h 15m 51s	0	3.9715%	3.2986%	3.7352%	-100.0%
10	1	KIAD	Feb-14	fuel opt	73,232	6,471,104	7h 15m 51s	0	3.9715%	3.2986%	3.7352%	-100.0%
10	10	KIAD	Feb-14	fuel opt	73,232	6,471,104	7h 15m 51s	0	3.9715%	3.2986%	3.7352%	-100.0%

D. Numeric results - Hybrid mitigation

β_{grnd}	β_{prof}	Dest	Atm	Mode	dm [kg]	ds [m]	dt [h:m:s]	ct _{tot} [m]	% dm	% ds	% dt	% CT
0	0	CYWG	Feb-14	fuel opt	77,564	6,839,002	7h 40m 39s	2,238,395	0.0000%	0.0000%	0.0000%	0.0%
0	0.0001	CYWG	Feb-14	fuel opt	77,577	6,839,034	7h 40m 39s	2,078,679	0.0173%	0.0005%	0.0011%	-7.1%
0	0.001	CYWG	Feb-14	fuel opt	77,554	6,836,666	7h 40m 30s	1,888,730	-0.0124%	-0.0341%	-0.0326%	-15.6%
0	0.01	CYWG	Feb-14	fuel opt	76,931	6,778,405	7h 36m 37s	1,471,199	-0.8166%	-0.8860%	-0.8753%	-34.3%
0	0.1	CYWG	Feb-14	fuel opt	77,790	6,842,879	7h 40m 55s	1,428,213	0.2919%	0.0567%	0.0582%	-36.2%
0	1	CYWG	Feb-14	fuel opt	76,976	6,772,219	7h 36m 13s	1,303,692	-0.7578%	-0.9765%	-0.9637%	-41.8%
0	10	CYWG	Feb-14	fuel opt	77,861	6,840,601	7h 40m 45s	1,147,467	0.3833%	0.0234%	0.0233%	-48.7%
0.01	0	CYWG	Feb-14	fuel opt	77,555	6,837,999	7h 40m 35s	2,348,628	-0.0113%	-0.0147%	-0.0139%	4.9%
0.01	0.0001	CYWG	Feb-14	fuel opt	77,578	6,839,076	7h 40m 39s	2,078,721	0.0182%	0.0011%	0.0015%	-7.1%
0.01	0.001	CYWG	Feb-14	fuel opt	77,554	6,836,671	7h 40m 30s	1,883,734	-0.0124%	-0.0341%	-0.0325%	-15.8%
0.01	0.01	CYWG	Feb-14	fuel opt	76,996	6,782,891	7h 36m 55s	1,350,633	-0.7322%	-0.8205%	-0.8091%	-39.7%
0.01	0.1	CYWG	Feb-14	fuel opt	76,980	6,777,731	7h 36m 35s	1,281,565	-0.7533%	-0.8959%	-0.8845%	-42.7%
0.01	1	CYWG	Feb-14	fuel opt	77,808	6,843,368	7h 40m 57s	1,303,685	0.3148%	0.0638%	0.0651%	-41.8%
0.01	10	CYWG	Feb-14	fuel opt	77,862	6,840,601	7h 40m 45s	1,152,469	0.3846%	0.0234%	0.0233%	-48.5%
0.03	0	CYWG	Feb-14	fuel opt	76,602	6,771,409	7h 35m 25s	1,325,949	-1.2399%	-0.9883%	-1.1352%	-40.8%
0.03	0.0001	CYWG	Feb-14	fuel opt	76,606	6,771,409	7h 35m 25s	1,215,000	-1.2355%	-0.9883%	-1.1358%	-45.7%
0.03	0.001	CYWG	Feb-14	fuel opt	76,611	6,771,409	7h 35m 25s	1,212,380	-1.2294%	-0.9883%	-1.1354%	-45.8%
0.03	0.01	CYWG	Feb-14	fuel opt	76,617	6,771,409	7h 35m 25s	1,092,432	-1.2209%	-0.9883%	-1.1357%	-51.2%
0.03	0.1	CYWG	Feb-14	fuel opt	76,640	6,771,409	7h 35m 25s	890,709	-1.1918%	-0.9883%	-1.1353%	-60.2%
0.03	1	CYWG	Feb-14	fuel opt	76,643	6,771,409	7h 35m 26s	1,012,843	-1.1874%	-0.9883%	-1.1338%	-54.8%
0.03	10	CYWG	Feb-14	fuel opt	76,643	6,771,409	7h 35m 26s	1,012,856	-1.1871%	-0.9883%	-1.1342%	-54.8%
0.1	0	CYWG	Feb-14	fuel opt	76,602	6,771,409	7h 35m 25s	1,325,949	-1.2399%	-0.9883%	-1.1352%	-40.8%
0.1	0.0001	CYWG	Feb-14	fuel opt	76,606	6,771,409	7h 35m 25s	1,215,000	-1.2355%	-0.9883%	-1.1358%	-45.7%
0.1	0.001	CYWG	Feb-14	fuel opt	76,614	6,771,409	7h 35m 25s	1,212,379	-1.2243%	-0.9883%	-1.1360%	-45.8%
0.1	0.01	CYWG	Feb-14	fuel opt	76,621	6,771,409	7h 35m 25s	1,092,430	-1.2160%	-0.9883%	-1.1362%	-51.2%
0.1	0.1	CYWG	Feb-14	fuel opt	76,641	6,771,409	7h 35m 26s	1,012,860	-1.1902%	-0.9883%	-1.1337%	-54.8%
0.1	1	CYWG	Feb-14	fuel opt	76,641	6,771,409	7h 35m 25s	890,713	-1.1905%	-0.9883%	-1.1352%	-60.2%
0.1	10	CYWG	Feb-14	fuel opt	76,642	6,771,409	7h 35m 26s	1,012,857	-1.1891%	-0.9883%	-1.1338%	-54.8%
0.3	0	CYWG	Feb-14	fuel opt	76,650	6,776,869	7h 35m 41s	1,277,949	-1.1788%	-0.9085%	-1.0781%	-42.9%
0.3	0.0001	CYWG	Feb-14	fuel opt	76,647	6,776,869	7h 35m 41s	1,289,951	-1.1827%	-0.9085%	-1.0785%	-42.4%
0.3	0.001	CYWG	Feb-14	fuel opt	76,663	6,776,869	7h 35m 41s	1,042,482	-1.1610%	-0.9085%	-1.0790%	-53.4%
0.3	0.01	CYWG	Feb-14	fuel opt	76,665	6,776,869	7h 35m 41s	1,042,494	-1.1588%	-0.9085%	-1.0793%	-53.4%
0.3	0.1	CYWG	Feb-14	fuel opt	76,683	6,776,869	7h 35m 41s	968,113	-1.1356%	-0.9085%	-1.0766%	-56.7%
0.3	1	CYWG	Feb-14	fuel opt	76,694	6,776,869	7h 35m 41s	956,930	-1.1223%	-0.9085%	-1.0767%	-57.2%
0.3	10	CYWG	Feb-14	fuel opt	76,690	6,776,869	7h 35m 42s	956,895	-1.1272%	-0.9085%	-1.0764%	-57.3%
1	0	CYWG	Feb-14	fuel opt	86,356	7,583,977	8h 29m 34s	203,601	11.3350%	10.8930%	10.6182%	-90.9%
1	0.0001	CYWG	Feb-14	fuel opt	86,352	7,583,977	8h 29m 34s	195,612	11.3306%	10.8930%	10.6176%	-91.3%
1	0.001	CYWG	Feb-14	fuel opt	86,369	7,583,977	8h 29m 34s	75,000	11.3514%	10.8930%	10.6178%	-96.6%
1	0.01	CYWG	Feb-14	fuel opt	86,372	7,583,977	8h 29m 33s	0	11.3554%	10.8930%	10.6166%	-100.0%
1	0.1	CYWG	Feb-14	fuel opt	86,372	7,583,977	8h 29m 33s	0	11.3554%	10.8930%	10.6166%	-100.0%
1	1	CYWG	Feb-14	fuel opt	86,372	7,583,977	8h 29m 33s	0	11.3554%	10.8930%	10.6166%	-100.0%
1	10	CYWG	Feb-14	fuel opt	86,372	7,583,977	8h 29m 33s	0	11.3554%	10.8930%	10.6166%	-100.0%
3	0	CYWG	Feb-14	fuel opt	88,093	7,725,277	8h 39m 2s	235,000	13.5743%	12.9591%	12.6746%	-89.5%
3	0.0001	CYWG	Feb-14	fuel opt	88,073	7,725,277	8h 39m 2s	35,000	13.5486%	12.9591%	12.6747%	-98.4%
3	0.001	CYWG	Feb-14	fuel opt	88,073	7,725,277	8h 39m 2s	35,000	13.5486%	12.9591%	12.6747%	-98.4%
3	0.01	CYWG	Feb-14	fuel opt	88,073	7,725,277	8h 39m 2s	35,000	13.5486%	12.9591%	12.6747%	-98.4%
3	0.1	CYWG	Feb-14	fuel opt	88,076	7,725,277	8h 39m 2s	0	13.5520%	12.9591%	12.6732%	-100.0%
3	1	CYWG	Feb-14	fuel opt	88,076	7,725,277	8h 39m 2s	0	13.5521%	12.9591%	12.6732%	-100.0%
3	10	CYWG	Feb-14	fuel opt	88,076	7,725,277	8h 39m 2s	0	13.5521%	12.9591%	12.6732%	-100.0%
10	0	CYWG	Feb-14	fuel opt	88,576	7,766,087	8h 41m 42s	235,000	14.1978%	13.5559%	13.2534%	-89.5%
10	0.0001	CYWG	Feb-14	fuel opt	88,557	7,766,087	8h 41m 42s	35,000	14.1723%	13.5559%	13.2533%	-98.4%
10	0.001	CYWG	Feb-14	fuel opt	88,557	7,766,087	8h 41m 42s	35,000	14.1723%	13.5559%	13.2533%	-98.4%
10	0.01	CYWG	Feb-14	fuel opt	88,557	7,766,087	8h 41m 42s	35,000	14.1723%	13.5559%	13.2533%	-98.4%
10	0.1	CYWG	Feb-14	fuel opt	88,559	7,766,087	8h 41m 42s	0	14.1758%	13.5559%	13.2519%	-100.0%
10	1	CYWG	Feb-14	fuel opt	88,559	7,766,087	8h 41m 42s	0	14.1758%	13.5559%	13.2519%	-100.0%
10	10	CYWG	Feb-14	fuel opt	88,559	7,766,087	8h 41m 42s	0	14.1759%	13.5559%	13.2519%	-100.0%

β_{grnd}	β_{prof}	Dest	Atm	Mode	dm [kg]	ds [m]	dt [h:m:s]	ct _{tot} [m]	% dm	% ds	% dt	% CT
0	0	CYVR	Feb-14	fuel opt	88,254	7,766,065	8h 40m 7s	1,550,551	0.0000%	0.0000%	0.0000%	0.0%
0	0.0001	CYVR	Feb-14	fuel opt	88,237	7,766,065	8h 40m 7s	1,345,551	-0.0187%	0.0000%	0.0003%	-13.2%
0	0.001	CYVR	Feb-14	fuel opt	88,237	7,766,065	8h 40m 7s	1,385,716	-0.0186%	0.0000%	0.0005%	-10.6%
0	0.01	CYVR	Feb-14	fuel opt	88,239	7,766,065	8h 40m 7s	1,260,146	-0.0169%	0.0000%	-0.0004%	-18.7%
0	0.1	CYVR	Feb-14	fuel opt	88,295	7,766,065	8h 40m 7s	806,876	0.0473%	0.0000%	0.0005%	-48.0%
0	1	CYVR	Feb-14	fuel opt	88,244	7,766,065	8h 40m 7s	824,822	-0.0109%	0.0000%	0.0019%	-46.8%
0	10	CYVR	Feb-14	fuel opt	88,244	7,766,065	8h 40m 7s	824,822	-0.0109%	0.0000%	0.0019%	-46.8%
0.01	0	CYVR	Feb-14	fuel opt	88,257	7,766,065	8h 40m 7s	1,708,582	0.0040%	0.0000%	0.0005%	10.2%
0.01	0.0001	CYVR	Feb-14	fuel opt	88,237	7,766,065	8h 40m 7s	1,345,551	-0.0187%	0.0000%	0.0003%	-13.2%
0.01	0.001	CYVR	Feb-14	fuel opt	88,239	7,766,065	8h 40m 7s	1,305,653	-0.0170%	0.0000%	0.0000%	-15.8%
0.01	0.01	CYVR	Feb-14	fuel opt	88,238	7,766,065	8h 40m 7s	1,053,831	-0.0171%	0.0000%	0.0012%	-32.0%
0.01	0.1	CYVR	Feb-14	fuel opt	88,253	7,766,065	8h 40m 7s	824,822	-0.0007%	0.0000%	0.0017%	-46.8%
0.01	1	CYVR	Feb-14	fuel opt	88,253	7,766,065	8h 40m 7s	824,823	-0.0006%	0.0000%	0.0017%	-46.8%
0.01	10	CYVR	Feb-14	fuel opt	88,292	7,766,065	8h 40m 7s	806,876	0.0441%	0.0000%	-0.0003%	-48.0%
0.03	0	CYVR	Feb-14	fuel opt	88,296	7,770,655	8h 40m 17s	1,378,117	0.0480%	0.0591%	0.0320%	-11.1%
0.03	0.0001	CYVR	Feb-14	fuel opt	88,276	7,770,655	8h 40m 17s	1,142,102	0.0256%	0.0591%	0.0319%	-26.3%
0.03	0.001	CYVR	Feb-14	fuel opt	88,278	7,770,655	8h 40m 17s	1,102,205	0.0273%	0.0591%	0.0316%	-28.9%
0.03	0.01	CYVR	Feb-14	fuel opt	88,272	7,770,655	8h 40m 17s	984,730	0.0205%	0.0591%	0.0311%	-36.5%
0.03	0.1	CYVR	Feb-14	fuel opt	88,340	7,770,655	8h 40m 17s	711,589	0.0977%	0.0591%	0.0326%	-54.1%
0.03	1	CYVR	Feb-14	fuel opt	88,286	7,770,655	8h 40m 17s	744,548	0.0373%	0.0591%	0.0326%	-52.0%
0.03	10	CYVR	Feb-14	fuel opt	88,285	7,770,655	8h 40m 17s	744,547	0.0361%	0.0591%	0.0327%	-52.0%
0.1	0	CYVR	Feb-14	fuel opt	88,529	7,787,835	8h 41m 33s	1,338,100	0.3119%	0.2803%	0.2776%	-13.7%
0.1	0.0001	CYVR	Feb-14	fuel opt	88,509	7,787,835	8h 41m 33s	1,092,076	0.2895%	0.2803%	0.2774%	-29.6%
0.1	0.001	CYVR	Feb-14	fuel opt	88,513	7,787,835	8h 41m 33s	853,101	0.2935%	0.2803%	0.2765%	-45.0%
0.1	0.01	CYVR	Feb-14	fuel opt	88,507	7,787,835	8h 41m 33s	855,758	0.2872%	0.2803%	0.2764%	-44.8%
0.1	0.1	CYVR	Feb-14	fuel opt	88,517	7,787,835	8h 41m 33s	759,555	0.2985%	0.2803%	0.2775%	-51.0%
0.1	1	CYVR	Feb-14	fuel opt	88,523	7,787,835	8h 41m 33s	756,897	0.3049%	0.2803%	0.2775%	-51.2%
0.1	10	CYVR	Feb-14	fuel opt	88,571	7,787,835	8h 41m 33s	620,585	0.3600%	0.2803%	0.2766%	-60.0%
0.3	0	CYVR	Feb-14	fuel opt	89,467	7,871,833	8h 46m 43s	773,620	1.3749%	1.3619%	1.2688%	-50.1%
0.3	0.0001	CYVR	Feb-14	fuel opt	89,463	7,871,833	8h 46m 43s	780,626	1.3710%	1.3619%	1.2683%	-49.7%
0.3	0.001	CYVR	Feb-14	fuel opt	89,470	7,871,833	8h 46m 43s	651,064	1.3788%	1.3619%	1.2679%	-58.0%
0.3	0.01	CYVR	Feb-14	fuel opt	89,471	7,871,833	8h 46m 43s	535,931	1.3792%	1.3619%	1.2702%	-65.4%
0.3	0.1	CYVR	Feb-14	fuel opt	89,486	7,871,833	8h 46m 42s	518,045	1.3965%	1.3619%	1.2666%	-66.6%
0.3	1	CYVR	Feb-14	fuel opt	89,491	7,871,833	8h 46m 42s	518,011	1.4024%	1.3619%	1.2665%	-66.6%
0.3	10	CYVR	Feb-14	fuel opt	89,491	7,871,833	8h 46m 43s	518,012	1.4018%	1.3619%	1.2684%	-66.6%
1	0	CYVR	Feb-14	fuel opt	89,467	7,871,833	8h 46m 43s	773,620	1.3749%	1.3619%	1.2688%	-50.1%
1	0.0001	CYVR	Feb-14	fuel opt	89,463	7,871,833	8h 46m 43s	780,626	1.3710%	1.3619%	1.2683%	-49.7%
1	0.001	CYVR	Feb-14	fuel opt	89,463	7,871,833	8h 46m 43s	780,626	1.3710%	1.3619%	1.2683%	-49.7%
1	0.01	CYVR	Feb-14	fuel opt	89,495	7,871,833	8h 46m 42s	538,022	1.4063%	1.3619%	1.2676%	-65.3%
1	0.1	CYVR	Feb-14	fuel opt	89,500	7,871,833	8h 46m 43s	447,894	1.4130%	1.3619%	1.2685%	-71.1%
1	1	CYVR	Feb-14	fuel opt	89,483	7,871,833	8h 46m 43s	518,016	1.3927%	1.3619%	1.2684%	-66.6%
1	10	CYVR	Feb-14	fuel opt	89,491	7,871,833	8h 46m 43s	518,010	1.4027%	1.3619%	1.2684%	-66.6%
3	0	CYVR	Feb-14	fuel opt	89,467	7,871,833	8h 46m 43s	773,620	1.3749%	1.3619%	1.2688%	-50.1%
3	0.0001	CYVR	Feb-14	fuel opt	89,463	7,871,833	8h 46m 43s	780,626	1.3710%	1.3619%	1.2683%	-49.7%
3	0.001	CYVR	Feb-14	fuel opt	89,465	7,871,833	8h 46m 43s	662,734	1.3727%	1.3619%	1.2681%	-57.3%
3	0.01	CYVR	Feb-14	fuel opt	89,520	7,871,833	8h 46m 43s	467,829	1.4356%	1.3619%	1.2695%	-69.8%
3	0.1	CYVR	Feb-14	fuel opt	89,486	7,871,833	8h 46m 42s	518,045	1.3966%	1.3619%	1.2666%	-66.6%
3	1	CYVR	Feb-14	fuel opt	89,490	7,871,833	8h 46m 42s	518,014	1.4015%	1.3619%	1.2665%	-66.6%
3	10	CYVR	Feb-14	fuel opt	89,491	7,871,833	8h 46m 43s	518,010	1.4024%	1.3619%	1.2684%	-66.6%
10	0	CYVR	Feb-14	fuel opt	-	-	-	-	-	-	-	-
10	0.0001	CYVR	Feb-14	fuel opt	-	-	-	-	-	-	-	-
10	0.001	CYVR	Feb-14	fuel opt	-	-	-	-	-	-	-	-
10	0.01	CYVR	Feb-14	fuel opt	-	-	-	-	-	-	-	-
10	0.1	CYVR	Feb-14	fuel opt	-	-	-	-	-	-	-	-
10	1	CYVR	Feb-14	fuel opt	-	-	-	-	-	-	-	-
10	10	CYVR	Feb-14	fuel opt	-	-	-	-	-	-	-	-

D. Numeric results - Hybrid mitigation

β_{grnd}	β_{prof}	Dest	Atm	Mode	dm [kg]	ds [m]	dt [h:m:s]	ct_{tot} [m]	% dm	% ds	% dt	% CT
0	0	KIAD	Feb-17	fuel opt	67,195	6,062,762	6h 41m 29s	0	0.0000%	0.0000%	0.0000%	0.0%
0	0.0001	KIAD	Feb-17	fuel opt	67,195	6,062,762	6h 41m 29s	0	0.0000%	0.0000%	0.0000%	0.0%
0	0.001	KIAD	Feb-17	fuel opt	67,195	6,062,762	6h 41m 29s	0	0.0000%	0.0000%	0.0000%	0.0%
0	0.01	KIAD	Feb-17	fuel opt	67,195	6,062,762	6h 41m 29s	0	0.0000%	0.0000%	0.0000%	0.0%
0	0.1	KIAD	Feb-17	fuel opt	67,195	6,062,762	6h 41m 29s	0	0.0000%	0.0000%	0.0000%	0.0%
0	1	KIAD	Feb-17	fuel opt	67,195	6,062,762	6h 41m 29s	0	0.0000%	0.0000%	0.0000%	0.0%
0	10	KIAD	Feb-17	fuel opt	67,195	6,062,762	6h 41m 29s	0	0.0000%	0.0000%	0.0000%	0.0%
0.01	0	KIAD	Feb-17	fuel opt	67,196	6,062,762	6h 41m 28s	0	0.0023%	0.0000%	-0.0005%	0.0%
0.01	0.0001	KIAD	Feb-17	fuel opt	67,195	6,062,762	6h 41m 29s	0	0.0000%	0.0000%	0.0000%	0.0%
0.01	0.001	KIAD	Feb-17	fuel opt	67,195	6,062,762	6h 41m 29s	0	0.0000%	0.0000%	0.0000%	0.0%
0.01	0.01	KIAD	Feb-17	fuel opt	67,195	6,062,762	6h 41m 29s	0	0.0000%	0.0000%	0.0000%	0.0%
0.01	0.1	KIAD	Feb-17	fuel opt	67,195	6,062,762	6h 41m 29s	0	0.0000%	0.0000%	0.0000%	0.0%
0.01	1	KIAD	Feb-17	fuel opt	67,195	6,062,762	6h 41m 29s	0	0.0000%	0.0000%	0.0000%	0.0%
0.01	10	KIAD	Feb-17	fuel opt	67,195	6,062,762	6h 41m 29s	0	0.0000%	0.0000%	0.0000%	0.0%
0.03	0	KIAD	Feb-17	fuel opt	67,196	6,062,762	6h 41m 28s	0	0.0023%	0.0000%	-0.0005%	0.0%
0.03	0.0001	KIAD	Feb-17	fuel opt	67,195	6,062,762	6h 41m 29s	0	0.0000%	0.0000%	0.0000%	0.0%
0.03	0.001	KIAD	Feb-17	fuel opt	67,195	6,062,762	6h 41m 29s	0	0.0000%	0.0000%	0.0000%	0.0%
0.03	0.01	KIAD	Feb-17	fuel opt	67,195	6,062,762	6h 41m 29s	0	0.0000%	0.0000%	0.0000%	0.0%
0.03	0.1	KIAD	Feb-17	fuel opt	67,195	6,062,762	6h 41m 29s	0	0.0000%	0.0000%	0.0000%	0.0%
0.03	1	KIAD	Feb-17	fuel opt	67,195	6,062,762	6h 41m 29s	0	0.0000%	0.0000%	0.0000%	0.0%
0.03	10	KIAD	Feb-17	fuel opt	67,195	6,062,762	6h 41m 29s	0	0.0000%	0.0000%	0.0000%	0.0%
0.1	0	KIAD	Feb-17	fuel opt	67,234	6,066,302	6h 41m 42s	0	0.0590%	0.0584%	0.0540%	0.0%
0.1	0.0001	KIAD	Feb-17	fuel opt	67,233	6,066,302	6h 41m 42s	0	0.0564%	0.0584%	0.0545%	0.0%
0.1	0.001	KIAD	Feb-17	fuel opt	67,233	6,066,302	6h 41m 42s	0	0.0564%	0.0584%	0.0545%	0.0%
0.1	0.01	KIAD	Feb-17	fuel opt	67,233	6,066,302	6h 41m 42s	0	0.0564%	0.0584%	0.0545%	0.0%
0.1	0.1	KIAD	Feb-17	fuel opt	67,233	6,066,302	6h 41m 42s	0	0.0564%	0.0584%	0.0545%	0.0%
0.1	1	KIAD	Feb-17	fuel opt	67,233	6,066,302	6h 41m 42s	0	0.0564%	0.0584%	0.0545%	0.0%
0.1	10	KIAD	Feb-17	fuel opt	67,233	6,066,302	6h 41m 42s	0	0.0564%	0.0584%	0.0545%	0.0%
0.3	0	KIAD	Feb-17	fuel opt	67,234	6,066,302	6h 41m 42s	0	0.0590%	0.0584%	0.0540%	0.0%
0.3	0.0001	KIAD	Feb-17	fuel opt	67,233	6,066,302	6h 41m 42s	0	0.0564%	0.0584%	0.0545%	0.0%
0.3	0.001	KIAD	Feb-17	fuel opt	67,233	6,066,302	6h 41m 42s	0	0.0564%	0.0584%	0.0545%	0.0%
0.3	0.01	KIAD	Feb-17	fuel opt	67,233	6,066,302	6h 41m 42s	0	0.0564%	0.0584%	0.0545%	0.0%
0.3	0.1	KIAD	Feb-17	fuel opt	67,233	6,066,302	6h 41m 42s	0	0.0564%	0.0584%	0.0545%	0.0%
0.3	1	KIAD	Feb-17	fuel opt	67,233	6,066,302	6h 41m 42s	0	0.0564%	0.0584%	0.0545%	0.0%
0.3	10	KIAD	Feb-17	fuel opt	67,233	6,066,302	6h 41m 42s	0	0.0564%	0.0584%	0.0545%	0.0%
1	0	KIAD	Feb-17	fuel opt	67,331	6,076,542	6h 42m 10s	240,699	0.2034%	0.2273%	0.1709%	0.0%
1	0.0001	KIAD	Feb-17	fuel opt	67,233	6,066,302	6h 41m 42s	0	0.0564%	0.0584%	0.0545%	0.0%
1	0.001	KIAD	Feb-17	fuel opt	67,233	6,066,302	6h 41m 42s	0	0.0564%	0.0584%	0.0545%	0.0%
1	0.01	KIAD	Feb-17	fuel opt	67,233	6,066,302	6h 41m 42s	0	0.0564%	0.0584%	0.0545%	0.0%
1	0.1	KIAD	Feb-17	fuel opt	67,233	6,066,302	6h 41m 42s	0	0.0564%	0.0584%	0.0545%	0.0%
1	1	KIAD	Feb-17	fuel opt	67,233	6,066,302	6h 41m 42s	0	0.0564%	0.0584%	0.0545%	0.0%
1	10	KIAD	Feb-17	fuel opt	67,233	6,066,302	6h 41m 42s	0	0.0564%	0.0584%	0.0545%	0.0%
3	0	KIAD	Feb-17	fuel opt	67,331	6,076,542	6h 42m 10s	240,699	0.2034%	0.2273%	0.1709%	0.0%
3	0.0001	KIAD	Feb-17	fuel opt	67,329	6,076,542	6h 42m 10s	120,547	0.2005%	0.2273%	0.1713%	0.0%
3	0.001	KIAD	Feb-17	fuel opt	67,329	6,076,542	6h 42m 10s	120,547	0.2005%	0.2273%	0.1713%	0.0%
3	0.01	KIAD	Feb-17	fuel opt	67,329	6,076,542	6h 42m 10s	120,547	0.2005%	0.2273%	0.1713%	0.0%
3	0.1	KIAD	Feb-17	fuel opt	67,329	6,076,542	6h 42m 10s	120,547	0.2005%	0.2273%	0.1713%	0.0%
3	1	KIAD	Feb-17	fuel opt	67,329	6,076,542	6h 42m 10s	120,547	0.2005%	0.2273%	0.1713%	0.0%
3	10	KIAD	Feb-17	fuel opt	67,329	6,076,542	6h 42m 10s	120,547	0.2005%	0.2273%	0.1713%	0.0%
10	0	KIAD	Feb-17	fuel opt	67,331	6,076,542	6h 42m 10s	240,699	0.2034%	0.2273%	0.1709%	0.0%
10	0.0001	KIAD	Feb-17	fuel opt	67,329	6,076,542	6h 42m 10s	120,547	0.2005%	0.2273%	0.1713%	0.0%
10	0.001	KIAD	Feb-17	fuel opt	67,329	6,076,542	6h 42m 10s	120,547	0.2005%	0.2273%	0.1713%	0.0%
10	0.01	KIAD	Feb-17	fuel opt	67,329	6,076,542	6h 42m 10s	120,547	0.2005%	0.2273%	0.1713%	0.0%
10	0.1	KIAD	Feb-17	fuel opt	67,329	6,076,542	6h 42m 10s	120,547	0.2005%	0.2273%	0.1713%	0.0%
10	1	KIAD	Feb-17	fuel opt	67,329	6,076,542	6h 42m 10s	120,547	0.2005%	0.2273%	0.1713%	0.0%
10	10	KIAD	Feb-17	fuel opt	67,324	6,076,542	6h 42m 10s	120,156	0.1925%	0.2273%	0.1700%	0.0%

β_{grnd}	β_{prof}	Dest	Atm	Mode	dm [kg]	ds [m]	dt [h:m:s]	ct _{tot} [m]	% dm	% ds	% dt	% CT
0	0	CYWG	Feb-17	fuel opt	71,749	6,471,289	7h 7m 41s	515,195	0.0000%	0.0000%	0.0000%	0.0%
0	0.0001	CYWG	Feb-17	fuel opt	71,749	6,471,289	7h 7m 41s	515,195	0.0000%	0.0000%	0.0000%	0.0%
0	0.001	CYWG	Feb-17	fuel opt	71,749	6,471,289	7h 7m 41s	455,549	-0.0003%	0.0000%	-0.0001%	-11.6%
0	0.01	CYWG	Feb-17	fuel opt	71,838	6,471,289	7h 7m 41s	280,000	0.1232%	0.0000%	0.0002%	-45.7%
0	0.1	CYWG	Feb-17	fuel opt	71,818	6,471,289	7h 7m 42s	0	0.0956%	0.0000%	0.0053%	-100.0%
0	1	CYWG	Feb-17	fuel opt	71,818	6,471,289	7h 7m 42s	0	0.0956%	0.0000%	0.0053%	-100.0%
0	10	CYWG	Feb-17	fuel opt	71,818	6,471,289	7h 7m 42s	0	0.0956%	0.0000%	0.0053%	-100.0%
0.01	0	CYWG	Feb-17	fuel opt	71,752	6,471,289	7h 7m 41s	509,193	0.0035%	0.0000%	0.0001%	-1.2%
0.01	0.0001	CYWG	Feb-17	fuel opt	71,749	6,471,289	7h 7m 41s	515,195	0.0000%	0.0000%	0.0000%	0.0%
0.01	0.001	CYWG	Feb-17	fuel opt	71,749	6,471,289	7h 7m 41s	455,549	-0.0003%	0.0000%	-0.0001%	-11.6%
0.01	0.01	CYWG	Feb-17	fuel opt	71,755	6,471,289	7h 7m 41s	450,639	0.0083%	0.0000%	0.0005%	-12.5%
0.01	0.1	CYWG	Feb-17	fuel opt	71,818	6,471,289	7h 7m 42s	0	0.0956%	0.0000%	0.0053%	-100.0%
0.01	1	CYWG	Feb-17	fuel opt	71,818	6,471,289	7h 7m 42s	0	0.0956%	0.0000%	0.0053%	-100.0%
0.01	10	CYWG	Feb-17	fuel opt	71,818	6,471,289	7h 7m 42s	0	0.0956%	0.0000%	0.0053%	-100.0%
0.03	0	CYWG	Feb-17	fuel opt	71,752	6,471,289	7h 7m 41s	509,193	0.0035%	0.0000%	0.0001%	-1.2%
0.03	0.0001	CYWG	Feb-17	fuel opt	71,749	6,471,289	7h 7m 41s	515,195	0.0000%	0.0000%	0.0000%	0.0%
0.03	0.001	CYWG	Feb-17	fuel opt	71,749	6,471,289	7h 7m 41s	455,549	-0.0003%	0.0000%	-0.0001%	-11.6%
0.03	0.01	CYWG	Feb-17	fuel opt	71,769	6,471,289	7h 7m 41s	410,239	0.0272%	0.0000%	0.0000%	-20.4%
0.03	0.1	CYWG	Feb-17	fuel opt	71,818	6,471,289	7h 7m 42s	0	0.0956%	0.0000%	0.0053%	-100.0%
0.03	1	CYWG	Feb-17	fuel opt	71,818	6,471,289	7h 7m 42s	0	0.0956%	0.0000%	0.0053%	-100.0%
0.03	10	CYWG	Feb-17	fuel opt	71,818	6,471,289	7h 7m 42s	0	0.0956%	0.0000%	0.0053%	-100.0%
0.1	0	CYWG	Feb-17	fuel opt	71,752	6,471,289	7h 7m 41s	509,193	0.0035%	0.0000%	0.0001%	-1.2%
0.1	0.0001	CYWG	Feb-17	fuel opt	71,749	6,471,289	7h 7m 41s	515,195	0.0000%	0.0000%	0.0000%	0.0%
0.1	0.001	CYWG	Feb-17	fuel opt	71,749	6,471,289	7h 7m 41s	455,549	-0.0003%	0.0000%	-0.0001%	-11.6%
0.1	0.01	CYWG	Feb-17	fuel opt	71,818	6,471,289	7h 7m 42s	0	0.0956%	0.0000%	0.0053%	-100.0%
0.1	0.1	CYWG	Feb-17	fuel opt	71,818	6,471,289	7h 7m 42s	0	0.0956%	0.0000%	0.0053%	-100.0%
0.1	1	CYWG	Feb-17	fuel opt	71,818	6,471,289	7h 7m 42s	0	0.0956%	0.0000%	0.0053%	-100.0%
0.1	10	CYWG	Feb-17	fuel opt	71,818	6,471,289	7h 7m 42s	0	0.0956%	0.0000%	0.0053%	-100.0%
0.3	0	CYWG	Feb-17	fuel opt	73,261	6,600,968	7h 16m 3s	0	2.1065%	2.0039%	1.9573%	-100.0%
0.3	0.0001	CYWG	Feb-17	fuel opt	73,258	6,600,968	7h 16m 3s	0	2.1029%	2.0039%	1.9572%	-100.0%
0.3	0.001	CYWG	Feb-17	fuel opt	73,258	6,600,968	7h 16m 3s	0	2.1029%	2.0039%	1.9572%	-100.0%
0.3	0.01	CYWG	Feb-17	fuel opt	73,258	6,600,968	7h 16m 3s	0	2.1029%	2.0039%	1.9572%	-100.0%
0.3	0.1	CYWG	Feb-17	fuel opt	73,258	6,600,968	7h 16m 3s	0	2.1029%	2.0039%	1.9572%	-100.0%
0.3	1	CYWG	Feb-17	fuel opt	73,258	6,600,968	7h 16m 3s	0	2.1029%	2.0039%	1.9572%	-100.0%
0.3	10	CYWG	Feb-17	fuel opt	73,258	6,600,968	7h 16m 3s	0	2.1029%	2.0039%	1.9572%	-100.0%
1	0	CYWG	Feb-17	fuel opt	73,261	6,600,968	7h 16m 3s	0	2.1065%	2.0039%	1.9573%	-100.0%
1	0.0001	CYWG	Feb-17	fuel opt	73,258	6,600,968	7h 16m 3s	0	2.1029%	2.0039%	1.9572%	-100.0%
1	0.001	CYWG	Feb-17	fuel opt	73,258	6,600,968	7h 16m 3s	0	2.1029%	2.0039%	1.9572%	-100.0%
1	0.01	CYWG	Feb-17	fuel opt	73,258	6,600,968	7h 16m 3s	0	2.1029%	2.0039%	1.9572%	-100.0%
1	0.1	CYWG	Feb-17	fuel opt	73,258	6,600,968	7h 16m 3s	0	2.1029%	2.0039%	1.9572%	-100.0%
1	1	CYWG	Feb-17	fuel opt	73,258	6,600,968	7h 16m 3s	0	2.1029%	2.0039%	1.9572%	-100.0%
1	10	CYWG	Feb-17	fuel opt	73,258	6,600,968	7h 16m 3s	0	2.1029%	2.0039%	1.9572%	-100.0%
3	0	CYWG	Feb-17	fuel opt	73,261	6,600,968	7h 16m 3s	0	2.1065%	2.0039%	1.9573%	-100.0%
3	0.0001	CYWG	Feb-17	fuel opt	73,258	6,600,968	7h 16m 3s	0	2.1029%	2.0039%	1.9572%	-100.0%
3	0.001	CYWG	Feb-17	fuel opt	73,258	6,600,968	7h 16m 3s	0	2.1029%	2.0039%	1.9572%	-100.0%
3	0.01	CYWG	Feb-17	fuel opt	73,258	6,600,968	7h 16m 3s	0	2.1029%	2.0039%	1.9572%	-100.0%
3	0.1	CYWG	Feb-17	fuel opt	73,258	6,600,968	7h 16m 3s	0	2.1029%	2.0039%	1.9572%	-100.0%
3	1	CYWG	Feb-17	fuel opt	73,258	6,600,968	7h 16m 3s	0	2.1029%	2.0039%	1.9572%	-100.0%
3	10	CYWG	Feb-17	fuel opt	73,258	6,600,968	7h 16m 3s	0	2.1029%	2.0039%	1.9572%	-100.0%
10	0	CYWG	Feb-17	fuel opt	73,261	6,600,968	7h 16m 3s	0	2.1065%	2.0039%	1.9573%	-100.0%
10	0.0001	CYWG	Feb-17	fuel opt	73,258	6,600,968	7h 16m 3s	0	2.1029%	2.0039%	1.9572%	-100.0%
10	0.001	CYWG	Feb-17	fuel opt	73,258	6,600,968	7h 16m 3s	0	2.1029%	2.0039%	1.9572%	-100.0%
10	0.01	CYWG	Feb-17	fuel opt	73,258	6,600,968	7h 16m 3s	0	2.1029%	2.0039%	1.9572%	-100.0%
10	0.1	CYWG	Feb-17	fuel opt	73,258	6,600,968	7h 16m 3s	0	2.1029%	2.0039%	1.9572%	-100.0%
10	1	CYWG	Feb-17	fuel opt	73,258	6,600,968	7h 16m 3s	0	2.1029%	2.0039%	1.9572%	-100.0%
10	10	CYWG	Feb-17	fuel opt	73,258	6,600,968	7h 16m 3s	0	2.1029%	2.0039%	1.9572%	-100.0%

D. Numeric results - Hybrid mitigation

β_{grnd}	β_{prof}	Dest	Atm	Mode	dm [kg]	ds [m]	dt [h:m:s]	ct _{tot} [m]	% dm	% ds	% dt	% CT
0	0	CYVR	Feb-17	fuel opt	86,867	7,739,677	8h 32m 6s	1,145,812	0.0000%	0.0000%	0.0000%	0.0%
0	0.0001	CYVR	Feb-17	fuel opt	86,868	7,739,677	8h 32m 6s	1,140,817	0.0002%	0.0000%	0.0000%	-0.4%
0	0.001	CYVR	Feb-17	fuel opt	86,884	7,739,677	8h 32m 5s	780,679	0.0195%	0.0000%	-0.0018%	-31.9%
0	0.01	CYVR	Feb-17	fuel opt	86,874	7,739,677	8h 32m 6s	800,953	0.0071%	0.0000%	-0.0002%	-30.1%
0	0.1	CYVR	Feb-17	fuel opt	86,963	7,739,677	8h 32m 8s	647,354	0.1105%	0.0000%	0.0080%	-43.5%
0	1	CYVR	Feb-17	fuel opt	86,898	7,739,677	8h 32m 7s	692,785	0.0350%	0.0000%	0.0046%	-39.5%
0	10	CYVR	Feb-17	fuel opt	86,901	7,739,677	8h 32m 7s	572,362	0.0391%	0.0000%	0.0051%	-50.0%
0.01	0	CYVR	Feb-17	fuel opt	86,870	7,739,677	8h 32m 5s	1,141,802	0.0026%	0.0000%	-0.0006%	-0.3%
0.01	0.0001	CYVR	Feb-17	fuel opt	86,868	7,739,677	8h 32m 6s	1,140,823	0.0004%	0.0000%	0.0000%	-0.4%
0.01	0.001	CYVR	Feb-17	fuel opt	86,881	7,739,677	8h 32m 5s	900,953	0.0158%	0.0000%	-0.0013%	-21.4%
0.01	0.01	CYVR	Feb-17	fuel opt	86,877	7,739,677	8h 32m 5s	680,679	0.0108%	0.0000%	-0.0008%	-40.6%
0.01	0.1	CYVR	Feb-17	fuel opt	86,899	7,739,677	8h 32m 7s	692,652	0.0358%	0.0000%	0.0056%	-39.5%
0.01	1	CYVR	Feb-17	fuel opt	86,901	7,739,677	8h 32m 7s	687,665	0.0382%	0.0000%	0.0056%	-40.0%
0.01	10	CYVR	Feb-17	fuel opt	86,900	7,739,677	8h 32m 7s	687,633	0.0372%	0.0000%	0.0056%	-40.0%
0.03	0	CYVR	Feb-17	fuel opt	86,883	7,740,377	8h 32m 8s	1,130,767	0.0174%	0.0090%	0.0064%	-1.3%
0.03	0.0001	CYVR	Feb-17	fuel opt	86,880	7,740,377	8h 32m 8s	1,140,778	0.0148%	0.0090%	0.0070%	-0.4%
0.03	0.001	CYVR	Feb-17	fuel opt	86,904	7,740,377	8h 32m 7s	721,077	0.0420%	0.0090%	0.0061%	-37.1%
0.03	0.01	CYVR	Feb-17	fuel opt	86,896	7,740,377	8h 32m 8s	761,334	0.0332%	0.0090%	0.0088%	-33.6%
0.03	0.1	CYVR	Feb-17	fuel opt	86,919	7,740,377	8h 32m 9s	696,833	0.0595%	0.0090%	0.0124%	-39.2%
0.03	1	CYVR	Feb-17	fuel opt	86,912	7,740,377	8h 32m 9s	687,693	0.0512%	0.0090%	0.0125%	-40.0%
0.03	10	CYVR	Feb-17	fuel opt	86,909	7,740,377	8h 32m 10s	692,527	0.0479%	0.0090%	0.0134%	-39.6%
0.1	0	CYVR	Feb-17	fuel opt	86,883	7,740,377	8h 32m 8s	1,130,767	0.0174%	0.0090%	0.0064%	-1.3%
0.1	0.0001	CYVR	Feb-17	fuel opt	86,880	7,740,377	8h 32m 8s	1,140,778	0.0148%	0.0090%	0.0070%	-0.4%
0.1	0.001	CYVR	Feb-17	fuel opt	86,902	7,740,377	8h 32m 8s	836,418	0.0394%	0.0090%	0.0065%	-27.0%
0.1	0.01	CYVR	Feb-17	fuel opt	86,897	7,740,377	8h 32m 9s	761,200	0.0338%	0.0090%	0.0097%	-33.6%
0.1	0.1	CYVR	Feb-17	fuel opt	86,899	7,740,377	8h 32m 9s	731,693	0.0366%	0.0090%	0.0108%	-36.1%
0.1	1	CYVR	Feb-17	fuel opt	86,916	7,740,377	8h 32m 10s	567,301	0.0563%	0.0090%	0.0130%	-50.5%
0.1	10	CYVR	Feb-17	fuel opt	86,911	7,740,377	8h 32m 10s	692,688	0.0506%	0.0090%	0.0128%	-39.5%
0.3	0	CYVR	Feb-17	fuel opt	87,780	7,820,234	8h 37m 2s	767,495	1.0502%	1.0408%	0.9656%	-33.0%
0.3	0.0001	CYVR	Feb-17	fuel opt	87,777	7,820,234	8h 37m 2s	770,491	1.0474%	1.0408%	0.9660%	-32.8%
0.3	0.001	CYVR	Feb-17	fuel opt	87,793	7,820,234	8h 37m 3s	645,719	1.0656%	1.0408%	0.9671%	-43.6%
0.3	0.01	CYVR	Feb-17	fuel opt	87,801	7,820,234	8h 37m 3s	525,492	1.0748%	1.0408%	0.9676%	-54.1%
0.3	0.1	CYVR	Feb-17	fuel opt	87,824	7,820,234	8h 37m 3s	0	1.1011%	1.0408%	0.9689%	-100.0%
0.3	1	CYVR	Feb-17	fuel opt	87,823	7,820,234	8h 37m 3s	241,944	1.1004%	1.0408%	0.9691%	-78.9%
0.3	10	CYVR	Feb-17	fuel opt	87,792	7,820,234	8h 37m 3s	425,926	1.0648%	1.0408%	0.9679%	-62.8%
1	0	CYVR	Feb-17	fuel opt	91,667	8,147,440	9h 58m 32s	376,193	5.5256%	5.2685%	5.1621%	-67.2%
1	0.0001	CYVR	Feb-17	fuel opt	91,665	8,147,440	9h 58m 32s	310,320	5.5226%	5.2685%	5.1624%	-72.9%
1	0.001	CYVR	Feb-17	fuel opt	91,665	8,147,440	9h 58m 32s	310,320	5.5226%	5.2685%	5.1624%	-72.9%
1	0.01	CYVR	Feb-17	fuel opt	91,676	8,147,440	9h 58m 32s	0	5.5356%	5.2685%	5.1644%	-100.0%
1	0.1	CYVR	Feb-17	fuel opt	91,676	8,147,440	9h 58m 32s	0	5.5356%	5.2685%	5.1644%	-100.0%
1	1	CYVR	Feb-17	fuel opt	91,676	8,147,440	9h 58m 32s	0	5.5356%	5.2685%	5.1644%	-100.0%
1	10	CYVR	Feb-17	fuel opt	91,676	8,147,440	9h 58m 32s	0	5.5356%	5.2685%	5.1644%	-100.0%
3	0	CYVR	Feb-17	fuel opt	97,765	8,650,620	9h 31m 55s	627,446	12.5456%	11.7698%	11.6828%	-45.2%
3	0.0001	CYVR	Feb-17	fuel opt	97,766	8,650,620	9h 31m 54s	400,205	12.5458%	11.7698%	11.6802%	-65.1%
3	0.001	CYVR	Feb-17	fuel opt	97,766	8,650,620	9h 31m 54s	305,048	12.5458%	11.7698%	11.6802%	-73.4%
3	0.01	CYVR	Feb-17	fuel opt	97,768	8,650,620	9h 31m 55s	64,921	12.5486%	11.7698%	11.6811%	-94.3%
3	0.1	CYVR	Feb-17	fuel opt	97,768	8,650,620	9h 31m 55s	64,921	12.5486%	11.7698%	11.6811%	-94.3%
3	1	CYVR	Feb-17	fuel opt	97,768	8,650,620	9h 31m 55s	64,921	12.5486%	11.7698%	11.6811%	-94.3%
3	10	CYVR	Feb-17	fuel opt	97,768	8,650,620	9h 31m 55s	64,921	12.5486%	11.7698%	11.6811%	-94.3%
10	0	CYVR	Feb-17	fuel opt	97,765	8,650,620	9h 31m 55s	627,446	12.5456%	11.7698%	11.6828%	-45.2%
10	0.0001	CYVR	Feb-17	fuel opt	97,766	8,650,620	9h 31m 54s	400,205	12.5458%	11.7698%	11.6802%	-65.1%
10	0.001	CYVR	Feb-17	fuel opt	97,768	8,650,620	9h 31m 55s	184,787	12.5488%	11.7698%	11.6815%	-83.9%
10	0.01	CYVR	Feb-17	fuel opt	97,768	8,650,620	9h 31m 55s	64,921	12.5486%	11.7698%	11.6811%	-94.3%
10	0.1	CYVR	Feb-17	fuel opt	97,768	8,650,620	9h 31m 55s	64,921	12.5486%	11.7698%	11.6811%	-94.3%
10	1	CYVR	Feb-17	fuel opt	97,768	8,650,620	9h 31m 55s	64,921	12.5486%	11.7698%	11.6811%	-94.3%
10	10	CYVR	Feb-17	fuel opt	97,768	8,650,620	9h 31m 55s	64,921	12.5486%	11.7698%	11.6811%	-94.3%

β_{grnd}	β_{prof}	Dest	Atm	Mode	dm [kg]	ds [m]	dt [h:m:s]	ct _{tot} [m]	% dm	% ds	% dt	% CT
0	0	KIAD	May-17	fuel opt	64,630	5,871,104	6h 26m 58s	1,165,000	0.0000%	0.0000%	0.0000%	0.0%
0	0.0001	KIAD	May-17	fuel opt	64,638	5,871,104	6h 26m 58s	855,580	0.0122%	0.0000%	0.0000%	-26.6%
0	0.001	KIAD	May-17	fuel opt	64,656	5,871,104	6h 26m 58s	560,574	0.0401%	0.0000%	0.0001%	-51.9%
0	0.01	KIAD	May-17	fuel opt	64,687	5,871,104	6h 26m 58s	0	0.0890%	0.0000%	0.0022%	-100.0%
0	0.1	KIAD	May-17	fuel opt	64,675	5,871,104	6h 26m 58s	0	0.0692%	0.0000%	0.0017%	-100.0%
0	1	KIAD	May-17	fuel opt	64,675	5,871,104	6h 26m 58s	0	0.0692%	0.0000%	0.0017%	-100.0%
0	10	KIAD	May-17	fuel opt	64,678	5,871,104	6h 26m 58s	0	0.0751%	0.0000%	0.0012%	-100.0%
0.01	0	KIAD	May-17	fuel opt	64,638	5,871,146	6h 26m 59s	1,106,000	0.0122%	0.0007%	0.0057%	-5.1%
0.01	0.0001	KIAD	May-17	fuel opt	64,635	5,871,146	6h 26m 59s	1,130,000	0.0086%	0.0007%	0.0056%	-3.0%
0.01	0.001	KIAD	May-17	fuel opt	64,658	5,871,146	6h 26m 59s	590,574	0.0439%	0.0007%	0.0057%	-49.3%
0.01	0.01	KIAD	May-17	fuel opt	64,662	5,871,146	6h 26m 59s	331,663	0.0500%	0.0007%	0.0069%	-71.5%
0.01	0.1	KIAD	May-17	fuel opt	64,680	5,871,146	6h 26m 59s	0	0.0773%	0.0007%	0.0070%	-100.0%
0.01	1	KIAD	May-17	fuel opt	64,680	5,871,146	6h 26m 59s	0	0.0773%	0.0007%	0.0070%	-100.0%
0.01	10	KIAD	May-17	fuel opt	64,680	5,871,146	6h 26m 59s	0	0.0773%	0.0007%	0.0070%	-100.0%
0.03	0	KIAD	May-17	fuel opt	64,665	5,873,644	6h 27m 9s	662,000	0.0551%	0.0433%	0.0474%	-43.2%
0.03	0.0001	KIAD	May-17	fuel opt	64,663	5,873,644	6h 27m 9s	685,000	0.0514%	0.0433%	0.0471%	-41.2%
0.03	0.001	KIAD	May-17	fuel opt	64,667	5,873,644	6h 27m 9s	495,000	0.0570%	0.0433%	0.0476%	-57.5%
0.03	0.01	KIAD	May-17	fuel opt	64,695	5,873,644	6h 27m 9s	0	0.1007%	0.0433%	0.0485%	-100.0%
0.03	0.1	KIAD	May-17	fuel opt	64,695	5,873,644	6h 27m 9s	0	0.1007%	0.0433%	0.0485%	-100.0%
0.03	1	KIAD	May-17	fuel opt	64,695	5,873,644	6h 27m 9s	0	0.1007%	0.0433%	0.0485%	-100.0%
0.03	10	KIAD	May-17	fuel opt	64,695	5,873,644	6h 27m 9s	0	0.1007%	0.0433%	0.0485%	-100.0%
0.1	0	KIAD	May-17	fuel opt	64,711	5,880,182	6h 27m 20s	721,193	0.1254%	0.1546%	0.0977%	-38.1%
0.1	0.0001	KIAD	May-17	fuel opt	64,709	5,880,182	6h 27m 20s	731,166	0.1220%	0.1546%	0.0977%	-37.2%
0.1	0.001	KIAD	May-17	fuel opt	64,715	5,880,182	6h 27m 21s	360,000	0.1315%	0.1546%	0.1008%	-69.1%
0.1	0.01	KIAD	May-17	fuel opt	64,717	5,880,182	6h 27m 21s	260,000	0.1355%	0.1546%	0.1007%	-77.7%
0.1	0.1	KIAD	May-17	fuel opt	64,738	5,880,182	6h 27m 20s	0	0.1666%	0.1546%	0.0973%	-100.0%
0.1	1	KIAD	May-17	fuel opt	64,743	5,880,182	6h 27m 21s	0	0.1756%	0.1546%	0.1004%	-100.0%
0.1	10	KIAD	May-17	fuel opt	64,737	5,880,182	6h 27m 21s	0	0.1663%	0.1546%	0.1006%	-100.0%
0.3	0	KIAD	May-17	fuel opt	65,251	5,929,684	6h 30m 35s	348,565	0.9607%	0.9978%	0.9365%	-70.1%
0.3	0.0001	KIAD	May-17	fuel opt	65,246	5,929,684	6h 30m 34s	230,000	0.9527%	0.9978%	0.9325%	-80.3%
0.3	0.001	KIAD	May-17	fuel opt	65,249	5,929,684	6h 30m 34s	166,174	0.9574%	0.9978%	0.9332%	-85.7%
0.3	0.01	KIAD	May-17	fuel opt	65,258	5,929,684	6h 30m 35s	0	0.9711%	0.9978%	0.9340%	-100.0%
0.3	0.1	KIAD	May-17	fuel opt	65,258	5,929,684	6h 30m 35s	0	0.9711%	0.9978%	0.9340%	-100.0%
0.3	1	KIAD	May-17	fuel opt	65,259	5,929,684	6h 30m 35s	0	0.9730%	0.9978%	0.9340%	-100.0%
0.3	10	KIAD	May-17	fuel opt	65,258	5,929,684	6h 30m 35s	0	0.9711%	0.9978%	0.9340%	-100.0%
1	0	KIAD	May-17	fuel opt	65,433	5,947,674	6h 31m 38s	256,494	1.2428%	1.3042%	1.2060%	-78.0%
1	0.0001	KIAD	May-17	fuel opt	65,431	5,947,674	6h 31m 38s	260,503	1.2394%	1.3042%	1.2059%	-77.6%
1	0.001	KIAD	May-17	fuel opt	65,434	5,947,674	6h 31m 38s	125,575	1.2448%	1.3042%	1.2066%	-89.2%
1	0.01	KIAD	May-17	fuel opt	65,441	5,947,674	6h 31m 38s	0	1.2552%	1.3042%	1.2091%	-100.0%
1	0.1	KIAD	May-17	fuel opt	65,441	5,947,674	6h 31m 38s	0	1.2550%	1.3042%	1.2077%	-100.0%
1	1	KIAD	May-17	fuel opt	65,441	5,947,674	6h 31m 38s	0	1.2552%	1.3042%	1.2091%	-100.0%
1	10	KIAD	May-17	fuel opt	65,441	5,947,674	6h 31m 38s	0	1.2552%	1.3042%	1.2091%	-100.0%
3	0	KIAD	May-17	fuel opt	67,980	6,179,691	6h 46m 17s	410,000	5.1837%	5.2560%	4.9953%	-64.8%
3	0.0001	KIAD	May-17	fuel opt	67,978	6,179,691	6h 46m 17s	425,000	5.1800%	5.2560%	4.9950%	-63.5%
3	0.001	KIAD	May-17	fuel opt	67,981	6,179,691	6h 46m 18s	325,846	5.1848%	5.2560%	4.9957%	-72.0%
3	0.01	KIAD	May-17	fuel opt	67,994	6,179,691	6h 46m 18s	165,846	5.2052%	5.2560%	4.9957%	-85.8%
3	0.1	KIAD	May-17	fuel opt	67,986	6,179,691	6h 46m 18s	65,922	5.1932%	5.2560%	4.9971%	-94.3%
3	1	KIAD	May-17	fuel opt	68,017	6,179,691	6h 46m 18s	166,769	5.2404%	5.2560%	4.9966%	-85.7%
3	10	KIAD	May-17	fuel opt	68,017	6,179,691	6h 46m 18s	166,769	5.2404%	5.2560%	4.9966%	-85.7%
10	0	KIAD	May-17	fuel opt	70,590	6,382,891	7h 1m 5s	120,639	9.2220%	8.7171%	8.8166%	-89.6%
10	0.0001	KIAD	May-17	fuel opt	70,588	6,382,891	7h 1m 5s	120,639	9.2182%	8.7171%	8.8164%	-89.6%
10	0.001	KIAD	May-17	fuel opt	70,588	6,382,891	7h 1m 5s	120,639	9.2182%	8.7171%	8.8164%	-89.6%
10	0.01	KIAD	May-17	fuel opt	70,593	6,382,891	7h 1m 5s	0	9.2263%	8.7171%	8.8169%	-100.0%
10	0.1	KIAD	May-17	fuel opt	70,593	6,382,891	7h 1m 5s	0	9.2263%	8.7171%	8.8169%	-100.0%
10	1	KIAD	May-17	fuel opt	70,593	6,382,891	7h 1m 5s	0	9.2263%	8.7171%	8.8169%	-100.0%
10	10	KIAD	May-17	fuel opt	70,593	6,382,891	7h 1m 5s	0	9.2263%	8.7171%	8.8169%	-100.0%

D. Numeric results - Hybrid mitigation

β_{grnd}	β_{prof}	Dest	Atm	Mode	dm [kg]	ds [m]	dt [h:m:s]	ct _{tot} [m]	% dm	% ds	% dt	% CT
0	0	CYWG	May-17	fuel opt	72,577	6,613,080	7h 12m 17s	1,360,000	0.0000%	0.0000%	0.0000%	0.0%
0	0.0001	CYWG	May-17	fuel opt	72,577	6,613,080	7h 12m 17s	1,360,000	0.0000%	0.0000%	0.0000%	0.0%
0	0.001	CYWG	May-17	fuel opt	72,582	6,613,080	7h 12m 18s	812,729	0.0065%	0.0000%	0.0008%	-40.2%
0	0.01	CYWG	May-17	fuel opt	72,613	6,613,080	7h 12m 18s	218,133	0.0490%	0.0000%	0.0006%	-84.0%
0	0.1	CYWG	May-17	fuel opt	72,613	6,613,080	7h 12m 18s	218,133	0.0490%	0.0000%	0.0006%	-84.0%
0	1	CYWG	May-17	fuel opt	72,613	6,613,080	7h 12m 18s	218,117	0.0489%	0.0000%	0.0009%	-84.0%
0	10	CYWG	May-17	fuel opt	72,617	6,613,080	7h 12m 18s	218,133	0.0551%	0.0000%	0.0007%	-84.0%
0.01	0	CYWG	May-17	fuel opt	72,582	6,613,255	7h 12m 17s	1,182,000	0.0065%	0.0026%	-0.0001%	-13.1%
0.01	0.0001	CYWG	May-17	fuel opt	72,577	6,613,255	7h 12m 17s	1,200,000	-0.0002%	0.0026%	0.0000%	-11.8%
0.01	0.001	CYWG	May-17	fuel opt	72,580	6,613,255	7h 12m 18s	920,863	0.0040%	0.0026%	0.0006%	-32.3%
0.01	0.01	CYWG	May-17	fuel opt	72,597	6,613,255	7h 12m 18s	218,133	0.0273%	0.0026%	0.0009%	-84.0%
0.01	0.1	CYWG	May-17	fuel opt	72,597	6,613,255	7h 12m 18s	218,117	0.0273%	0.0026%	0.0012%	-84.0%
0.01	1	CYWG	May-17	fuel opt	72,598	6,613,255	7h 12m 18s	218,117	0.0281%	0.0026%	0.0012%	-84.0%
0.01	10	CYWG	May-17	fuel opt	72,601	6,613,255	7h 12m 18s	218,117	0.0326%	0.0026%	0.0012%	-84.0%
0.03	0	CYWG	May-17	fuel opt	72,582	6,613,255	7h 12m 17s	1,182,000	0.0065%	0.0026%	-0.0001%	-13.1%
0.03	0.0001	CYWG	May-17	fuel opt	72,577	6,613,255	7h 12m 17s	1,200,000	-0.0002%	0.0026%	0.0000%	-11.8%
0.03	0.001	CYWG	May-17	fuel opt	72,581	6,613,255	7h 12m 18s	831,577	0.0053%	0.0026%	0.0006%	-38.9%
0.03	0.01	CYWG	May-17	fuel opt	72,590	6,613,255	7h 12m 18s	393,886	0.0178%	0.0026%	0.0014%	-71.0%
0.03	0.1	CYWG	May-17	fuel opt	72,597	6,613,255	7h 12m 18s	218,133	0.0268%	0.0026%	0.0009%	-84.0%
0.03	1	CYWG	May-17	fuel opt	72,600	6,613,255	7h 12m 18s	218,117	0.0317%	0.0026%	0.0012%	-84.0%
0.03	10	CYWG	May-17	fuel opt	72,598	6,613,255	7h 12m 18s	218,133	0.0283%	0.0026%	0.0009%	-84.0%
0.1	0	CYWG	May-17	fuel opt	73,161	6,665,746	7h 15m 37s	463,000	0.8041%	0.7964%	0.7697%	-66.0%
0.1	0.0001	CYWG	May-17	fuel opt	73,158	6,665,746	7h 15m 37s	470,000	0.7999%	0.7964%	0.7691%	-65.4%
0.1	0.001	CYWG	May-17	fuel opt	73,157	6,665,746	7h 15m 37s	250,000	0.7986%	0.7964%	0.7695%	-81.6%
0.1	0.01	CYWG	May-17	fuel opt	73,170	6,665,746	7h 15m 37s	0	0.8170%	0.7964%	0.7700%	-100.0%
0.1	0.1	CYWG	May-17	fuel opt	73,170	6,665,746	7h 15m 37s	0	0.8170%	0.7964%	0.7700%	-100.0%
0.1	1	CYWG	May-17	fuel opt	73,170	6,665,746	7h 15m 37s	0	0.8170%	0.7964%	0.7700%	-100.0%
0.1	10	CYWG	May-17	fuel opt	73,170	6,665,746	7h 15m 37s	0	0.8170%	0.7964%	0.7700%	-100.0%
0.3	0	CYWG	May-17	fuel opt	73,683	6,707,026	7h 18m 37s	315,000	1.5231%	1.4206%	1.4616%	-76.8%
0.3	0.0001	CYWG	May-17	fuel opt	73,680	6,707,026	7h 18m 36s	330,000	1.5186%	1.4206%	1.4607%	-75.7%
0.3	0.001	CYWG	May-17	fuel opt	73,683	6,707,026	7h 18m 36s	230,904	1.5235%	1.4206%	1.4612%	-83.0%
0.3	0.01	CYWG	May-17	fuel opt	73,688	6,707,026	7h 18m 37s	0	1.5301%	1.4206%	1.4615%	-100.0%
0.3	0.1	CYWG	May-17	fuel opt	73,688	6,707,026	7h 18m 37s	0	1.5301%	1.4206%	1.4615%	-100.0%
0.3	1	CYWG	May-17	fuel opt	73,688	6,707,026	7h 18m 37s	0	1.5301%	1.4206%	1.4615%	-100.0%
0.3	10	CYWG	May-17	fuel opt	73,688	6,707,026	7h 18m 37s	0	1.5301%	1.4206%	1.4615%	-100.0%
1	0	CYWG	May-17	fuel opt	73,911	6,726,331	7h 19m 53s	305,000	1.8380%	1.7125%	1.7574%	-77.6%
1	0.0001	CYWG	May-17	fuel opt	73,908	6,726,331	7h 19m 53s	315,000	1.8334%	1.7125%	1.7566%	-76.8%
1	0.001	CYWG	May-17	fuel opt	73,913	6,726,331	7h 19m 53s	220,901	1.8402%	1.7125%	1.7570%	-83.8%
1	0.01	CYWG	May-17	fuel opt	73,924	6,726,331	7h 19m 53s	70,000	1.8552%	1.7125%	1.7572%	-94.9%
1	0.1	CYWG	May-17	fuel opt	73,916	6,726,331	7h 19m 53s	0	1.8449%	1.7125%	1.7574%	-100.0%
1	1	CYWG	May-17	fuel opt	73,916	6,726,331	7h 19m 53s	0	1.8449%	1.7125%	1.7574%	-100.0%
1	10	CYWG	May-17	fuel opt	73,916	6,726,331	7h 19m 53s	0	1.8449%	1.7125%	1.7574%	-100.0%
3	0	CYWG	May-17	fuel opt	79,938	7,241,571	7h 53m 47s	437,000	10.1423%	9.5038%	9.5991%	-67.9%
3	0.0001	CYWG	May-17	fuel opt	79,935	7,241,571	7h 53m 47s	445,000	10.1379%	9.5038%	9.5987%	-67.3%
3	0.001	CYWG	May-17	fuel opt	79,941	7,241,571	7h 53m 47s	195,000	10.1456%	9.5038%	9.5989%	-85.7%
3	0.01	CYWG	May-17	fuel opt	79,943	7,241,571	7h 53m 47s	141,065	10.1484%	9.5038%	9.5989%	-89.6%
3	0.1	CYWG	May-17	fuel opt	79,942	7,241,571	7h 53m 47s	0	10.1475%	9.5038%	9.5994%	-100.0%
3	1	CYWG	May-17	fuel opt	79,942	7,241,571	7h 53m 47s	0	10.1475%	9.5038%	9.5994%	-100.0%
3	10	CYWG	May-17	fuel opt	79,942	7,241,571	7h 53m 47s	0	10.1475%	9.5038%	9.5994%	-100.0%
10	0	CYWG	May-17	fuel opt	79,938	7,241,571	7h 53m 47s	437,000	10.1423%	9.5038%	9.5991%	-67.9%
10	0.0001	CYWG	May-17	fuel opt	79,935	7,241,571	7h 53m 47s	445,000	10.1379%	9.5038%	9.5987%	-67.3%
10	0.001	CYWG	May-17	fuel opt	79,941	7,241,571	7h 53m 47s	195,000	10.1456%	9.5038%	9.5989%	-85.7%
10	0.01	CYWG	May-17	fuel opt	79,943	7,241,571	7h 53m 47s	156,066	10.1483%	9.5038%	9.5989%	-88.5%
10	0.1	CYWG	May-17	fuel opt	79,942	7,241,571	7h 53m 47s	0	10.1475%	9.5038%	9.5994%	-100.0%
10	1	CYWG	May-17	fuel opt	79,942	7,241,571	7h 53m 47s	0	10.1476%	9.5038%	9.5994%	-100.0%
10	10	CYWG	May-17	fuel opt	79,942	7,241,571	7h 53m 47s	0	10.1475%	9.5038%	9.5994%	-100.0%

β_{grnd}	β_{prof}	Dest	Atm	Mode	dm [kg]	ds [m]	dt [h:m:s]	ct _{tot} [m]	% dm	% ds	% dt	% CT
0	0	CYVR	May-17	fuel opt	87,780	7,931,614	8h 36m 55s	1,037,044	0.0000%	0.0000%	0.0000%	0.0%
0	0.0001	CYVR	May-17	fuel opt	87,780	7,931,614	8h 36m 55s	961,108	-0.0002%	0.0000%	-0.0003%	-7.3%
0	0.001	CYVR	May-17	fuel opt	87,814	7,931,614	8h 36m 55s	192,123	0.0383%	0.0000%	0.0001%	-81.5%
0	0.01	CYVR	May-17	fuel opt	87,823	7,931,614	8h 36m 56s	70,000	0.0491%	0.0000%	0.0028%	-93.3%
0	0.1	CYVR	May-17	fuel opt	87,809	7,931,614	8h 36m 54s	0	0.0327%	0.0000%	-0.0013%	-100.0%
0	1	CYVR	May-17	fuel opt	87,809	7,931,614	8h 36m 54s	0	0.0327%	0.0000%	-0.0013%	-100.0%
0	10	CYVR	May-17	fuel opt	87,809	7,931,614	8h 36m 54s	0	0.0327%	0.0000%	-0.0013%	-100.0%
0.01	0	CYVR	May-17	fuel opt	87,783	7,931,614	8h 36m 55s	1,022,041	0.0032%	0.0000%	-0.0003%	-1.4%
0.01	0.0001	CYVR	May-17	fuel opt	87,780	7,931,614	8h 36m 55s	961,108	-0.0002%	0.0000%	-0.0003%	-7.3%
0.01	0.001	CYVR	May-17	fuel opt	87,814	7,931,614	8h 36m 55s	192,123	0.0383%	0.0000%	0.0001%	-81.5%
0.01	0.01	CYVR	May-17	fuel opt	87,809	7,931,614	8h 36m 54s	0	0.0327%	0.0000%	-0.0013%	-100.0%
0.01	0.1	CYVR	May-17	fuel opt	87,809	7,931,614	8h 36m 54s	0	0.0327%	0.0000%	-0.0013%	-100.0%
0.01	1	CYVR	May-17	fuel opt	87,809	7,931,614	8h 36m 54s	0	0.0327%	0.0000%	-0.0013%	-100.0%
0.01	10	CYVR	May-17	fuel opt	87,809	7,931,614	8h 36m 54s	0	0.0327%	0.0000%	-0.0013%	-100.0%
0.03	0	CYVR	May-17	fuel opt	87,783	7,931,614	8h 36m 55s	1,022,041	0.0032%	0.0000%	-0.0003%	-1.4%
0.03	0.0001	CYVR	May-17	fuel opt	87,780	7,931,614	8h 36m 55s	961,108	-0.0002%	0.0000%	-0.0003%	-7.3%
0.03	0.001	CYVR	May-17	fuel opt	87,817	7,931,614	8h 36m 55s	70,000	0.0421%	0.0000%	0.0015%	-93.3%
0.03	0.01	CYVR	May-17	fuel opt	87,809	7,931,614	8h 36m 54s	0	0.0327%	0.0000%	-0.0013%	-100.0%
0.03	0.1	CYVR	May-17	fuel opt	87,809	7,931,614	8h 36m 54s	0	0.0327%	0.0000%	-0.0013%	-100.0%
0.03	1	CYVR	May-17	fuel opt	87,809	7,931,614	8h 36m 54s	0	0.0327%	0.0000%	-0.0013%	-100.0%
0.03	10	CYVR	May-17	fuel opt	87,809	7,931,614	8h 36m 54s	0	0.0327%	0.0000%	-0.0013%	-100.0%
0.1	0	CYVR	May-17	fuel opt	87,894	7,938,204	8h 37m 30s	917,986	0.1298%	0.0831%	0.1127%	-11.5%
0.1	0.0001	CYVR	May-17	fuel opt	87,891	7,938,204	8h 37m 30s	841,057	0.1264%	0.0831%	0.1128%	-18.9%
0.1	0.001	CYVR	May-17	fuel opt	87,902	7,938,204	8h 37m 30s	0	0.1388%	0.0831%	0.1118%	-100.0%
0.1	0.01	CYVR	May-17	fuel opt	87,902	7,938,204	8h 37m 30s	0	0.1388%	0.0831%	0.1118%	-100.0%
0.1	0.1	CYVR	May-17	fuel opt	87,902	7,938,204	8h 37m 30s	0	0.1388%	0.0831%	0.1118%	-100.0%
0.1	1	CYVR	May-17	fuel opt	87,905	7,938,204	8h 37m 30s	0	0.1425%	0.0831%	0.1135%	-100.0%
0.1	10	CYVR	May-17	fuel opt	87,905	7,938,204	8h 37m 30s	0	0.1425%	0.0831%	0.1135%	-100.0%
0.3	0	CYVR	May-17	fuel opt	88,481	7,990,746	8h 40m 41s	497,057	0.7982%	0.7455%	0.7306%	-52.1%
0.3	0.0001	CYVR	May-17	fuel opt	88,478	7,990,746	8h 40m 42s	501,057	0.7950%	0.7455%	0.7310%	-51.7%
0.3	0.001	CYVR	May-17	fuel opt	88,487	7,990,746	8h 40m 41s	122,095	0.8059%	0.7455%	0.7308%	-88.2%
0.3	0.01	CYVR	May-17	fuel opt	88,490	7,990,746	8h 40m 42s	0	0.8090%	0.7455%	0.7311%	-100.0%
0.3	0.1	CYVR	May-17	fuel opt	88,490	7,990,746	8h 40m 42s	0	0.8090%	0.7455%	0.7311%	-100.0%
0.3	1	CYVR	May-17	fuel opt	88,490	7,990,746	8h 40m 42s	0	0.8090%	0.7455%	0.7311%	-100.0%
0.3	10	CYVR	May-17	fuel opt	88,490	7,990,746	8h 40m 42s	0	0.8090%	0.7455%	0.7311%	-100.0%
1	0	CYVR	May-17	fuel opt	89,799	8,104,466	8h 47m 56s	486,605	2.3005%	2.1793%	2.1322%	-53.1%
1	0.0001	CYVR	May-17	fuel opt	89,797	8,104,466	8h 47m 56s	371,057	2.2975%	2.1793%	2.1327%	-64.2%
1	0.001	CYVR	May-17	fuel opt	89,801	8,104,466	8h 47m 56s	0	2.3027%	2.1793%	2.1328%	-100.0%
1	0.01	CYVR	May-17	fuel opt	89,801	8,104,466	8h 47m 56s	0	2.3027%	2.1793%	2.1328%	-100.0%
1	0.1	CYVR	May-17	fuel opt	89,801	8,104,466	8h 47m 56s	0	2.3027%	2.1793%	2.1328%	-100.0%
1	1	CYVR	May-17	fuel opt	89,801	8,104,466	8h 47m 56s	0	2.3027%	2.1793%	2.1328%	-100.0%
1	10	CYVR	May-17	fuel opt	89,801	8,104,466	8h 47m 56s	0	2.3027%	2.1793%	2.1328%	-100.0%
3	0	CYVR	May-17	fuel opt	93,680	8,419,506	9h 9m 14s	0	6.7219%	6.1512%	6.2526%	-100.0%
3	0.0001	CYVR	May-17	fuel opt	93,678	8,419,506	9h 9m 14s	0	6.7187%	6.1512%	6.2531%	-100.0%
3	0.001	CYVR	May-17	fuel opt	93,678	8,419,506	9h 9m 14s	0	6.7187%	6.1512%	6.2531%	-100.0%
3	0.01	CYVR	May-17	fuel opt	93,678	8,419,506	9h 9m 14s	0	6.7187%	6.1512%	6.2531%	-100.0%
3	0.1	CYVR	May-17	fuel opt	93,678	8,419,506	9h 9m 14s	0	6.7187%	6.1512%	6.2531%	-100.0%
3	1	CYVR	May-17	fuel opt	93,678	8,419,506	9h 9m 14s	0	6.7187%	6.1512%	6.2531%	-100.0%
3	10	CYVR	May-17	fuel opt	93,678	8,419,506	9h 9m 14s	0	6.7187%	6.1512%	6.2531%	-100.0%
10	0	CYVR	May-17	fuel opt	93,680	8,419,506	9h 9m 14s	0	6.7219%	6.1512%	6.2526%	-100.0%
10	0.0001	CYVR	May-17	fuel opt	93,678	8,419,506	9h 9m 14s	0	6.7187%	6.1512%	6.2531%	-100.0%
10	0.001	CYVR	May-17	fuel opt	93,678	8,419,506	9h 9m 14s	0	6.7187%	6.1512%	6.2531%	-100.0%
10	0.01	CYVR	May-17	fuel opt	93,678	8,419,506	9h 9m 14s	0	6.7187%	6.1512%	6.2531%	-100.0%
10	0.1	CYVR	May-17	fuel opt	93,678	8,419,506	9h 9m 14s	0	6.7187%	6.1512%	6.2531%	-100.0%
10	1	CYVR	May-17	fuel opt	93,678	8,419,506	9h 9m 14s	0	6.7187%	6.1512%	6.2531%	-100.0%
10	10	CYVR	May-17	fuel opt	93,678	8,419,506	9h 9m 14s	0	6.7187%	6.1512%	6.2531%	-100.0%

D. Numeric results - Hybrid mitigation

β_{grnd}	β_{prof}	Dest	Atm	Mode	dm [kg]	ds [m]	dt [h:m:s]	ct _{tot} [m]	% dm	% ds	% dt	% CT
0	0	KIAD	Feb-14	time opt	74,108	5,937,317	6h 16m 15s	2,315,000	0.0000%	0.0000%	0.0000%	0.0%
0	0.0001	KIAD	Feb-14	time opt	74,108	5,937,317	6h 16m 15s	2,315,000	0.0000%	0.0000%	0.0000%	0.0%
0	0.001	KIAD	Feb-14	time opt	74,108	5,937,317	6h 16m 15s	2,315,000	0.0000%	0.0000%	0.0000%	0.0%
0	0.01	KIAD	Feb-14	time opt	74,729	6,056,837	6h 26m 20s	688,336	0.8378%	2.0130%	2.6759%	-70.3%
0	0.1	KIAD	Feb-14	time opt	73,257	5,929,677	6h 19m 27s	115,000	-1.1493%	-0.1287%	0.8491%	-95.0%
0	1	KIAD	Feb-14	time opt	73,229	5,929,677	6h 19m 30s	115,000	-1.1864%	-0.1287%	0.8632%	-95.0%
0	10	KIAD	Feb-14	time opt	73,229	5,929,677	6h 19m 30s	115,000	-1.1864%	-0.1287%	0.8632%	-95.0%
0.01	0	KIAD	Feb-14	time opt	74,023	5,929,677	6h 15m 46s	2,424,057	-0.1150%	-0.1287%	-0.1299%	4.7%
0.01	0.0001	KIAD	Feb-14	time opt	74,108	5,937,317	6h 16m 15s	2,315,000	0.0000%	0.0000%	0.0000%	0.0%
0.01	0.001	KIAD	Feb-14	time opt	73,709	5,936,952	6h 16m 53s	1,160,000	-0.5383%	-0.0062%	0.1662%	-49.9%
0.01	0.01	KIAD	Feb-14	time opt	74,712	6,060,136	6h 26m 58s	403,333	0.8151%	2.0686%	2.8475%	-82.6%
0.01	0.1	KIAD	Feb-14	time opt	73,229	5,929,677	6h 19m 30s	115,000	-1.1864%	-0.1287%	0.8632%	-95.0%
0.01	1	KIAD	Feb-14	time opt	73,257	5,929,677	6h 19m 26s	115,000	-1.1487%	-0.1287%	0.8444%	-95.0%
0.01	10	KIAD	Feb-14	time opt	73,250	5,929,677	6h 19m 13s	295,816	-1.1585%	-0.1287%	0.7874%	-87.2%
0.03	0	KIAD	Feb-14	time opt	74,052	5,933,817	6h 15m 57s	2,365,197	-0.0763%	-0.0590%	-0.0811%	2.2%
0.03	0.0001	KIAD	Feb-14	time opt	74,149	5,942,347	6h 16m 30s	2,260,000	0.0554%	0.0847%	0.0632%	-2.4%
0.03	0.001	KIAD	Feb-14	time opt	74,149	5,942,347	6h 16m 30s	2,260,000	0.0554%	0.0847%	0.0632%	-2.4%
0.03	0.01	KIAD	Feb-14	time opt	74,674	6,060,470	6h 26m 52s	238,337	0.7630%	2.0742%	2.8193%	-89.7%
0.03	0.1	KIAD	Feb-14	time opt	74,697	6,060,538	6h 26m 49s	238,337	0.7940%	2.0754%	2.8066%	-89.7%
0.03	1	KIAD	Feb-14	time opt	74,678	6,060,457	6h 26m 52s	238,337	0.7687%	2.0740%	2.8193%	-89.7%
0.03	10	KIAD	Feb-14	time opt	74,731	6,060,602	6h 26m 51s	238,336	0.8399%	2.0764%	2.8153%	-89.7%
0.1	0	KIAD	Feb-14	time opt	74,940	6,018,623	6h 20m 16s	990,003	1.1229%	1.3694%	1.0675%	-57.2%
0.1	0.0001	KIAD	Feb-14	time opt	75,056	6,028,022	6h 20m 52s	880,000	1.2787%	1.5277%	1.2235%	-62.0%
0.1	0.001	KIAD	Feb-14	time opt	75,056	6,028,022	6h 20m 52s	880,000	1.2787%	1.5277%	1.2235%	-62.0%
0.1	0.01	KIAD	Feb-14	time opt	76,008	6,147,136	6h 30m 26s	133,336	2.5632%	3.5339%	3.7669%	-94.2%
0.1	0.1	KIAD	Feb-14	time opt	76,026	6,147,178	6h 30m 22s	133,336	2.5872%	3.5346%	3.7518%	-94.2%
0.1	1	KIAD	Feb-14	time opt	76,000	6,147,914	6h 30m 27s	123,335	2.5533%	3.5470%	3.7722%	-94.7%
0.1	10	KIAD	Feb-14	time opt	76,000	6,147,949	6h 30m 27s	123,335	2.5533%	3.5476%	3.7733%	-94.7%
0.3	0	KIAD	Feb-14	time opt	75,511	6,068,225	6h 23m 8s	771,605	1.8929%	2.2048%	1.8292%	-66.7%
0.3	0.0001	KIAD	Feb-14	time opt	75,575	6,073,426	6h 23m 28s	660,000	1.9797%	2.2924%	1.9150%	-71.5%
0.3	0.001	KIAD	Feb-14	time opt	75,575	6,073,426	6h 23m 28s	660,000	1.9797%	2.2924%	1.9150%	-71.5%
0.3	0.01	KIAD	Feb-14	time opt	76,697	6,198,585	6h 33m 8s	208,335	3.4931%	4.4004%	4.4829%	-91.0%
0.3	0.1	KIAD	Feb-14	time opt	76,630	6,196,150	6h 33m 1s	123,337	3.4023%	4.3594%	4.4547%	-94.7%
0.3	1	KIAD	Feb-14	time opt	76,630	6,196,150	6h 33m 1s	123,337	3.4023%	4.3594%	4.4547%	-94.7%
0.3	10	KIAD	Feb-14	time opt	76,630	6,196,150	6h 33m 1s	123,337	3.4023%	4.3594%	4.4547%	-94.7%
1	0	KIAD	Feb-14	time opt	75,906	6,100,165	6h 25m 1s	692,545	2.4263%	2.7428%	2.3295%	-70.1%
1	0.0001	KIAD	Feb-14	time opt	76,014	6,108,760	6h 25m 33s	575,000	2.5719%	2.8875%	2.4714%	-75.2%
1	0.001	KIAD	Feb-14	time opt	76,014	6,108,760	6h 25m 33s	575,000	2.5719%	2.8875%	2.4714%	-75.2%
1	0.01	KIAD	Feb-14	time opt	77,075	6,228,881	6h 34m 53s	123,336	4.0031%	4.9107%	4.9521%	-94.7%
1	0.1	KIAD	Feb-14	time opt	77,075	6,228,881	6h 34m 53s	123,336	4.0031%	4.9107%	4.9521%	-94.7%
1	1	KIAD	Feb-14	time opt	77,075	6,228,881	6h 34m 53s	123,336	4.0031%	4.9107%	4.9521%	-94.7%
1	10	KIAD	Feb-14	time opt	77,075	6,228,881	6h 34m 53s	123,336	4.0031%	4.9107%	4.9521%	-94.7%
3	0	KIAD	Feb-14	time opt	89,838	7,172,740	7h 33m 19s	209,120	21.2256%	20.8078%	20.4784%	-91.0%
3	0.0001	KIAD	Feb-14	time opt	89,924	7,179,581	7h 33m 44s	80,000	21.3416%	20.9230%	20.5914%	-96.5%
3	0.001	KIAD	Feb-14	time opt	89,924	7,179,581	7h 33m 44s	80,000	21.3416%	20.9230%	20.5914%	-96.5%
3	0.01	KIAD	Feb-14	time opt	89,924	7,179,581	7h 33m 44s	80,000	21.3416%	20.9230%	20.5914%	-96.5%
3	0.1	KIAD	Feb-14	time opt	89,924	7,179,581	7h 33m 44s	80,000	21.3416%	20.9230%	20.5914%	-96.5%
3	1	KIAD	Feb-14	time opt	89,924	7,179,581	7h 33m 44s	80,000	21.3416%	20.9230%	20.5914%	-96.5%
3	10	KIAD	Feb-14	time opt	89,924	7,179,581	7h 33m 44s	80,000	21.3416%	20.9230%	20.5914%	-96.5%
10	0	KIAD	Feb-14	time opt	90,046	7,189,540	7h 34m 22s	208,920	21.5064%	21.0907%	20.7586%	-91.0%
10	0.0001	KIAD	Feb-14	time opt	90,111	7,194,726	7h 34m 41s	80,000	21.5938%	21.1781%	20.8442%	-96.5%
10	0.001	KIAD	Feb-14	time opt	90,111	7,194,726	7h 34m 41s	80,000	21.5938%	21.1781%	20.8442%	-96.5%
10	0.01	KIAD	Feb-14	time opt	90,111	7,194,726	7h 34m 41s	80,000	21.5938%	21.1781%	20.8442%	-96.5%
10	0.1	KIAD	Feb-14	time opt	90,111	7,194,726	7h 34m 41s	80,000	21.5938%	21.1781%	20.8442%	-96.5%
10	1	KIAD	Feb-14	time opt	90,111	7,194,726	7h 34m 41s	80,000	21.5938%	21.1781%	20.8442%	-96.5%
10	10	KIAD	Feb-14	time opt	90,111	7,194,726	7h 34m 41s	80,000	21.5938%	21.1781%	20.8442%	-96.5%

β_{grnd}	β_{prof}	Dest	Atm	Mode	dm [kg]	ds [m]	dt [h:m:s]	ct _{tot} [m]	% dm	% ds	% dt	% CT
0	0	CYWG	Feb-14	time opt	85,065	6,777,028	7h 10m 9s	2,940,000	0.0000%	0.0000%	0.0000%	0.0%
0	0.0001	CYWG	Feb-14	time opt	85,065	6,777,028	7h 10m 9s	2,940,000	0.0000%	0.0000%	0.0000%	0.0%
0	0.001	CYWG	Feb-14	time opt	85,065	6,777,028	7h 10m 9s	2,940,000	0.0000%	0.0000%	0.0000%	0.0%
0	0.01	CYWG	Feb-14	time opt	85,919	6,955,512	7h 28m 59s	1,126,356	1.0049%	2.6337%	4.3775%	-61.7%
0	0.1	CYWG	Feb-14	time opt	85,901	6,955,660	7h 29m 30s	963,072	0.9834%	2.6358%	4.4982%	-67.2%
0	1	CYWG	Feb-14	time opt	85,906	6,955,617	7h 29m 33s	963,026	0.9895%	2.6352%	4.5089%	-67.2%
0	10	CYWG	Feb-14	time opt	85,876	6,953,962	7h 29m 13s	1,144,367	0.9538%	2.6108%	4.4306%	-61.1%
0.01	0	CYWG	Feb-14	time opt	84,974	6,770,462	7h 9m 42s	2,726,633	-0.1066%	-0.0969%	-0.1075%	-7.3%
0.01	0.0001	CYWG	Feb-14	time opt	84,985	6,777,215	7h 10m 11s	2,325,000	-0.0936%	0.0028%	0.0054%	-20.9%
0.01	0.001	CYWG	Feb-14	time opt	84,985	6,777,215	7h 10m 11s	2,325,000	-0.0936%	0.0028%	0.0054%	-20.9%
0.01	0.01	CYWG	Feb-14	time opt	86,501	6,955,418	7h 27m 12s	1,223,058	1.6889%	2.6323%	3.9611%	-58.4%
0.01	0.1	CYWG	Feb-14	time opt	86,064	6,957,424	7h 29m 17s	1,114,467	1.1753%	2.6619%	4.4449%	-62.1%
0.01	1	CYWG	Feb-14	time opt	86,067	6,957,422	7h 29m 15s	1,114,461	1.1785%	2.6618%	4.4406%	-62.1%
0.01	10	CYWG	Feb-14	time opt	86,067	6,957,422	7h 29m 15s	1,114,461	1.1785%	2.6618%	4.4406%	-62.1%
0.03	0	CYWG	Feb-14	time opt	85,292	6,796,563	7h 11m 12s	1,647,734	0.2670%	0.2882%	0.2416%	-44.0%
0.03	0.0001	CYWG	Feb-14	time opt	85,358	6,802,142	7h 11m 33s	1,535,000	0.3446%	0.3706%	0.3237%	-47.8%
0.03	0.001	CYWG	Feb-14	time opt	85,358	6,802,142	7h 11m 33s	1,535,000	0.3446%	0.3706%	0.3237%	-47.8%
0.03	0.01	CYWG	Feb-14	time opt	86,496	6,926,836	7h 21m 26s	1,000,472	1.6824%	2.2105%	2.6234%	-66.0%
0.03	0.1	CYWG	Feb-14	time opt	86,265	6,927,884	7h 22m 22s	810,474	1.4116%	2.2260%	2.8373%	-72.4%
0.03	1	CYWG	Feb-14	time opt	86,265	6,927,884	7h 22m 22s	810,474	1.4116%	2.2260%	2.8373%	-72.4%
0.03	10	CYWG	Feb-14	time opt	86,265	6,927,884	7h 22m 22s	810,474	1.4116%	2.2260%	2.8373%	-72.4%
0.1	0	CYWG	Feb-14	time opt	85,428	6,807,353	7h 11m 53s	1,469,524	0.4274%	0.4475%	0.4016%	-50.0%
0.1	0.0001	CYWG	Feb-14	time opt	85,551	6,817,294	7h 12m 30s	1,365,000	0.5718%	0.5941%	0.5466%	-53.6%
0.1	0.001	CYWG	Feb-14	time opt	85,551	6,817,294	7h 12m 30s	1,365,000	0.5718%	0.5941%	0.5466%	-53.6%
0.1	0.01	CYWG	Feb-14	time opt	86,352	6,879,889	7h 16m 46s	1,218,498	1.5139%	1.5178%	1.5374%	-58.3%
0.1	0.1	CYWG	Feb-14	time opt	86,372	6,837,250	7h 23m 2s	697,260	1.5369%	2.3642%	2.9951%	-76.3%
0.1	1	CYWG	Feb-14	time opt	86,395	6,936,726	7h 23m 15s	696,721	1.5641%	2.3565%	3.0448%	-76.3%
0.1	10	CYWG	Feb-14	time opt	86,395	6,936,708	7h 23m 14s	696,703	1.5634%	2.3562%	3.0418%	-76.3%
0.3	0	CYWG	Feb-14	time opt	86,661	6,905,110	7h 17m 54s	1,030,281	1.8763%	1.8899%	1.7990%	-65.0%
0.3	0.0001	CYWG	Feb-14	time opt	86,760	6,913,182	7h 18m 24s	915,000	1.9936%	2.0091%	1.9167%	-68.9%
0.3	0.001	CYWG	Feb-14	time opt	86,760	6,913,182	7h 18m 24s	915,000	1.9936%	2.0091%	1.9167%	-68.9%
0.3	0.01	CYWG	Feb-14	time opt	86,760	6,913,182	7h 18m 24s	915,000	1.9936%	2.0091%	1.9167%	-68.9%
0.3	0.1	CYWG	Feb-14	time opt	87,418	6,978,688	7h 23m 50s	677,146	2.7671%	2.9756%	3.1803%	-77.0%
0.3	1	CYWG	Feb-14	time opt	87,411	6,979,162	7h 23m 45s	677,623	2.7578%	2.9826%	3.1607%	-77.0%
0.3	10	CYWG	Feb-14	time opt	87,413	6,979,159	7h 23m 46s	677,620	2.7606%	2.9826%	3.1643%	-77.0%
1	0	CYWG	Feb-14	time opt	88,035	7,015,429	7h 24m 35s	875,601	3.4918%	3.5178%	3.3536%	-70.2%
1	0.0001	CYWG	Feb-14	time opt	88,146	7,024,375	7h 25m 9s	755,000	3.6228%	3.6498%	3.4841%	-74.3%
1	0.001	CYWG	Feb-14	time opt	88,146	7,024,375	7h 25m 9s	755,000	3.6228%	3.6498%	3.4841%	-74.3%
1	0.01	CYWG	Feb-14	time opt	88,146	7,024,375	7h 25m 9s	755,000	3.6228%	3.6498%	3.4841%	-74.3%
1	0.1	CYWG	Feb-14	time opt	88,838	7,086,552	7h 29m 47s	657,972	4.4365%	4.5673%	4.5642%	-77.6%
1	1	CYWG	Feb-14	time opt	88,838	7,086,552	7h 29m 47s	657,972	4.4365%	4.5673%	4.5642%	-77.6%
1	10	CYWG	Feb-14	time opt	88,838	7,086,552	7h 29m 47s	657,972	4.4365%	4.5673%	4.5642%	-77.6%
3	0	CYWG	Feb-14	time opt	100,691	7,979,054	8h 25m 56s	427,225	18.3702%	17.7368%	17.6158%	-85.5%
3	0.0001	CYWG	Feb-14	time opt	-	-	-	-	-	-	-	-
3	0.001	CYWG	Feb-14	time opt	-	-	-	-	-	-	-	-
3	0.01	CYWG	Feb-14	time opt	-	-	-	-	-	-	-	-
3	0.1	CYWG	Feb-14	time opt	-	-	-	-	-	-	-	-
3	1	CYWG	Feb-14	time opt	-	-	-	-	-	-	-	-
3	10	CYWG	Feb-14	time opt	-	-	-	-	-	-	-	-
10	0	CYWG	Feb-14	time opt	113,295	8,930,784	9h 25m 51s	245,956	33.1867%	31.7802%	31.5459%	-91.6%
10	0.0001	CYWG	Feb-14	time opt	-	-	-	-	-	-	-	-
10	0.001	CYWG	Feb-14	time opt	-	-	-	-	-	-	-	-
10	0.01	CYWG	Feb-14	time opt	-	-	-	-	-	-	-	-
10	0.1	CYWG	Feb-14	time opt	-	-	-	-	-	-	-	-
10	1	CYWG	Feb-14	time opt	-	-	-	-	-	-	-	-
10	10	CYWG	Feb-14	time opt	-	-	-	-	-	-	-	-

D. Numeric results - Hybrid mitigation

β_{grnd}	β_{prof}	Dest	Atm	Mode	dm [kg]	ds [m]	dt [h:m:s]	ct_{tot} [m]	% dm	% ds	% dt	% CT
0	0	CYVR	Feb-14	time opt	97,849	7,786,731	8h 12m 9s	2,700,000	0.0000%	0.0000%	0.0000%	0.0%
0	0.0001	CYVR	Feb-14	time opt	97,849	7,786,731	8h 12m 9s	2,700,000	0.0000%	0.0000%	0.0000%	0.0%
0	0.001	CYVR	Feb-14	time opt	97,849	7,786,731	8h 12m 9s	2,700,000	0.0000%	0.0000%	0.0000%	0.0%
0	0.01	CYVR	Feb-14	time opt	97,421	7,782,597	8h 12m 23s	1,863,833	-0.4384%	-0.0531%	0.0502%	-31.0%
0	0.1	CYVR	Feb-14	time opt	98,203	7,905,441	8h 22m 49s	1,339,153	0.3615%	1.5245%	2.1674%	-50.4%
0	1	CYVR	Feb-14	time opt	98,252	7,905,917	8h 23m 12s	1,280,713	0.4115%	1.5306%	2.2467%	-52.6%
0	10	CYVR	Feb-14	time opt	98,192	7,905,524	8h 23m 14s	1,280,659	0.3500%	1.5256%	2.2545%	-52.6%
0.01	0	CYVR	Feb-14	time opt	97,735	7,777,291	8h 11m 33s	2,806,544	-0.1166%	-0.1212%	-0.1208%	3.9%
0.01	0.0001	CYVR	Feb-14	time opt	97,849	7,786,731	8h 12m 9s	2,700,000	0.0000%	0.0000%	0.0000%	0.0%
0.01	0.001	CYVR	Feb-14	time opt	97,849	7,786,731	8h 12m 9s	2,700,000	0.0000%	0.0000%	0.0000%	0.0%
0.01	0.01	CYVR	Feb-14	time opt	97,423	7,782,595	8h 12m 23s	1,863,833	-0.4356%	-0.0531%	0.0497%	-31.0%
0.01	0.1	CYVR	Feb-14	time opt	98,332	7,905,370	8h 22m 8s	1,275,912	0.4934%	1.5236%	2.0284%	-52.7%
0.01	1	CYVR	Feb-14	time opt	98,198	7,905,244	8h 23m 13s	1,338,961	0.3562%	1.5220%	2.2508%	-50.4%
0.01	10	CYVR	Feb-14	time opt	98,210	7,905,807	8h 23m 14s	1,280,660	0.3688%	1.5292%	2.2543%	-52.6%
0.03	0	CYVR	Feb-14	time opt	97,759	7,778,991	8h 11m 41s	2,685,244	-0.0921%	-0.0994%	-0.0953%	-0.5%
0.03	0.0001	CYVR	Feb-14	time opt	97,851	7,786,731	8h 12m 10s	2,575,000	0.0015%	0.0000%	0.0041%	-4.6%
0.03	0.001	CYVR	Feb-14	time opt	97,851	7,786,731	8h 12m 10s	2,575,000	0.0015%	0.0000%	0.0041%	-4.6%
0.03	0.01	CYVR	Feb-14	time opt	97,488	7,787,662	8h 12m 44s	1,748,833	-0.3698%	0.0120%	0.1185%	-35.2%
0.03	0.1	CYVR	Feb-14	time opt	98,264	7,910,384	8h 23m 5s	1,204,098	0.4235%	1.5880%	2.2212%	-55.4%
0.03	1	CYVR	Feb-14	time opt	98,251	7,905,856	8h 23m 7s	1,140,711	0.4107%	1.5298%	2.2293%	-57.8%
0.03	10	CYVR	Feb-14	time opt	98,258	7,910,664	8h 23m 6s	1,140,794	0.4175%	1.5916%	2.2251%	-57.7%
0.1	0	CYVR	Feb-14	time opt	97,928	7,791,011	8h 12m 29s	2,455,264	0.0798%	0.0550%	0.0687%	-9.1%
0.1	0.0001	CYVR	Feb-14	time opt	97,996	7,796,867	8h 12m 51s	2,330,000	0.1495%	0.1302%	0.1439%	-13.7%
0.1	0.001	CYVR	Feb-14	time opt	97,996	7,796,867	8h 12m 51s	2,330,000	0.1495%	0.1302%	0.1439%	-13.7%
0.1	0.01	CYVR	Feb-14	time opt	98,692	7,920,849	8h 22m 34s	1,148,157	0.8611%	1.7224%	2.1179%	-57.5%
0.1	0.1	CYVR	Feb-14	time opt	98,554	7,921,001	8h 22m 60s	945,720	0.7203%	1.7243%	2.2043%	-65.0%
0.1	1	CYVR	Feb-14	time opt	98,552	7,920,870	8h 23m 23s	945,591	0.7177%	1.7227%	2.2826%	-65.0%
0.1	10	CYVR	Feb-14	time opt	98,549	7,920,866	8h 23m 23s	945,591	0.7154%	1.7226%	2.2827%	-65.0%
0.3	0	CYVR	Feb-14	time opt	99,673	7,924,810	8h 20m 54s	1,725,063	1.8641%	1.7733%	1.7794%	-36.1%
0.3	0.0001	CYVR	Feb-14	time opt	99,779	7,933,462	8h 21m 27s	1,610,000	1.9715%	1.8844%	1.8900%	-40.4%
0.3	0.001	CYVR	Feb-14	time opt	99,779	7,933,462	8h 21m 27s	1,610,000	1.9715%	1.8844%	1.8900%	-40.4%
0.3	0.01	CYVR	Feb-14	time opt	99,395	7,933,395	8h 21m 47s	925,000	1.5792%	1.8835%	1.9589%	-65.7%
0.3	0.1	CYVR	Feb-14	time opt	99,182	7,934,311	8h 22m 44s	737,515	1.3622%	1.8953%	2.1523%	-72.7%
0.3	1	CYVR	Feb-14	time opt	99,251	7,933,344	8h 22m 29s	732,418	1.4324%	1.8829%	2.0992%	-72.9%
0.3	10	CYVR	Feb-14	time opt	99,181	7,934,213	8h 23m 6s	737,419	1.3609%	1.8940%	2.2266%	-72.7%
1	0	CYVR	Feb-14	time opt	101,317	8,051,229	8h 28m 48s	1,562,482	3.5441%	3.3968%	3.3834%	-42.1%
1	0.0001	CYVR	Feb-14	time opt	101,425	8,060,044	8h 29m 21s	1,440,000	3.6543%	3.5100%	3.4959%	-46.7%
1	0.001	CYVR	Feb-14	time opt	101,425	8,060,044	8h 29m 21s	1,440,000	3.6543%	3.5100%	3.4959%	-46.7%
1	0.01	CYVR	Feb-14	time opt	101,035	8,060,043	8h 29m 42s	745,000	3.2559%	3.5100%	3.5686%	-72.4%
1	0.1	CYVR	Feb-14	time opt	101,014	8,060,429	8h 29m 52s	717,540	3.2343%	3.5149%	3.6008%	-73.4%
1	1	CYVR	Feb-14	time opt	101,019	8,060,349	8h 30m 14s	717,455	3.2389%	3.5139%	3.6749%	-73.4%
1	10	CYVR	Feb-14	time opt	101,019	8,060,349	8h 30m 14s	717,455	3.2389%	3.5139%	3.6749%	-73.4%
3	0	CYVR	Feb-14	time opt	101,785	8,086,569	8h 31m 2s	1,519,822	4.0224%	3.8506%	3.8389%	-43.7%
3	0.0001	CYVR	Feb-14	time opt	101,895	8,095,493	8h 31m 36s	1,395,000	4.1344%	3.9652%	3.9527%	-48.3%
3	0.001	CYVR	Feb-14	time opt	101,895	8,095,493	8h 31m 36s	1,395,000	4.1344%	3.9652%	3.9527%	-48.3%
3	0.01	CYVR	Feb-14	time opt	101,505	8,095,492	8h 31m 57s	695,000	3.7357%	3.9652%	4.0254%	-74.3%
3	0.1	CYVR	Feb-14	time opt	101,485	8,095,874	8h 32m 7s	672,535	3.7155%	3.9701%	4.0596%	-75.1%
3	1	CYVR	Feb-14	time opt	101,490	8,095,822	8h 32m 27s	672,479	3.7207%	3.9695%	4.1256%	-75.1%
3	10	CYVR	Feb-14	time opt	101,445	8,095,533	8h 32m 28s	667,479	3.6743%	3.9658%	4.1309%	-75.3%
10	0	CYVR	Feb-14	time opt	-	-	-	-	-	-	-	-
10	0.0001	CYVR	Feb-14	time opt	-	-	-	-	-	-	-	-
10	0.001	CYVR	Feb-14	time opt	-	-	-	-	-	-	-	-
10	0.01	CYVR	Feb-14	time opt	-	-	-	-	-	-	-	-
10	0.1	CYVR	Feb-14	time opt	-	-	-	-	-	-	-	-
10	1	CYVR	Feb-14	time opt	-	-	-	-	-	-	-	-
10	10	CYVR	Feb-14	time opt	-	-	-	-	-	-	-	-

β_{grnd}	β_{prof}	Dest	Atm	Mode	dm [kg]	ds [m]	dt [h:m:s]	ct _{tot} [m]	% dm	% ds	% dt	% CT
0	0	KIAD	Feb-17	time opt	72,513	5,922,568	6h 8m 16s	1,975,000	0.0000%	0.0000%	0.0000%	0.0%
0	0.0001	KIAD	Feb-17	time opt	72,513	5,922,568	6h 8m 16s	1,975,000	0.0000%	0.0000%	0.0000%	0.0%
0	0.001	KIAD	Feb-17	time opt	71,840	5,922,568	6h 9m 43s	670,000	-0.9289%	0.0000%	0.3929%	-66.1%
0	0.01	KIAD	Feb-17	time opt	71,641	5,922,568	6h 10m 7s	437,203	-1.2033%	0.0000%	0.5054%	-77.9%
0	0.1	KIAD	Feb-17	time opt	71,622	5,922,568	6h 10m 12s	314,727	-1.2289%	0.0000%	0.5253%	-84.1%
0	1	KIAD	Feb-17	time opt	71,561	5,922,568	6h 10m 20s	255,809	-1.3132%	0.0000%	0.5622%	-87.0%
0	10	KIAD	Feb-17	time opt	71,580	5,922,568	6h 10m 15s	132,203	-1.2870%	0.0000%	0.5380%	-93.3%
0.01	0	KIAD	Feb-17	time opt	72,515	5,922,868	6h 8m 16s	1,897,000	0.0028%	0.0051%	0.0005%	-3.9%
0.01	0.0001	KIAD	Feb-17	time opt	72,514	5,922,868	6h 8m 16s	1,920,000	0.0006%	0.0051%	0.0008%	-2.8%
0.01	0.001	KIAD	Feb-17	time opt	71,843	5,922,868	6h 9m 42s	610,000	-0.9248%	0.0051%	0.3923%	-69.1%
0.01	0.01	KIAD	Feb-17	time opt	71,620	5,922,868	6h 10m 10s	192,203	-1.2315%	0.0051%	0.5157%	-90.3%
0.01	0.1	KIAD	Feb-17	time opt	71,630	5,922,868	6h 10m 10s	215,859	-1.2179%	0.0051%	0.5169%	-89.1%
0.01	1	KIAD	Feb-17	time opt	71,649	5,922,868	6h 9m 44s	132,249	-1.1924%	0.0051%	0.4937%	-93.3%
0.01	10	KIAD	Feb-17	time opt	71,587	5,922,868	6h 10m 13s	132,203	-1.2770%	0.0051%	0.5311%	-93.3%
0.03	0	KIAD	Feb-17	time opt	72,552	5,934,968	6h 8m 22s	1,282,000	0.0532%	0.2094%	0.0282%	-35.1%
0.03	0.0001	KIAD	Feb-17	time opt	72,540	5,934,968	6h 8m 23s	1,305,000	0.0368%	0.2094%	0.0326%	-33.9%
0.03	0.001	KIAD	Feb-17	time opt	72,540	5,934,968	6h 8m 23s	1,305,000	0.0368%	0.2094%	0.0326%	-33.9%
0.03	0.01	KIAD	Feb-17	time opt	71,913	5,934,968	6h 9m 44s	207,014	-0.8280%	0.2094%	0.4001%	-89.5%
0.03	0.1	KIAD	Feb-17	time opt	71,905	5,934,968	6h 9m 41s	177,014	-0.8387%	0.2094%	0.3860%	-91.0%
0.03	1	KIAD	Feb-17	time opt	71,877	5,934,968	6h 9m 48s	220,586	-0.8771%	0.2094%	0.4157%	-88.8%
0.03	10	KIAD	Feb-17	time opt	71,650	5,934,968	6h 11m 18s	132,014	-1.1901%	0.2094%	0.8241%	-93.3%
0.1	0	KIAD	Feb-17	time opt	72,999	5,971,778	6h 10m 32s	487,000	0.6701%	0.8309%	0.6161%	-75.3%
0.1	0.0001	KIAD	Feb-17	time opt	72,996	5,971,778	6h 10m 32s	500,000	0.6653%	0.8309%	0.6170%	-74.7%
0.1	0.001	KIAD	Feb-17	time opt	72,996	5,971,778	6h 10m 32s	500,000	0.6653%	0.8309%	0.6170%	-74.7%
0.1	0.01	KIAD	Feb-17	time opt	72,710	5,971,778	6h 11m 8s	103,440	0.2706%	0.8309%	0.7775%	-94.8%
0.1	0.1	KIAD	Feb-17	time opt	72,656	5,971,778	6h 11m 35s	45,000	0.1969%	0.8309%	0.9001%	-97.7%
0.1	1	KIAD	Feb-17	time opt	72,659	5,971,778	6h 11m 34s	45,000	0.2013%	0.8309%	0.8963%	-97.7%
0.1	10	KIAD	Feb-17	time opt	72,659	5,971,778	6h 11m 34s	45,000	0.2013%	0.8309%	0.8963%	-97.7%
0.3	0	KIAD	Feb-17	time opt	72,999	5,971,778	6h 10m 32s	487,000	0.6701%	0.8309%	0.6161%	-75.3%
0.3	0.0001	KIAD	Feb-17	time opt	72,996	5,971,778	6h 10m 32s	500,000	0.6653%	0.8309%	0.6170%	-74.7%
0.3	0.001	KIAD	Feb-17	time opt	72,996	5,971,778	6h 10m 32s	500,000	0.6653%	0.8309%	0.6170%	-74.7%
0.3	0.01	KIAD	Feb-17	time opt	72,710	5,971,778	6h 11m 8s	103,440	0.2706%	0.8309%	0.7775%	-94.8%
0.3	0.1	KIAD	Feb-17	time opt	72,659	5,971,778	6h 11m 34s	45,000	0.2013%	0.8309%	0.8963%	-97.7%
0.3	1	KIAD	Feb-17	time opt	72,659	5,971,778	6h 11m 34s	45,000	0.2013%	0.8309%	0.8963%	-97.7%
0.3	10	KIAD	Feb-17	time opt	72,659	5,971,778	6h 11m 34s	45,000	0.2013%	0.8309%	0.8963%	-97.7%
1	0	KIAD	Feb-17	time opt	74,348	6,083,926	6h 17m 13s	227,000	2.5304%	2.7245%	2.4326%	-88.5%
1	0.0001	KIAD	Feb-17	time opt	74,346	6,083,926	6h 17m 13s	240,000	2.5266%	2.7245%	2.4332%	-87.8%
1	0.001	KIAD	Feb-17	time opt	74,346	6,083,926	6h 17m 13s	240,000	2.5266%	2.7245%	2.4332%	-87.8%
1	0.01	KIAD	Feb-17	time opt	74,298	6,083,926	6h 17m 22s	60,000	2.4611%	2.7245%	2.4705%	-97.0%
1	0.1	KIAD	Feb-17	time opt	74,224	6,083,926	6h 17m 30s	35,000	2.3590%	2.7245%	2.5090%	-98.2%
1	1	KIAD	Feb-17	time opt	74,224	6,083,926	6h 17m 30s	35,000	2.3590%	2.7245%	2.5090%	-98.2%
1	10	KIAD	Feb-17	time opt	74,224	6,083,926	6h 17m 30s	35,000	2.3590%	2.7245%	2.5090%	-98.2%
3	0	KIAD	Feb-17	time opt	77,213	6,315,486	6h 31m 23s	154,000	6.4806%	6.6343%	6.2785%	-92.2%
3	0.0001	KIAD	Feb-17	time opt	77,210	6,315,486	6h 31m 23s	165,000	6.4764%	6.6343%	6.2791%	-91.6%
3	0.001	KIAD	Feb-17	time opt	77,210	6,315,486	6h 31m 23s	165,000	6.4764%	6.6343%	6.2791%	-91.6%
3	0.01	KIAD	Feb-17	time opt	77,210	6,315,486	6h 31m 23s	165,000	6.4764%	6.6343%	6.2791%	-91.6%
3	0.1	KIAD	Feb-17	time opt	76,870	6,315,486	6h 32m 23s	0	6.0076%	6.6343%	6.5493%	-100.0%
3	1	KIAD	Feb-17	time opt	76,870	6,315,486	6h 32m 23s	0	6.0076%	6.6343%	6.5494%	-100.0%
3	10	KIAD	Feb-17	time opt	76,870	6,315,486	6h 32m 23s	0	6.0076%	6.6343%	6.5494%	-100.0%
10	0	KIAD	Feb-17	time opt	85,362	6,960,300	7h 11m 20s	42,000	17.7192%	17.5217%	17.1278%	-97.9%
10	0.0001	KIAD	Feb-17	time opt	85,360	6,960,300	7h 11m 20s	50,000	17.7164%	17.5217%	17.1280%	-97.5%
10	0.001	KIAD	Feb-17	time opt	85,360	6,960,300	7h 11m 20s	50,000	17.7164%	17.5217%	17.1280%	-97.5%
10	0.01	KIAD	Feb-17	time opt	85,360	6,960,300	7h 11m 20s	50,000	17.7164%	17.5217%	17.1280%	-97.5%
10	0.1	KIAD	Feb-17	time opt	85,280	6,960,300	7h 11m 29s	0	17.6058%	17.5217%	17.1651%	-100.0%
10	1	KIAD	Feb-17	time opt	85,280	6,960,300	7h 11m 29s	0	17.6058%	17.5217%	17.1651%	-100.0%
10	10	KIAD	Feb-17	time opt	85,280	6,960,300	7h 11m 29s	0	17.6058%	17.5217%	17.1651%	-100.0%

D. Numeric results - Hybrid mitigation

β_{grnd}	β_{prof}	Dest	Atm	Mode	dm [kg]	ds [m]	dt [h:m:s]	ct _{tot} [m]	% dm	% ds	% dt	% CT
0	0	CYWG	Feb-17	time opt	80,129	6,481,044	6h 45m 48s	1,325,000	0.0000%	0.0000%	0.0000%	0.0%
0	0.0001	CYWG	Feb-17	time opt	80,129	6,481,044	6h 45m 48s	1,325,000	0.0000%	0.0000%	0.0000%	0.0%
0	0.001	CYWG	Feb-17	time opt	80,129	6,481,044	6h 45m 48s	1,325,000	0.0000%	0.0000%	0.0000%	0.0%
0	0.01	CYWG	Feb-17	time opt	79,705	6,481,044	6h 46m 35s	460,000	-0.5292%	0.0000%	0.1915%	-65.3%
0	0.1	CYWG	Feb-17	time opt	79,320	6,481,044	6h 49m 28s	181,490	-1.0091%	0.0000%	0.9014%	-86.3%
0	1	CYWG	Feb-17	time opt	79,331	6,481,044	6h 49m 41s	0	-0.9962%	0.0000%	0.9563%	-100.0%
0	10	CYWG	Feb-17	time opt	79,323	6,481,044	6h 49m 27s	181,490	-1.0062%	0.0000%	0.9000%	-86.3%
0.01	0	CYWG	Feb-17	time opt	80,132	6,481,044	6h 45m 48s	1,317,000	0.0032%	0.0000%	-0.0008%	-0.6%
0.01	0.0001	CYWG	Feb-17	time opt	80,129	6,481,044	6h 45m 48s	1,325,000	0.0000%	0.0000%	0.0000%	0.0%
0.01	0.001	CYWG	Feb-17	time opt	80,129	6,481,044	6h 45m 48s	1,325,000	0.0000%	0.0000%	0.0000%	0.0%
0.01	0.01	CYWG	Feb-17	time opt	79,705	6,481,044	6h 46m 35s	460,000	-0.5292%	0.0000%	0.1915%	-65.3%
0.01	0.1	CYWG	Feb-17	time opt	79,331	6,481,044	6h 49m 41s	0	-0.9962%	0.0000%	0.9563%	-100.0%
0.01	1	CYWG	Feb-17	time opt	79,331	6,481,044	6h 49m 41s	0	-0.9962%	0.0000%	0.9563%	-100.0%
0.01	10	CYWG	Feb-17	time opt	79,323	6,481,044	6h 49m 27s	181,490	-1.0062%	0.0000%	0.9000%	-86.3%
0.03	0	CYWG	Feb-17	time opt	80,132	6,481,044	6h 45m 48s	1,317,000	0.0032%	0.0000%	-0.0008%	-0.6%
0.03	0.0001	CYWG	Feb-17	time opt	80,129	6,481,044	6h 45m 48s	1,325,000	0.0000%	0.0000%	0.0000%	0.0%
0.03	0.001	CYWG	Feb-17	time opt	80,129	6,481,044	6h 45m 48s	1,325,000	0.0000%	0.0000%	0.0000%	0.0%
0.03	0.01	CYWG	Feb-17	time opt	79,331	6,481,044	6h 49m 41s	0	-0.9962%	0.0000%	0.9563%	-100.0%
0.03	0.1	CYWG	Feb-17	time opt	79,331	6,481,044	6h 49m 41s	0	-0.9962%	0.0000%	0.9563%	-100.0%
0.03	1	CYWG	Feb-17	time opt	79,331	6,481,044	6h 49m 41s	0	-0.9962%	0.0000%	0.9563%	-100.0%
0.03	10	CYWG	Feb-17	time opt	79,323	6,481,044	6h 49m 27s	181,490	-1.0062%	0.0000%	0.9000%	-86.3%
0.1	0	CYWG	Feb-17	time opt	80,209	6,487,384	6h 46m 12s	1,240,000	0.1000%	0.0978%	0.0981%	-6.4%
0.1	0.0001	CYWG	Feb-17	time opt	80,209	6,487,384	6h 46m 12s	1,250,000	0.0998%	0.0978%	0.0981%	-5.7%
0.1	0.001	CYWG	Feb-17	time opt	80,209	6,487,384	6h 46m 12s	1,250,000	0.0998%	0.0978%	0.0981%	-5.7%
0.1	0.01	CYWG	Feb-17	time opt	79,501	6,487,384	6h 48m 12s	90,000	-0.7841%	0.0978%	0.5923%	-93.2%
0.1	0.1	CYWG	Feb-17	time opt	79,501	6,487,384	6h 48m 12s	90,000	-0.7841%	0.0978%	0.5923%	-93.2%
0.1	1	CYWG	Feb-17	time opt	79,501	6,487,384	6h 48m 12s	90,000	-0.7841%	0.0978%	0.5923%	-93.2%
0.1	10	CYWG	Feb-17	time opt	79,501	6,487,384	6h 48m 12s	90,000	-0.7841%	0.0978%	0.5923%	-93.2%
0.3	0	CYWG	Feb-17	time opt	80,684	6,527,944	6h 48m 32s	982,000	0.6932%	0.7236%	0.6744%	-25.9%
0.3	0.0001	CYWG	Feb-17	time opt	80,685	6,527,944	6h 48m 32s	985,000	0.6937%	0.7236%	0.6743%	-25.7%
0.3	0.001	CYWG	Feb-17	time opt	80,685	6,527,944	6h 48m 32s	985,000	0.6937%	0.7236%	0.6743%	-25.7%
0.3	0.01	CYWG	Feb-17	time opt	80,404	6,527,944	6h 49m 9s	480,000	0.3435%	0.7236%	0.8254%	-63.8%
0.3	0.1	CYWG	Feb-17	time opt	80,037	6,527,944	6h 52m 30s	0	-0.1143%	0.7236%	1.6481%	-100.0%
0.3	1	CYWG	Feb-17	time opt	80,037	6,527,944	6h 52m 30s	0	-0.1143%	0.7236%	1.6481%	-100.0%
0.3	10	CYWG	Feb-17	time opt	80,029	6,527,944	6h 52m 15s	181,232	-0.1247%	0.7236%	1.5880%	-86.3%
1	0	CYWG	Feb-17	time opt	85,518	6,896,839	7h 12m 8s	281,000	6.7255%	6.4156%	6.4898%	-78.8%
1	0.0001	CYWG	Feb-17	time opt	85,516	6,896,839	7h 12m 9s	285,000	6.7232%	6.4156%	6.4903%	-78.5%
1	0.001	CYWG	Feb-17	time opt	85,516	6,896,839	7h 12m 9s	285,000	6.7232%	6.4156%	6.4903%	-78.5%
1	0.01	CYWG	Feb-17	time opt	85,516	6,896,839	7h 12m 9s	285,000	6.7232%	6.4156%	6.4903%	-78.5%
1	0.1	CYWG	Feb-17	time opt	85,234	6,896,839	7h 13m 19s	0	6.3713%	6.4156%	6.7791%	-100.0%
1	1	CYWG	Feb-17	time opt	85,234	6,896,839	7h 13m 19s	0	6.3713%	6.4156%	6.7791%	-100.0%
1	10	CYWG	Feb-17	time opt	85,234	6,896,839	7h 13m 19s	0	6.3713%	6.4156%	6.7791%	-100.0%
3	0	CYWG	Feb-17	time opt	85,989	6,932,669	7h 14m 26s	266,000	7.3130%	6.9684%	7.0537%	-79.9%
3	0.0001	CYWG	Feb-17	time opt	85,987	6,932,669	7h 14m 26s	270,000	7.3103%	6.9684%	7.0543%	-79.6%
3	0.001	CYWG	Feb-17	time opt	85,987	6,932,669	7h 14m 26s	270,000	7.3103%	6.9684%	7.0543%	-79.6%
3	0.01	CYWG	Feb-17	time opt	85,712	6,932,669	7h 15m 34s	0	6.9678%	6.9684%	7.3331%	-100.0%
3	0.1	CYWG	Feb-17	time opt	85,712	6,932,669	7h 15m 34s	0	6.9678%	6.9684%	7.3331%	-100.0%
3	1	CYWG	Feb-17	time opt	85,712	6,932,669	7h 15m 34s	0	6.9678%	6.9684%	7.3331%	-100.0%
3	10	CYWG	Feb-17	time opt	85,712	6,932,669	7h 15m 34s	0	6.9678%	6.9684%	7.3331%	-100.0%
10	0	CYWG	Feb-17	time opt	101,046	8,096,909	8h 27m 13s	43,000	26.1037%	24.9322%	24.9892%	-96.8%
10	0.0001	CYWG	Feb-17	time opt	101,043	8,096,909	8h 27m 13s	45,000	26.1009%	24.9322%	24.9897%	-96.6%
10	0.001	CYWG	Feb-17	time opt	101,043	8,096,909	8h 27m 13s	45,000	26.1009%	24.9322%	24.9897%	-96.6%
10	0.01	CYWG	Feb-17	time opt	101,043	8,096,909	8h 27m 13s	45,000	26.1009%	24.9322%	24.9897%	-96.6%
10	0.1	CYWG	Feb-17	time opt	100,956	8,096,909	8h 27m 21s	0	25.9918%	24.9322%	25.0233%	-100.0%
10	1	CYWG	Feb-17	time opt	100,956	8,096,909	8h 27m 21s	0	25.9918%	24.9322%	25.0233%	-100.0%
10	10	CYWG	Feb-17	time opt	100,956	8,096,909	8h 27m 21s	0	25.9918%	24.9322%	25.0233%	-100.0%

β_{grnd}	β_{prof}	Dest	Atm	Mode	dm [kg]	ds [m]	dt [h:m:s]	ct _{tot} [m]	% dm	% ds	% dt	% CT
0	0	CYVR	Feb-17	time opt	95,609	7,725,148	8h 1m 8s	1,395,000	0.0000%	0.0000%	0.0000%	0.0%
0	0.0001	CYVR	Feb-17	time opt	95,609	7,725,148	8h 1m 8s	1,395,000	0.0000%	0.0000%	0.0000%	0.0%
0	0.001	CYVR	Feb-17	time opt	95,609	7,725,148	8h 1m 8s	1,395,000	0.0000%	0.0000%	0.0000%	0.0%
0	0.01	CYVR	Feb-17	time opt	95,128	7,725,148	8h 2m 2s	565,000	-0.5026%	0.0000%	0.1879%	-59.5%
0	0.1	CYVR	Feb-17	time opt	94,818	7,725,148	8h 2m 56s	366,713	-0.8276%	0.0000%	0.3732%	-73.7%
0	1	CYVR	Feb-17	time opt	94,753	7,725,148	8h 3m 12s	364,583	-0.8953%	0.0000%	0.4300%	-73.9%
0	10	CYVR	Feb-17	time opt	94,649	7,725,148	8h 4m 26s	296,384	-1.0042%	0.0000%	0.6850%	-78.8%
0.01	0	CYVR	Feb-17	time opt	95,610	7,725,148	8h 1m 8s	1,364,000	0.0010%	0.0000%	0.0004%	-2.2%
0.01	0.0001	CYVR	Feb-17	time opt	95,609	7,725,148	8h 1m 8s	1,395,000	0.0000%	0.0000%	0.0000%	0.0%
0.01	0.001	CYVR	Feb-17	time opt	95,609	7,725,148	8h 1m 8s	1,395,000	0.0000%	0.0000%	0.0000%	0.0%
0.01	0.01	CYVR	Feb-17	time opt	95,128	7,725,148	8h 2m 2s	565,000	-0.5026%	0.0000%	0.1879%	-59.5%
0.01	0.1	CYVR	Feb-17	time opt	94,680	7,725,148	8h 4m 16s	298,441	-0.9715%	0.0000%	0.6521%	-78.6%
0.01	1	CYVR	Feb-17	time opt	94,647	7,725,148	8h 4m 25s	296,384	-1.0059%	0.0000%	0.6839%	-78.8%
0.01	10	CYVR	Feb-17	time opt	94,754	7,725,148	8h 3m 12s	364,583	-0.8937%	0.0000%	0.4311%	-73.9%
0.03	0	CYVR	Feb-17	time opt	95,629	7,727,058	8h 1m 13s	1,153,000	0.0206%	0.0247%	0.0178%	-17.3%
0.03	0.0001	CYVR	Feb-17	time opt	95,626	7,727,058	8h 1m 13s	1,160,000	0.0180%	0.0247%	0.0178%	-16.8%
0.03	0.001	CYVR	Feb-17	time opt	95,626	7,727,058	8h 1m 13s	1,160,000	0.0180%	0.0247%	0.0178%	-16.8%
0.03	0.01	CYVR	Feb-17	time opt	95,186	7,727,058	8h 2m 4s	488,686	-0.4424%	0.0247%	0.1947%	-65.0%
0.03	0.1	CYVR	Feb-17	time opt	95,025	7,727,058	8h 2m 25s	298,441	-0.6102%	0.0247%	0.2671%	-78.6%
0.03	1	CYVR	Feb-17	time opt	95,035	7,727,058	8h 2m 24s	298,441	-0.6004%	0.0247%	0.2654%	-78.6%
0.03	10	CYVR	Feb-17	time opt	95,036	7,727,058	8h 2m 24s	298,441	-0.5988%	0.0247%	0.2653%	-78.6%
0.1	0	CYVR	Feb-17	time opt	95,629	7,727,058	8h 1m 13s	1,153,000	0.0206%	0.0247%	0.0178%	-17.3%
0.1	0.0001	CYVR	Feb-17	time opt	95,626	7,727,058	8h 1m 13s	1,160,000	0.0180%	0.0247%	0.0178%	-16.8%
0.1	0.001	CYVR	Feb-17	time opt	95,626	7,727,058	8h 1m 13s	1,160,000	0.0180%	0.0247%	0.0178%	-16.8%
0.1	0.01	CYVR	Feb-17	time opt	95,171	7,727,058	8h 2m 4s	390,000	-0.4574%	0.0247%	0.1955%	-72.0%
0.1	0.1	CYVR	Feb-17	time opt	95,035	7,727,058	8h 2m 24s	298,441	-0.6004%	0.0247%	0.2654%	-78.6%
0.1	1	CYVR	Feb-17	time opt	95,032	7,727,058	8h 2m 25s	298,441	-0.6029%	0.0247%	0.2658%	-78.6%
0.1	10	CYVR	Feb-17	time opt	95,035	7,727,058	8h 2m 24s	298,441	-0.6003%	0.0247%	0.2653%	-78.6%
0.3	0	CYVR	Feb-17	time opt	96,684	7,807,408	8h 6m 17s	882,000	1.1247%	1.0648%	1.0708%	-36.8%
0.3	0.0001	CYVR	Feb-17	time opt	96,682	7,807,408	8h 6m 17s	890,000	1.1230%	1.0648%	1.0705%	-36.2%
0.3	0.001	CYVR	Feb-17	time opt	96,682	7,807,408	8h 6m 17s	890,000	1.1230%	1.0648%	1.0705%	-36.2%
0.3	0.01	CYVR	Feb-17	time opt	96,376	7,807,408	8h 6m 53s	400,000	0.8029%	1.0648%	1.1948%	-71.3%
0.3	0.1	CYVR	Feb-17	time opt	96,237	7,807,408	8h 7m 14s	308,432	0.6571%	1.0648%	1.2667%	-77.9%
0.3	1	CYVR	Feb-17	time opt	96,237	7,807,408	8h 7m 14s	308,432	0.6571%	1.0648%	1.2667%	-77.9%
0.3	10	CYVR	Feb-17	time opt	96,237	7,807,408	8h 7m 14s	308,432	0.6571%	1.0648%	1.2667%	-77.9%
1	0	CYVR	Feb-17	time opt	101,626	8,176,239	8h 30m 0s	282,000	6.2939%	5.8393%	6.0002%	-79.8%
1	0.0001	CYVR	Feb-17	time opt	101,623	8,176,239	8h 30m 0s	285,000	6.2909%	5.8393%	6.0001%	-79.6%
1	0.001	CYVR	Feb-17	time opt	101,623	8,176,239	8h 30m 0s	285,000	6.2909%	5.8393%	6.0001%	-79.6%
1	0.01	CYVR	Feb-17	time opt	101,328	8,176,239	8h 31m 10s	0	5.9815%	5.8393%	6.2437%	-100.0%
1	0.1	CYVR	Feb-17	time opt	101,328	8,176,239	8h 31m 10s	0	5.9815%	5.8393%	6.2437%	-100.0%
1	1	CYVR	Feb-17	time opt	101,328	8,176,239	8h 31m 10s	0	5.9815%	5.8393%	6.2437%	-100.0%
1	10	CYVR	Feb-17	time opt	101,328	8,176,239	8h 31m 10s	0	5.9815%	5.8393%	6.2437%	-100.0%
3	0	CYVR	Feb-17	time opt	102,106	8,212,069	8h 32m 17s	267,000	6.7952%	6.3031%	6.4759%	-80.9%
3	0.0001	CYVR	Feb-17	time opt	102,102	8,212,069	8h 32m 17s	270,000	6.7918%	6.3031%	6.4759%	-80.6%
3	0.001	CYVR	Feb-17	time opt	102,102	8,212,069	8h 32m 17s	270,000	6.7918%	6.3031%	6.4759%	-80.6%
3	0.01	CYVR	Feb-17	time opt	102,085	8,212,069	8h 32m 28s	85,000	6.7740%	6.3031%	6.5141%	-93.9%
3	0.1	CYVR	Feb-17	time opt	101,814	8,212,069	8h 33m 25s	0	6.4902%	6.3031%	6.7109%	-100.0%
3	1	CYVR	Feb-17	time opt	101,814	8,212,069	8h 33m 25s	0	6.4902%	6.3031%	6.7109%	-100.0%
3	10	CYVR	Feb-17	time opt	101,814	8,212,069	8h 33m 25s	0	6.4902%	6.3031%	6.7109%	-100.0%
10	0	CYVR	Feb-17	time opt	-	-	-	-	-	-	-	-
10	0.0001	CYVR	Feb-17	time opt	-	-	-	-	-	-	-	-
10	0.001	CYVR	Feb-17	time opt	-	-	-	-	-	-	-	-
10	0.01	CYVR	Feb-17	time opt	-	-	-	-	-	-	-	-
10	0.1	CYVR	Feb-17	time opt	-	-	-	-	-	-	-	-
10	1	CYVR	Feb-17	time opt	-	-	-	-	-	-	-	-
10	10	CYVR	Feb-17	time opt	-	-	-	-	-	-	-	-

**Faculty of
Aerospace Engineering**
Kluyverweg 1
2629 HS Delft
The Netherlands

www.tudelft.nl